A non-contact co-culture method for studying metabolic interactions in the human microbiome

Timothy Rozday

Doctor of Philosophy

University of York
Biology

September 2018

0.1 Abstract

Neisseria meningitidis is a commensal of the upper respiratory tract (URT) that can sporadically cause invasive meningococcal disease (IMD). Utilisation of propionic acid by *N. meningitidis* is a known pathogenicity factor, and *N. meningitidis* is associated with propionic acid-producing bacteria of the URT microbiome, in particular *Porphyromonas*.

An *in vitro* non-contact co-culture assay is proposed to study metabolic interactions between *N. meningitidis* and *Porphyromonas gingivalis* via propionic acid. This assay is modelled using ordinary differential equations showing that it is feasible when permeability of oxygen and propionic acid is balanced, and that quantification can be achieved only when *N. meningitidis* growth is limited by both oxygen and propionic acid. Parameter values from a verified model, fitted to *in vitro* data, would quantify the metabolic interaction.

The apparatus was designed using limits and rules discovered by the model analysis, and by an iterative development process. The ability to capture *N. meningitidis* growth dynamics, and generate anaerobic conditions for *P. gingivalis*, was demonstrated. Growth inhibition by propionic acid, and yields of *N. meningitidis* from glucose, pyruvate and propionic acid were measured. Other important aspects of *N. meningitidis* growth were identified using plate reader experiments.

The developed assay is not fully demonstrated. However, all results indicate that it is suitable for quantifying metabolic interactions between the aerobic *N. meningitidis* and the anaerobic *P. gingivalis*. Insights into this metabolic interaction would be useful for developing novel therapeutics to prevent IMD. This methodology is also of general interest for studying metabolic interactions in the human microbiome.

0.2 Author's declaration

I declare that this thesis is a presentation of original work and I am the sole author. This work has not previously been presented for an award at this, or any other, University. All sources are acknowledged as References.

0.3 Acknowledgements

Writing a thesis requires patience. I would not have been able to complete my thesis without the patience of so many people around me.

In particular I want to thank Tiff, my wife. Thinking back on the late-night phone calls from the lab and after long days of writing up, you weren't just cheering me on from the sidelines, you were in the race with me.

I wouldn't be where I am without the constant love, care, support, concern and joy that my parents have given me. From you I inherited a love of education and academia, and I join you now in a shared love for Jesus.

My church family at York Evangelical Church, and more recently at Hope Community Church, have kept me fed, watered and rested. You did more than this though, you were true brothers and sisters to me.

Many thanks my friends in the CIDCATS program, L1 corridor, Chong lab and the Moir lab. You gave me a reason to keep coming back to the lab after so many failed experiments, and you made the rare successes that much more thrilling.

Thank you to my supervisors: James, Jon and Steve. Your excitement for all things curious is an inspiration to me, thank you for your attempts to teach me this and countless other things. Thank you to James and Marjan (my thesis advisory panel) for holding me to your high standards. My thinking is stronger, and this thesis is more useful, as a result of your inputs.

It has been a gift knowing all of you.

I'm humbled to have been able to dive a little deeper into the world that God has made. The frustrations involved in these efforts speak only to the limitless wisdom of the creator, and a longing to search him out. I thank this God for being the beginning, middle and end of my thesis.

Contents

List of Figures

Chapter 1

Introduction

1.1 *Neisseria meningitidis*

Invasive meningococcal disease (IMD) was first described in 1805 (Vieusseux, 1805), and *Neisseria meningitidis* (or meningococcus) was first discovered as the causative agent in 1887 (Weichselbaum, 1887; Koyfman & Takayesu, 2011). *N. meningitidis* causes both sporadic and epidemic disease in humans (Stephens *et al.*, 2007). Since the development of antibiotics the fatality rate of IMD has dropped significantly from ~80% however it has since remained at 7-15 % (Black *et al.*, 2012).

The microbiology of *N. meningitidis* is reviewed in Rouphael & Stephens, 2012a. In short: *N. meningitidis* is a Gram-negative β proteobacterium and an aerobic diplococcus. It is fastidious and cannot survive more than a few hours outside of favourable conditions. In the lab optimal growth conditions are 35-37 °C and 5-10% CO_2. Many *N. meningitidis* strains are surrounded by a capsule which provides protection, enables transmission between hosts and survival within hosts. The capsule is the basis for serotyping which is the most common classification system of *N. meningitidis*. There are 13 serotypes, of which 6 are pathogenic (A, B, C, W-135, X and Y). Other further classifications are based on the outer membrane porins PorA and PorB, and immonotyping based on lipooligosaccharide (LOS) structure. More recently, multi-locus sequence typing (MLST), based on genome sequencing, has been used to define clonal complexes. *N. meningitidis* has a transformable genome, it is known to transfer DNA with other *N. meningitidis* strains, with the closely-related *N. gonorrhoeae*, and with *Haemophilus*

which also causes meningitis in humans. *N. meningitidis* is most closely related to *N. gonorrhoeae*, a pathogen that causes gonorrhoea, and *N. lactamica*, a commensal of the human upper respiratory tract (URT).

The human nasopharynx, part of the URT, is the only known reservoir of *N. meningitidis* (Trivedi *et al.*, 2011). *N. meningitidis* almost always acts as a commensal during colonisation of this site (Moxon & Jansen, 2005). Meningococcal carriage is an important part of IMD because colonisation almost always precedes invasion and pathogenesis (Gabutti *et al.*, 2015), and because the nasopharynx acts as a reservoir from which other hosts are infected (Moir, 2015).

This project examines the role that microbiota of the URT play in affecting colonisation, carriage and pathogenicity of *N. meningitidis* in the human host.

1.2 Human cost of invasive meningococcal disease (IMD)

1.2.1 Global incidence

1.2.1.1 Global distribution of IMD

IMD occurs throughout the globe, with incidences varying by region (Fig1.1). It is sporadic with occasional outbreaks (Dretler *et al.*, 2018), and in the past has repeatedly resulted in epidemics (Stephens *et al.*, 2007). Many countries have surveillance systems in place to monitor incidence of IMD. These systems vary in their coverage and methodology for verifying IMD, this skews the reported incidence rates (Harrison *et al.*, 2009). The area of the world most affected by IMD is a region spanning 26 countries in sub-Saharan Africa known as the "meningitis belt", it stretches west to east from Senegal to Ethiopia (Harrison *et al.*, 2009; Borrow *et al.*, 2017).

The global incidence of IMD has been reviewed recently in Acevedo *et al.*, 2019, to summarise: the USA has the most thorough surveillance system for IMD, and as of 2017 the overall incidence was 0.12 in 100,000. Elsewhere in North America, the incidence was 0.3 per 100,000 in Canada and 0.01-0.02 per 100,000 in Mexico. In Europe, as of 2018, the incidence was 0.7 per 100,000. South East Asian countries have reported re-

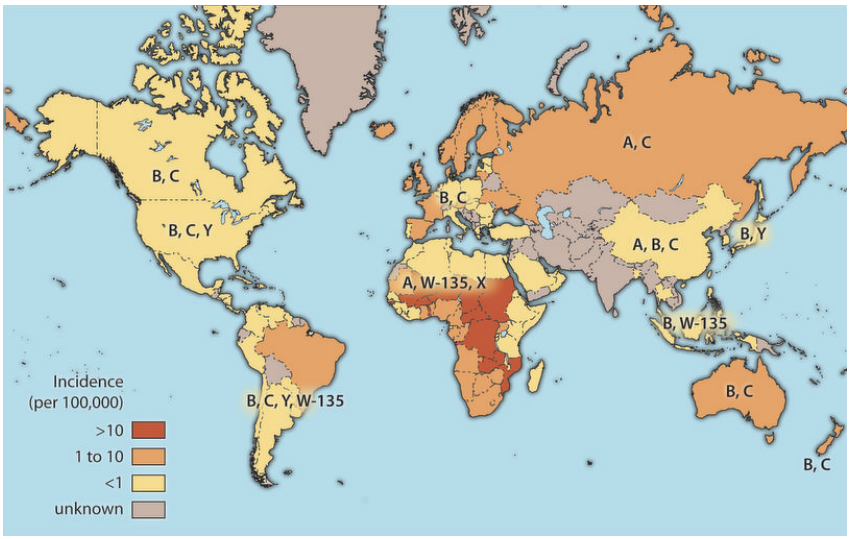

Figure 1.1: Global distribution of IMD incidence and distribution of IMD-causing serogroups. It should be noted that, as of 2013, incidence of IMD has since become much lower in the sub-Saharan meningitidis belt (Acevedo *et al.*, 2019). From Black *et al.*, 2012

latively low incidences, 0.05 per 100,000 in China, and <0.03 per 100,000 in Taiwan, South Korea and Japan. In South and Central America, incidence was also relatively low with <0.1 per 100,000 in Bolivia, Cuba, Paraguay and Peru. However, Brazil had an incidence of 2 per 100,000. The meningitis belt in sub-Saharan Africa, as of 2013, had an incidence of 0.02 per 100,000. This is following deployment of the MenAfriVac vaccine in 2010. Before this, the incidence was around 100 per 100,000 (this change in incidence rate is not displayed in Fig1.1). Despite this progress, the meningitis belt had around 20,000 recorded cases of IMD in 2015 with one region experiencing a cumulative attack rate of 992 per 100,000 (WHO, 2016). Other countries mentioned are New Zealand with an incidence of 1.6 per 100,000 in 2016, Russia with an incidence of 0.45-1.0 per 100,000 between 2010-2016, and Morocco with an incidence of 2-3.6 per 100,000 between 2012-2016.

Serogroups are geographically distributed. Serogroup B is the most important cause of IMD in North America, South America, Australia, North Africa and Europe. Serogroup C is most prevalent in Brazil, China, Russia, India (along with serogroup A), Niger and Nigeria. Serogroups W and Y predominate in some countries such as Mozambique and Japan respectively. (Acevedo *et al.*, 2019)

1.2.1.2 Epidemics and outbreaks

Historically, Serogroup A used to cause outbreaks in China before the 1980s (Harrison *et al.*, 2009) and predominated in Europe before World War II (Stephens *et al.*, 2007), however this is no longer the case. In the meningitis belt there have been periodic epidemics of serogroup A IMD since the 1940's with incidences exceeding 1000 per 100,000 (Stephens *et al.*, 2007). In particular, the epidemic of 1996-1997 resulted in over 25,000 fatalities (Harrison *et al.*, 2009). However, outbreaks of IMD caused by serogroup A have been practically eliminated since the introduction of the MenAfriVac vaccine in 2010 (Dretler *et al.*, 2018). Epidemics of IMD have been associated with the Hajj pilgrimage in 1987, 2000 and 2001. These have prompted preventative measures such as the current Saudi Arabian policy of mandatory vaccinations for all pilgrims (Dretler *et al.*, 2018; Acevedo *et al.*, 2019).

There are occasional outbreaks in cities such as in Delhi (India) in 2005 and Baguio City (Philippines) in 2005 (Harrison *et al.*, 2009).

Outbreaks in countries with advanced economies are typically centred around universities, primary and secondary schools, nursing homes and the community (Harrison *et al.*, 2009). There have been university campus outbreaks at Ohio University in 2008-2010, at Princeton University in 2013-2014 and at Rutgers University in 2016 (Acevedo *et al.*, 2019). Other outbreaks have occurred at the World Scout Jamboree in 2015 (Japan), and at a Norwegian "russefeiring" event in 2011 where around 60,000 adolescents party for several weeks (Acevedo *et al.*, 2019). These outbreaks were relatively small involving <10 cases of IMD.

1.2.1.3 Global decline in IMD cases

Global incidence of IMD has been steadily decreasing for decades both in countries with advanced and developing economies. This is partly due to the development of vaccines, however the trend existed before deployment of these vaccines (Dretler *et al.*, 2018). Possible explanations include a decrease in risky behaviour, such as smoking (Acevedo *et al.*, 2019), and a general increase in administration of antibiotics (Dretler *et al.*, 2018). Also, there appear to be natural changes in incidence (Dretler *et al.*, 2018) as serogroups and clonal complexes emerge and decline (Tzeng & Stephens, 2000). For example, the emergence of the virulent clonal complex ST-11 in the otherwise non-

virulent serogroup W (Borrow *et al.*, 2017).

1.2.2 Morbidity and mortality

It is estimated that there are ~135,000 deaths each year due to IMD from a total of ~1.2 million cases (Rouphael & Stephens, 2012b), an overall mortality rate of 11.25%. IMD causes severe symptoms and death if not treated promptly, and before the antibiotic era mortality rates for IMD were much higher at ~70-85% (Dretler *et al.*, 2018). Onset of disease is rapid, quick recognition of symptoms and application of treatment is essential to prevent death or permanent consequences for the patient (Stephens *et al.*, 2007; Black *et al.*, 2012).

Meningitis (inflammation of the layer surrounding the brain and spinal cord) is the most common presentation of IMD occurring in ~50% of cases. Bacteriaemia (infection of the blood) occurs in ~40% of cases and sudden onset of organ failure and blood clot development (fulminant meningococcemia) occurs in ~10-20% of cases. Overall fatality rates are around ~10%, permanent pathology following a case of IMD occurs in ~20% of cases. These permanent consequences include limb amputations, scarring of the skin, loss of hearing, loss of sight and neurological damage. (Gabutti *et al.*, 2015)

Fatality rate varies with country, for example in Niger the mortality rate was ~12% while in Europe it was ~7% (Trotter & Maiden, 2014). Despite advances in healthcare systems, fatality rates remain high in countries with advanced economies due to the rapid onset and progression of IMD (Yogev & Tan, 2011; Dretler *et al.*, 2018).

IMD disproportionally affects infants (<1 years old) (Fig1.2) (Dretler *et al.*, 2018) due to the lack of natural immunity against *N. meningitidis* (Gabutti *et al.*, 2015). Individuals that survive the infection can still be faced with "a lifetime of rehabilitation, chronic medical care and financial support" due to neurological damage and other pathologies (Yogev & Tan, 2011).

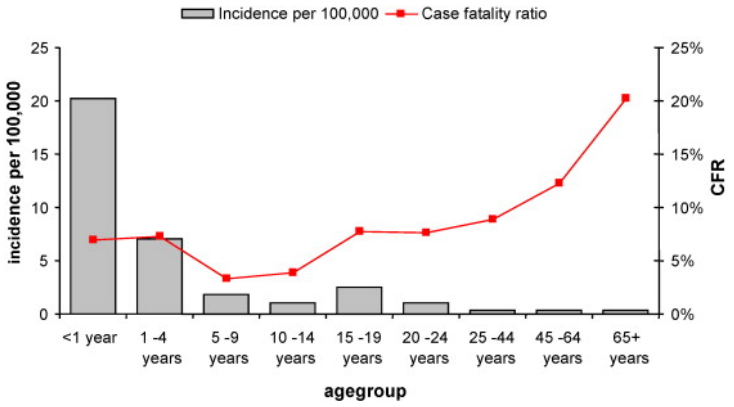

Figure 1.2: IMD incidence by age in 27 European countries in 2006, from Harrison *et al.*, 2009

1.3 *N. meningitidis* transmission and carriage

1.3.1 Importance of carriage

The only known stable reservoir of *N. meningitidis* is the human nasopharynx (Trivedi *et al.*, 2011). Although it is routinely found in other locations in human hosts (Gabutti *et al.*, 2015), carriage at these sites is transient. In the vast majority of cases, *N. meningitidis* acts as a commensal in the nasopharynx and only rarely causes disease (Trivedi *et al.*, 2011), in fact *N. meningitidis* has become regarded as an "accidental pathogen" since pathogenesis is so rare and it does not benefit the invasive meningococci (Moxon & Jansen, 2005; Schoen *et al.*, 2014). Carriage is a prerequisite for disease (Gabutti *et al.*, 2015) with most IMD occurring within 2 weeks of colonisation (Stephens *et al.*, 2007). However most colonisation events lead to a commensal population which can be either transient or stable, lasting weeks and sometimes months (Tzeng & Stephens, 2000).

Carriage rates in human populations vary widely based on geographical location, climate and other risk factors. For healthy individuals its average ranges from 8-25%, while in the meningitis belt during an epidemic the overall carriage rates are typically ~10% (Stephens *et al.*, 2007). Carriage rates are much higher in adolescents/young adults Christensen *et al.*, 2010, Fig1.3), in large groups of people coming together (such as crowded social gatherings, university students, army recruits and pilgrims), and in individuals engaging in risky behaviour (such as intimate kissing and smoking) (Stephens *et al.*, 2007). Carriage rates have been found as high as 55% in university students in the UK, 86% in male Hajj attendees (Balmer *et al.*, 2018) and 60% in army recruits

(Dellicour & Greenwood, 2007).

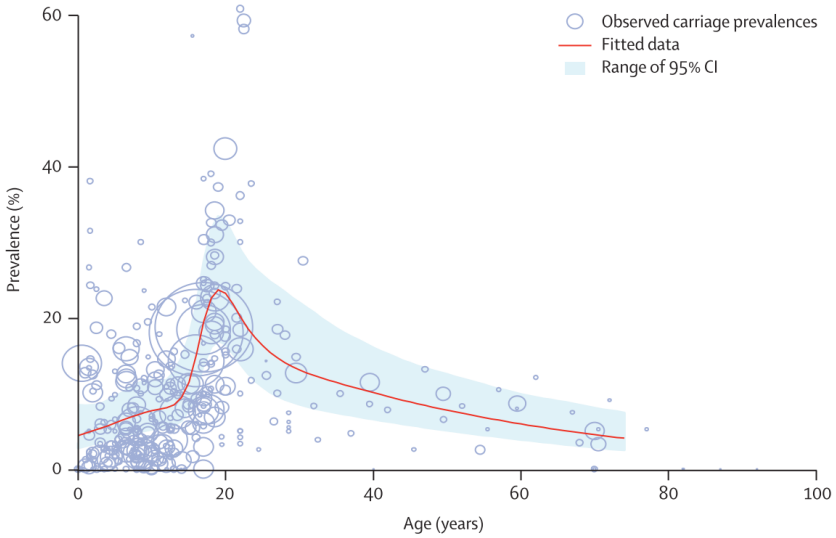

Figure 1.3: *N. meningitidis* carriage by age. From Christensen *et al.*, 2010 where a meta-analysis of carriage studies was performed.

Carriage is an essential part of IMD providing a stable reservoir from which transmissions and colonisations leading to invasive disease can occur. In Europe and North America adolescents and young adults act as a source of infection in this way (Gabutti *et al.*, 2015; Moir, 2015).

1.3.2 Transmission and adhesion

N. meningitidis is transmitted from person to person by transfer of nasal and oral secretions, either via direct contact or aerosol (Tzeng & Stephens, 2000). *N. meningitidis* strains may be encapsulated which enhances transmission at this stage by protecting against desiccation (Stephens *et al.*, 2007). A successful colonisation event occurs when contact is made with a mucosal surface, the mucus layer is penetrated, *N. meningitidis* adheres to the epithelial layer, and a microcolony forms (Tzeng & Stephens, 2000; Stephens *et al.*, 2007). Non-ciliated cells of the epithelium provide the site for attachment of *N. meningitidis* (Stephens *et al.*, 1983).

Meningococcal twitching motility, mediated by pili, enables penetration through the mucus to the epithelial layer (Stephens *et al.*, 2007). Type IV pili (Tfp) with a PilC tip mediate binding to CD46 (among other host cell surface markers) and adhesion to the

epithelium. Interactions between PilX components of the Tfp cause *N. meningitidis* to aggregate into microcolonies. Release of *N. meningitidis* from these microcolonies may occur through glycosylation of pilins reducing the pilin-pilin interactions that kept the bacteria aggregated. This enables spreading to other sites and transmission to other hosts and occurs in a phase-variable manner (Trivedi *et al.*, 2011, Fig1.4). The size of the inoculum needed for successful colonisation is not known (Stephens *et al.*, 2007).

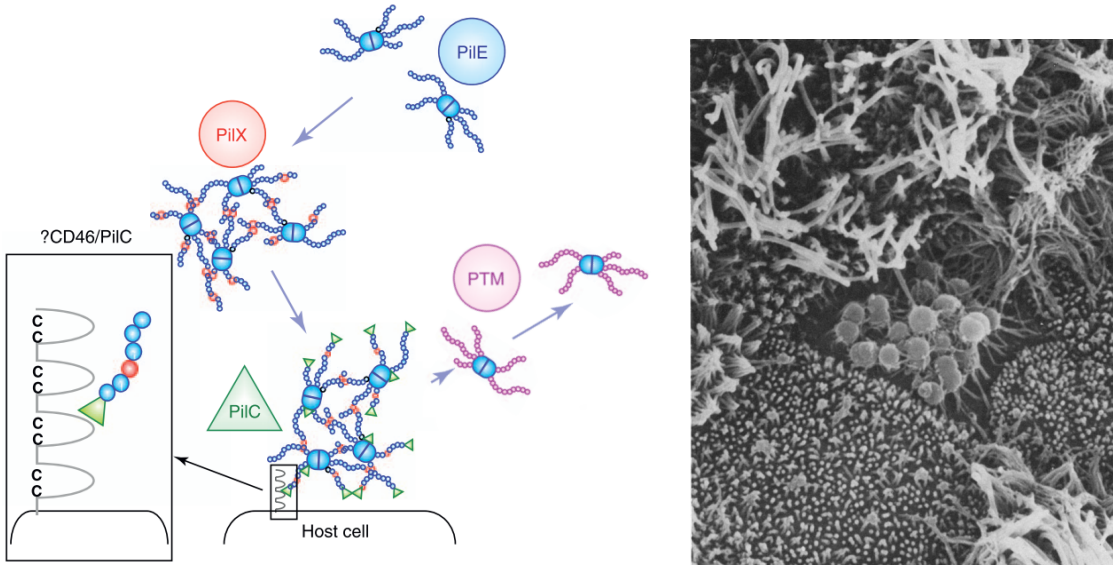

Figure 1.4: *N. meningitidis* adhesion to the mucosal surface.
a) The type IV pili (Tfp) with PilE, PilX and PilC tips mediate penetration and binding to the host epithelial cells, post-translational modification of the pili mediate release and spread to other sites, adapted from Trivedi *et al.*, 2011.
b) Scanning electron microscope (SEM) image of *N. meningitidis* adhered to non-ciliated cell of mucosal epithelium, from Stephens *et al.*, 1983.

1.3.3 Survival and colonisation in the upper respiratory tract (URT)

1.3.3.1 The upper respiratory tract

N. meningitidis colonises mucosal surfaces of the upper respiratory tract (URT) (Fig1.5 & 1.6). The nasopharynx is the only known reservoir of *N. meningitidis*, however other adjacent mucosal surfaces can be colonised such as the middle meatus (main nasal passage that drains the frontal and maxillary sinuses) (Ramakrishnan *et al.*, 2013) and

the throat (Donati *et al.*, 2016). It is not clear how long-term or transient the carriage is in these adjacent regions, there is some evidence of persistence in the throat (Donati *et al.*, 2016).

The URT is a point of entry for air and respiratory pathogens, it can also act as a reservoir for these pathogens. There are several barriers to colonisation of this site. (Weyand, 2017)

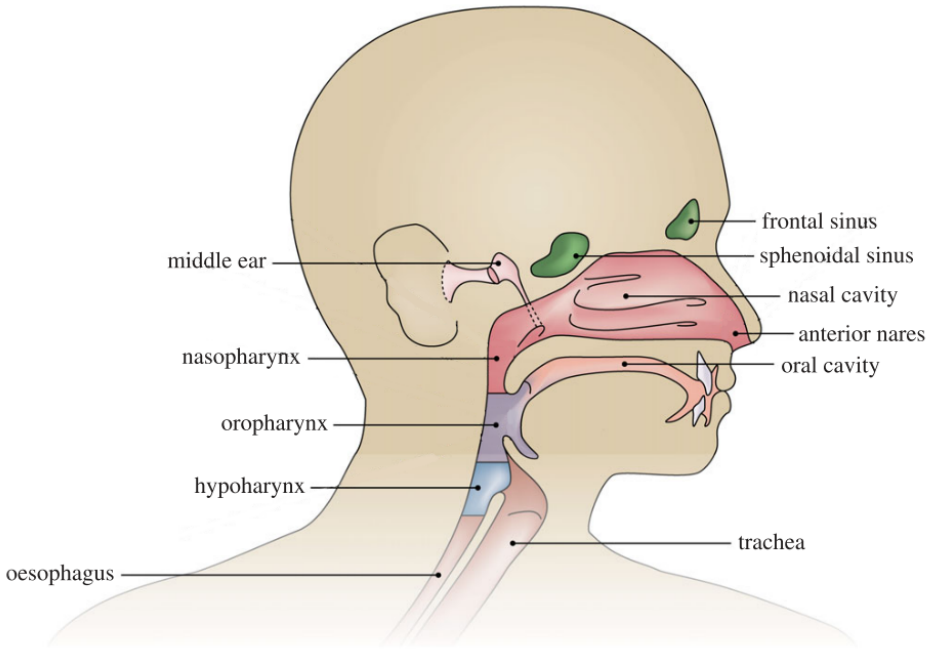

Figure 1.5: Upper respiratory tract anatomy, adapted from de Steenhuijsen Piters *et al.*, 2015

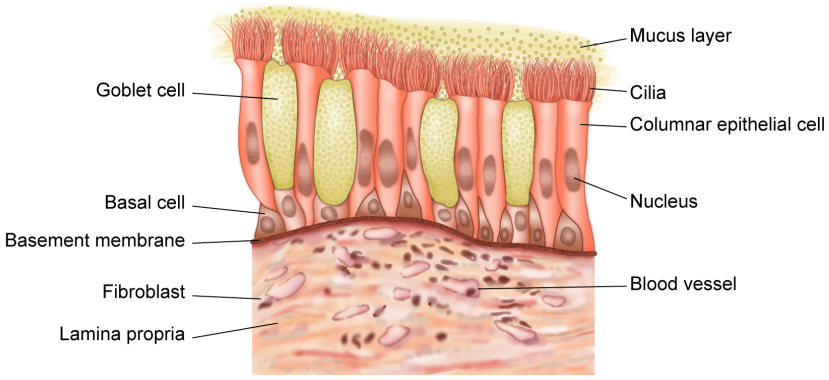

Figure 1.6: Upper respiratory tract mucosal surface structure, from Brugger *et al.*, 2016

1.3.3.2 Mucus barrier

A major barrier to colonisation of the URT is the mucus layer. Mucus is made up of mostly glycoproteins and water. It is secreted by the sinuses, moved by the action of ciliary beating through the nasal cavity to the nasopharynx, down the oeosophagus and ultimately to the gastrointestinal tract. The mucus serves to trap pathogens and deliver antigens to lymphoid tissues, it also has innate antimicrobial properties. Similar functions are fulfilled by other nasal secretions and saliva. (Weyand, 2017)

A common factor expressed by colonisers of the URT, including *N. meningitidis*, that enables penetration this barrier to reach the epithelium is a polysaccharide capsule (Siegel & Weiser, 2015). This capsule resists entrapment by the mucus and protects from the activity of antimicrobial proteins and peptides (Siegel & Weiser, 2015). Once through this layer, *N. meningitidis* overcomes the mechanical force from the mucus flow by adhering to the epithelial surface (Trivedi *et al.*, 2011). This involves reducing expression of Tfp (which mediates initial adherence) and the capsule so that lipopolysaccharide (LPS) and outer membrane proteins (Opa and Opc) can mediate a tighter adherence to this surface, recruitment of cholesterol to form cortical plaques, and formation a biofilm in which cells are embedded in a matrix of polysaccharides, lipids and DNA (Schoen *et al.*, 2014; Trivedi *et al.*, 2011).

1.3.3.3 Immune system

The innate and adaptive immune systems present another barrier to meningococcal colonisation of the URT. The capsule expressed by *N. meningitidis* enables evasion of complement- and opsonin-based detection mechanisms (Trivedi *et al.*, 2011). Various *N. meningitidis* factors also confer resistance: export pumps remove anti-microbial peptides from the cell, metabolism of nitric oxide (released by host cells) protects against its antimicrobial properties (this metabolism may also contribute to the survival of *N. meningitidis* in microaerobic environments), and secretion of a protease prevents opsonisation by cleaving secreted IgA (Trivedi *et al.*, 2011).

However, once *N. meningitidis* reaches the epithelium, it is detected by the innate immune system via Toll-like receptors (TLRs) and nucleotide-binding oligomerisation domain (Nod) receptors leading to recruitment of neutrophils (that help clear *N. meningitidis* by phagocytosis) and the recruitment of the adaptive immune system (Siegel &

Weiser, 2015).

The interaction of *N. meningitidis* with the adaptive immune system during colonisation is evidenced by the fact that carriage is an "immunising event" and results in protective immunity (Stephens *et al.*, 2007). However, *N. meningitidis* has some resistance to the adaptive immune response: capsule switching (changing expression of capsule components by phase variation and horizontal gene transfer) can allow escape from an immune response that targets capsule components, and *N. meningitidis* can also evade an immune response by molecular mimicry since some LOS components expressed on the outer membrane of *N. meningitidis* are identical to human I and i antigens (Stephens *et al.*, 2007). There is a significant regulatory T-cell response to carriage in older children and adults that suppresses the immune response against *N. meningitidis* (Trivedi *et al.*, 2011). This indicates that *N. meningitidis* is able to evade an adaptive immune response, and that carriage is tolerated and managed by the host immune system.

1.3.3.4 Nutritional immunity

Limitation of nutrients is a major barrier for microbes colonising the human host (Schoen *et al.*, 2014). Essential nutrients such as iron and zinc are sequestered forming a so-called "nutritional immunity" (Stork *et al.*, 2013). Additionally, the host microbiome competes for these limited resources excluding their use by invading pathogens (Ramakrishnan *et al.*, 2013). This competition and lack of nutrients is especially strong in biofilms, particularly during oxygen limitation (Schoen *et al.*, 2014). In response to this, invading microbes such as *N. meningitidis* display "nutritional virulence" by expressing adaptations that enable the exploitation of host resources (Abu Kwaik & Bumann, 2013).

Nutritional virulence adaptations of *N. meningitidis* are reviewed in Schoen *et al.*, 2014 which explains that: *N. meningitidis* is able to use glucose, lactate and pyruvate as sole carbon sources. Lactate (produced by lactic acid bacteria) is particularly relevant, increasing colonisation efficiency by 10 times due to the lack of competition for lactate as a carbon source (lactate is much more abundant than glucose in saliva and mucosal environments including the nasopharynx). For aerobic respiration, *N. meningitidis* uses cytochrome cbb_3 oxidase permitting growth in oxygen-limited environments such as biofilms. Sulphur is preferentially acquired from cysteine and cystine, although other sources can be used. Nitrogen is acquired by uptake of glutamate. *N. meningitidis*

can only synthesise glutamate in the presence of high levels on ammonia and so it is generally acquired from the environment. Iron acquisition is from host proteins such as transferrin, lactoferrin and haemoglobin, and siderophores secreted by other bacteria may also be used. Zinc, manganese, copper, cobalt and calcium transporters have been discovered in the *N. meningitidis* genome. The importance of nutritional virulence is displayed by the fact that adaptations that allow *N. meningitidis* to compensate for limitations of key nutrients (e.g. sulphur and amino acids) are important for long-term colonisation the URT.

1.3.3.5 Propionic acid utilisation

Propionic acid can be used as a carbon source by *N. meningitidis* via the methylcitrate cycle (Catenazzi *et al.*, 2014). Propionic acid in the URT is primarily a product of anaerobic fermentation by the resident microbiota. The significance of this is shown by the dramatic difference in carriage rates between infants and adolescents/young adults: as infants grow older their sinuses grow (Weyand, 2017), biofilms develop and so the prevalence of anaerobes in the microbiome greatly increases (Brugger *et al.*, 2016). This coincides with increased *N. meningitidis* carriage (Fig1.3) and incidence of IMD (Fig1.2) (Moir, 2015). The rates of carriage and IMD incidence decreases in older adults, possibly due to a decrease in other risk factors such as crowded social gatherings and intimate kissing (section 1.3.1). The high level of carriage in adolescents/young adults causes more than just increased IMD in this age-group, it acts as a reservoir from which all age-groups, including infants, are infected (Gabutti *et al.*, 2015; Moir, 2015).

Propionic acid also has antimicrobial properties, for instance inhibiting the growth of common enteric (Levison, 1973) and oral (Huang *et al.*, 2011) bacteria. This growth inhibition is dependent on concentration and pH (Levison, 1973; Ghorbani *et al.*, 2015). The pH dependence of the antimicrobial activity indicates that dissociated propionic acid is the active agent (Levison, 1973). The mechanism of this antimicrobial activity is via binding with coenzyme A to form propionate-CoA which inhibits the activity of pyruvate dehydrogenase complex, an enzyme complex that links the glycolysis pathway to the citric acid cycle (Maruyama & Kitamura, 1985). The antimicrobial effects of propionic acid vary widely between species (Huang *et al.*, 2011). A measurement of *N. meningitidis* growth inhibition has not been published in scientific literature, however the concentration that causes a 50% growth inhibition (IC50) in *Neisseria gonorrhoeae*

(a closely-related pathogen of the same genus) has been reported at $10\,\mathrm{mM}$ (Miller *et al.*, 1977).

1.3.3.6 Biofilm

Biofilms are composed of bacterial cells embedded in a matrix of protein, polysaccharide and DNA, this provides a stable environment that is resistant to physical dislocation and attack by antimicrobial compounds. (Fastenberg *et al.*, 2016)

It is hypothesised that *N. meningitidis* carriage is made possible by biofilm formation on host mucosal surfaces (Neil & Apicella, 2009). Biofilm is known to provide resistance to complement factors, antibodies and other factors (e.g. antibiotics, and reactive oxygen or nitrogen species) since the intracellular matrix in a biofilm immobilises these factors. Additionally, a subset of a microbial community within a biofilm may be able to persist through an antimicrobial challenge while the rest of the population is susceptible. This persistence may be genetic, or it may be due to a stationary-phase level of metabolic activity. (Anderson & O'Toole, 2008)

N. meningitidis biofilms are present in the carriage state, and they are more common than swabbing would indicate (Sim *et al.*, 2000) (because swabs were not able to detect microcolonies present beneath the epithelial surface in the URT).

1.4 Upper respiratory tract microbiome

1.4.1 Interaction between *N. meningitidis* and the URT microbiome

The microbiome is important in determining URT health and disease. It acts as a disease modifier by shaping the ecological environment (e.g. niche competition) and shaping the host immune system (Ramakrishnan *et al.*, 2013). Due to the importance of host microbiota, colonisation by *N. meningitidis* can be thought of as an event in a process of ecological succession (Moir, 2015) where microbiome developments must occur before *N. meningitidis* colonisation is permitted.

Specific metabolic interactions between *N. meningitidis* and the microbiome via lactate (section 1.3.3.4) and propionic acid (section 1.3.3.5) have already been described.

Also, the general importance of the microbiome is demonstrated clearly in Deasy *et al.*, 2015 where inoculation of university students with *Neisseria lactamica* caused *N. meningitidis* carriage to fall from 24.2% to 6.7% after 4 weeks. The mechanism appeared to be by competition for the same ecological niche rather than by an interaction with the immune system. The magnitude of carriage reduction was greater than that of the MenACWY conjugate vaccine (in use at the time of the study) showing that ecological interactions are at least as important as adaptive immune responses in affecting *N. meningitidis* carriage.

1.4.2 URT microbiome structure and function

Since the status of the URT microbiome is important in *N. meningitidis* carriage, it is important to understand the typical structure, function, organising principles and behaviours of the URT microbiome.

The composition of the commensal flora is somewhat consistent throughout the URT (Allen *et al.*, 2014; Ramakrishnan *et al.*, 2017; Earl *et al.*, 2018) although the oral microbiome is distinct from the nasopharyngeal microbiome (Allen *et al.*, 2014) and the URT contains a wide range of micro-habitats with varying oxygen and carbon dioxide levels (de Steenhuijsen Piters *et al.*, 2015). In the nasopharynx, the major phyla are *Firmicutes*, *Actinobacteria*, *Proteobacteria*, *Bacteroidetes* and *Fusobacteria* (Allen *et al.*, 2014; Bogaert *et al.*, 2011), the most abundant genera being *Alloiococcus*, *Corynebacterium*, *Staphylococcus*, *Haemophilus*, *Propionibacterium* and *Streptococcus* (Allen *et al.*, 2014). In the paranasal sinuses and middle meatus (a site used as a proxy for the sinuses due to its relative ease of sampling), the dominant phyla are similar with notable genera being *Streptococcus*, *Staphylococcus*, *Prevotella*, *Propionibacterium* and *Corynebacterium* (Ramakrishnan *et al.*, 2013; Ramakrishnan *et al.*, 2017).

Microbial growth in the URT is supported by carbon sources derived from the host. In the nostrils, sebum secreted by follicles provides a carbon source for the microbiota, notably propionibacteria (Mourelatos *et al.*, 2007). *Propionibacterium acnes* has been shown to metabolise glycerol in the sebum to produce propionic acid (Shu *et al.*, 2013). Mucin in the URT and lower respiratory tract also acts as a nutrient source for the microbiota. Mucin-degraders such as have *Veillonella parvula*, *Fusobacterium nucleatum*, *Prevotella melaninogenica* and *Streptococcus parasanguinis* have been shown to mobilise

this nutrient source in the airways by releasing products (such as propionic acid) that can be metabolised by other members of the microbiome (Flynn *et al.*, 2016). The main growth substrates in the oral cavity are glycoproteins. These complex substrates are utilised by consortia of bacteria where the degradation of each member is part of a chain of reactions that produce end products such as propionic acid and methane (Wade, 2013).

The ecological processes that shape the development of the URT microbiome are 1) dispersal, in which sites are initially colonised following birth of the host and continuously colonised from neighbouring sites and exogenous sources, 2) selection, with each of the myriad different niches that develop in the URT providing a different selection pressure, and 3) speciation and ecological drift, where isolated populations evolve to adapt to their environment and specialise in a niche (de Steenhuijsen Piters *et al.*, 2015).

The URT is colonised by microbes from the age of just a few months. This includes anaerobes, although the healthy infant URT microbiome is dominated by aerobes (Könönen, 2005). The development of sinuses (Weyand, 2017) and eruption of teeth (Könönen, 2005) associated with infant development provides more environments for anaerobes to thrive in. From these sites, other sites in the URT may be colonised, and so the presence and abundance of anaerobes can increase (Moir, 2015). The composition of the URT microbiome at an early age is mainly *Firmicutes* and *Proteobacteria* along with some *Actinobacteria* and *Bacteroidetes* (Bogaert *et al.*, 2011). However, in puberty *Actinobacteria* comes to dominate the microbiome, particularly the genera *Corynebacterium* and *Propionibacterium* (Brugger *et al.*, 2016). This could be due to physiological changes associated with a shift in hormone levels (Kumar, 2013). It has been demonstrated in the nostrils that increased sebum secretions in puberty cause an increase in *Propionibacterium acnes* abundance (an anaerobe that produces propionic acid as a fermentation product) (Mourelatos *et al.*, 2007). In adulthood, anaerobes greatly outnumber aerobes on mucosal surfaces of the URT at a ratio of around 10:1, and maybe as high as 100:1 (Brook, 2002; Brook, 2006).

The anaerobic conditions required for obligate anaerobes are generated in the URT by aerobic metabolism. These strict anaerobic conditions are generated in biofilms (Moir, 2015; Welch *et al.*, 2016). Biofilms are a common feature in the URT, which is unsurprising since biofilm is the most common form in which bacteria exist outside of the lab (Fastenberg *et al.*, 2016).

1.4.3 Association with disease

The URT microbiome is an important modulator of many diseases (Ramakrishnan *et al.*, 2013). The most important pathogens of the URT are *Streptococcus pneumoniae*, *Haemophilus influenzae*, *N. meningitidis*, *Staphylococcus aureus* and *Moraxella catarrhalis* (Bogaert *et al.*, 2011; Könönen, 2005). Together these pathogens cause pneumonia, sepsis and meningitis. However, they are also commonly found in the healthy microbiome as transient commensals (Bogaert *et al.*, 2011) and are considered to be part of the healthy microbiome (de Steenhuijsen Piters *et al.*, 2015). The mechanism by which these pathobionts shift from acting as a commensal to a pathogen is not fully known, however it is known that interactions with the microbiome are important in the process (Brugger *et al.*, 2016; Ramakrishnan *et al.*, 2013; Bogaert *et al.*, 2011).

The microbiome has a role in providing "nutritional immunity" by competing for resources and excluding pathogens in the URT (section 1.3.3.4). Additionally a decrease in biodiversity, evenness and population density of commensals is associated with a greater abundance of URT pathogens (e.g. *Streptococcus*, *Haemophilus*) (de Steenhuijsen Piters *et al.*, 2015). The role of this dysbiosis has been shown *in vivo*: mice with depleted sinus microbiomes are left more vulnerable to disease following colonisation by the pathogen *Corynebacterium tuberculostearicum* (Abreu *et al.*, 2012). Specific mechanisms for pathogen growth inhibition by the microbiota have been described: hydrogen peroxide produced by *S. pneumoniae* directly inhibits *S. aureus*, bacteriocins produced by the commensal *S. salivarius* may inhibit *S. pyogenes* (de Steenhuijsen Piters *et al.*, 2015), short-chain fatty acid production by Bacteroidetes and *Propionibacterium* spp inhibits growth and virulence of pathogens such as *S. aureus* (Brugger *et al.*, 2016; de Steenhuijsen Piters *et al.*, 2015). And so, it is shown that pathobiont pathogenicity is caused by a failure of the resident flora (and the host immune system) to prevent overgrowth of these otherwise commensal bacteria (de Steenhuijsen Piters *et al.*, 2015).

Other resident microbiota of the URT can also actively increase pathogenicity in pathobionts. For example, *Propionibacterium* spp can produce factors that induce and enhance *S. aureus* virulence (Brugger *et al.*, 2016), and anaerobic mucin-degraders in the airways can mobilise nutrients for use by potential pathogens (Flynn *et al.*, 2016). Also, more generally, there appears to be a synergy between pathogens in otitis (inflammation of the ear) and anaerobic commensals since they are often co-localised (Könönen, 2005).

1.4.4 Propionic acid production by the URT microbiome

Propionic acid production by the URT microbiome has a role in IMD by providing *N. meningitidis* with another carbon source (section 1.3.3.5, Catenazzi *et al.*, 2014, Moir, 2015). Propionic acid is also associated with pathogen exclusion (section 1.4.3), and mobilisation of nutrients from mucin for use by pathogens (section 1.4.2).

This propionic acid is produced by anaerobic metabolism. Levels of propionic acid vary between sites and with microbiome status. In healthy human adult gingival crevices (between the teeth and the gums), concentrations of $0.8\,\mathrm{mM}$ ($\pm 0.3\,\mathrm{mM}$) were measured (Niederman *et al.*, 1997). In the saliva of healthy adults, the concentration was measured at $0.06\,\mathrm{mM}$ (Takeda *et al.*, 2009). This shows that propionic acid is typically produced by the oral microbiome in health. In the oral cavity during peridontitis, the concentration of propionic acid in the gingival crevices reaches $9.5\,\mathrm{mM}$ ($\pm 1.8\,\mathrm{mM}$), 10 times higher than in health (Niederman *et al.*, 1997).

The concentration of propionic acid in the URT is likely to change with other factors since the abundance of propionic acid producers changes with age (Mourelatos *et al.*, 2007; Brugger *et al.*, 2016), season (Bogaert *et al.*, 2011), and whether the subject smokes (Charlson *et al.*, 2010).

The major propionic acid producers of the oral microbiome are *Porphyromonas gingivalis*, *Bacteroides loescheii* and *Fusobacterium nucleatum* (Kurita-Ochiai *et al.*, 1995). In the URT, *Veillonella parvula*, *F. nucleatum*, *Prevotella melaninogenica* and *Streptococcus parasanguinis* have been identified as key mucin degraders that produce propionic acid (Flynn *et al.*, 2016). *Propionibacterium* spp are also particularly important due to their prevalence (92.9%) and relative abundance (14.7%) in the nasal cavity (Ramakrishnan *et al.*, 2013), and they are implicated in several interactions with pathogens mediated by propionic acid (Brugger *et al.*, 2016; de Steenhuijsen Piters *et al.*, 2015).

Porphyromonas has been shown to correlate with *Neisseria* across several studies (Catenazzi *et al.*, 2014). *Porphyromonas gingivalis* is a key member of the oral microbiome that is involved in head and neck infections in a wide variety of sites (Brook, 2002), but is not itself a pathogen. It is known as a "keystone pathogen" due to its central role in the formation of "pathogenic polymicrobial plaques" (Tan *et al.*, 2014). It enables the development of pathogenicity via metabolic interactions, for example, by producing glycine which mediates an interaction with *Treponema denticola*, or by pro-

ducing short chain fatty acids which inhibit the host immune response (Kurita-Ochiai *et al.*, 1995). It is a strict anaerobe that grows in the oral cavity in the interior of subgingival plaque and deep in periodontal pockets (between the teeth and the gums) (Tan *et al.*, 2014) where anaerobic conditions are maintained by aerobic respiration. Also, *F. nucleatum* has a role in protecting *P. gingivalis* from oxidising conditions (Diaz *et al.*, 2002; Welch *et al.*, 2016). *P. gingivalis* is only present at low levels of abundance, if at all, in healthy individuals and only increases in abundance during disease (Diaz *et al.*, 2002).

The abundance of *Porphyromonas*, along with that of *Fusobacterium*, coincides with a significant increase of IMD incidence in teenagers and young adults (Catenazzi *et al.*, 2014). Although *P. gingivalis* is primarily a member of the oral microbiome (rather than the nasopharynx) there is a constant route to colonisation of the nasopharynx via saliva(Könönen, 2005). And so, this provides a possible mechanistic explanation for the correlation between *Porphyromonas* and IMD.

1.5 *N. meningitidis* invasion and pathogenesis

1.5.1 Mechanisms

1.5.1.1 Invasion

Following colonisation, to cause IMD *N. meningitidis* must cross the host epithelium and enter the bloodstream (Coureuil *et al.*, 2019).

It is likely that *N. meningitidis* crosses the epithelium by transcytosis (through the epithelial cells) rather than paracytosis (around the epithelial cells, breaking through the tight junctions connecting them) (Sutherland *et al.*, 2010; Coureuil *et al.*, 2019). At the epithelial surface, meningococcal outer membrane opacity-associated (Opa) proteins interact with epithelial carcinoembryonic antigen-related cell adhesion molecules (CEACAMs), mainly CEACAM1 and CEACAM3 but also CEA and CEACAM6, to cause adhesion and endocytosis (Schmitter *et al.*, 2007; Takahashi *et al.*, 2011). Meningococcal outer membrane protein Opc also has a role in adhesion and endocytosis (Takahashi *et al.*, 2011). The adhesin Nad2 has a role in transport within the epithelial cell to the basal surface as well as initial adherence and endocytosis (Bozza *et al.*, 2014). Influx of

L-glutamate into meningococcus mediated by the GltT-GltM ABC Transporter is known to be important in initiation of endocytosis (Takahashi *et al.*, 2011), and interactions between meningococcal porins and host cell Toll-like receptor 2 (TLR2) are known to enhance endocytosis (Toussi *et al.*, 2016). The capsule is also an important factor in this process, not for entry into cells but for survival during transcytosis and exit at the basolateral pole of the epithelium (Sutherland *et al.*, 2010).

In addition to this, damaged epithelium (e.g. due to smoking or URT infection) may provide a more direct route for *N. meningitidis* to enter the bloodstream (Tzeng & Stephens, 2000).

These invasion events may be more frequent than is apparent from clinical data since they would go undetected if they do not lead to a recognisable infection (Tzeng & Stephens, 2000). Following invasion, survival and growth in the bloodstream is dependent on evasion of the host immune response and acquisition of nutrients. The mechanisms by which the immune system is evaded in the bloodstream are similar to those in the nasopharynx (section 1.3.3.3). The capsule in particular protects meningococcus from phagocytosis and the complement system (Janowski & Newland, 2017). This is shown by the tendency for *N. meningitidis* strains from invasive cases to be encapsulated while encapsulation in strains isolated from the nasopharyngeal carriage is not as common (Tzeng & Stephens, 2000). Molecular mimicry (Tzeng & Stephens, 2000) and capsule switching (Harrison *et al.*, 2009) allow further evasion of adaptive immune responses in the bloodstream. The ability to overcome nutritional immunity (section 1.3.3.4) is also vital for enabling *N. meningitidis* to cause invasive disease (Schoen *et al.*, 2014).

1.5.1.2 Systemic infection

Pathogenicity is caused by meningococcus proliferating in the blood (Stephens *et al.*, 2007) and adhering to several sites in the host. These sites include the meninges that surrounds the central nervous system (CNS), the pericardium that surrounds the heart, and large bone joints (Tzeng & Stephens, 2000). Rapid multiplication of meningococcus in the blood, combined with a humoral immune response, causes the release of bacterial cell fragments and components including lipopolysaccharides (LPS) and LOS (Stephens *et al.*, 2007). LPS and LOS in particular are recognised by activation of Toll-like receptor 4 (TLR4) (Beutler *et al.*, 2001; Pridmore *et al.*, 2003) leading to a massive

and destructive immune response (Pathan *et al.*, 2003). This pathology may progress to cause fulminant meningococcal septicaemia, where kidney and lung function is impaired, blood clots cause tissue damage and the circulatory system progressively fails (Stephens *et al.*, 2007). This ultimately leads to death of the host if left untreated (Stephens *et al.*, 2007).

The other major mechanism of pathogenicity is by causing meningitis. At the meninges, *N. meningitidis* is able to breach the blood brain barrier and proliferate rapidly in the CNS which lacks a humoral immune system to oppose infection. Direct damage and inflammation caused by the release of meningococcal cell components and secreted substances (such as LPS, LOS, and proteases that degrade the extra-cellular matrix) cause damage in the CNS (Janowski & Newland, 2017; Kim, 2003). This, again, often causes death of the host if left untreated.

Disease progression and outcomes vary between outbreaks. For example, in Africa, fulminant septicaemia is less common than in the West (Stephens *et al.*, 2007). Patients often present with neck stiffness, a distinctive rash, aversion to light, fever and headache (Dretler *et al.*, 2018). However, ~30% of patients do not display these symptoms in a distinct way (Stephens *et al.*, 2007). Disease progression from when the first symptoms are displayed can occur over the course of a few hours or up to 14 days (Black *et al.*, 2012). The disease endpoint is death for 7-15% of patients (Black *et al.*, 2012). Of the patients who present with fulminant septicaemia the fatality rate is much higher at ~40-50%. Of the patients that survive IMD, 11-19% are left with permanent disability such as limb amputation, hearing loss or brain damage and developmental disabilities Black *et al.*, 2012; Dretler *et al.*, 2018.

1.5.2 Risk factors

Virulence of *N. meningitidis* is associated with risk factors, such as the bacterial strain involved in infection, the host's biology and behaviour, and the conditions of the surrounding environment.

1.5.2.1 Strain factors

Some *N. meningitidis* strains are more likely to cause IMD than others. This is shown by the fact that strains isolated from the blood and cerebrospinal fluid of IMD patients are more homogenous than strains isolated from carriage (Balmer *et al.*, 2018). Of the twelve defined *N. meningitidis* serogroups, only A, B, C, W, X and Y significantly cause IMD (Tzeng *et al.*, 2016). *N. meningitidis* strains are also grouped by clonal complex (CC) and called by their sequence type (ST). A small subset of these CCs cause the majority of IMD cases (Donati *et al.*, 2016; Harrison *et al.*, 2009). In serogroup A, the main hypervirulent strain has been ST-5 (subgroup III), although since the 1990s ST-7 and ST-2859 have become more important in the meningitidis belt (Harrison *et al.*, 2009). In Serogroup B, ST-32 and ST-41/44 (lineage 3) have been important causes of IMD, also ST-269 has emerged recently causing an outbreak in Quebec starting in 2003 (Harrison *et al.*, 2009; Law *et al.*, 2006). In Serogroup C, the main cause of IMD has been ST-11, although ST-8 (cluster A4) has also been an important hypervirulent strain. In Serogroup W-135, ST-11 is the only invasive strain. Since ST-11 is strongly associated with serogroup C, it is likely that a capsular switch event from C to W-135 occurred (Harrison *et al.*, 2009).

On a global scale, the predominant serogroups of each region differ (section 1.2.1.1, Dretler *et al.*, 2018, Acevedo *et al.*, 2019). Strains are also geographically distributed, emerging in one part of the world and spreading to others. For example, ST-5 (subgroup III) was endemic in China in the 1960s and spread to Moscow, Finland, Norway and Brazil over the next decade. ST-5 (subgroup III) then re-emerged in China in the 1980s, caused an outbreak in Hajj pilgrims in 1987 and then spread throughout Africa over the following decade (Harrison *et al.*, 2009). ST-7 and ST-2859 have emerged as strains localised to the meningitidis belt. Serogroup B strains have caused localised outbreaks, such as ST-32 in Norway, Spain, Brazil, Cuba, Chile & Oregon, and ST-41/44 (lineage III) in the Netherlands and New Zealand (Harrison *et al.*, 2009).

These strain differences are caused by differential expression of virulence factors, such as capsule components and metabolic factors. The effect of serogroup on invasiveness (Tzeng & Stephens, 2000) demonstrates the impact of capsule component expression on disease since serogroups mainly differ from each in the makeup of their capsules. *N. meningitidis* capsules are made from polysaccharide: serogroup B capsules are made from $\alpha 2 \rightarrow 8$ linked sialic acid, serogroup C capsules are made from partially

O-acetylated α2→9 linked sialic acid, serogroup Y capsules are made from alternating monomers of D-glucose and partially O-acetylated sialic acid, serogroup W capsules are made from alternating monomers of D-galactose and partially O-acetylated sialic acid, serogroup A capsules are made from α1→6 linked N-acetylmannosamine 1-phosphate, and serogroup X capusules are made from α1→4 linked N-acetylglucosamine 1-phosphate (Tzeng *et al.*, 2016).

These molecular differences cause *N. meningitidis* to interact with a human host in different ways. All the major invasive serogroups inhibit activation of complement via the classical pathway, since they prevent the formation of a C1 complex (Agarwal *et al.*, 2014). However, the sialic acid of serogroup B and C capsules are also recognised by complement factor H which inhibits alternative complement pathway (AP) activation via C3b binding (Tzeng *et al.*, 2016). Serogroup A capsules do not suppress AP activation, however they do provide resistance to the bactericidal activity of the complement system (Tzeng *et al.*, 2016). In a similar way, serogroup W and Y capsules also provide protection from complement, however they actually enhance AP activation by acting as targets for C3b binding (Ram *et al.*, 2011). The different serogroup capsule compositions also affect interactions with host cell cytoskeletons. Serogroup B capsules are able to directly interact with microtubules meaning that they are able to multiply and spread within epithelial cells using this environment as protection from phagocytosis (Tala *et al.*, 2014).

Differences in transcription profiles of *N. meningitidis* metabolic genes show that expression levels of these factors determine a strain's ability to survive in the blood and infect a host (Schoen *et al.*, 2014). In a whole-blood model of meningococcal septicaemia, enzymes involved in glycolysis, the citric acid cycle and the 2-methylcitrate cycle are upregulated (Echenique-Rivera *et al.*, 2011). The 2-methylcitrate cycle is proposed to have a role in meningococcal colonisation of the nasopharynx since it enables *N. meningitidis* to utilise propionic acid as a carbon source (section 1.3.3.5), however it is unclear what role this may have in invasive disease. A study measuring transcriptional changes during long-term colonisation (Hey *et al.*, 2013) noted that the observed changes in metabolic factors resembled previously reported measurements from a whole blood model of invasive disease (Hedman *et al.*, 2012). Therefore, it is possible that the changes in 2-methylcitrate cycle regulation are in fact associated with host contact rather than being specific to invasive disease.

Uptake and metabolism of glutamate (Hedman *et al.*, 2012; Schoen *et al.*, 2014) and

sulphur (Hey *et al.*, 2013; Grifantini *et al.*, 2002) are also upregulated in invasive disease. Additionally, a lactate transport protein (LctP) and an iron uptake regulator (Fur) have been shown to increase survival of *N. meningitidis* in the blood (Echenique-Rivera *et al.*, 2011).

1.5.2.2 Host factors

Some hosts are more vulnerable to IMD than others. Individuals that have deficiencies in their humoral immune response or complement system are more likely to suffer from IMD (Tzeng & Stephens, 2000; Dretler *et al.*, 2018; Stephens *et al.*, 2007). This may be due to a congenital condition such as asplenia (Dretler *et al.*, 2018), or one of a variety of hereditary complement deficiencies which affect around 0.03% of the global population (Lewis & Ram, 2014; Tzeng *et al.*, 2016). Genome wide association studies have shown that mutations in the region of the *CFH* gene (which encodes for complement factor H) are strongly associated with IMD (Davila *et al.*, 2010; Martinon-Torres *et al.*, 2016). Immune deficiencies may also be acquired from HIV infection, cancers affecting immune cells (e.g. leukaemia, myeloma), alcoholism or immunosuppression (e.g. the complement inhibitor eculizumab), to name a few (Tzeng & Stephens, 2000; Dretler *et al.*, 2018; Gabutti *et al.*, 2015). The presence of IgA antibodies in the serum is a key determinant of IMD risk (Stephens *et al.*, 2007). A host can acquire these antibodies following *N. meningitidis* colonisation. Protective IgA antibodies are typically present in the serum around 2 weeks after colonisation (Dretler *et al.*, 2018). This priming of the immune system can also be caused by exposure to non-meningococcal bacterial species (Tzeng & Stephens, 2000). Infants are at greater risk of IMD since they have not yet acquired these protective IgA antibodies, and so when immunity acquired from antibodies in human milk decreases then the child is left at a greater risk of acquiring IMD (Stephens *et al.*, 2007; Janowski & Newland, 2017).

Other known host risk factors include ABO blood group antigen secretor status, with non-secretors being more likely to develop IMD (Tzeng & Stephens, 2000), and the host microbiome (section 1.4.1).

1.5.2.3 Environmental and behavioural factors

Factors that damage the epithelium and permit invasion of the blood by *N. meningitidis* include co-infections and smoking (section 1.5.1.1) (Tzeng & Stephens, 2000). This is reflected by the fact that infections such as influenza (Harrison *et al.*, 2009; Tzeng & Stephens, 2000) and exposure to tobacco smoke (MacLennan *et al.*, 2006; Dretler *et al.*, 2018) increase the risk of developing IMD.

Climate is also an important contributory factor: in sub-Saharan Africa, epidemic IMD is associated with the hot, dry and dusty season (Harrison *et al.*, 2009; Dretler *et al.*, 2018) which again could be due to damage of the URT epithelium. In more temperate climates, IMD is associated with winter when URT infection and dysbiosis are more common (section 1.4.3, Weyand, 2017).

N. meningitidis is an infectious pathogen and so close contact with individuals with IMD increases the risk of contracting IMD 500-2000 fold (Tzeng & Stephens, 2000). Travelling to regions where IMD is more prevalent (such as the meningitidis belt) is also a known risk factor (Dretler *et al.*, 2018).

Other risk factors of IMD mirror those that affect *N. meningitidis* carriage (outlined in section 1.3.1). Factors such as crowding, migration, kissing, pub visits, and university attendance are all also risk factors for IMD due to their impact on meningococcal carriage and transmission (Dretler *et al.*, 2018; Acevedo *et al.*, 2019). This is unsurprising since carriage is a prerequisite for IMD (Gabutti *et al.*, 2015).

1.6 Current treatments

1.6.1 Antibiotics

Use of antibiotics to treat IMD has greatly reduced morbidity from this disease. The mortality rate before the antibiotic era was ~70-85%, while today it is ~10-15% (Rouphael & Stephens, 2012a).

The antibiotics commonly used to treat and prevent IMD are beta-lactams (e.g. benzylpenicillin, cefotaxime, and ceftriaxone) which target cell wall synthesis, sulfonamides which target folate synthesis, quinolones (e.g. ciprofloxacin) which target DNA

Gyrase, rifampicin which targets RNA polymerase, and chloramphenicol which targets protein synthesis (Stephens *et al.*, 2007; Kapoor *et al.*, 2017).

Stephens *et al.*, 2007 provides a good summary of the strategies used for treating IMD: when a case of IMD is identified, the priority for treatment is prompt administration of antibiotics. This is because an antibiotic dose effectively halts the growth and spread of *N. meningitidis* in the host's blood and CNS. The rapid proliferation of *N. meningitidis* and potentially rapid progression of IMD makes this a priority, so much so that, in many countries, antibiotics are administered before the patient is admitted to a hospital. Such is the effectiveness of antibiotics that a single dose of chloramphenicol or ceftriaxone is often sufficient for treatment and has been administered as a single dose during epidemics in developing economies. In developed economies, cefotaxime or ceftriaxone combined with vancomycin is typically used before a case is confirmed as IMD. Once an IMD case is confirmed then benzylpenicillin or a third-generation cephalosporin is used. Treatment typically lasts 3-4 days and is combined with other interventions to manage septicaemia and prevent death by circulatory collapse (e.g. adding fluids to increase the volume of blood in circulation).

Another use of antibiotics is to prevent IMD in subjects that have been in close contact with an individual with IMD, since this contact greatly increases the risk of developing the disease (section 1.5.2.3) (Tzeng & Stephens, 2000). The aim of this prevention strategy is to eliminate *N. meningitidis* from the nasopharynx, therefore rifampicin and quinolones are typically used. This prevention strategy is not used on a wide scale since it would accelerate the rate of development of antimicrobial resistance (AMR). (Stephens *et al.*, 2007)

AMR has been detected in *N. meningitidis* for most antibiotics commonly used to treat IMD (Acevedo *et al.*, 2019). Sulfonamides were once the main antibiotic used to treat IMD until resistance emerged in the 1970s. Rate of resistance increased until around 30% of meningococcal isolates in the UK were no longer susceptible to this class of antibiotics (Riley & Brown, 1991). A study of *N. meningitidis* clinical isolates, collected mainly from Europe during 1945-2006, showed that 65% had reduced susceptibility to penicillin G (Taha *et al.*, 2007). Penicillin G resistant strains have also shown increased resistance to other beta-lactams, such as cefotaxime and ceftriaxone (Deghmane *et al.*, 2017). In China, resistance to ciprofloxacin has recently emerged with 84% of strains showing some non-susceptibility during 2005-2013 (Chen *et al.*, 2015). Chloramphenicol resistance was first detected in Vietnam during 1987–1996 (Galimand *et al.*, 1998)

and in Australia during 1994-1997 (Shultz *et al.*, 2003), and has since become widespread in South East Asia (Batty *et al.*, 2020). Rifampicin resistance has also been detected, however it is rare and remains confined to Europe (Acevedo *et al.*, 2019).

Despite the fact that some degree of AMR has been detected for all major antibiotics used to treat IMD, cases of IMD with AMR strains are still rare. There are, however, concerns that AMR may become a problem in the near future thus reversing the global progress that has been made in combating IMD. (Acevedo *et al.*, 2019)

As well as being limited by AMR, antibiotics are limited by being a reactionary treatment. IMD is a sporadic disease (Harrison *et al.*, 2009) with rapid onset and high morbidity/mortality if left untreated. Even when treated, minimising the delay before treatment is critical, but this can be difficult since presenting symptoms can be non-specific. For this reason, the IMD mortality rate in economically developed countries remains at around 7-15% (Black *et al.*, 2012). Therefore prevention by vaccination has been the focus of efforts to reduce IMD morbidity and mortality (Dretler *et al.*, 2018).

1.6.2 Vaccines

1.6.2.1 Polysaccharide vaccines

The first successful vaccines used purified meningococcal capsule polysaccharide, and were developed around 1970 (Dretler *et al.*, 2018). These polysaccharide vaccines were limited to protecting against specific serogroups, and vaccines against all major IMD-causing serogroups, except serogroup B, were developed (Trotter & Maiden, 2014). These vaccines were effective at promoting immunity against IMD, showing a clinical success rate of over 85% (Dretler *et al.*, 2018).

However, capsular polysaccharides are type 2 T-cell independent (TI) antigens (Weintraub, 2003). This means they do not induce long-term protection by memory B-cells but instead activate B-cells previously primed by natural exposure to *N. meningitidis* (e.g. during colonisation of the nasopharynx) (Zahlanie *et al.*, 2014). Therefore, the duration of protection is short with repeat vaccinations recommended every 3-5 years (Zahlanie *et al.*, 2014). These repeat vaccinations, however, induce hyporesponsiveness since primed B-cells are activated and differentiated in response to the vaccine but not replenished (Poolman & Borrow, 2011). The mechanism of immunisation by

capsular polysaccharide antigens involves activation of complement factor C3d which ultimately binds to B-cell complement receptor 2 (CD21) expressed by marginal-zone (MZ) B-cells in the spleen (Klouwenberg & Bont, 2008). However, in neonate and infants under 2 years of age, the expression of complement is low, numbers of MZ B-cells are low and these B-cells have low expression of CD21 (Klouwenberg & Bont, 2008). Therefore, polysaccharides are not effective at protecting infants less than 2 years of age from IMD (Zahlanie *et al.*, 2014).

Due to these limitations, they were mainly used during epidemics and outbreaks (Trotter & Maiden, 2014) rather than in routine widespread vaccination programs.

1.6.2.2 Conjugate vaccines

In the 1990's, meningococcal conjugate vaccines were developed by conjugating capsular polysaccharide to a protein that would elicit a T-cell immune response (e.g. tetanus toxoid) (Trotter & Maiden, 2014). This meant that the vaccines would generate a higher-affinity IgG antibody response with a longer term immune memory, an immune response in infants, and the ability to be boosted by subsequent doses (Trotter & Maiden, 2014; Gabutti *et al.*, 2015; Dretler *et al.*, 2018). Immunogenicity of these vaccines, as measured by serum bactericidal antibody (SBA) titre, showed a higher efficacy when compared to polysaccharide vaccines (71-95%, compared to 57-83% from polysaccharide vaccines) (Dretler *et al.*, 2018). These advantages meant that meningoccocal conjugate vaccines have since been replacing the polysaccharide vaccines (Dretler *et al.*, 2018).

The first conjugate vaccine was introduced in the UK in 1999 (Dretler *et al.*, 2018), it led to a decrease in IMD of over 97% in 2007 compared to 1998 (Trotter & Maiden, 2014). Similar success stories have been reported in Brazil where a 2010 vaccination program led to a 64-92% reduction of IMD in infants, in the Netherlands where IMD incidence was reduced by 99% in the target population and a 93% in the general population, and in the USA where IMD rates were reduced by 91-95% in adolescents (Dretler *et al.*, 2018). In the African meningitis belt, the MenAfriVac vaccine has been deployed with unprecedented success: IMD rates fell from 100 cases per 100,000 to just 0.02 (2013 compared to 2011), a reduction of over 99.9% (Acevedo *et al.*, 2019; Dretler *et al.*, 2018). However, other data (WHO, 2016) indicates that the success is more moderate than this with ~20,000 cases in 2015, which is more like a 90% when compared to

2011. The success of these conjugate vaccines has been due to direct protection of vaccinated individuals, reduction of *N. meningitidis* transmission, and herd immunity (Trotter & Maiden, 2014; Gabutti *et al.*, 2015)

1.6.2.3 Herd immunity

Herd immunity is an phenomenon in which non-immunised individuals in a population are protected from a disease by the presence of immunised individuals in the same population. This effect relies on immunisation causing reduced pathogen carriage and transmission in immunised individuals (Trotter & Maiden, 2014).

Conjugate vaccines are effective at reducing *N. meningitidis* carriage: in the UK a serogroup C vaccine caused a reduction in carriage rate of 75% over the course of two years (Yogev & Tan, 2011). In Chad a 98% reduction in carriage was observed following deployment of a serogroup A vaccine (Dretler *et al.*, 2018). The MenAfriVac vaccine caused a ~95% reduction in carriage over 2 years (Gabutti *et al.*, 2015), and in Burkina Faso it caused a >95% reduction in carriage over one year (Balmer *et al.*, 2018). These reductions in carriage have had the effect of causing a reduction in IMD rates in non-vaccinated individuals: in the Netherlands, IMD decreased by 93% in non-vaccinated groups (Dretler *et al.*, 2018). In the UK, herd immunity caused IMD rates to remain low in vaccinated groups even after direct protection had waned (Trotter & Maiden, 2014).

It has been estimated that ~50% of the protection conferred by meningococcus conjugate vaccines is due to herd immunity (Dretler *et al.*, 2018). Other conjugate vaccines against URT pathogens (e.g. *Haemophilus influenzae* and *Streptococcus pneumoniae*) also exhibit significant herd immunity (Trotter & Maiden, 2014). This is in contrast to polysaccharide vaccines which confer little, if any, herd immunity (Dellicour & Greenwood, 2007).

1.6.2.4 Protein-based vaccines

One shortcoming of meningococcal polysaccharide and conjugate vaccines has been that a serogroup B vaccine was never developed. This is due to structural similarities between the serogroup B capsular components and human foetal neural tissue (McCoy

et al., 1985; Stephens *et al.*, 2007). This is significant because serogroup B is the most important cause of IMD in North America, South America, Australia, North Africa and Europe (section 1.2.1.1) (Acevedo *et al.*, 2019).

Protein-based vaccines have been developed that use alternate antigens that are not part of the meningococcal capsule (Trotter & Maiden, 2014), such as LPS, outer membrane vesicles (OMVs), outer membrane porins and other surface proteins (Nadel & Ninis, 2018). OMVs initiate complement activation, they are naturally released by *N. meningitidis* as a mechanism to evade the bactericidal activity of complement by initiating complement activation elsewhere (Nadel & Ninis, 2018). These antigens are not specific to each serogroup and are primarily used in vaccines to protect against serogroup B disease in the absence of a suitable polysaccharide vaccines (Trotter & Maiden, 2014). However, due to the diversity of *N. meningitidis* strains, the antigens are strain-specific, and so the vaccines do not confer protection for all serogroup B strains (Dretler *et al.*, 2018). Vaccines based on OMVs that contain porin A (PorA), have been developed and successfully used during outbreaks in Norway, Chile, Cuba, Brazil and New Zealand (Trotter & Maiden, 2014). However, these vaccines were not suitable for routine immunisation due to their narrow strain-specificity (Dretler *et al.*, 2018).

Reverse vaccinology has been used to identify other antigens and develop the MenB-4C and MenB-FHp vaccines. MenB-FHp contains two variants of complement factor H binding protein (fHbp) as antigens (McCarthy *et al.*, 2018). MenB-4C contains four antigenic components: outer membrane vesicles from strain NZ98/254 (containing PorA), fHbp, *Neisseria* adhesin A (NadA) and Neisserial Heparin Binding Antigen (NHBA) (McCarthy *et al.*, 2018). MenB-4C has been shown to have an effectiveness of 82.9% against all serogroup B strains indicating its suitability for routine immunisation programs (Dretler *et al.*, 2018; Acevedo *et al.*, 2019). Immunisation of infants with the MenB-4C vaccine in the UK has caused a significant reduction in serogroup B IMD in the target group (Acevedo *et al.*, 2019). There is no evidence for herd immunity caused by these protein-based vaccines (Acevedo *et al.*, 2019) or OMV vaccines (Trotter & Maiden, 2014). The MenB-4C vaccine does cause a significant reduction in carriage of 26.6% (Read *et al.*, 2014), but this is much less than what is caused by the conjugate vaccines (section 1.6.2.3).

1.6.2.5 Future developments

There are ongoing concerns that vaccinations against specific strains and serogroups may drive serogroup replacement and antigenic changes that reduce the efficacy of current vaccines (Harrison *et al.*, 2009). Additionally, the costs of developing new vaccines are increasing (Dretler *et al.*, 2018). Cost has been a limiting factor particularly in the meningitidis belt where the predicted benefit of a vaccination program must be balanced with the money available (Yaesoubi *et al.*, 2018; Dretler *et al.*, 2018). Therefore a focus of future vaccine development is to reduce costs of vaccinations, along with developing vaccines that protect against the emerging serogroups C, Y, W and X as well as serogroup A in Africa (Dretler *et al.*, 2018).

1.7 Microbiome-based approach to preventing IMD

Due to the lack of vaccines that provide long-term protection of vulnerable groups against a broad range of invasive serogroups and strains, a microbiome-based approach for preventing IMD has been explored.

Inoculation of the nasopharynx with the commensal *Neisseria lactamica* has been found to reduce meningococcal carriage (Deasy *et al.*, 2015). Results showed a greater reduction in carriage than conjugate vaccines over the first several months. This may be useful for reducing IMD risk in targeted groups, such as university students, pilgrims or military recruits (Dellicour & Greenwood, 2007). A microbiome approach may indeed have several advantages over vaccines when used to target at-risk groups, such as being faster acting, and affecting a broader range of serogroups/strains (Deasy *et al.*, 2015). The reduction in carriage was found to be due to competition for the same ecological niche (Deasy *et al.*, 2015). This demonstrates the importance that the microbiome has on *N. meningitidis* carriage.

Other specific interactions between the URT microbiome and *N. meningitidis* via metabolites, such as propionic acid, have been discovered (section 1.4.1). In particular, propionic acid production by the microbiome has been proposed as a mechanism for the observed increased carriage in adolescents/young adults as compared to children (Moir, 2015).

This reduction in carriage is important because meningococcal carriage and disease are inextricably linked. Carriage must precede IMD (section 1.3.1), and there is evidence that the rate of carriage is linked to the rate of IMD in a population. Risk factors for carriage are very similar to risk factors for disease (section 1.5.2.3) which implies a shared mechanism. Also, it is known that adolescents/young adults have a higher carriage rate, something that leads to increased IMD incidence in both adolescents and infants (since adolescents act as a reservoir from which infants can be infected) (Gabutti *et al.*, 2015, Moir, 2015, section 1.3.3.5). A causal relationship between carriage and disease can be seen in that herd immunity, induced by conjugate vaccines, reduces incidence of IMD (Gabutti *et al.*, 2015). Mass vaccination with conjugate vaccines have had the effect of reducing IMD in both vaccinated and unvaccinated individuals (section 1.6.2.3). This has not been observed in polysaccharide or protein-based vaccines, which have a much smaller effect on carriage rates (sections 1.6.2.3 and 1.6.2.4).

The importance of the microbiome in IMD is in line with what is known about other similar pathogens (section 1.4.3). *N. meningitidis* is part of a class of organisms known as "pathobionts", named for their behaviour as both commensals and pathogens. Microbiome-derived treatments (such as pre- or pro-biotics) have been proposed as a good method to promote commensal behaviour and so prevent pathobiont disease (Brugger *et al.*, 2016).

Microbiome treatments may also have a role in reducing the prophylactic use of antibiotics to prevent IMD by offering an alternative to this practice. This would aid in slowing the emergence of AMR (section 1.6.1).

1.8 Approach, hypothesis and aims

Propionic acid, produced by the URT microbiome (section 1.4.4), has a potential role in IMD since it can be used by *N. meningitidis* as a carbon source (section 1.3.3.5). Nutrition limitation (or "nutritional immunity") in the URT means that any extra carbon sources are particularly important. This is shown by the 10-times increase in meningococcal colonisation efficiency due to lactic-acid producing bacteria (Schoen *et al.*, 2014, section 1.3.3.4), and by the effect of mucin degraders on pathogen growth in the lower respiratory tract airways (section 1.4.3).

Catenazzi *et al.*, 2014 reports that the *N. meningitidis* genome contains a gene cluster with methylcitrate cycle genes, the same metabolic pathway used by other pathogens to utilise propionic acid. *N. meningitidis* was confirmed to use propionic acid as a carbon source *in vitro*. These genes were also shown to be present in the closely-related pathogen *N. gonorrhoeae* but not the closely-related commensal *N. lactamica* indicating that this is a pathogenicity factor.

This project aims to study the role that propionic acid production by the host microbiome plays in *N. meningitidis* carriage, and therefore how the host microbiome may be used/modified to prevent IMD.

1.8.1 *P. gingivalis* as a model propionic acid-producer

Several propionic acid-producers of the URT have been identified (section 1.4.4). However, the genus *Porphyromonas* has been singled out as a propionic acid-producing member of the URT microbiome that consistently co-occurs with *N. meningitidis* in 16S rDNA sequencing datasets (Catenazzi *et al.*, 2014). *P. gingivalis* is a member of the URT microbiome that produces propionic acid and is known as a "keystone pathogen" due to its role in facilitating the pathogenicity of other bacteria (section 1.4.4). Therefore, it was chosen to be used as a model propionic acid-producer. Interactions with *N. meningitidis* will be studied using a *in vitro* assay that is able to isolate the interactions mediated by propionic acid.

1.8.2 Experimental methods for studying microbial metabolic interactions

There are a variety of methods that have been used to study metabolic interactions in microbial communities.

Methods based on well-defined mixed cultures have been used. For example, pairwise mixed cultures of a 6-member model of the mouse gut microbiome have been used to understand the emergent metabolic behaviour of the system (Medlock *et al.*, 2018). Two-member co-cultures were compared to mono-cultures, optical density and qPCR measurements were used to calculate population sizes of the microbes, and nuclear magnetic resonance was used to measure production and consumption of metabolites.

A combination of population density time-series measurements and metabolomic data were used to construct a simple mathematical model of the system. This was used to test the feasibility of predicted metabolic relationships.

Using mixed cultures to study metabolic interactions between aerobes and anaerobes involves additional technical challenges, however some methods have been developed and used. For example, in order to study the gut microbiome, co-cultures of aerobic epithelial tissue with anaerobic bacteria have been set up. These are reviewed in Martels *et al.*, 2017 and include a 6-well plate modified with inserts that divide each well in two with semi-permeable membranes, anaerobic nutrient agar overlaid with a layer of epithelial cells, and a variety of microfluidic solutions. Interactions between aerobic and anaerobic bacteria of the oral microbiome have been studied by submerging a biofilm in continuous aerobic culture (Bradshaw *et al.*, 1996). The aerobes depleted the oxygen thus maintaining anaerobic conditions in the biofilm.

Methods based on spent culture media have also been used. These work by supplementing one culture with the media from the "spent" media from another culture, and allows either of the cultures to be aerobic or anaerobic since the media can be modified before-hand accordingly. The interactions captured by this method are directional from the donor culture to the recipient culture. This method has been used in conjunction with microbiome population data to characterise interactions in poly-microbial urinary tract infections (Vos *et al.*, 2017).

Non-contact co-cultures in various forms have been used to prevent contact-dependent interactions in co-cultures and so isolate the effects that are mediated instead by metabolites and other diffusible compounds. Techniques used include dialysis tubing containing one culture submerged by another culture in a flask (Shi *et al.*, 2017), use of modified glassware to join two flasks together with a flat face sandwiching a semi-permeable membrane (Paul *et al.*, 2013), and a similar construction of an array of smaller co-cultures that fit in a standard 96-well plate reader (Moutinho *et al.*, 2017).

The study of microbial communities, particularly community assembly, has been identified as a area where a combined mathematical and experimental biology approach is be beneficial (Zaccaria *et al.*, 2017). Indeed, many of the above example studies used some form of mathematical modelling to interpret the experiments.

1.8.3 Chosen method

For this study, the chosen *in vitro* assay should:

1. study the metabolic interaction between two cultures
2. capture two-way interactions
3. produce data useful for quantification of the interaction

Therefore, I have chosen to use a non-contact co-culture of two well-mixed liquid cultures as the experimental platform of this study.

A co-culture based method was chosen in order to capture a more complete view of the metabolic interactions, compared to what mono-cultures would provide. Spent-media experiments were a possible alternative, however these may not be able to capture two-way interactions between the cultures (e.g. utilisation of propionic acid leading to an increase *N. meningitidis* growth due to increased nutrient availability, along with an increase in *P. gingivalis* growth due to reduced product inhibition).

Due to the potentially incompatible growth requirements of the two microbes (e.g. oxygen requirement), a non-contact co-culture was chosen where the conditions in each culture chamber could be controlled separately. A biofilm-based method where a *P. gingivalis* biofilm is submerged in a *N. meningitidis* liquid culture was an alternate option (Bradshaw *et al.*, 1996), however a non-contact co-culture has the advantages of also preventing contact-dependent interactions, and enabling high resolution non-destructive measurements of both cultures.

Well-mixed liquid cultures were also chosen as they are more amenable to mathematical modelling using well-established ordinary differential equation (ODE) based models of microbial growth. These models can be kept simple for greater clarity of analysis, and can be based on previously validated modelling techniques. A close, parallel development of both the mathematical model and the experimental system will ensure that the model is valid with a suitable methodology and accurate parameter values. Modelling of the system will be used for development and implementation of the assay, and for deciding the experimental conditions required for quantifying the metabolic interaction. Modelling may also increase the general utility of the assay since it could be used to adapt the experimental conditions for the study of organisms with different growth rates, nutritional requirements and metabolic interactions. Modulation of

pathogenicity by propionic acid is not unique to *N. meningitidis* and so this method may be of use in studying other interactions between other microbes.

1.8.4 Hypothesis

The system being studied operates on the following hypothesis: propionic acid produced by *P. gingivalis* is used as a carbon source by *N. meningitidis* (Fig1.7a) in the human URT, and this affects carriage rate (population size) of *N. meningitidis*.

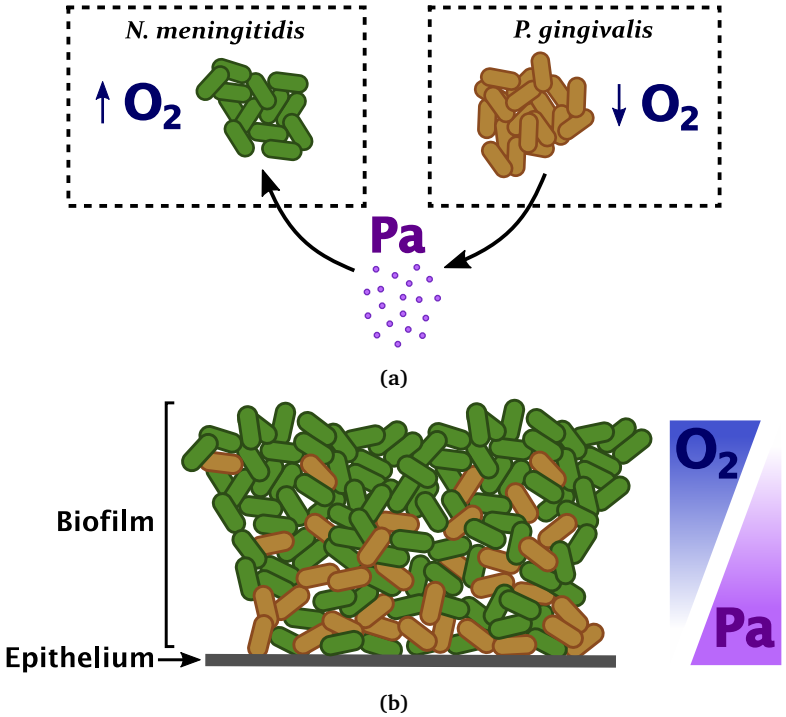

Figure 1.7: Hypothesis of metabolic interaction between *N. meningitidis* and *P. gingivalis*.
(a) *P. gingivalis* grows in an anaerobic habitat and produces propionic acid (Pa) which can be used as a carbon source by *N. meningitidis* growing in an aerobic habitat.
(b) These neighbouring aerobic and anaerobic habitats may exist in a mixed biofilm, *P. gingivalis* would preferentially grow deep in the biofilm where aerobic metabolism produces anaerobic conditions, this anaerobic metabolism would provide a source of propionic acid (Pa) that is used by *N. meningitidis* growing in the more aerobic areas of the biofilm.

P. gingivalis is known to reside preferentially in the oral cavity, rather than the nasopharynx where *N. meningitidis* is known to commonly reside. Interactions between the two species in the URT could be due to colonisation of the nasopharynx by *P. gingivalis* so that it mixes with *N. meningitidis* within the same biofilm structure (Fig1.7b).

Alternatively, interactions could be by transfer of material (saliva and mucus) between the oral cavity and the nasopharynx.

1.8.5 Aims

This project aims to develop an *in vitro* assay to study this interaction for the purpose of:

1. Measuring production/utilisation rates of propionic acid in the system, and measuring the effect this has on meningococcal population size
2. Determining the conditions under which the metabolic interaction is relevant, and assessing how important it is *in vivo*
3. Establishing a method that can be used to compare the relationship with different strains/species and in different growth conditions

This will contribute to our understanding of the role that the human microbiome plays in IMD, it will assist in forming health advice for preventing IMD, and it may aid in the development of therapies (such as pre- or pro-biotics) to reduce IMD incidence.

Chapter 2

Mathematical modelling of non-contact co-culture assay

2.1 Introduction

A non-contact co-culture *in vitro* assay with well-mixed liquid cultures has been chosen to study metabolic interactions between *N. meningitidis* and *P. gingivalis* (section 1.8.3).

The assay will first be modelled mathematically in order to:

1. Determine feasibility of a co-culture between the aerobe *N. meningitidis* and the anaerobe *P. gingivalis*, showing what experimental conditions are required for a co-culture to be established and maintained.
2. Aid design and development of the non-contact co-culture assay by defining limits on the physical dimensions of the experimental apparatus.
3. Aid experiment design by determining good experimental conditions for conducting useful experiments. A useful experiment is one in which the phenomenon being studied (microbial metabolic interaction) causes a change in the variable being measured (time series of microbial population density). Modelling will be used to assess under what conditions an experiment is useful. This will inform experimental parameters such as starting population densities of cultures, resource concentrations in the growth media, and lengths of experiments.
4. Interpret results from these experiments, e.g. by providing models that will be

fitted using experimental data, or by highlighting features to be measured from which important values can be measured. This will be used to validate the model and measure important parameters.

2.2 Literature summary of microbial metabolic interaction mathematical modelling

Mathematical modelling is a standard technique studying and understanding microbial interactions. The models commonly used can be broadly categorised into genome-scale metabolic models and dynamic models, although there is some crossover between these categories.

2.2.1 Whole-genome models

In whole-genome models, metabolic networks are constructed based on the predicted expression of enzymes (as predicted by genome annotation). This can be used to measure "resource overlap" and so predict cooperative or competitive interactions between microbes (Freilich *et al.*, 2011). Whole-genome models can also be used for flux balance analysis (FBA) where the fluxes of various metabolic pathways are predicted at steady state.

To extend these to study metabolic interactions between microbes, dynamic FBAs (dFBA) involving multiple FBA models have been used. The metabolic activity of each FBA model is repeatedly applied to the environment in time-steps, therefore allowing exchange of metabolites between multiple FBA models (Hanly & Henson, 2013). dFBA has been applied to study the development of cross-feeding in the gut microbiome and its production of short chain fatty acids (SCFAs), such as propionic acid (Hoek & Merks, 2017). To achieve this, the metabolic networks were simplified and, for practical reasons, only the pathways important to this aspect of the gut microbiome were modelled.

2.2.2 Dynamic models

Dynamic models describe the dynamics of microbial populations and chemicals through continuous time.

One common method is the use of generalised Lotka-Volterra equations. These have been applied to study microbiomes, for example, co-occurrence, calculated from longitudinal population abundance data (16S), was used to parametrise Lotka-Volterra equations for each pair of bacteria in the microbiome (Stein *et al.*, 2013). However, since chemicals are not explicit these models (Vos *et al.*, 2017), they fail to capture many important phenomena (Momeni *et al.*, 2017).

In one study, dynamical models in which chemicals are represented by variables, were used to study the response of the gut microbiome to environmental changes, such as change in pH (Kettle *et al.*, 2015). The gut microbiome was modelled as 10 functional groups that each represented a group of species with similar metabolic function. Dynamic models have also been used in more theoretical way to study the effect of distance and diffusion geometry on metabolic interactions between two pure cultures (Peaudecerf *et al.*, 2018). The simplicity of this model enabled analysis that is applicable to microbial metabolic interactions in general.

2.3 Modelling approach

The data from the non-contact co-culture assay will be in the form of a high resolution time series of microbe population densities (calculated from optical density measurements). Systems of ordinary differential equations (ODEs) can model smooth and continuous change in variables through time, and their use in modelling bacterial growth is well established (Wade *et al.*, 2016). ODEs are typically used by modelling bacterial populations with a single variable, which is a suitable representation of the mixed liquid culture. This method can be used to model the co-culture system since spatial heterogeneity is not expected to be an important factor.

Use of a model that builds upon existing ODE models of bacterial growth will be beneficial because of the wealth of variations and extensions that can be drawn upon if needed (such as diauxic growth, growth inhibition, or thermodynamic considerations).

This is particularly useful if this method is to be applied to metabolic interactions beyond *N. meningitidis* and *P. gingivalis* via propionic acid.

An ODE-based model that includes only the factors that are pertinent to the system being studied can yield clearer and more useful predictions than a modelling strategy that seeks greater accuracy by including all potentially relevant mechanistic aspects of the system. That being said, it is important that the model is grounded in mechanistic knowledge of the system so that predictions can be made with confidence. Therefore, a system of ODEs with a minimum set of resources that can be expanded as needed is a good strategy for modelling this system.

Therefore, for these reasons, and those discussed in section 2.2.2, I have chosen to model the non-contact co-culture assay as a dynamical system using a system of ordinary differential equations (ODEs). In this model, bacterial populations and resources (growth substrates and metabolites) will be modelled explicitly as variables.

2.4 Methods

Numerical solutions to ODE systems were calculated using the "scipy.integrate.odeint" function from the Python library SciPy. It used the Runge-Kutta method to do this (Press *et al.*, 1992). Successful numerical solutions were often dependent on providing the Jacobian matrix of the ODE system being solved, which was generated using the symbolic solver library SymPy for Python. Analytical solutions were constructed by hand, on occasion this was also done with the aid of SymPy. All plots were made using the Python library matplotlib.

2.5 Model description

2.5.1 Terminology

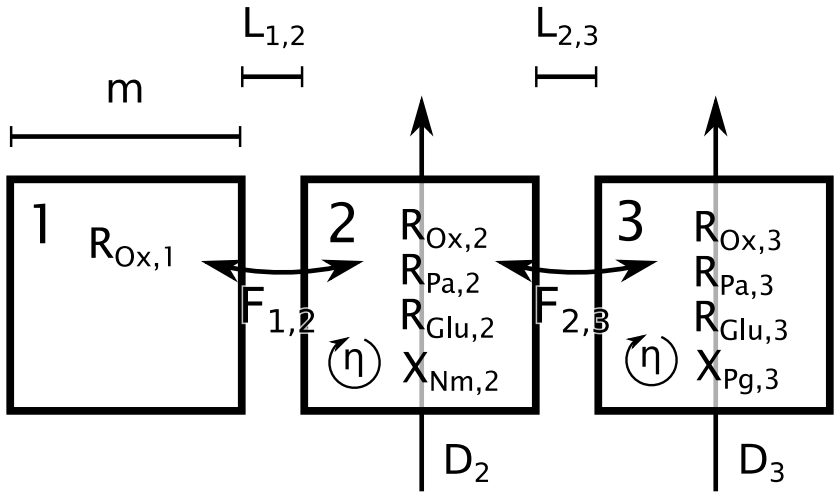

Figure 2.1: Diagram of the model terminology

Figure 2.1 shows the chamber dimensions (m), membrane thicknesses (L), locations (1, 2, 3) of bacterial cultures (X_{Nm}, X_{Pg}) and growth resources (R_{Ox}, R_{Pa}, R_{Glu}), diffusion fluxes (F), mixing factors (η) and dilutions (D) associated with the three chambers of the non-contact co-culture device being modelled.

The *N. meningitidis* culture has biomass density X_{Nm}, for *P. gingivalis* this is X_{Pg}. Glucose has concentration R_{Glu}, oxygen has concentration R_{Ox} and for propionic acid this is R_{Pa}.

There are three chambers. Chamber 1 contains oxygen with concentration $R_{Ox,1}$. Chamber 2 contains a *N. meningitidis* culture with biomass density $X_{Nm,2}$ and oxygen, propionic acid and glucose with concentrations $R_{Ox,2}$, $R_{Pa,2}$ and $R_{Glu,2}$. Chamber C contains a *P. gingivalis* culture, oxygen, propionic acid and glucose ($X_{Pg,3}$, $R_{Ox,3}$, $R_{Pa,3}$ and $R_{Glu,3}$ respectively).

The chambers neighbour each other as shown in figure 2.1. They have characteristic length m ($m = volume/surface\ area$) and are separated from each other by membranes of thickness L (e.g. $L_{2,3}$ is the thickness of the membrane between chambers 2 and 3). In the case of continuous culture, the chambers may be diluted at a rate D (e.g.

D_2 is the dilution rate of chamber 2). In this model all chambers have the same dimensions and so have the same m. This constraint was chosen to simplify the question of the optimum scale for the apparatus. Although a vast array of different chamber shapes and methods of diffusion can be imagined, analysing this simpler shape will help reveal some generally applicable limitations.

Flux of oxygen and propionic acid by diffusion between chambers is represented by F (e.g. $F_{Ox,1,2}$ is the flux of oxygen between chambers 1 and 2). Glucose cannot diffuse between the chambers across the membrane. Flux is a product of permeability P and concentration gradient (e.g. $R_{Ox,1} - R_{Ox,2}$ is the concentration gradient of oxygen between chambers 1 and 2). Permeability P is a function of saturation constants S (e.g. $S_{Ox,aq}$ is the saturation constant of oxygen in water), diffusion coefficients C (e.g. $C_{Pa,pdms}$ is the diffusion coefficient of propionic acid in polydimethylsiloxane, i.e. PDMS, which is the material that the membranes are made of) and chamber mixing factor η. All chambers are mixed to the same degree and so have the same η.

Diffusion is affected by a partition coefficient S^P (e.g. S^P_{Pa}) which describes the preference a solute has to dissolve in one solvent over another (e.g. S^P_{Pa} is the ratio of propionic acid saturation constant in water and PDMS). Propionic acid diffusion is also affected by the dissociation coefficient J_{Pa} which determines how pH affects the proportion of propionic acid molecules in the undissociated volatile form.

In this model, bacterial populations utilise resources for growth. For *N. meningitidis* in chamber 2, $X_{Nm,2}$ grows at a growth rate $\mu_{Nm,2}$ which is a function of the maximum growth rate μ^{max}_{Nm} and Michaelis-Menten equation terms M, which are functions of resource concentration R and half-rate constants K. So, for the example of *N. meningitidis* growth due to oxygen in chamber 2, $M_{Nm,Ox,2}$ is a function of $R_{Ox,2}$ and $K_{Nm,Ox}$.

Yield constants, Y, describe resource quantities that bacterial populations utilise to produce biomass, and they describe quantities of resources that they produce proportional to their growth. For example, *N. meningitidis* converts glucose to biomass at a yield of $Y_{Nm,Ox}$, and *P. gingivalis* produces propionic acid when using glucose as a growth substrate with a yield of $Y_{Pg,Glu,Pa}$.

A summary of variables and properties used in this model is given in 2.1, a summary of the parameters is given in table 2.2.

2.5.2 Logistic growth

P. gingivalis in batch culture is modelled with a logistic growth model (Verhulst, 1838):

$$\frac{dX_{Pg,3}}{dt} = \mu_{Pg}^{max} \cdot X_{Pg,3} \cdot \frac{H_{Pg} - X_{Pg,3}}{H_{Pg}} \tag{2.1}$$

where μ_{Pg}^{max} is the intrinsic growth rate and H_{Pg} is the carrying capacity.

Solving 2.1 for time, $X_{Pg,3}^{t}$ ($X_{Pg,3}$ at time t) is

$$X_{Pg,3}^{t} = H_{Pg} \cdot \frac{e^{\mu_{Pg}^{max} \cdot t}}{\frac{H_{Pg}}{X_{Pg,3}^{0}} - 1 + e^{\mu_{Pg}^{max} \cdot t}} \tag{2.2}$$

where $X_{Pg,3}^{0}$ is the starting biomass density of the *P. gingivalis* culture in chamber 3 (i.e. $X_{Pg,3}^{t}$ when $t = 0$). Time for $X_{Pg,3}$ to reach $X_{Pg,3}^{t}$ (i.e. t^*) is described by:

$$t^* = \frac{1}{\mu_{Pg}^{max}} \cdot \left(ln\left(\frac{H_{Pg}}{X_{Pg,3}^{0}} - 1 \right) - ln\left(\frac{H_{Pg}}{X_{Pg,3}^{t}} - 1 \right) \right). \tag{2.3}$$

2.5.3 Monod equation

2.5.3.1 Single resource

With the Monod equation (Monod, 1949), growth of bacterial population of biomass X (e.g. $X_{Nm,2}$) is described as

$$\frac{dX}{dt} = \mu \cdot X \tag{2.4}$$

where μ (e.g. $\mu_{Nm,2}$), the growth rate, is dependent on the resource concentration R (e.g. $R_{Ox,2}$) such that

$$\mu = \mu_{max} \cdot \frac{R}{R + K} \tag{2.5}$$

where μ_{max} is the maximum growth rate of X (e.g. μ_{Nm}^{max}) and K is the half rate constant (e.g. $K_{Nm,Ox}$).

This model has the behaviour of X growing exponentially at maximum growth rate when R is in abundance. And as R decreases to approach K, then $\frac{R}{R+K}$ decreases. When $R = K$ then $\mu = \frac{1}{2} \cdot \mu_{max}$ and when $R = 0$ then $\mu = 0$.

2.5.3.2 Resource consumption

Resources R are consumed as they are converted into biomass X with a constant yield Y, such that

$$\frac{dR}{dt} = \frac{1}{Y} \cdot \mu \cdot X. \tag{2.6}$$

For instance, consumption of glucose by *P. gingivalis* for growth in chamber 3 is described by

$$\frac{dR_{Glu,3}}{dt} = \frac{1}{Y_{Pg,Glu}} \cdot \mu_{Pg,3} \cdot X_{Pg,3}.$$

2.5.3.3 Oxygen and single carbon source

When growth of $X_{Nm,2}$ is dependent on more than one resource, in this instance $R_{Ox,2}$ and $R_{Glu,2}$, then $\mu_{Nm,2}$ is described as

$$\mu_{Nm,2} = \mu_{Nm}^{max} \cdot \frac{R_{Ox,2}}{R_{Ox,2} + K_{Nm,Ox}} \cdot \frac{R_{Pa,2}}{R_{Pa,2} + K_{Nm,Pa}} \tag{2.7}$$

and so both oxygen and propionic acid must be present for growth, and growth rate is primarily determined by the resource that is most limiting.

2.5.3.4 Diauxic growth on different carbon sources

N. meningitidis can use both glucose and propionic acid as a carbon source, but preferentially uses glucose first. This observation is based on observations that propionic acid

consumption began when glucose was depleted (Catenazzi *et al.*, 2014). This diauxic growth is modelled with a modified Monod equation (Lee *et al.*, 1974) where growth is split into partial growths corresponding to each resource.

$$\begin{aligned}
\mu_{Nm,2,Pa} &= \mu^{max}_{Nm,Pa} \cdot \frac{R_{Pa,2}}{R_{Pa,2} + K_{Nm,Pa}} \cdot \frac{K^R_{Nm,Glu}}{K^R_{Nm,Glu} + R_{Glu,2}} \cdot \frac{R_{Ox,2}}{R_{Ox,2} + K_{Nm,Ox}}, \\
\mu_{Nm,2,Glu} &= \mu^{max}_{Nm,Glu} \cdot \frac{R_{Glu,2}}{R_{Glu,2} + K_{Nm,Glu}} \cdot \frac{R_{Ox,2}}{R_{Ox,2} + K_{Nm,Ox}}, \\
\mu_{Nm,2} &= \mu_{Nm,2,Pa} + \mu_{Nm,2,Glu}.
\end{aligned} \tag{2.8}$$

where K^R is a repression half-rate parameter. $K^R_{Nm,Glu}/(K^R_{Nm,Glu} + R_{Glu,2})$ is small when glucose concentration is high, therefore this term has the effect of repressing growth due to propionic acid ($\mu_{Nm,2,Pa}$) when glucose is present.

Consumption of propionic acid ($R_{Pa,2}$) and glucose ($R_{Glu,2}$) is

$$\begin{aligned}
\frac{dR_{Pa,2}}{dt} &= \frac{1}{Y_{Nm,Pa}} \cdot \mu_{Nm,2,Pa} \cdot X_{Nm,2}, \\
\frac{dR_{Glu,2}}{dt} &= \frac{1}{Y_{Nm,Glu}} \cdot \mu_{Nm,2,Glu} \cdot X_{Nm,2}.
\end{aligned} \tag{2.9}$$

and so propionic acid is only utilised by *N. meningitidis* when glucose is depleted.

2.5.4 Diffusion of resources across a membrane

2.5.4.1 Oxygen diffusion

Polydimethylsiloxane (PDMS) was chosen as the material for the membranes because it is compatible with microbial cultures, permeable to gasses and volatile substances (including propionic acid), impermeable to other dissolved substances (e.g. glucose),

resists damage during sterilisation by autoclaving, ethanol or strongly acidic/alkaline solutions, and it is convenient to acquire and use in a biology lab (section 3.2.2.4.1).

Diffusion of oxygen from atmosphere across a PDMS membrane into the aqueous chamber contents was modelled using a method that does not assume perfect mixing (Lee *et al.*, 2006). Although perfect mixing is an important assumption of the model, particularly for microbial growth and resource consumption, diffusion of resources proceeds on a much faster time-scale and so imperfect mixing in apparatus used to implement the system *in vitro* will have a more significant effect on diffusion. Therefore this must be factored into the model.

In this imperfect-mixing diffusion model, the oxygen transfer coefficient is made up of two components, one for diffusion across the membrane (with permeability P^{mem}), and the other for diffusion through the chamber contents (with permeability P^{mix}). In this model, flux is determined by the partition coefficient S^P_{Ox} (the ratio of the solubility in the aqueous culture media and the PDMS membrane) and the diffusion coefficient of the solute in the membrane. Flux of oxygen between chambers 1 and 2 ($F_{Ox,1,2}$) is described by

$$F_{Ox,1,2} = P_{Ox,1,2} \cdot \Delta R_{Ox,1,2} \tag{2.10}$$

where $\Delta R_{Ox,1,2} = R_{Ox,1} - R_{Ox,2}$ (i.e. the oxygen gradient between chambers 1 and 2), and where $P_{Ox,1,2}$ is the harmonic mean of the permeability through the membrane ($P^{mem}_{Ox,1,2}$) and through the chamber ($P^{mix}_{Ox,1,2}$):

$$P_{Ox,1,2} = \frac{1}{\frac{1}{P^{mem}_{Ox,1,2}} + \frac{1}{P^{mix}_{Ox,1,2}}}. \tag{2.11}$$

Equation 2.11 shows that P is limited by the smaller of the two terms P^{mem} and P^{mix}, and that when $P^{mem} = P^{mix}$ then $P = \frac{1}{2} \cdot P^{mem} = \frac{1}{2} \cdot P^{mix}$.

These permeabilities are a function of diffusion coefficients (C), saturation concentrations (S), chamber dimensions (m), membrane thickness (L) and chamber mixing (η). For example, diffusion of oxygen between chambers 1 and 2 depends on the diffusion coefficient of oxygen in water ($C_{Ox,aq}$) and in PDMS ($C_{Ox,pdms}$), the saturation

concentrations of oxygen in water and PDMS ($S_{Ox,aq}$ and $S_{Ox,pdms}$ respectively), the dimensions $L_{1,2}$ & m, and the mixing factors η.

$P^{mem}_{Ox,1,2}$ is described by

$$P^{mem}_{Ox,1,2} = \frac{C_{Ox,pdms} \cdot S^P_{Ox}}{L_{1,2} \cdot m}. \tag{2.12}$$

where

$$S^P_{Ox} = \frac{S_{Ox,pdms}}{S_{Ox,aq}}$$

$P^{mix}_{Ox,1,2}$ depends on the chamber contents of chambers 1 and 2. In this model, chamber 1 is used to supply oxygen to chamber 2. When chamber 1 is filled with gas (e.g. atmosphere) then mixing is assumed to be perfect in chamber 1, and so

$$P^{mix}_{Ox,1,2} = \frac{2 \cdot \eta \cdot C_{Ox,aq}}{m^2}. \tag{2.13}$$

If chamber 1 is instead filled with an aqueous solution of oxygen then

$$P^{mix}_{Ox,1,2} = \frac{\eta \cdot C_{Ox,aq}}{m^2}. \tag{2.14}$$

Equation 2.14 is used for diffusion of oxygen and propionic acid between chambers 2 and 3.

These equations show that when P is limited by P^{mix} (i.e. $P^{mix} \ll P^{mem}$) then P is primarily a function of mixing (η and m). Whereas, when P is limited by P^{mem} (i.e. $P_{mem} \ll P^{mix}$) then P is primarily of function of membrane thickness (L and m).

The effects of m, L and η on P are shown in figure 2.2. Figure 2.2a shows that P cannot be maximised by simply decreasing membrane thickness (L) relative to chamber size. When the membrane is thin, then P is limited by P^{mix} (i.e. limited by imperfect mixing) and so decreasing the membrane thickness further does not change P significantly. Conversely, as the membrane is thickened then P becomes more limited by P^{mem} and so P decreases tending towards 0.

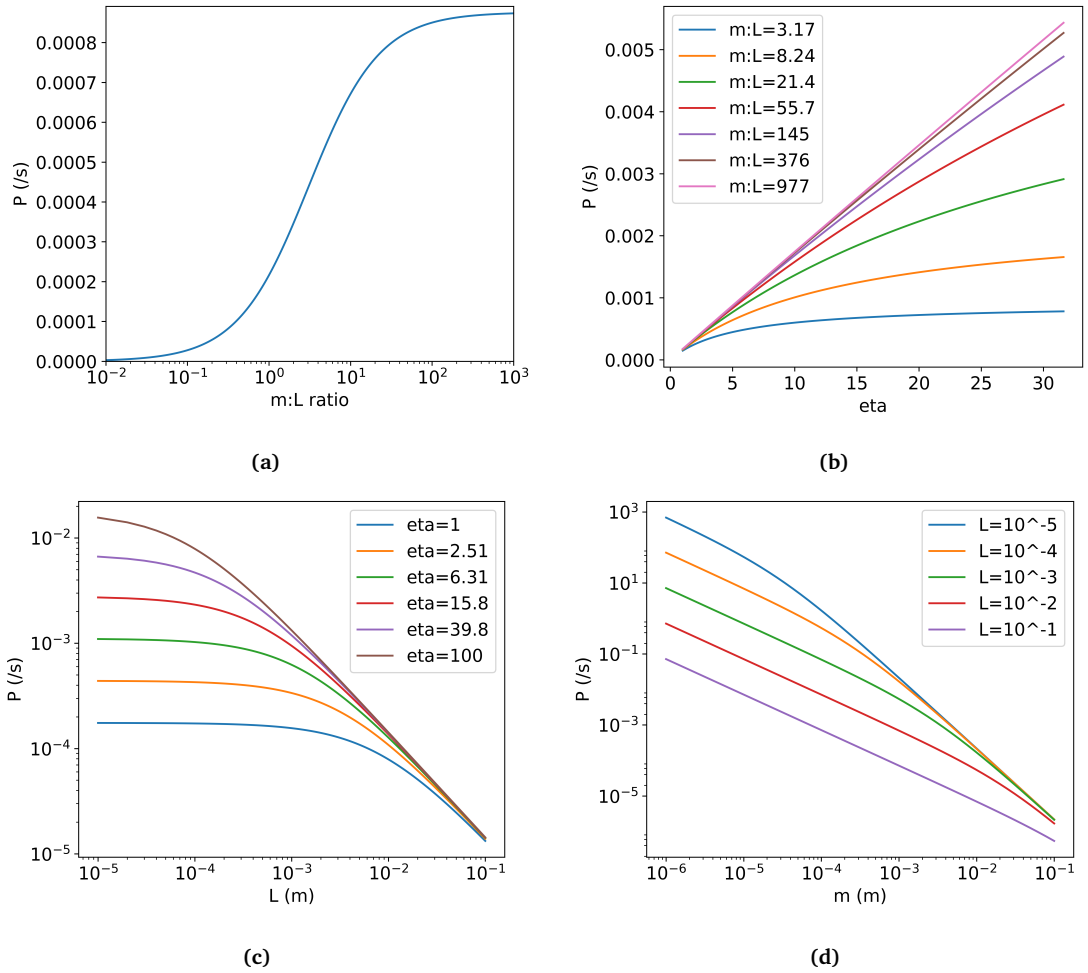

Figure 2.2: Effect of chamber dimension (m), membrane thickness (L) and mixing rate (eta) on oxygen permeability between chambers (P). a) the effect that $m : L$ ratio has on P at a fixed mixing rate (eta), the $m : L$ ratio was varied by changing L. b) the effect that mixing rate (eta) has on P at various $m : L$ ratios, the $m : L$ ratio was also varied by changing L. c) the effect that L has on P at various mixing rates. d) the effect that varying both m and L independently has on P. Graphs generated by evaluating equation 2.11 with parameter values: $\eta = 5$, $L = 1 \times 10^{-4}\,\mathrm{m}$, $m = 5 \times 10^{-3}\,\mathrm{m}$ and as shown in table 2.2, unless otherwise specified.

Figure 2.2b shows that when P is limited by P^{mix} then the relationship between P and η is linear (with gradient $(2 \cdot C_{Ox,aq})/m^2$), and when P is limited by P^{mem} then η has no significant effect on P.

When P is limited by P^{mem} then $P \propto 1/L$, and when P is limiting by P^{mix} then L has no significant effect on P. Figures 2.2c&d show this: at higher values of η or m, P is limited by P^{mem}, at lower values of η or m, P is limited by P^{mix}.

2.5.4.2 Propionic acid diffusion

Diffusion of propionic acid is different to diffusion of oxygen since propionic acid partially dissociates in solution. Therefore, a solution-diffusion model is used where the solute from one side diffuses into the membrane and then diffuses to the other side along a concentration gradient. In this model, the dissociation coefficient J_{Pa} (the ratio of dissociated to undissociated molecules at steady state) is important, along with the partition coefficient (S^P_{Ox}) and diffusion coefficients ($C_{Pa,aq}$ and $C_{Pa,pdms}$) of the solute in the membrane.

This model is appropriate because the PDMS membrane is relatively thick and non-porous. PDMS membranes above a thickness of $50\,\mu\mathrm{m}$ show a permeability proportional to thickness (Firpo *et al.*, 2015), meaning that flux can be calculated as a function of a permeability coefficient and diffusion distance.

Volatile fatty acids have been shown to diffuse through thin PDMS membranes (Netke *et al.*, 1995; Hasanoglu *et al.*, 2009), however the flux is low because PDMS is hydrophobic and so propionic acid can only diffuse in PDMS as an undissociated, uncharged molecule. The dissociation coefficient J_{Pa} describes the relationship between proportion of undissociated molecules and pH in aqueous solution, such that

$$pH = J_{Pa} + log_{10}\left(\frac{[A^-]}{[AH]}\right)$$

where $[A^-]$ is the concentration of the dissociated form and $[AH]$ is the concentration of the un-dissociated form. This is solved such that

$$J^*_{Pa,3} = \frac{1}{1+10^{pH_3 - J_{Pa}}}$$

where pH_3 is the pH of chamber 3, and $J^*_{Pa,3}$ is the fraction of propionic acid in undissociated form in chamber 3 ($[AH]/([AH]+[A^-])$). $J^*_{Pa,3} \cdot R_{Pa,3}$ gives the concentration propionic acid in undissociated form (in chamber 3).

Flux of propionic acid (e.g. $F_{Pa,2,3}$) is defined in a similar way to oxygen flux (eq 2.10) but with the concentration gradient adjusted for dissociation ($\Delta R_{Pa,3,2} = J^*_{Pa,3} \cdot R_{Pa,3} - J^*_{Pa,2} \cdot R_{Pa,2}$). Permeability is the same as equation 2.11, where P^{mix} is described by equation 2.14 and P^{mem} is described by equation 2.12, but with diffusion rate $C_{Pa,aq}$ and partition coefficient S^P_{Pa}. Therefore, to summarise:

$$F_{Pa,2,3} = P_{Pa,2,3} \cdot \Delta R_{Pa,3,2} \ ,$$

$$\Delta R_{Pa,3,2} = J^*_{Pa,3} \cdot R_{Pa,3} - J^*_{Pa,2} \cdot R_{Pa,2} \ ,$$

$$P^{mix}_{Pa,2,3} = \frac{\eta \cdot C_{Pa,aq}}{m^2}$$

and

$$P^{mem}_{Pa,2,3} = \frac{C_{Pa,pdms} \cdot S^P_{Pa}}{L_{2,3} \cdot m} \ .$$

2.6 Parameter values

Evaluations of the mathematical models are carried out in order to assess the dynamics of *N. meningitidis*, *P. gingivalis*, glucose, oxygen and propionic acid in non-contact co-culture, and to determine appropriate equipment and experiment design.

Parameter values for these evaluations have been taken from scientific literature and other resources. Not all parameter values have been published or measured, so in these cases parameter values of equivalent processes were used instead with the intention of measuring the relevant parameter values experimentally once the system is implemented *in vitro*. The parameter values and their sources are summarised in table 2.2.

2.6.1 *N. meningitidis* parameters

Yields of *N. meningitidis* from various resources have been calculated using a whole genome flux balance analysis (FBA) model (Baart *et al.*, 2007). Yield from propionic acid was not calculated, however several other relevant values were reported: $10.7\,\mathrm{g\,Cmol^{-1}}$ from glucose, $9.6\,\mathrm{g\,Cmol^{-1}}$ from lactate, $8.2\,\mathrm{g\,Cmol^{-1}}$ from glutamate, and $6.3\,\mathrm{g\,Cmol^{-1}}$ from acetate/glutamate (1:1 Cmol/Cmol) where Cmol is a mole of carbon.

This acetate/glutamate yield value was converted into an estimated yield per mol of propionic acid by multiplying by the number of carbon atoms in propionic acid (three). This was reasoned to be equivalent since both acetate and propionic acid are volatile

fatty acids of similar molecular weight, and also glutamate has similar R-group chemistry to propionic acid.

For yield of *N. meningitidis* from oxygen, the value for *Escherichia coli* was used since *E. coli* is also a fast-growing Gram negative aerobe. The yield of *E. coli* per oxygen is $0.49\ g(dw) \cdot g(O_2)^{-1}$ (Hron *et al.*, 2014).

Maximum growth rate of *N. meningitidis* has been reported as $0.9\,\mathrm{h}^{-1}$ (Schoen *et al.*, 2014).

The half-rate constant K for *E. coli* and O_2 has been reported as $121\,\mathrm{nM}$ (Stolper *et al.*, 2010), and for *E. Coli* and glucose a value of $35\,\mu\mathrm{g\,L}^{-1}$ has been reported (Füchslin *et al.*, 2012). A model of a microbial consortium utilising propionic acid (Vaveilin & Lokshina, 1996) used a half rate constant K of $100\,\mathrm{mg\,L}^{-1}$. These values were used for *N. meningitidis* under the assumption that there is no significant difference, or difference of such a magnitude as to significantly affect the model evaluations, between these values and values for *N. meningitidis*.

2.6.2 *P. gingivalis* parameters

Maximum growth rate of *P. gingivalis* in Brain-heart infusion medium (BHI) was reported as $0.15\,\mathrm{h}^{-1}$ (Milner *et al.*, 1996).

Fitting of logistic growth function (2.5.2) to results from section 4.3.3 of a time-series of optical density measurements of a *P. gingivalis* batch culture in enriched tryptic soy broth gives an intrinsic growth rate (μ_{Pg}^{max}) of $0.259\,\mathrm{h}^{-1}$ and a carrying capacity (H_{Pg}) of 1.06 (OD_{600}).

Values for yields of *P. gingivalis* from glucose and production of propionic acid from this anaerobic metabolism of glucose were not available. However, yields are reported in studies for *Propionibacterium acidipropionici*. This genus is anaerobic, produces propionic acid and is a part of the upper respiratory tract (URT) microbiome (Ramakrishnan *et al.*, 2013) and so may serve as a source of parameter values until they can be measured in *P. gingivalis*. The yield of *P. acidipropionici* growing anaerobically on glucose is reported as $0.24\ g(dw) \cdot g(glucose)^{-1}$, and the yield of propionic acid from glucose by *P. acidipropionici* has been reported as $0.389\ g \cdot g^{-1}$ (Lewis & Yang, 1992).

Similarly to *N. meningitidis* half-rate constants, the half-rate constant K for *E. Coli*

and glucose was applied to *P. gingivalis* growing on glucose: $35\,\mu g\,L^{-1}$ (Füchslin *et al.*, 2012).

2.6.3 Oxygen diffusion across a PDMS membrane

Diffusion rates and saturation constants of oxygen in water and PDMS from Lee *et al.*, 2006 were used in this model, listed in table 2.2. Also, rates for the mixing parameter η were reported. They were able to achieve $\eta = 13$ which roughly corresponded to a mixing time of $5\,s$ (time for dye to mix completely with water estimated by visual inspection). Based on this information, I estimated that a plausible value of η for the apparatus to implement this assay *in vitro* would be between $5\text{-}10$. This range is used as a starting point for this analysis.

2.6.4 Propionic acid diffusion across a PDMS membrane

The dissociation coefficient, J_{Pa}, for propionic acid is 4.88 ("Propionate | C3H5O2 - PubChem").

Partition coefficients are specific to each solute and the two solvents (in this case water and PDMS), and there are no reported values for propionic acid or other volatile fatty acids in both water and PDMS. However, the octanol/water partition coefficient ($S^{P,oct}$) is a commonly used metric of lipophobicity, and there is a log-log relationship between the octanol/water partition coefficient and the partition coefficient between water and PDMS (S^P) such that $log(S^P) = 0.83 \cdot log(S^{P,oct}) + 0.07$ (Difilippo & Eganhouse, 2010). For propionic acid, $log(S^{P,oct}_{Pa}) = 0.33$ ("Propionate | C3H5O2 - PubChem"), and so $log(S^P_{Pa}) = 0.344$, and so the partition coefficient between water and PDMS is estimated to be $S^P_{Pa} = 2.21$. In Difilippo & Eganhouse, 2010, the lowest value of $log(S^{P,oct})$ used to fit the relationship was around 1. $log(S^{P,oct}_{Pa})$ is beyond this range, and so the log-log relationship may not still apply. However, this value can still be used as an initial estimate of S^P_{Pa}.

The diffusion coefficient of propionic acid in PDMS has not been measured. However it has been measured for propanol (Duineveld *et al.*, 2002) which is a molecule of similar molecular weight, composition and octanol/water partition coefficient ($S^{P,oct}$). The diffusion coefficient of propanol in PDMS is $2.7 \times 10^{-11}\,m^2\,s^{-1}$ ("1-Propanol | C3H8O -

PubChem"), and this is used as an initial estimate for $C_{Pa,pdms}$.

The diffusion coefficient of propionic acid in water is reported as $1.06 \times 10^{-9}\,\mathrm{m}^2\,\mathrm{s}^{-1}$ (Dunn & Stokes, 1965).

2.6.5 Table of model variables and properties

Name	Units	Description
$X_{a,b}$	$g \cdot m^{-3}$	Density of a culture (a) in a culture chamber (b)
$R_{a,b}$	$mol \cdot m^{-3}$	Concentration of a growth resource (a) in a culture chamber (b)
$\Delta R_{a,b,c}$	$mol \cdot m^{-3}$	Concentration gradient of a growth resource (a) from one chamber (b) to another (c)
$L_{a,b}$	m	Thickness of membrane separating culture chambers (a and b)
m	m	Unit length of the culture chambers
$M_{a,b.c}$	-	Michaelis-Menten term describing growth rate of a culture (a) in a chamber (b) due to a resource (c)
$F_{a,b,c}$	$mol \cdot m^{-3} \cdot s^{-1}$	Flux of a growth resource (b) between chambers (b and c) due to diffusion
$P_{a,b,c}$	s^{-1}	Permeability of the membrane separating chambers (b and c) to a substance (a).
$\mu_{a,b}$	s^{-1}	Growth rate of a culture (a) in a chamber (b)
D_a	s^{-1}	Dilution rate of a chamber (a)
$y_{a,b,c}$	$g \cdot m^{-3} \cdot s^{-1}$	Partial yield (section 2.7.1.2) of the density of a culture (a) in a chamber (b) from a growth resource (c)

Table 2.1: Terminology of variables and properties of the ODE model.

2.6.6 Table of parameter values

Name	Value	Reference	Description
$Y_{Nm,Ox}$	$15.68\ g \cdot mol^{-1}$	(Hron *et al.*, 2014)	Yield of *Nm* from O_2
$Y_{Nm,Pa}$	$18.9\ g \cdot mol^{-1}$	(Baart *et al.*, 2007)	Yield of *Nm* from Pa
$Y_{Nm,Glu}$	$64.2\ g \cdot mol^{-1}$	(Baart *et al.*, 2007)	Yield of *Nm* from glucose
$K_{Nm,Ox}$	$1.21 \times 10^{-4}\ mol \cdot m^{-3}$	(Stolper *et al.*, 2010)	Half-rate constant for *Nm* and O_2
$K_{Nm,Pa}$	$1.35\ mol \cdot m^{-3}$	(Vaveilin & Lokshina, 1996)	Half-rate constant for *Nm* and Pa
$K_{Nm,Glu}$	$1.94 \times 10^{-4}\ mol \cdot m^{-3}$	(Füchslin *et al.*, 2012)	Half-rate constant for *Nm* and glucose
$\mu^{max}_{Nm,Glu}$	$2.50 \times 10^{-4}\ s^{-1}$	(Schoen *et al.*, 2014)	Maximum growth rate of *Nm* utilising glucose
$\mu^{max}_{Nm,Pa}$	$2.50 \times 10^{-4}\ s^{-1}$	(Schoen *et al.*, 2014)	Maximum growth rate of *Nm* utilising Pa
$Y_{Pg,Glu}$	$43.2\ g \cdot mol^{-1}$	(Lewis & Yang, 1992)	Yield of *Pg* from glucose
$Y_{Pg,Glu,Pa}$	$0.946\ mol \cdot mol^{-1}$	(Lewis & Yang, 1992)	Yield of Pa from glucose metabolised by *Pg*
$K_{Pg,Glu}$	$1.94 \times 10^{-4}\ mol \cdot m^{-3}$	(Füchslin *et al.*, 2012)	Half-rate constant for *Pg* and glucose
μ^{max}_{Pa}	$4.17 \times 10^{-5}\ s^{-1}$	(Milner *et al.*, 1996)	Maximum growth rate for *Pg*
$C_{Ox,pdms}$	$2.15 \times 10^{-9}\ m^2 \cdot s^{-1}$	(Lee *et al.*, 2006)	Diffusion coefficient of O_2 in PDMS
$C_{Ox,aq}$	$2.19 \times 10^{-9}\ m^2 \cdot s^{-1}$	(Lee *et al.*, 2006)	Diffusion coefficient of O_2 in water
$C_{Pa,pdms}$	$2.7 \times 10^{-11}\ m^2 \cdot s^{-1}$	(Duineveld *et al.*, 2002)	Diffusion coefficient of Pa in PDMS
$C_{Pa,aq}$	$1.06 \times 10^{-9}\ m^2 \cdot s^{-1}$	(Dunn & Stokes, 1965)	Diffusion coefficient of Pa in water
$S_{Ox,pdms}$	$0.9\ mol \cdot m^{-3}$	(Lee *et al.*, 2006)	Saturation concentration of O_2 in PDMS
$S_{Ox,aq}$	$0.27\ mol \cdot m^{-3}$	(Lee *et al.*, 2006)	Saturation concentration of O_2 in water
S^P_{Pa}	2.21	("Propionate | C3H5O2 - PubChem")	Partition coefficient of Pa between PDMS and water
J_{Pa}	4.88	("Propionate | C3H5O2 - PubChem")	Dissociation coefficient of Pa
μ^{max}_{Pg}	$0.259\ s^{-1}$	Section 4.3.3	Intrinsic growth rate of *Pg*
H_{Pg}	1.06 OD_{600}	Section 4.3.3	Carrying capacity of *Pg* batch culture
$W_{OD,g}$	$360g(dw) \cdot m^{-3} \cdot OD_{600}{}^{-1}$	(Ren *et al.*, 2013)	Conversion constant of culture density to OD

Table 2.2: Parameter values used in evaluations and analysis of the mathematical models. *Nm* refers to *N. meningitidis*, *Pg* refers to *P. gingivalis*, Pa refers to propionic acid and OD refers to optical density.

2.7 Non-contact co-culture modelling and analysis

2.7.1 Oxygen and glucose utilisation by *N. meningitidis*

2.7.1.1 ODE system

A simple model with two chambers, one *N. meningitidis* culture chamber and one oxygen supply chamber, is used to study *N. meningitidis* oxygen consumption in a culture chamber, and to predict

1. if and when anaerobic conditions will be generated
2. resource consumption and *N. meningitidis* growth under oxygen-limited conditions

The system of ODEs is as follows:

$$\begin{aligned}
\frac{dX_{Nm,2}}{dt} &= \mu_{Nm,2} \cdot X_{Nm,2}, \\
\mu_{Nm,2} &= \mu_{Nm}^{max} \cdot \frac{R_{Ox,2}}{R_{Ox,2} + K_{Nm,Ox}}, \\
\frac{dR_{Ox,2}}{dt} &= \frac{1}{Y_{Nm,Ox}} \cdot \mu_{Nm,2} \cdot X_{Nm,2} + P_{Ox,1,2} \cdot \Delta R_{Ox,1,2}.
\end{aligned} \tag{2.15}$$

2.7.1.2 Anaerobic conditions

In the non-contact co-culture assay, oxygen consumption by an aerobic culture is proposed to generate anaerobic conditions. For this to happen *N. meningitidis* growth must be oxygen-limited, i.e. the maximum possible rate of oxygen consumption must be greater than the yield of *N. meningitidis* from the oxygen diffusing into the chamber, referred to in this analysis as the "partial yield". The partial yield, $y_{Nm,2,Ox}$ is defined as:

$$y_{Nm,2,Ox} = Y_{Nm,Ox} \cdot P_{Ox,1,2} \cdot R_{Ox,1} \ .$$

It represents the maximum potential growth rate of *N. meningitidis* biomass if growth is limited solely by oxygen. Partial yields from other growth resources are used in future sections of this chapter. The partial yields assume a maximum diffusion gradient (i.e. the definition of $y_{Nm,2,Ox}$ assumes no oxygen in chamber 2) which is reasonable when that resource is limiting *N. meningitidis* growth.

The maximum rate of oxygen consumption by a culture occurs when it is growing at the maximum possible rate (μ_{Nm}^{max}). Therefore, oxygen is limiting when the maximum growth rate from oxygen ($y_{Nm,2,Ox}$) is less than this, so:

$$y_{Nm,2,Ox} < X_{Nm,2} \cdot \mu_{Nm}^{max}$$

which can be used to find the minimum culture density of *N. meningitidis* needed to generate anaerobic conditions for a given oxygen supply and permeability.

2.7.1.3 Oxygen-limited growth

When *N. meningitidis* growth is oxygen limited, then $(dX_{Nm,2}/dt) = y_{Nm,2,Ox}$. In this model, $X_{Nm,2}$ would continue to increase at a constant rate, however a bacterial culture would eventually be limited by depletion of other resources such as carbon sources (e.g. glucose). In a model where glucose utilisation is essential for *N. meningitidis* culture growth:

$$\begin{aligned}
\frac{dX_{Nm,2}}{dt} &= \mu_{Nm,2} \cdot X_{Nm,2}, \\
\mu_{Nm,2} &= \mu_{Nm}^{max} \cdot \frac{R_{Ox,2}}{R_{Ox,B} + K_{Nm,Ox}} \cdot \frac{R_{Glu,2}}{R_{Glu,2} + K_{Nm,Glu}}, \\
\frac{dR_{Ox,2}}{dt} &= P_{Ox,1,2} \cdot \Delta R_{Ox,1,2} - \frac{1}{Y_{Nm,Ox}} \cdot \mu_{Nm,2} \cdot X_{Nm,2}, \\
\frac{dR_{Glu,2}}{dt} &= -\frac{1}{Y_{Nm,Glu}} \cdot \mu_{Nm,2} \cdot X_{Nm,2}.
\end{aligned} \tag{2.16}$$

When *N. meningitidis* growth is oxygen limited ($(dX_{Nm,2}/dt) = y_{Nm,2,Ox}$) then

$$\frac{dR_{Glu,2}}{dt} = -\frac{y_{Nm,2,Ox}}{Y_{Nm,Glu}}$$

which solved for t is

$$R^t_{Glu,2} = R^0_{Glu,2} - t \cdot \left(\frac{y_{Nm,2,Ox}}{Y_{Nm,Glu}} \right)$$

where $R^0_{Glu,2}$ is the starting concentration of glucose in chamber 2 (i.e. $R_{Glu,2}$ at $t = 0$). And so the time is takes for glucose to be depleted ($R^t_{Glu,2} = 0$) is

$$t^D_{Glu} = R^0_{Glu,2} \cdot \frac{Y_{Nm,Glu}}{y_{Nm,2,Ox}} \tag{2.17}$$

where t^D_{Glu} is the time to glucose depletion.

This is important because the chamber is only anaerobic until t^D_{Glu}, after which *N. meningitidis* growth ceases and oxygen levels increase in chamber 2 due to diffusion from the oxygen supply chamber.

2.7.1.4 Practical and useful parameter set

In order to assess the relative scales of the quantities involved in these solutions, and to generate practical and useful parameters to use in further analyses. A set of parameters has been generated based on a series of design choices and desired model outputs. These choices and targets are intended to be practical for implementation *in vitro*.

When the target change of *N. meningitidis* OD_{600} to be measured is 0.2 ($144\,\mathrm{g\,m^{-3}}$) then the initial glucose must be $72g \cdot m^{-3}/Y_{Nm,Glu} = 1.12\,\mathrm{mM}$.

When the target time for glucose depletion is $4\,\mathrm{h}$ then $y_{Nm,2,Ox} = 18.0\,\mathrm{g\,m^{-3}\,h^{-1}}$, and when the oxygen supply has atmospheric conditions then oxygen permeability between chamber 1 and 2 must be $4.25\,\mathrm{h^{-1}}$

With this partial yield from oxygen ($y_{Nm,2,Ox}$), the minimum culture density of *N. meningitidis* needed to generate anaerobic conditions is $18.0gm^{-3}h^{-1}/\mu^{max}_{Nm} = 16.2\,\mathrm{g\,m^{-3}}$, or 0.045 OD_{600}.

When the oxygen permeability is $4.25\,\mathrm{h}^{-1}$, the chamber unit length (m) is $5\,\mathrm{mm}$ and the mixing factor (η) is 10, then the membrane thickness ($L_{1,2}$) must be $0.397\,\mathrm{mm}$.

Using this set of parameters as a starting point, adjustments can be made. In order to adjust the duration of the experiment (i.e. the time to glucose depletion), a lower initial concentration of glucose can be used since the time of glucose depletion is directly proportional to initial glucose concentration. Also, a lower oxygen permeability can be used since this is inversely proportional to the duration of *N. meningitidis* growth due to glucose.

In order to increase the change in *N. meningitidis* culture density, either the glucose concentration can be increased (simultaneously increasing the duration of growth), or the rate of oxygen influx can be increased. There is a practical limit to how thin a PDMS membrane or how perfect the mixing can be. Diffusion rate can also be increased by decreasing the size (ie unit length m) of the chambers.

This parameter set is defined by the limitations due to oxygen supply and consumption. It lays a foundation onto which further limitations can be added and adjustments made based on different technical limitations that define what a "practical" parameter set is.

2.7.1.5 Dynamics of oxygen consumption

Numeric solutions to the ODE model show the dynamics of the variables (Fig2.3a). This is useful for analysing model behaviours when relevant analytical solutions do not exist, or when assumptions of these solutions need to be tested.

The amount of time it takes from the start of the experiment to when anaerobic conditions are formed in the culture chamber (chamber 2) can be predicted by taking the numerical solution of the system of ODEs (equations 2.16). When oxygen-limiting conditions are defined with the Monod term for $X_{Nm,2}$ utilising $R_{Ox,2}$: $M_{Nm,Ox,2} = R_{Ox,2}/(R_{Ox,2} + K_{Nm,Ox})$, and when an arbitrary threshold of $M_{Nm,Ox,2} < 0.9$ is used to define "anaerobic" (Fig2.3a), the time at which this happens (t^D_{Ox}) can be calculated from numerical solutions.

These results show that t^D_{Ox} varies with $P_{Ox,1,2}$ (Fig2.3b), and that when $P_{Ox,1,2}$ is higher then it takes longer for $X_{Nm,2}$ growth to become oxygen-limited. The smallest possible t^D_{Ox} (when $P_{Ox,1,2} \approx 0$) is around $15\,\mathrm{min}$, this is the time it takes for the initial oxygen

(in the media at $t = 0$) to be depleted by $X_{Nm,2}$ growth.

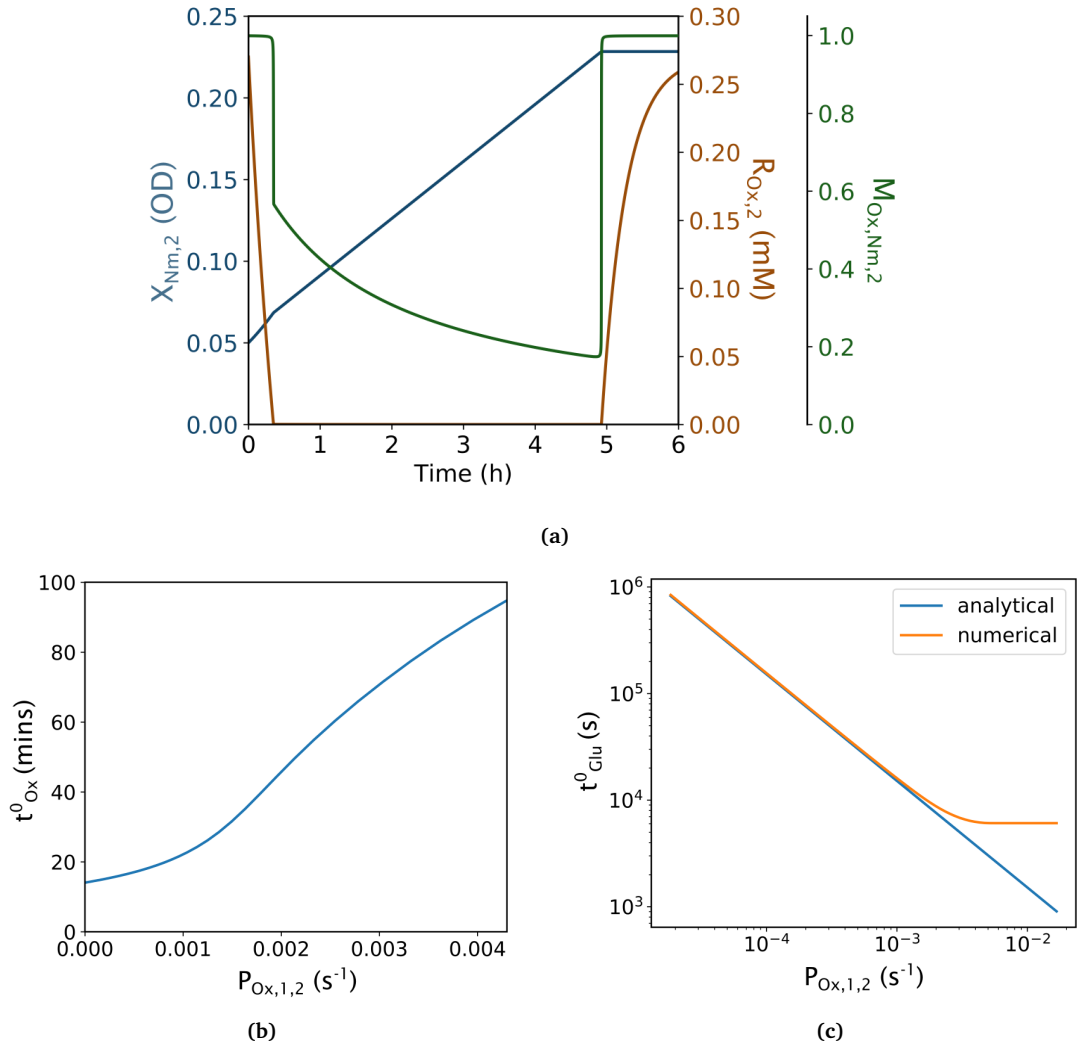

Figure 2.3: Oxygen depletion by *N. meningitidis* growth. Numerical solutions of an ODE system (section 2.7.1.3) show a) anaerobic conditions are generated quickly by *N. meningitidis* growth (anaerobic defined as $M_{Ox,Nm,2} < 0.9$), b) time by which anaerobic conditions are generated varies with $P_{Ox,1,2}$, c) time by which glucose is depleted ($t^D_{Glu,2}$) is accurately predicted by the analytical solution at lower values of $P_{Ox,1,2}$, and it varies with $P_{Ox,1,2}$. Parameter values were: $\eta = 5$, $L_{1,2} = 0.1\,\text{mm}$, $m = 5\,\text{mm}$, $R^0_{Glu} = 1\,\text{mM}$, $X^0_{Nm,2} = 0.05$ OD_{600} and as shown in table 2.2.

The time taken for generation of anaerobic conditions is important since glucose depletion must not occur before this time otherwise anaerobic conditions will never be established. This is because anaerobic conditions are required for any propionic acid production in the *P. gingivalis* chamber.

The analytical solution for t^D_{Glu} (equation 2.17) assumes oxygen-limiting conditions and

so does not take into account the time for oxygen to become depleted in the chamber. Analytical and numerical solutions have been compared to see what effect this has. The results (Fig2.3c) show that when $R^0_{Glu} = 1mM$ then this difference only becomes important for $X_{Nm,2}$ growth when $P_{Ox,1,2} > 10^{-3}s^{-1}$.

2.7.2 Propionic acid utilisation by *N. meningitidis*

2.7.2.1 *N. meningitidis* growth must be limited by both oxygen and propionic acid

In the planned non-contact co-culture assay, propionic acid utilisation by *N. meningitidis* will cause a change in *N. meningitidis* growth. The data collected from this assay will be in the form of culture density dynamics as a function of time. This will enable the study of metabolic interactions between *N. meningitidis* and *P. gingivalis* by observing how the culture density changes as a result of the co-culture.

To achieve this, *N. meningitidis* growth should be limited by propionic acid, because then, any amount of propionic acid production by *P. gingivalis* will have a measurable effect on *N. meningitidis* growth. However, oxygen must limit the growth of *N. meningitidis* so that anaerobic conditions can be maintained. This presents a dilemma, because When growth is oxygen-limited then propionic acid production by *P. gingivalis* will not have any effect on *N. meningitidis* growth.

Therefore, experimental conditions must be developed where *N. meningitidis* growth is limited by both oxygen and propionic acid. In batch cultures this can be achieved with an oxygen-limited phase followed by a propionic acid-limited phase. This is achievable when growth follows three phases:

1. Oxygen-limited growth, utilising glucose as a carbon source until it is depleted. Propionic acid diffuses into the culture chamber and accumulates in this phase.
2. Utilisation of the accumulated propionic acid, growth is still oxygen-limited.
3. Compromising of anaerobic conditions as propionic acid concentrations drop to the point at which oxygen is not longer limiting.

For all of these phases to be present, sufficient propionic acid must be allowed to accumulate, and flux of propionic acid must not be so high as to outpace consumption of

propionic acid by the oxygen-limited *N. meningitidis* culture. This scenario is modelled using an extended version of the ODE model in section 2.7.1.3.

2.7.2.2 ODE system

Diauxic growth is modelled as described in section 2.5.3.4, propionic acid diffusion is modelled as described in section 2.5.4.2.

$$
\begin{aligned}
\frac{dX_{Nm,2}}{dt} &= (\mu_{Nm,2,Glu} + \mu_{Nm,2,Pa}) \cdot X_{Nm,2}, \\
\mu_{Nm,2,Glu} &= \mu^{max}_{Nm,Glu} \cdot \frac{R_{Glu,2}}{R_{Glu,2} + K_{Nm,Glu}} \cdot \frac{R_{Ox,2}}{R_{Ox,2} + K_{Nm,Ox}}, \\
\mu_{Nm,2,Pa} &= \mu^{max}_{Nm,Pa} \cdot \frac{R_{Pa,2}}{R_{Pa,2} + K_{Nm,Pa}} \cdot \frac{K^R_{Nm,Glu}}{K^R_{Nm,Glu} + R_{Glu,2}} \cdot \frac{R_{Ox,2}}{R_{Ox,2} + K_{Nm,Ox}}, \\
\frac{dR_{Ox,2}}{dt} &= P_{Ox,1,2} \cdot \Delta R_{Ox,1,2} + P_{Ox,2,3} \cdot \Delta R_{Ox,3,2} - \frac{1}{Y_{Nm,Ox}} \cdot (\mu_{Nm,2,Glu} + \mu_{Nm,2,Pa}) \cdot X_{Nm,2}, \\
\frac{dR_{Pa,2}}{dt} &= P_{Pa,1,2} \cdot \Delta R_{Pa,1,2} + P_{Pa,2,3} \cdot \Delta R_{Pa,3,2} - \frac{1}{Y_{Nm,Pa}} \cdot \mu_{Nm,2,Pa} \cdot X_{Nm,2}, \\
\frac{dR_{Glu,2}}{dt} &= -\frac{1}{Y_{Nm,Glu}} \cdot \mu_{Nm,2,Glu} \cdot X_{Nm,2}
\end{aligned}
\tag{2.18}
$$

2.7.2.3 Conditions for oxygen and propionic acid limiting *N. meningitidis* growth

N. meningitidis growth rate due to propionic acid utilisation ($\mu_{Nm,2,Pa}$) only becomes significantly greater than 0 once glucose becomes depleted ($R_{Glu,2} \approx 0$). This is because $K^R_{Nm,Glu}$ is assumed to be equal to $K_{Nm,Glu}$ which is very low. This very low value means that the Michaelis-Menten term switches sharply from repressed to activated when glucose is depleted. When glucose is depleted, *N. meningitidis* growth becomes dependent on the partial yield (section 2.7.1.2) of either oxygen ($y_{Nm,2,Ox}$) or propionic

acid ($y_{Nm,2,Pa}$) depending on which one is most limiting.

The partial yields are defined as:

$$\begin{aligned} y_{Nm,Pa,2} &= Y_{Nm,Pa} \cdot P_{Pa,3,2} \cdot J^*_{Pa,3} \cdot R_{Pa,3}, \\ y_{Nm,Ox,2} &= Y_{Nm,Ox} \cdot P_{Ox,1,2} \cdot R_{Ox,1}. \end{aligned} \tag{2.19}$$

When $y_{Nm,2,Ox} < y_{Nm,2,Pa}$ then *N. meningitidis* growth is oxygen limited and propionic acid will always be in excess. When $y_{Nm,2,Ox} > y_{Nm,2,Pa}$ then propionic acid will become limiting once it begins to be utilised. While glucose is being utilised by *N. meningitidis*, propionic acid accumulates in the culture chamber (chamber 2). It is only after both the glucose and the accumulated propionic acid have been depleted, that *N. meningitidis* growth slows to the rate limited by propionic acid flux ($y_{Nm,2,Pa}$). Once growth is limited by propionic acid then oxygen is in excess and anaerobic conditions are compromised.

2.7.2.4 Propionic acid accumulation and depletion

In order to aid understanding of this system and design of useful experiments, analytical solutions have been generated. An analytical solution for the amount of propionic acid accumulated during glucose depletion is described. and a solution is formed describing the amount of time it takes for that propionic acid to become depleted.

For these solutions the following assumptions are made:

- Diffusion gradient of propionic acid between chambers 2 and 3 is far from equilibrium, therefore $\Delta R_{Pa,3,2} = J^*_{Pa,3} \cdot R_{Pa,3}$.
- Diffusion of propionic acid between chambers 1 and 2 is negligible, therefore $P_{Pa,1,2} = 0$.
- Oxygen is the resource that limits *N. meningitidis* growth (up until both glucose and propionic acid are depleted) therefore $R_{Ox,2} = 0$ and $\frac{dX_{Nm,2}}{dt} = Y_{Nm,Ox} \cdot P_{Ox,1,2} \cdot R_{Ox,1}$.

And so the amount of propionic acid accumulated in the period of time it takes for glucose to become depleted ($t^D_{Glu,2}$, defined by equation 2.17), i.e. $R^{t,Glu,0}_{Pa,2}$, is

$$R_{Pa,2}^{t,Glu,0} = P_{Pa,2,3} \cdot J_{Pa,3}^{*} \cdot R_{Pa,3} \cdot t_{Glu,0}^{D} \, ,$$

and the rate of propionic acid depletion ($\Delta R_{Pa,2}^{D}$) is

$$\Delta R_{Pa,2}^{D} = \frac{1}{Y_{Nm,Pa}} \cdot \left(y_{Nm,2,Ox} - y_{Nm,2,Pa} \right) .$$

Therefore, the time it takes for the accumulated propionic acid ($R_{Pa,2}^{t,Glu,0}$) to be depleted is

$$t_{Pa,2}^{D} = \frac{R_{Pa,2}^{t,Glu,0}}{\Delta R_{Pa,2}^{D}} = t_{Glu,2}^{D} \cdot \frac{y_{Nm,2,Pa}}{y_{Nm,2,Ox} - y_{Nm,2,Pa}}. \tag{2.20}$$

Oxygen and propionic acid permeabilities are a key factor in determining the partial yields $y_{Nm,2,Ox}$ and $y_{Nm,2,Pa}$. Figure 2.4 shows how the propionic acid duration is affected by both of these permeabilities. In this figure, the duration is expressed as a proportion of the glucose depletion duration ($y_{Nm,2,Pa}/(y_{Nm,2,Ox} - y_{Nm,2,Pa})$). It is clear that propionic acid duration is only much greater that 0 when the permeabilities are close to the point at which $y_{Nm,2,Ox} = y_{Nm,2,Pa}$. This range of permeability values covered in figure 2.4 was chosen in order to investigate a wide variety of chamber sizes and membrane thicknesses. This same range is used for further analyses in this chapter.

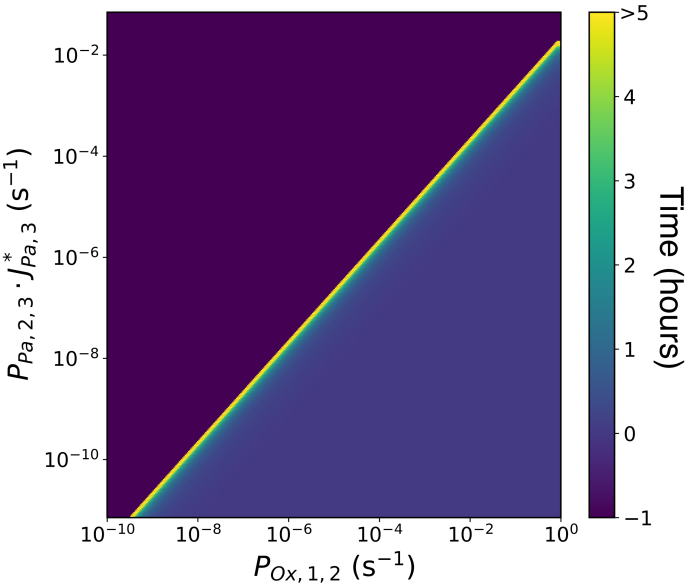

Figure 2.4: Duration of propionic acid depletion is affected by oxygen and propionic acid permeabilities. The analytical solution for $y_{Nm,2,Pa}/(y_{Nm,2,Ox} - y_{Nm,2,Pa})$ (i.e. the duration of propionic acid depletion relative to duration of glucose depletion) is displayed over a range of oxygen ($P_{Ox,1,2}$) and propionic acid ($P_{Pa,2,3}$) permeabilities. A value of -1 indicates that $y_{Nm,2,Pa} > y_{Nm,2,Ox}$ and so propionic acid does not deplete.
Parameter values used are $m = 5\,\text{mm}$, $\eta = 10$, $R_{Ox,1} = 100\%$ of saturation from air, $R_{Pa,3} = 10\,\text{mM}$, $pH_2 = 7.2$, $pH_3 = 6.0$, and as shown in table 2.2

The validity of this solution, with all of its assumptions, can be assessed by comparing the results with numerical solutions. From the results of the numerical solutions, $t^D_{Pa,2}$ is defined as the period of time between glucose being depleted and propionic acid being depleted. Resource depletion is defined using the Michaelis-Menten terms $M_{Nm,Glu,2}$ and $M_{Nm,Pa,2}$ with the conditions for depletion being $M_{Nm,Glu,2} < 0.9$ and $M_{Nm,Pa,2} < 0.15$. A lower threshold was used for propionic acid because $K_{Nm,Pa}$ is much larger than $K_{Nm,Glu}$ (table 2.2), and so the value of $M_{Nm,Pa,2}$ is lower at the point where propionic acid can be considered to be depleted (in a practical sense). The response of $M_{Nm,Glu,2}$ and $M_{Nm,Pa,2}$ to varying resource concentrations is shown in figure 2.5a.

Numerical solutions were found for a variety of parameter sets with a range of $y_{Nm,2,Pa}$: $y_{Nm,2,Ox}$ ratios. Comparing this analytical solution from equation 2.20 to the numerical solution for $t^D_{Pa,2}$ shows that the analytical solution is slightly higher (Fig2.5b). This is due to the assumption that propionic acid in the culture chamber (chamber 2) is 0 which leads to both an overestimation of propionic acid flux into chamber 2 ($F_{Pa,2,3}$) and an underestimation of propionic acid lost due to flux into chamber 1 ($F_{Pa,1,2}$). Both

of these factors artificially prolong the predicted time taken for propionic acid to be depleted.

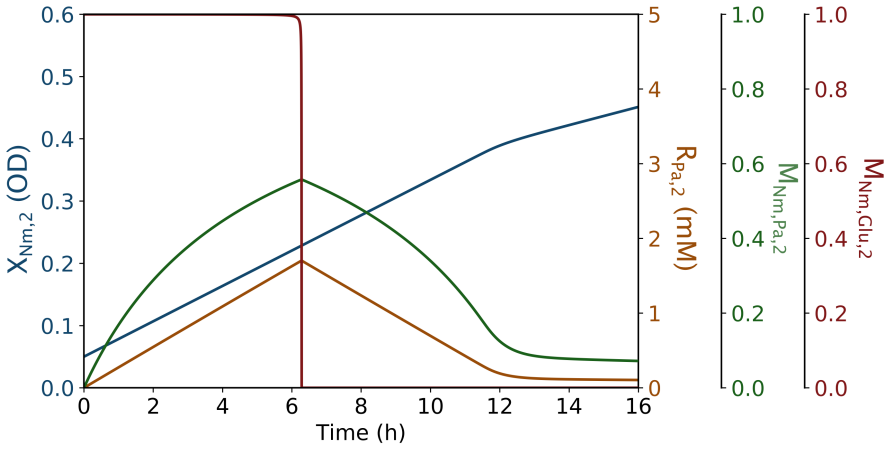

(a)

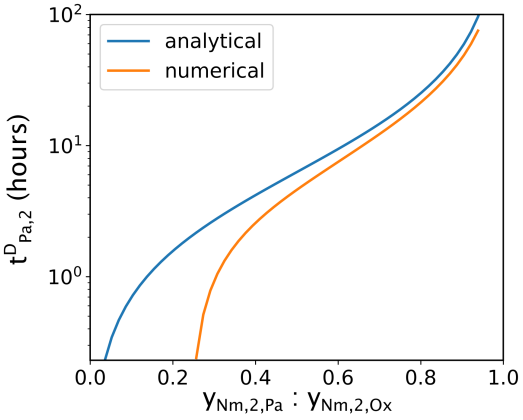

(b)

Figure 2.5: Propionic acid depletion times are affected by oxygen and propionic acid limitation.
a) Sample numerical solution showing how $M_{Nm,Glu,2}$ and $M_{Nm,Pa,2}$ vary as *N. meningitidis* utilises resources for growth while propionic acid accumulates and is depleted. Parameters: $\eta = 5$, $L_{1,2} = 0.5\,\text{mm}$, $L_{2,3} = 10\,\mu\text{m}$, $R_{Pa,3} = 6\,\text{mM}$, $R^0_{Glu,2} = 1\,\text{mM}$, $X^0_{Nm,2} = 0.05$ OD_{600}.
b) Comparison of analytical and numerical solutions for parameter sets giving a range of $y_{Nm,2,Pa} : y_{Nm,2,Ox}$ ratios. The output, $t^D_{Pa,2}$, shows good agreement with an offset. Parameters: $\eta = 5$, $L_{1,2} = 0.5\,\text{mm}$, $L_{2,3} = 10\,\mu\text{m}$, $R_{Pa,3} = 6\,\text{mM}$, $R^0_{Glu,2} = 1\,\text{mM}$, $X^0_{Nm,2} = 0.05$ OD_{600}.
Other parameter values are $m = 5\,\text{mm}$, $R_{Ox,1} = 100\%$ of saturation from air, $pH_2 = 7.2$, $pH_3 = 6.0$, and as shown in table 2.2

Therefore, when designing these experiments and analysing results, it is important to use numerical solutions to verify predictions from the analytical solutions.

2.7.2.5 Propionic acid utilisation without depletion

When propionic acid does not get depleted (when $y_{Nm,2,Pa} > y_{Nm,2,Ox}$), it instead accumulates. Although this is of limited use for investigating propionic acid utilisation by *N. meningitidis*, since propionic acid is not the factor limiting microbial growth, it may be useful for studying inhibition of growth by propionic acid. This growth inhibition is not a factor in the current ODE model but could be added if it is an important aspect of the metabolic interaction between *N. meningitidis* and *P. gingivalis*.

2.7.2.6 Practical and useful parameter sets

Analytical solutions show the limits that the requirement to have *N. meningitidis* growth limited by both oxygen and then propionic acid places on the model parameters (section 2.7.2.3). The solutions also show how the timings of the growth can be controlled by adjusting oxygen and propionic acid flux into the culture chamber (i.e. by varying membrane thickness, chamber dimensions, pH and concentration of propionic acid), and by adjusting the starting concentration of glucose (section 2.7.2.4). A wide variety of parameter sets are permitted by these findings, however it is clear that in this implementation of the assay (with parameters in table 2.2) the challenge is to have a high enough propionic acid diffusion rate relative to oxygen diffusion into the culture chamber. This is due to the relatively high permeability of PDMS to oxygen compared to propionic acid, and the need for the pH of chambers 2 and 3 to be compatible with their respective microbial cultures.

One possible set of parameter values that satisfies these limits is: $m = 5\,\mathrm{mm}$, $L_{1,2} = 0.9\,\mathrm{mm}$, $L_{2,3} = 10\,\mu\mathrm{m}$, $\eta = 5$ and $R_{Pa,3} = 10\,\mathrm{mM}$, pH of chamber 2 (pH_2) as 7.2, $pH_3 =$ 6.0, and $m = 5\,\mathrm{mm}$. With these parameters, $y_{Nm,2,Ox} = y_{Nm,2,Pa}$, and the dynamics (Fig2.6a) are as expected: first glucose is consumed as *N. meningitidis* grows, and during this period propionic acid accumulates in chamber 2. Once glucose is depleted then flux and consumption of propionic acid are balanced such that the concentration of propionic acid does not change. Oxygen is the resource that limits *N. meningitidis* growth throughout the entire experiment, and so conditions remain anaerobic. This parameter set has practical membrane thicknesses, chamber dimensions, time scales and chamber content concentrations/pH/culture densities.

Different $y_{Nm,2,Pa} : (y_{Nm,2,Ox} - y_{Nm,2,Pa})$ ratios change how oxygen and propionic

acid vary once glucose is depleted. When $y_{Nm,2,Pa} : (y_{Nm,2,Ox} - y_{Nm,2,Pa})$ is around $1 : 6$ then oxygen immediately rises after glucose becomes depleted (Fig2.6b). When $y_{Nm,2,Pa} : (y_{Nm,2,Ox} - y_{Nm,2,Pa})$ is around $1 : 1$ then oxygen still accumulates after glucose depletion, however this takes around the same amount of time as it took glucose to be depleted meaning there is a distinct phase in which *N. meningitidis* maintains anaerobic conditions while utilising propionic acid (Fig2.6c). When $y_{Nm,2,Ox} > y_{Nm,2,Pa}$ then propionic acid continues to accumulate, even after glucose is depleted, and so propionic acid never becomes a limiting factor in *N. meningitidis* growth (Fig2.6d).

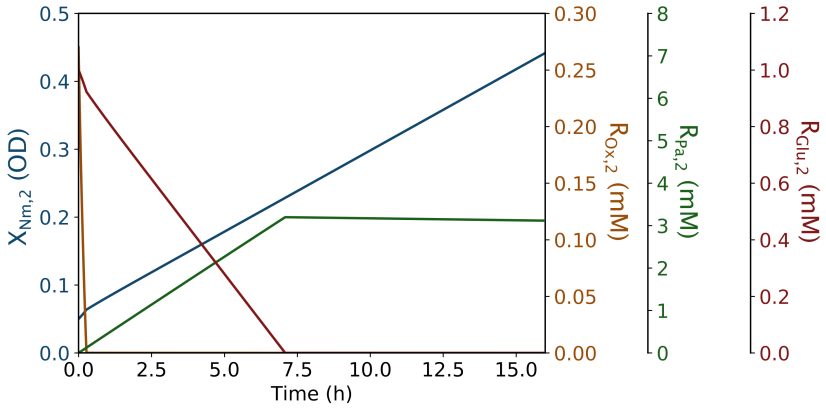

(a)

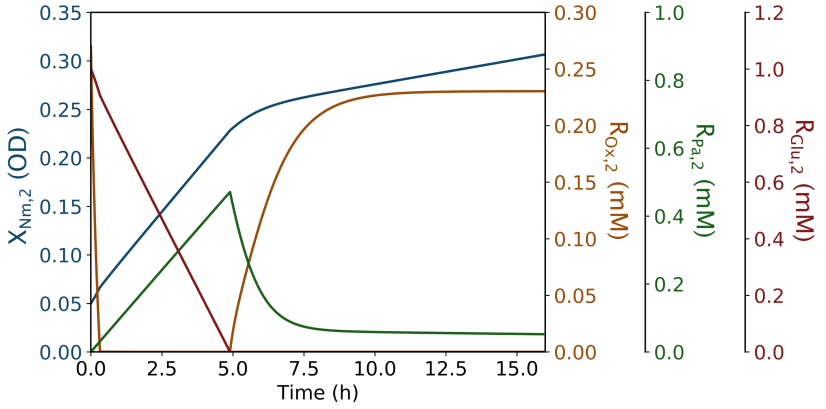

(b)

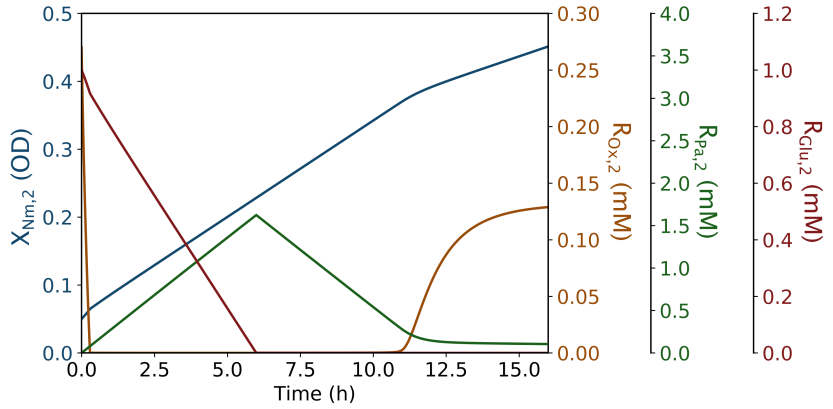

(c)

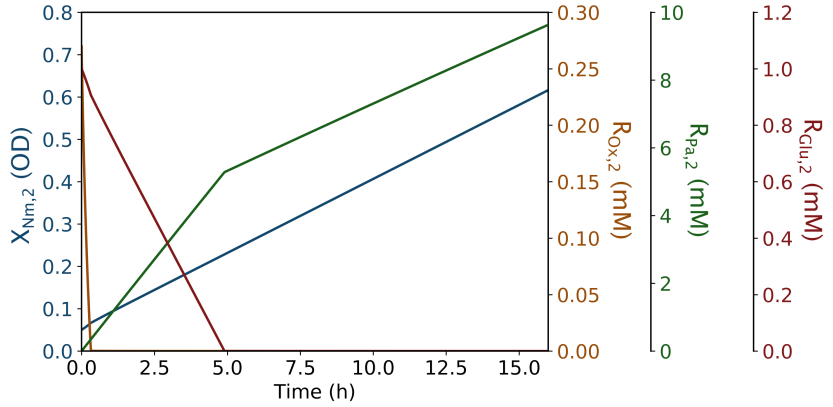

(d)

Figure 2.6: The effect of oxygen and propionic acid limitation on growth dynamics. Numerical solutions of *N. meningitidis* utilising propionic acid at different resource limitations.
a) $y_{Nm,2,Ox} = y_{Nm,2,Pa}$ ($L_{2,3} = 10\,\mu$m, $L_{1,2} = 0.9$ mm, $R_{Pa,3} = 10$ mM, $pH_C = 6.0$).
b) $y_{Nm,2,Pa} : (y_{Nm,2,Ox} - y_{Nm,2,Pa}) \approx 1 : 6$ ($L_{2,3} = 0.1$ mm, $L_{1,2} = 0.1$ mm, $R_{Pa,3} = 5$ mM, $pH_C = 6.0$).
c) $y_{Nm,2,Pa} : (y_{Nm,2,Ox} - y_{Nm,2,Pa}) \approx 1 : 1$ ($L_{2,3} = 10\,\mu$m, $L_{1,2} = 0.5$ mm, $R_{Pa,3} = 6$ mM, $pH_C = 6.0$).
d) $y_{Nm,2,Ox} > y_{Nm,2,Pa}$ ($L_{2,3} = 20\,\mu$m, $L_{1,2} = 0.1$ mm, $R_{Pa,3} = 10$ mM, $pH_C = 5.5$).
Other parameter values are $m = 5$ mm, $pH_B = 7.2$, $R^0_{Glu} = 1$ mM, $X^0_{Nm,2} = 0.05$ OD_{600} and as shown in table 2.2.

Having a practical parameter set and knowing how to control the behaviour of the system is vital for designing sets of experiments that allow quantification of propionic acid diffusion and utilisation in the non-contact co-culture assay. This analysis forms the basis for adding *P. gingivalis* to the system and start modelling a co-culture between *N. meningitidis* and *P. gingivalis*.

2.7.3 Propionic acid production by a batch culture of *P. gingivalis*, and utilisation by *N. meningitidis*

2.7.3.1 Purpose of modelling adjacent batch cultures of *N. meningitidis* and *P. gingivalis*

N. meningitidis dynamics with a constant supply of propionic acid diffusing into the culture chamber has been studied (section 2.7.2). However, propionic acid produced by an adjacent *P. gingivalis* culture (in chamber 3) would not necessarily provide such a stable source of propionic acid.

The *P. gingivalis* culture may exist as a batch or continuous culture. Batch culture represents the simplest form of culture, from a practical standpoint, since no intervention is required once the starting conditions have been established. Therefore, this scenario is analysed first. A *N. meningitidis* batch culture in chamber 2 utilises oxygen diffusing from chamber 1 (the oxygen supply chamber) and propionic acid diffusing from chamber 3. The propionic acid in chamber 3 is produced by a batch culture of *P. gingivalis* in that chamber, this culture grows by utilising glucose.

Since propionic acid is produced as a product of anaerobic fermentation, a batch culture of *P. gingivalis* would only produce propionic acid for a limited period of time (after lag phase and before stationary phase). This timing limitation will add to the timing constraints related to consumption of resources by the *N. meningitidis* culture (section 2.7.2.1).

The purpose of modelling this system is to determine the feasibility, robustness and usefulness of using a batch *P. gingivalis* culture in co-culture experiments. In particular, information about how to adjust parameters in order to coordinate the two batch cultures and measure a metabolic interaction between them will be vital for designing experiments.

2.7.3.2 ODE system

The *N. meningitidis* culture and resources in chamber 2 are modelled as in section 2.7.2.1 (equation 2.18). *P. gingivalis* growth is modelled using a logistic growth equation (section 2.5.2, equation 2.1). This is appropriate since logistic growth provides a

good fit to experimental data (section 4.3.3), modelling the timings of different phases of *P. gingivalis* growth in batch culture (lag, exponential, linear and stationary phases), and it is fully described by two parameters (maximum growth rate μ_{Pg}^{max} and carrying capacity H_{Pg}).

Therefore, *P. gingivalis* growth and the resources in chamber 3 are modelled with the following system of ODEs:

$$\begin{aligned}
\mu_{Pg,3} &= \mu_{Pg}^{max} \cdot \left(1 - \frac{X_{Pg,3}}{H_{Pg}}\right), \\
\frac{dX_{Pg,3}}{dt} &= \mu_{Pg,3} \cdot X_{Pg,3}, \\
\frac{dR_{Pa,3}}{dt} &= \frac{Y_{Pg,Glu,Pa}}{Y_{Pg,Glu}} \cdot \mu_{Pg,3} \cdot X_{Pg,3} + P_{Pa,2,3} \cdot \Delta R_{Pa,2,3}, \\
\frac{dR_{Ox,3}}{dt} &= P_{Ox,2,3} \cdot \Delta R_{Ox,2,3}.
\end{aligned} \tag{2.21}$$

2.7.3.3 Quantity of propionic acid produced by a batch culture of *P. gingivalis*

To determine if the *P. gingivalis* culture will produce enough propionic acid to have a measurable effect on *N. meningitidis* growth, the yield during each phase of growth can be calculated using parameter values from table 2.2.

Tryptic soy broth (TSB) is commonly used in liquid cultures of *P. gingivalis*, it typically contains $3.0\,\mathrm{g\,L^{-1}}$ of glucose which is $16.7\,\mathrm{mM}$. This value is used as a starting point for concentration of glucose in the *P. gingivalis* culture media (i.e. $R_{Glu,3}^{0}$).

Assuming that the *P. gingivalis* culture converts all of the available glucose to propionic acid with a yield of $Y_{Pg,Glu,Pa}$, then the concentration of propionic acid will $13.9 \cdot Y_{Pg,Glu,Pa} = 15.8\,\mathrm{mM}$. Assuming that all of this propionic acid ends up diffusing into the *N. meningitidis* culture chamber and is utilised for growth at a yield of $Y_{Nm,Pa}$, the change in *N. meningitidis* will be $13.1 \times 10^{-3} \cdot Y_{Nm,Pa} = 0.298\,\mathrm{g\,L^{-1}}$, or 0.107 OD_{600}.

Glucose in the *P. gingivalis* chamber is not modelled explicitly in equations 2.21, however it is represented in the carrying capacity H_{Pg} since this maximum culture density is

likely determined by the resources available to the culture. In the case of the parameter value for H_{Pg} in table 2.2, the glucose concentration was $16.7\,\mathrm{mM}$.

Overall, the relationship between change in *N. meningitidis* biomass due to the propionic acid ($\Delta X^{Pa}_{Nm,2}$) is

$$\Delta X^{Pa}_{Nm,2} = R^0_{Glu,3} \cdot Y_{Pg,Glu,Pa} \cdot Y_{Nm,Pa} \text{ ,}$$

and so, the magnitude of the effect on *N. meningitidis* culture density is directly proportional to the starting concentration of glucose in the *P. gingivalis* culture medium.

2.7.3.4 Timing of propionic acid production by a *P. gingivalis* batch culture

The temporal dynamics of *P. gingivalis* batch culture growth are captured in the logistic growth model. The growth curve can be split into four phases:

1. Lag phase, where growth rate is zero or very low
2. Exponential phase, where growth is uninhibited and exponential
3. Linear phase, where growth proceeds at a constant rate due to resource limitation
4. Stationary phase, where growth halts once the culture reaches its carrying capacity. This may be due to depletion of resources or accumulation of metabolic products that inhibit growth.

Although there is never a point at which $X_{Pg,3}$ is not growing in the model, there are phases at the beginning and end of the growth curve where the growth rate is negligible. These correspond to the lag phase and the stationary phase. Between these phases, in the exponential and linear phases, is where almost all of the growth and propionic acid production occurs. Production rate of propionic acid peaks mid-way through the linear phase where growth rate ($\mu_{Pg,3} \cdot X_{Pg,3}$) is highest.

Since the logistic model is continuous, in order to aid analysis, the transition between these phases are defined using threshold values of key variables. The end of the lag phase and start of the exponential phase is defined by the point at which $X_{Pg,3}$ exceeds 10% of the carrying capacity, and the start of the lag phase is defined by the point at which $X_{Pg,3}$ exceeds 90% of the carrying capacity.

The time it takes to reach each of these thresholds is described by equation 2.3. The only parameter in this equation that can be controlled is the starting culture density of *P. gingivalis*. This can be used to control the growth phase that *P. gingivalis* is in at the start of the experiment. However, the rate at which the culture transitions between phases is entirely determined by the intrinsic growth rate μ_{Pg}^{max} and carrying capacity H_{Pg} and so cannot be changed.

2.7.3.5 Coordination of propionic acid production by *P. gingivalis* with utilisation by *N. meningitidis*

Analytical solutions to this system are made more complicated due to diffusion between chambers 2 and 3. However, useful solutions can be produced by examining two different situations:

1. when permeability of propionic acid from chamber 3 to chamber 2 is very low. In this situation we can assume that the concentration of propionic acid in chamber 3 is unchanged by diffusion
2. when permeability of propionic acid between chambers 3 and 2 is very high. In this situation we can assume that the concentration of propionic acid in one chamber is directly proportional to concentration in the other chamber (the proportion being determined by partitioning due to the pH of each chamber)

The true behaviour of the system will fall somewhere between these two solutions. Which solution is more applicable can be determined by comparing the rates of propionic acid production, propionic acid diffusion and oxygen diffusion (i.e. glucose depletion).

In both of these situations, "success" (i.e. oxygen-limited growth followed by propionic acid-limited growth) of an experiment can be determined by comparing propionic acid influx into chamber 2 to consumption by *N. meningitidis*. If the influx is greater then the oxygen-limited growth of *N. meningitidis*, then anaerobic conditions will be maintained for *P. gingivalis*, and the effect of the co-culture on *N. meningitidis* can be studied by measuring the growth of this culture once the glucose is depleted.

2.7.3.5.1 Slow diffusion of propionic acid When the permeability of propionic acid is very low, then a large diffusion gradient is required for a sufficient influx. Therefore, there must be sufficient time to allow propionic acid to accumulate in chamber 3 before *N. meningitidis* begins utilising it. The maximum concentration will be reached once the *P. gingivalis* reaches stationary phase, however this would be in-effect a spent-media experiment and would not capture two-way interactions between the two cultures. Analysis of the co-culture system is used to determine under what conditions co-culture is possible and how long these co-cultures last.

If we assume that there is no diffusion from chamber 3 to 2 (situation 1 from section 2.7.3.5) then $R^t_{Pa,3}$ (propionic acid at time t) is proportional to $X^t_{Pg,3}$ (*P. gingivalis* at time t):

$$R^t_{Pa,3} - R^0_{Pa,3} = \frac{Y_{Pg,Glu,Pa}}{Y_{Pg,Glu}} \cdot \left(X^t_{Pg,3} - X^0_{Pg,3}\right) \tag{2.22}$$

where $R^0_{Pa,3}$ and $X^0_{Pg,3}$ are starting levels ($t = 0$) of propionic acid and *P. gingivalis* respectively. Since growth of *P. gingivalis* is modelled by the logistic growth equation (equation 2.1), equation 2.2 shows the solution of $X^t_{Pg,3}$ for time t.

To determine what value of $R^t_{Pa,3}$ is required, the maximum potential yields of *N. meningitidis* from oxygen ($y_{Nm,2,Ox}$) and propionic acid ($y_{Nm,2,Pa}$) are compared. When $y_{Nm,2,Ox} < y_{Nm,2,Pa}$ then $X_{Nm,2}$ growth is oxygen limited (section 2.7.2.3).

Together, these equations are used to calculate the time after which sufficient propionic acid has accumulated to support oxygen-limited growth of *N. meningitidis*.

2.7.3.5.2 Fast diffusion of propionic acid When the permeability of propionic acid is very high then we can assume that it is instantaneous (situation 2 from section 2.7.3.5). In this situation, anaerobic conditions are maintained when the production of propionic acid by *P. gingivalis* in chamber 3 exceeds the maximum consumption rate of propionic acid by *N. meningitidis* in chamber 2. This maximum consumption rate is limited by the diffusion rate of oxygen into chamber 2 from the oxygen supply chamber. This is similar to the condition in section 2.7.3.5.1 where anaerobic conditions are maintained when $y_{Nm,2,Ox} < y_{Nm,2,Pa}$. However, in the case of fast diffusion, $y_{Nm,2,Pa}$ is determined by the production rate of propionic acid in chamber 3 rather than the concentration, such that

$$y_{Nm,Pa,2} = Y_{Nm,Pa} \cdot \frac{Y_{Pg,Glu,Pa}}{Y_{Pg,Glu}} \cdot \frac{dX_{Pg,3}}{dt},$$
$$y_{Nm,Ox,2} = Y_{Nm,Ox} \cdot P_{Ox,1,2} \cdot R_{Ox,1}. \tag{2.23}$$

The relationship between $\frac{dX_{Pg,3}}{dt}$ and $X_{Pg,3}$ (equation 2.1) is quadratic (Fig2.7) with roots at $X_{Pg,3} = 0$ and $X_{Pg,3} = H_{Pg}$ and a maximum point halfway between the roots at $X_{Pg,3} = (H_{Pg}/2)$. At this maximum point, $\frac{dX_{Pg,3}}{dt} = \mu_P^{max} g \cdot (H_{Pg}/4)$.

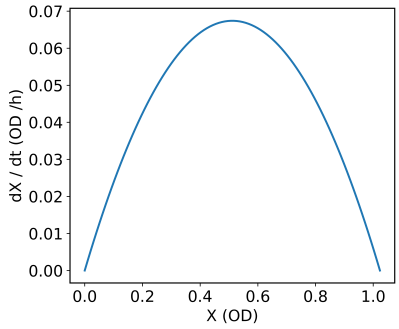

Figure 2.7: Quadratic relationship between $X_{Pg,3}$ and $dX_{Pg,3}/dt$ in logistic growth model. Parameter values are $\mu = 0.263\,\mathrm{h}^{-1}$ and $H_{Pg} = 1.02$ OD_{600}.

Solving using the quadratic formula gives

$$x_{Pg,3} = \frac{1}{2} \cdot \left(1 \pm \sqrt{1-q}\right) \tag{2.24}$$

where $x_{Pg,3}$ is $X_{Pg,3}$ expressed as a proportion of the maximum value H_{Pg}, and q is $\frac{dX_{Pg,3}}{dt}$ expressed as a proportion of the maximum value $\frac{\mu_{Pg}^{max} \cdot H_{Pg}}{4}$.

This shows that, given a threshold value for $\frac{dX_{Pg,3}}{dt}$, as $X_{Pg,3}$ grows it will exceed this threshold but then it will fall below it again (as long as this threshold value does not exceed what is possible given the maximum growth rate μ_{Pg}^{max}). This means that there is a period of time during which anaerobic conditions can be maintained by *P. gingivalis* propionic acid production.

When designing an experiment it is important that this time period is coordinated with the time it takes for glucose to be depleted by *N. meningitidis* growth in chamber 2.

The maximum value of $\frac{dX_{Pg,3}}{dt} = \mu_{Pg}^{max} \cdot (H_{Pg}/4)$ can be used to check if propionic acid

production will ever be high enough to support anaerobic conditions, if it cannot then oxygen influx into chamber 2 must be reduced.

2.7.3.6 Comparison of analytical and numerical solutions

The "fast diffusion" and "slow diffusion" analytical solutions describe two very different situations. It is not apparent which solution best applies to each parameter set without comparing each analytical solution to the numerical solution. To perform this comparison, a set of parameter values was chosen, and the permeability of the membranes between chambers 1 & 2 and 2 & 3 (i.e. $P_{Ox,1,2}$ and $P_{Pa,2,3}$) were varied by varying $L_{1,2}$ and $L_{2,3}$. The parameter values were $m = 5\,\mathrm{mm}$, $\eta = 5$, $pH_2 = 7.2$, $pH_3 = 6.0$ and $R_{Ox,1} = S_{Ox,aq}$ (i.e. at saturation level) or as described in table 2.2.

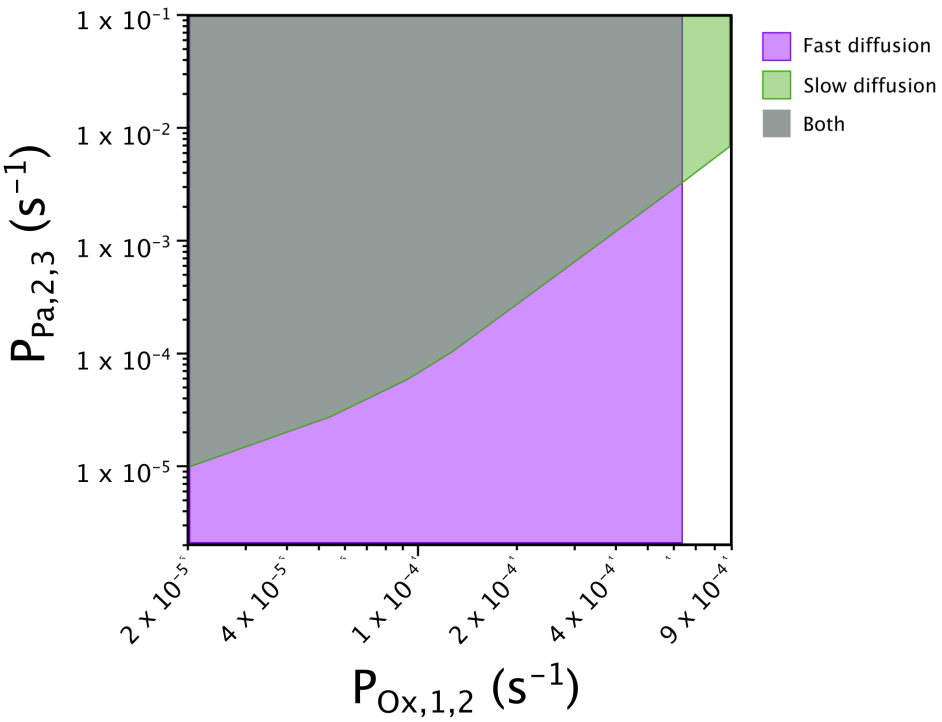

Figure 2.8: Analytical solutions to viability of *N. meningitidis* and *P. gingivalis* batch co-culture with varying permeabilities.
The successful maintenance of the co-culture was assessed by each of the solutions over a range of $P_{Ox,1,2}$ and $P_{Pa,2,3}$ values. Successful co-culture is indicated by the shaded areas. The two analytical solutions both place different limits on what permeability values are needed for a successful co-culture. The "fast diffusion" solution assumes a high $P_{Pa,2,3}$ such that diffusion of propionic acid is instantaneous, the "slow diffusion" solution assumes a low $P_{Pa,2,3}$ such that propionic acid accumulates in chamber 3 and does not decrease due to diffusion.
Parameters: $R_{Ox,1} = 100\%$ of saturation from, air, $pH_2 = 7.2$, $pH_3 = 6.0$, $R^0_{Glu,2} = 0.25\,\text{mM}$, $X^0_{Nm,2} = 0.02$ OD_{600}, $X^0_{Pg,3} = 0.2$ OD_{600}.

Figure 2.8 shows the analytical solutions as these permeabilities are varied. The shaded areas indicate when each analytical solution predicts that anaerobic conditions will be maintained. The "fast diffusion" solution places an upper limit on oxygen permeability since, over this limit, it is not possible for the *P. gingivalis* culture to produce propionic acid fast enough to ensure that there is an abundance of propionic acid for *N. meningitidis* growth. The "slow diffusion" model allows for higher oxygen permeability values but only at higher propionic acid permeabilities so that propionic acid can diffuse fast enough from where is has accumulated in chamber 3.

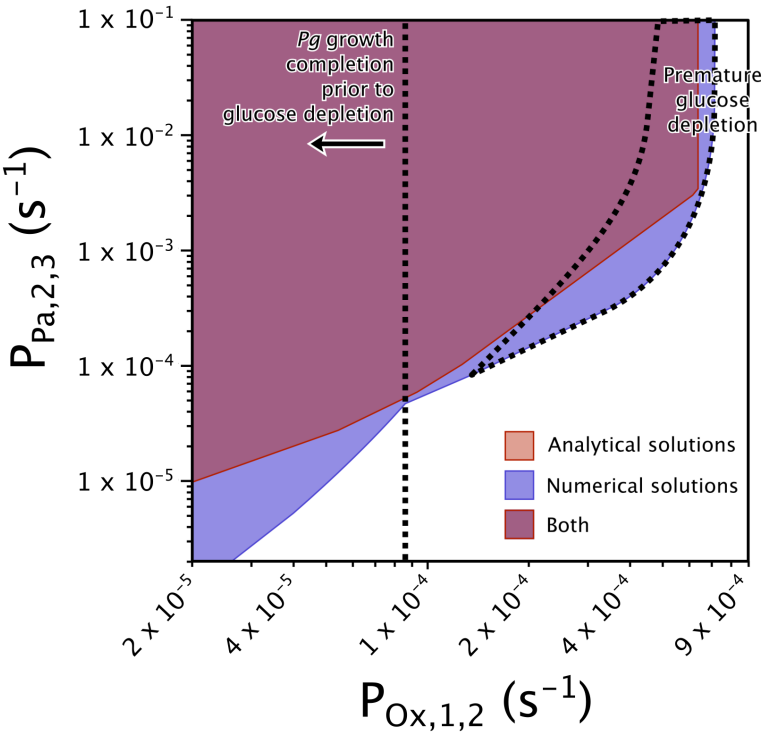

Figure 2.9: Comparison of analytical and numerical solutions to viability of *N. meningitidis* and *P. gingivalis* batch co-culture with varying permeabilities.
The numerical solutions are compared to the intersection of the two analytical solutions from figure 2.8 because it applies the "fast diffusion" solution at higher $P_{Pa,2,3}$ values and the "slow diffusion" solution at lower $P_{Pa,2,3}$ values. The zone of "premature glucose depletion" is where anaerobic conditions were temporarily compromised ($R_{Ox,2} > 0.056\,\mathrm{mM}$) before being restored. Also indicated is the $P_{Ox,1,2}$ value below which glucose depletion is slower than the effective end of *P. gingivalis* growth. When this happens, the co-culture is in-effect equivalent to a spent-media assay.
Parameters: $R_{Ox,1} = 100\%$ of saturation from air, $pH_2 = 7.2$, $pH_3 = 6.0$, $R^0_{Glu,2} = 0.25\,\mathrm{mM}$, $X^0_{Nm,2} = 0.02$ OD_{600}, $X^0_{Pg,3} = 0.2$ OD_{600}.

To verify these analytical solutions, numerical solutions of the ODE system described in section 2.7.3.2 were generated across the same range of permeability values. The parameter values used were the same as for the analytical solution, but with some changes: $\mu^{max}_{Nm,Pa} = 1.25 \times 10^{-4}\,\mathrm{s}^{-1}$ rather than $2.50 \times 10^{-4}\,\mathrm{s}^{-1}$ and $K^R_{Nm,Glu} = K_{Nm,Glu}$. The rational behind these parameter values is that growth is likely to be slower on propionic acid (it is unclear how much slower though), and the point at which propionic acid metabolism is repressed in *N. meningitidis* is likely to be the point at which glucose starts to become available.

The starting conditions were $X_{Nm,2} = 0.02$ OD_{600}, $X_{Pg,3} = 0.2$ OD_{600} and $R_{Glu,2} = 0.25\,\mathrm{mM}$. All other variables started at 0. The condition for a "successful" co-culture

was: if the anaerobic time period was at least 5% longer than the time it took for glucose to deplete. This definition is versatile since it is normalised to duration of the experiment (period of time consuming glucose + period of time consuming propionic acid, until anaerobic conditions are compromised), and it ensures that the duration of oxygen-limited growth on propionic acid is not so short as to be meaningless in an *in vitro* experiment.

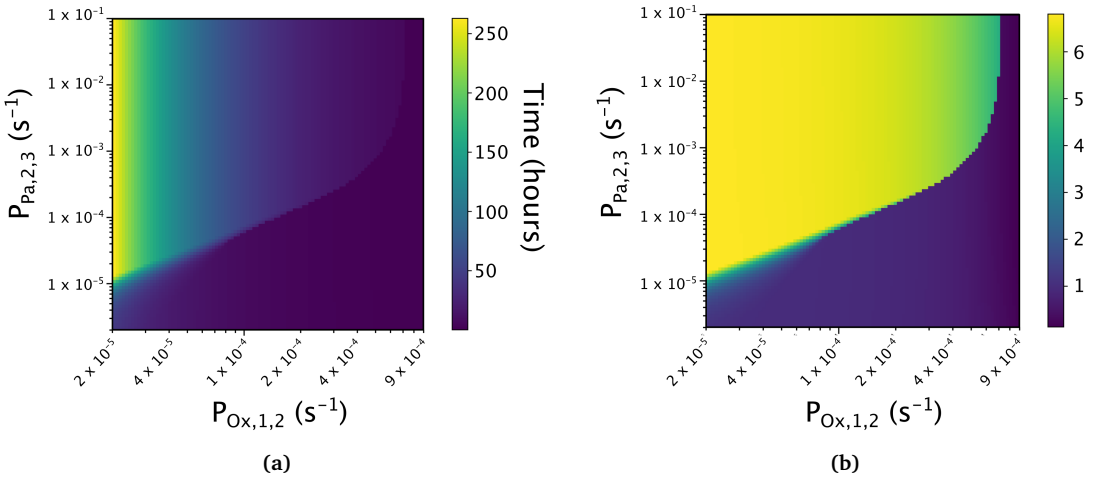

Figure 2.10: Oxygen and propionic acid permeabilities affect the duration of anaerobic conditions
Numerical solution results over a range of $P_{Ox,1,2}$ and $P_{Pa,2,3}$ values, showing:
a) Period of time anaerobic conditions are maintained by propionic acid production by *P. gingivalis* batch culture.
b) The period of time in (a) (i.e. Duration of anaerobic conditions due to *P. gingivalis* activity), normalised for glucose-depletion time.
Parameters: $R_{Ox,1}$ = 100% of saturation from air, pH_2 = 7.2, pH_3 = 6.0, $R^0_{Glu,2} = 0.25\,\text{mM}$, $X^0_{Nm,2}$ = 0.02 OD_{600}, $X^0_{Pg,3}$ = 0.2 OD_{600}.

Figure 2.9 shows a comparison the analytical solutions (represented together as the intersection of the "slow diffusion" and "fast diffusion" solutions) and the numerical solutions. The numerical solutions follow the "fast diffusion" solution closer at higher $P_{Pa,2,3}$ values and the "slow diffusion" solution more at lower $P_{Ox,2,3}$. Although there is a lot of deviation from the analytical solutions at low $P_{Ox,1,2}$ values, figure 2.10 shows that the co-culture durations of these deviating results are so small that they can be discounted. Also, as indicated in figure 2.9, when $P_{Ox,1,2}$ values are that low then *P. gingivalis* growth is completed before the glucose has been depleted. Therefore, two-way metabolic interactions would not captured in these cases limiting their usefulness.

There is a set of numerical solutions where there was successful co-culture but anaerobic conditions were compromised (labelled "premature glucose depletion" in figure

2.9). It is likely that this could be avoided by optimising the timings of glucose depletion and propionic acid production/accumulation (e.g. by increasing the starting glucose concentration). No such optimisation was carried out in this analysis, the same starting values were used for each numerical solution. Therefore, for this analysis, this set of solutions should be considered "successful".

Figure 2.9 shows numerical solutions with successful co-cultures beyond the limit set by the "fast diffusion" solution. This is due to accumulation of propionic acid in chamber 2 and 3, not captured in the "fast diffusion" analytical solution, which can support oxygen-limited growth until they are depleted.

There are also numerical solutions that show successful co-culture beyond the limit of the "slow diffusion" solution. This may be due to dynamics similar to those in a "fast diffusion" situation, or it may be due to phenomena not captured by the analytical solutions (such as accumulation of propionic acid in chamber 2).

This comparison between analytical and numerical solutions demonstrates that the two analytical solutions together provide a useful framework for understanding the system, but that numerical solutions are also required for accurate predictions of behaviour. Together, these models can provide a means by which to choose non-contact co-culture assay conditions and interpret the resulting data. This is particularly vital for coordinating the growth of the two cultures so that anaerobic conditions are not compromised due to the premature depletion of glucose in chamber 2 (Fig2.14).

2.7.3.7 Co-culture dynamics

Co-cultures where a successful co-culture is predicted must be verified by analysis of the dynamics to ensure that these situations can indeed be considered a practical co-culture. Also, numerical solutions of the batch co-culture model indicate successful co-cultures beyond the limits set by both the "fast-diffusion" and "slow-diffusion" analytical solutions. These situations must be explained by analysing the co-culture dynamics.

When propionic acid permeability is very low, then the slow-diffusion analytical solution assumes that propionic acid must accumulate in chamber 3 before a high diffusion gradient causes sufficient flux of propionic acid into chamber 2 to support oxygen-limited growth. A key assumption in this solution is that the flux of propionic acid is much smaller that the quantity of accumulated propionic acid, and so diffusion does

not cause a reduction in propionic acid in chamber 3. Therefore, propionic acid levels in chamber 3 are determined simply by *P. gingivalis* logistic growth. Figure 2.11 shows that, when propionic acid permeability is towards the low end of the parameter sets represented in figure 2.9, then levels of propionic acid in chamber 3 reduce slowly once *P. gingivalis* reaches stationary phase (the point at which propionic acid production effectively halts). *N. meningitidis* growth only ceases to be oxygen-limited once the concentration gradient falls below a threshold, once this happens then propionic acid levels in chamber 2 quickly deplete and anaerobic conditions are compromised. Therefore the assumptions of the analytical solution are, for the most part, reflected in the dynamics of the numerical solutions.

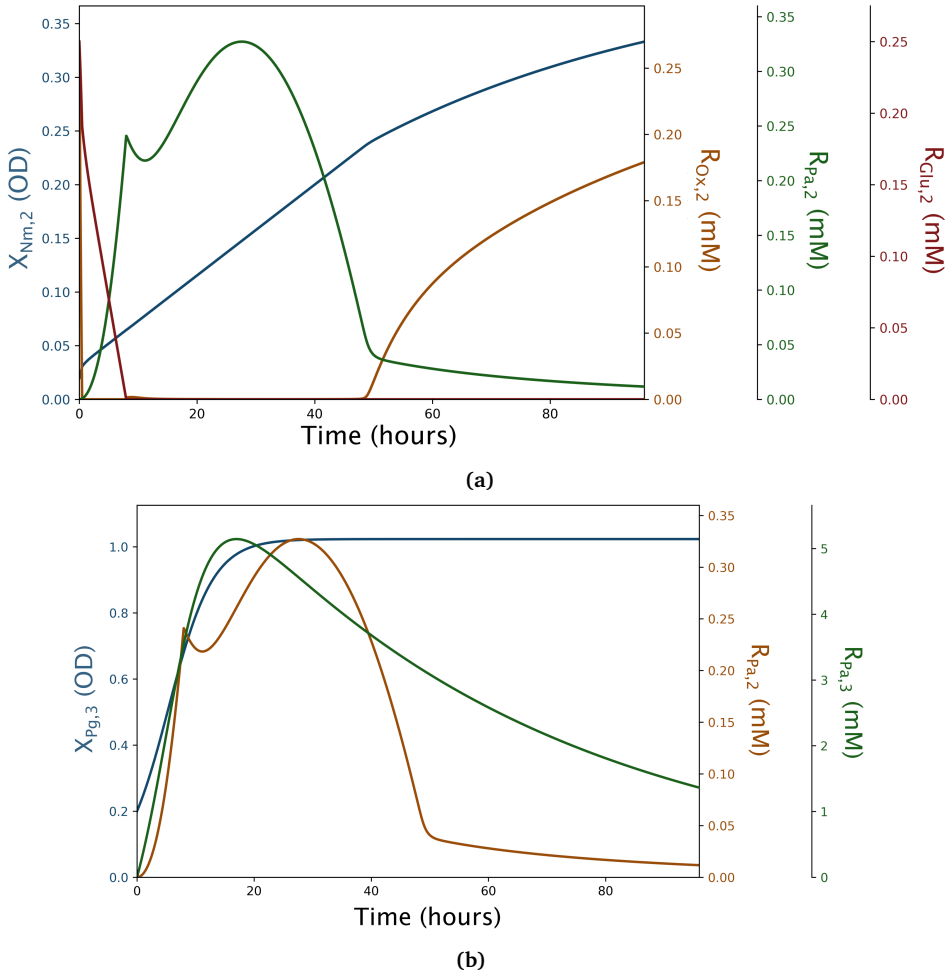

Figure 2.11: Dynamics of non-contact batch co-culture with very low permeability.
a) Dynamics of culture density ($X_{Nm,2}$), and oxygen ($R_{Ox,2}$), propionic acid ($R_{Pa,2}$) and glucose ($R_{Glu,2}$) concentrations in the *N. meningitidis* culture chamber.
b) Dynamics of culture density ($X_{Pg,3}$) and propionic acid ($R_{Pa,3}$) in the *P. gingivalis* culture chamber, along with concentration of propionic acid in the adjacent *N. meningitidis* culture chamber ($R_{Pa,2}$).
Parameters: $P_{Ox,1,2} = 1 \times 10^{-4}\,\mathrm{s}^{-1}$, $P_{Pa,2,3} = 7 \times 10^{-5}\,\mathrm{s}^{-1}$, ($L_{1,2} = 12.7\,\mathrm{mm}$, $L_{2,3} = 0.114\,\mathrm{mm}$, $m = 5\,\mathrm{mm}$, $\eta = 5$), $R_{Ox,1} = 100\%$ of saturation from air, $R^0_{Glu,2} = 0.25\,\mathrm{mM}$, $pH_2 = 7.2$, $pH_3 = 6.0$.

When propionic acid permeability is very high, then the fast-diffusion analytical solution assumes that propionic acid diffusion is instantaneous and so any propionic acid produced in chamber 3 can be utilised by *N. meningitidis* in chamber 2. This assumption is supported by the numerical solutions: when propionic acid permeability is towards the high end of the parameter sets represented in figure 2.9 then propionic acid levels in chamber 2 closely follow levels in chamber 3 (Fig2.12). In particular, they both approximate to 0 at the same time point. Propionic acid becomes depleted very soon after the *P. gingivalis* culture reaches stationary phase. This behaviour verifies this assump-

tion of the analytical solution. Accumulation of propionic acid in chamber 3 still has some effect, although it is small compared to the role of accumulation when propionic acid permeability is low. Dynamics due to accumulation are not captured at all in the fast-diffusion analytical solution.

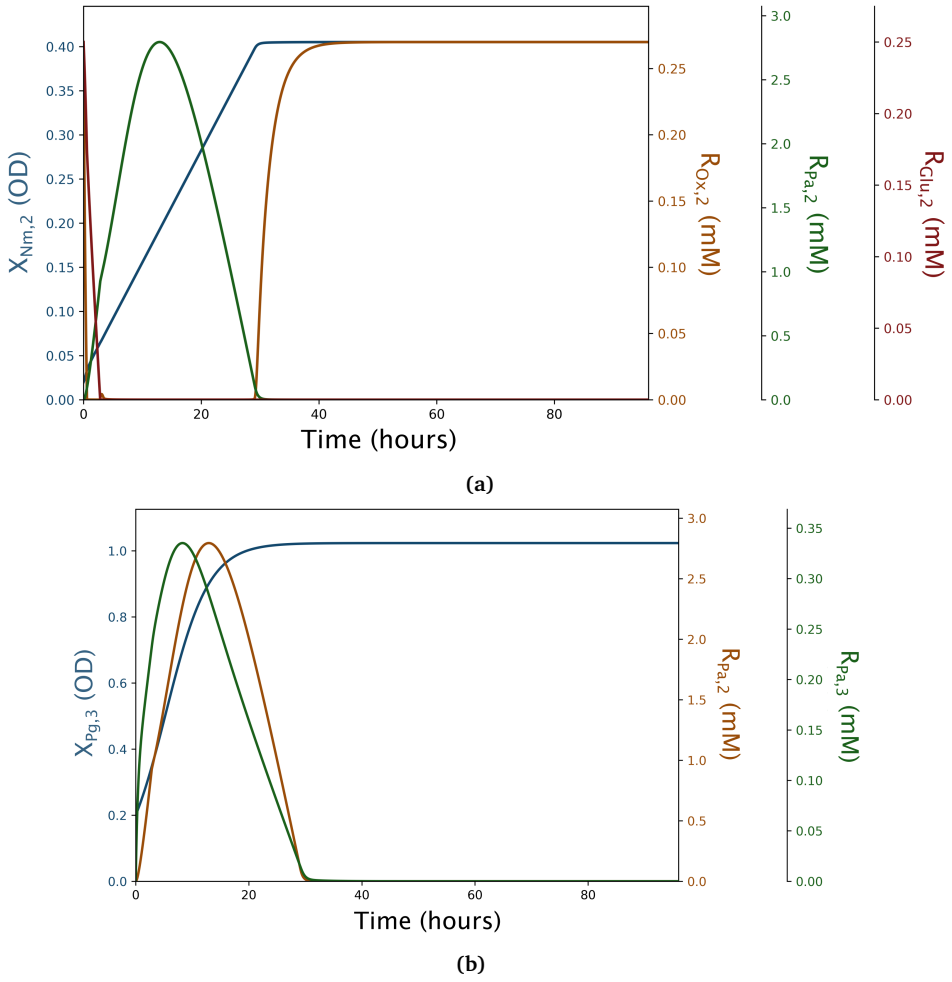

Figure 2.12: Dynamics of non-contact batch co-culture with very high permeability.
a) Dynamics of culture density ($X_{Nm,2}$), and oxygen ($R_{Ox,2}$), propionic acid ($R_{Pa,2}$) and glucose ($R_{Glu,2}$) concentrations in the *N. meningitidis* culture chamber.
b) Dynamics of culture density ($X_{Pg,3}$) and propionic acid ($R_{Pa,3}$) in the *P. gingivalis* culture chamber, along with concentration of propionic acid in the adjacent *N. meningitidis* culture chamber ($R_{Pa,2}$).
Parameters: $P_{Ox,1,2} = 3 \times 10^{-4}\,\mathrm{s}^{-1}$, $P_{Pa,2,3} = 1 \times 10^{-2}\,\mathrm{s}^{-1}$, ($L_{1,2} = 23.7\,\mathrm{mm}$, $L_{2,3} = 0.338\,\mu\mathrm{m}$, $m = 1\,\mathrm{mm}$, $\eta = 10$), $R_{Ox,1} = 100\%$ of saturation from air, $R^0_{Glu,2} = 0.25\,\mathrm{mM}$, $pH_2 = 7.2$, $pH_3 = 6.0$.

Most parameter sets represented in figure 2.9 fall in-between the two extremes of very high and very low propionic acid permeability. In these instances, the dynamics exhibit behaviours characteristic of both analytical solutions. For example, the dynamics shown

in figure 2.13 can be interpreted in two ways:

1. propionic acid in chamber 3 is able to accumulate to a sufficient level before glucose is depleted. And so, this "pool" of propionic acid is able to support oxygen-limited *N. meningitidis* until it is sufficiently depleted
2. *P. gingivalis* is producing propionic acid at a sufficiently high rate to replace that which is being consumed by *N. meningitidis* in chamber 2. Once *P. gingivalis* growth halts then propionic acid levels inevitably decline until anaerobic conditions are compromised

This shows that both of the analytical solutions together provide a useful tool for interpreting the dynamics of this non-contact co-culture of two batch cultures.

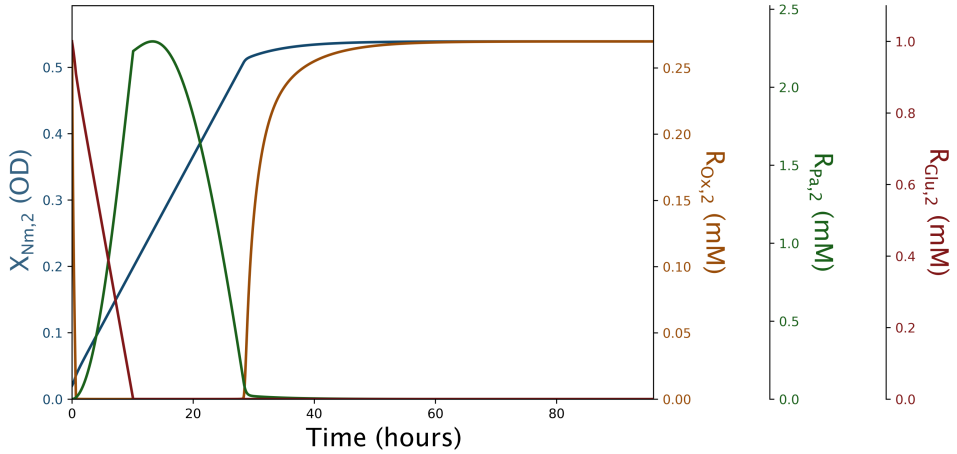

(a)

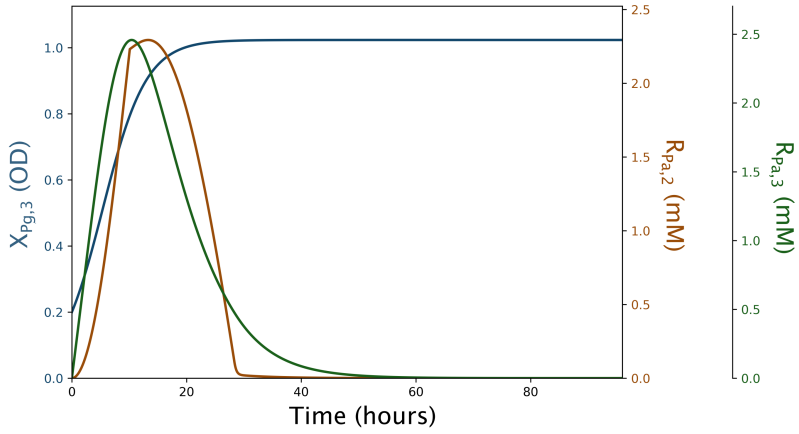

(b)

Figure 2.13: Dynamics of non-contact batch co-culture with intermediate permeability.
a) Dynamics of culture density ($X_{Nm,2}$), and oxygen ($R_{Ox,2}$), propionic acid ($R_{Pa,2}$) and glucose ($R_{Glu,2}$) concentrations in the *N. meningitidis* culture chamber.
b) Dynamics of culture density ($X_{Pg,3}$) and propionic acid ($R_{Pa,3}$) in the *P. gingivalis* culture chamber, along with concentration of propionic acid in the adjacent *N. meningitidis* culture chamber ($R_{Pa,2}$).
Parameters: $P_{Ox,1,2} = 4 \times 10^{-4}\,\mathrm{s}^{-1}$, $P_{Pa,2,3} = 6 \times 10^{-4}\,\mathrm{s}^{-1}$, ($L_{1,2} = 17.8\,\mathrm{mm}$, $L_{2,3} = 93.8\,\mu\mathrm{m}$, $m = 1\,\mathrm{mm}$, $\eta = 10$), $R_{Ox,1} = 100\%$ of saturation from air, $R^0_{Glu,2} = 1\,\mathrm{mM}$, $pH_2 = 7.2$, $pH_3 = 6.0$.

As mentioned in section 2.7.3.6, a set of numerical solutions showed successful maintenance anaerobic conditions, but were interrupted briefly due to a premature depletion of glucose in chamber 2. An example of this is shown in figure 2.14. Although there is a spike in oxygen levels in chamber 2, this oxygen is quickly consumed due to *N. meningitidis*. Therefore, it is apparent that, if glucose depletion had been slower, then the spike in oxygen levels would have never occurred. This demonstrates that the starting conditions are vital, since if the starting concentration of glucose had been higher then depletion of the glucose would have taken more time.

Similarly, especially in the case of high propionic acid permeability, a higher starting culture density of *P. gingivalis* would prevent premature glucose depletion since it would not take as long for propionic acid production to reach a rate high enough to support anaerobic conditions.

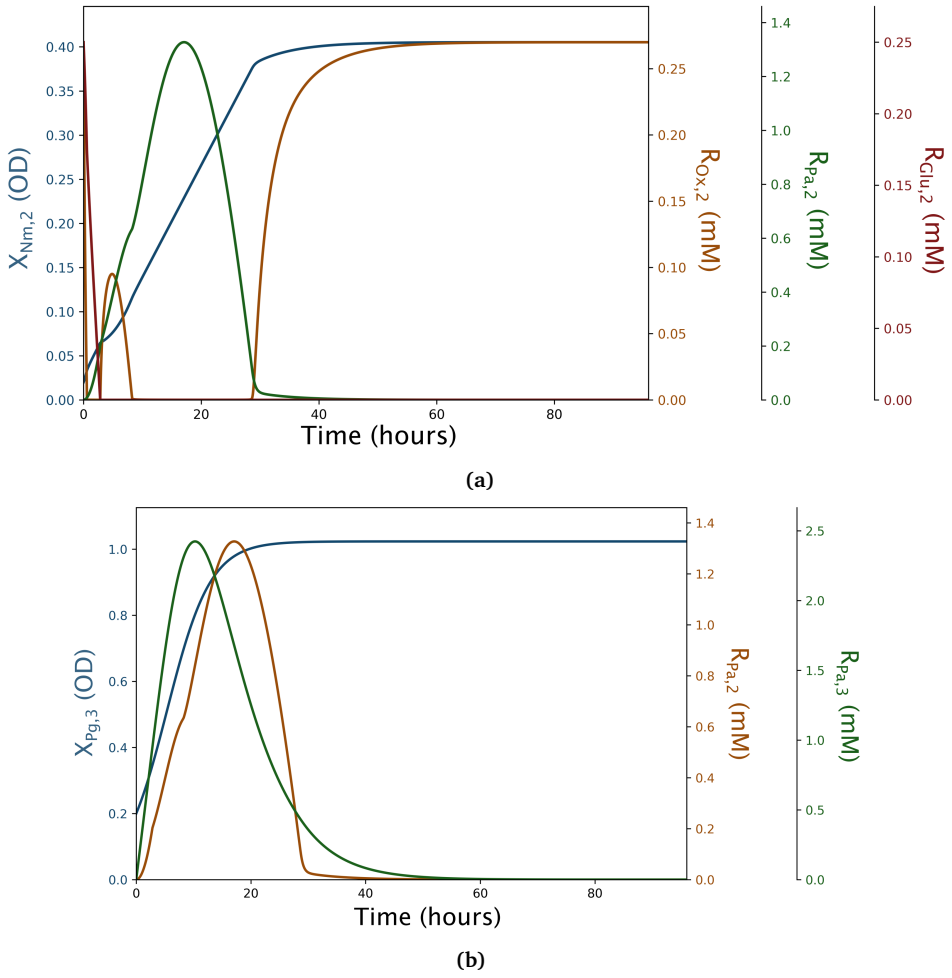

Figure 2.14: Dynamics of non-contact batch co-culture with a premature depletion of glucose.
a) Dynamics of culture density ($X_{Nm,2}$), and oxygen ($R_{Ox,2}$), propionic acid ($R_{Pa,2}$) and glucose ($R_{Glu,2}$) concentrations in the *N. meningitidis* culture chamber.
b) Dynamics of culture density ($X_{Pg,3}$) and propionic acid ($R_{Pa,3}$) in the *P. gingivalis* culture chamber, along with concentration of propionic acid in the adjacent *N. meningitidis* culture chamber ($R_{Pa,2}$).
Parameters: $P_{Ox,1,2} = 3 \times 10^{-4}\,\mathrm{s}^{-1}$, $P_{Pa,2,3} = 6 \times 10^{-4}\,\mathrm{s}^{-1}$, ($L_{1,2} = 23.7\,\mathrm{mm}$, $L_{2,3} = 93.8\,\mu\mathrm{m}$, $m = 1\,\mathrm{mm}$, $\eta = 10$), $R_{Ox,1} = 100\%$ of saturation from air, $R^0_{Glu,2} = 0.25\,\mathrm{mM}$, $pH_2 = 7.2$, $pH_3 = 6.0$.

2.7.3.8 Practical and useful parameter sets

The parameter sets used to exemplify different dynamics of the non-contact batch co-culture system (figures 2.11, 2.12, 2.13 and 2.14) have small chamber sizes ($m = 1\,\mathrm{mm}$). If the chamber size would be increased (e.g. to make fabrication of *in vitro* apparatus more practical) then membrane thicknesses would have to decrease in order to maintain the same permeability values. This limits the range of parameter sets that are practical to use in a physical lab experiment. Figure 2.15 shows one such parameter set, however this was only made possible by reducing the pH of chamber 3 to 5.5 and reducing the concentration of oxygen in chamber 1 to 30% of atmosphere. This may add other technical challenges to setting up the required apparatus. Also, it is unclear how a pH of 5.5 would affect the growth and metabolism of *P. gingivalis* in that chamber.

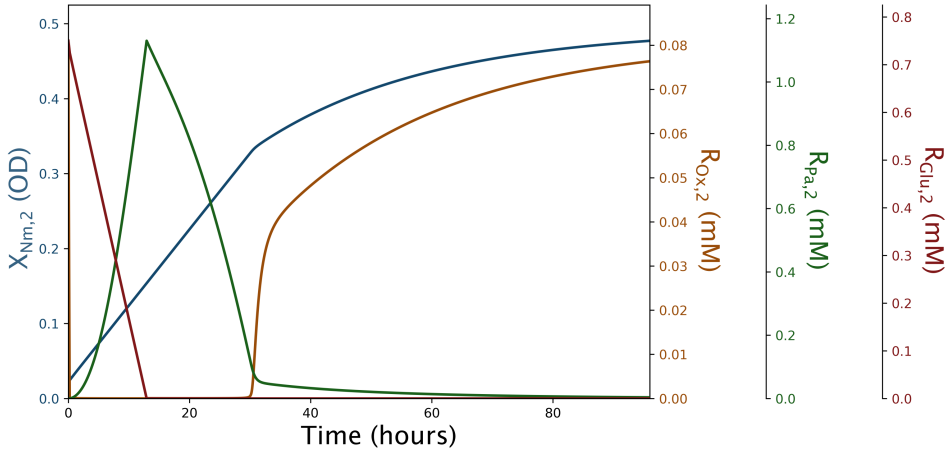

(a)

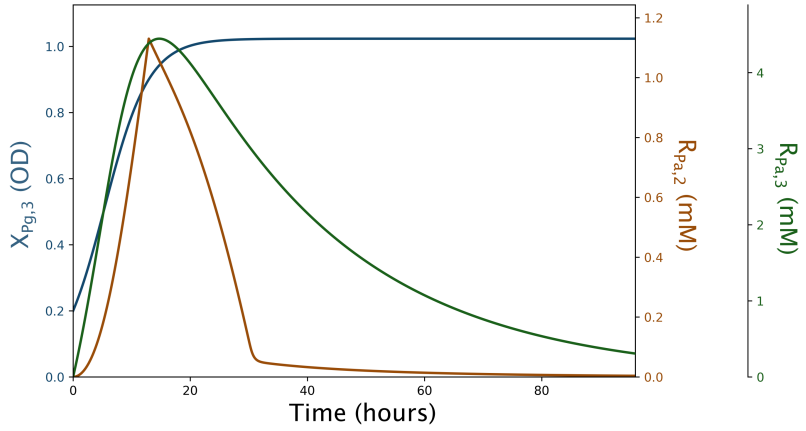

(b)

Figure 2.15: Non-contact batch culture numerical solution showing viable co-culture with sensible parameter values.
a) Dynamics of culture density ($X_{Nm,2}$), and oxygen ($R_{Ox,2}$), propionic acid ($R_{Pa,2}$) and glucose ($R_{Glu,2}$) concentrations in the *N. meningitidis* culture chamber.
b) Dynamics of culture density ($X_{Pg,3}$) and propionic acid ($R_{Pa,3}$) in the *P. gingivalis* culture chamber, along with concentration of propionic acid in the adjacent *N. meningitidis* culture chamber ($R_{Pa,2}$).
Parameters: $P_{Ox,1,2} = 8 \times 10^{-4}\,\mathrm{s}^{-1}$, $P_{Pa,2,3} = 5 \times 10^{-5}\,\mathrm{s}^{-1}$, ($L_{1,2} = 0.155\,\mathrm{mm}$, $L_{2,3} = 0.182\,\mathrm{mm}$, $m = 5\,\mathrm{mm}$, $\eta = 5$), $R_{Ox,1} = 30\%$ of saturation from air, $R^0_{Glu,2} = 0.75\,\mathrm{mM}$, $pH_2 = 7.2$, $pH_3 = 5.5$.

2.7.3.9 Weaknesses of using batch co-cultures

Despite the ability to interpret and control the batch co-culture system, there are several weaknesses that make using it in *in vitro* experiments less than ideal.

The system is sensitive to the starting conditions, therefore if either culture has a significant lag phase then it must be taken into account. If the lag phase is consistent, then a

simple control experiment could be used to account for this. However, if the lag phase is inconsistent due to unknown factors (i.e. slight variation in the preparation procedures) then this could present a significant source of noise. An ideal experiment would not be sensitive to the starting conditions (within reason, since the starting conditions of any such experiment would have to fall within some limits).

Another weakness of this system is that the concentration of propionic acid in chamber 3 has a firm limit set by the carrying capacity of *P. gingivalis* batch cultures. If this could be increased then propionic acid permeability would not have to be so high, and so a wider range of parameter sets could be used. These parameter sets would have larger, more manageable chamber sizes and membranes that are not so thin and fragile.

Ideally, an experimental strategy similar to that used for a constant-concentration propionic acid source (section 2.7.2) would be used. For this to work, the *P. gingivalis* culture must be a source of propionic acid with a constant concentration.

One possible solution to these weaknesses is to use continuous cultures rather than batch cultures.

2.7.4 Propionic acid production by a continuous culture of *P. gingivalis*

A continuous culture is a culture under constant dilution such that growth resources are constantly replenished and inhibitory metabolic products are constantly removed. Continuous cultures can be much denser than batch cultures, and they can therefore have greater total metabolic activity (i.e. $\mu_{Pg,3} \cdot X_{Pg,3}$).

Pure continuous cultures (i.e. with a single population) tend towards a steady state where influx of resources and dilution of the culture is balanced by resource consumption and microbial growth. This steady state is not determined by the starting conditions (as long as the culture starts with some cells and growth resources). Since the propionic acid concentration reaches steady state, the analytical solutions and experimental strategies for a constant-concentration propionic acid source (section 2.7.2) can be used.

These properties are beneficial for studying non-contact co-culture between *N. meningitidis* and *P. gingivalis*, however there are disadvantages to using continuous cultures

instead of batch cultures: namely the time required to reach steady state must be taken into account, and the greater complexity of the apparatus.

Despite these complications, the relative simplicity of a continuous culture ODE system and analytical solutions means it remains an attractive option.

2.7.4.1 ODE system

In continuous culture, *P. gingivalis* growth and the resources in chamber 3 are modelled with the following system of ODEs:

$$\begin{aligned}
\mu_{Pg,3} &= \mu_{Pg}^{max} \cdot \frac{R_{Glu,3}}{R_{Glu,3} + K_{Pg,Glu}}, \\
\frac{dX_{Pg,3}}{dt} &= (\mu_{Pg,3} - D_3) \cdot X_{Pg,3}, \\
\frac{dR_{Glu,3}}{dt} &= (R_{Glu,3}^{in} - R_{Glu,3}) \cdot D_3 - \frac{1}{Y_{Pg,Glu}} \cdot \mu_{Pg,3} \cdot X_{Pg,3}, \\
\frac{dR_{Pa,3}}{dt} &= \frac{Y_{Pg,Glu,Pa}}{Y_{Pg,Glu}} \cdot \mu_{Pg,3} \cdot X_{Pg,3} - R_{Pa,3} \cdot D_3 + P_{Pa,2,3} \cdot \Delta R_{Pa,2,3}.
\end{aligned} \tag{2.25}$$

where $R_{Glu,3}^{in}$ is the concentration of glucose in the diluting input media for chamber 3.

Growth is modelled with the Monod equation (section 2.5.3) with added terms for dilution:

- each variable (microbial population densities and resource concentrations) decreases according to dilution,
- glucose is replenished by the diluting input media ($R_{Glu,3}^{in}$).

In this model there is no propionic acid in the input media, only glucose.

2.7.4.2 Steady state solutions

At steady state the *P. gingivalis* culture density does not change ($dX_{Pg,3}/dt = 0$). Therefore the growth rate must be perfectly balanced by the dilution rate ($\mu_{Pg,3} = D_3$) (or the culture will be no more, i.e. the trivial case $X_{Pg,3} = 0$).

When $\mu_{Pg,3} = D_3$ then (from equations 2.25)

$$R^*_{Glu,3} = K_{Pg,Glu} \cdot \frac{D_3}{(\mu^{max}_{Pg}) - D_3},$$

$$X^*_{Pg,3} = Y_{Pg,Glu} \cdot (R^{in}_{Glu,3} - R^*_{Glu,3}), \tag{2.26}$$

$$R^*_{Pa,3} = \frac{D_3}{D_3 + P_{Pa,2,3} \cdot J^*_{Pa,3}} \cdot \frac{Y_{Pg,Glu,Pa}}{Y_{Pg,Glu}} \cdot X^*_{Pg,3} + \frac{P_{Pa,2,3} \cdot J^*_{Pa,2}}{P_{Pa,2,3} \cdot J^*_{Pa,3} + D_3} \cdot R_{Pa,2}.$$

Since $K_{Pg,Glu}$ is very small then $R^*_{Glu,3} \approx 0$, except when D_3 is very close to μ^{max}_{Pg} (e.g. $D_3 = \mu^{max}_{Pg} - K_{Pg,Glu}$). When $R^*_{Glu,3} = 0$ then

$$X^*_{Pg,3} = Y_{Pg,Glu} \cdot R^{in}_{Glu,3}. \tag{2.27}$$

This shows that the *P. gingivalis* culture density is directly controlled by the concentration of input glucose. In particular, it shows that the culture density is independent of dilution rate. Since the growth rate of the culture is equal to the dilution rate then increasing the dilution rate will increase the metabolic activity of the culture ($\mu_{Pg,3} \cdot X_{Pg,3}$).

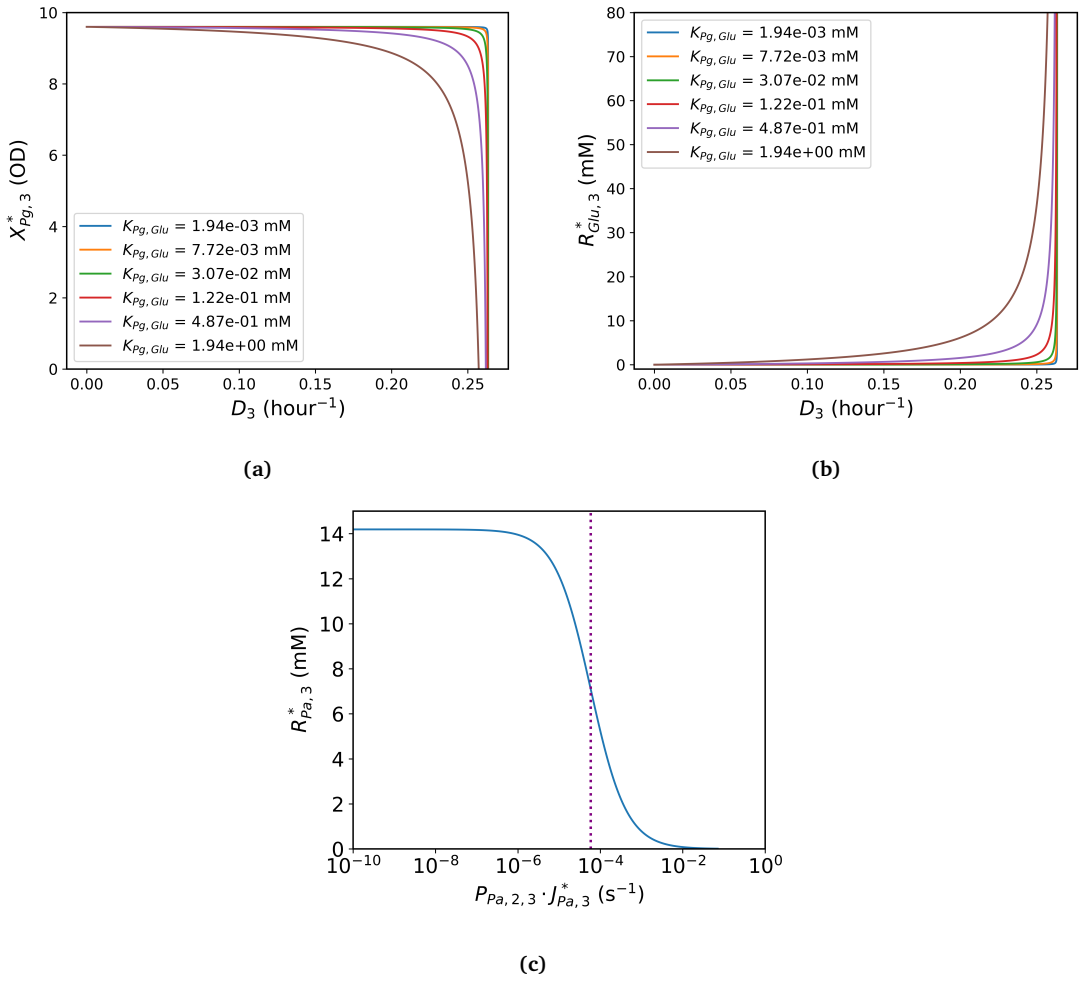

Figure 2.16: Dilution rate and propionic acid permeability affect the *P. gingivalis* culture at steady state.
a) increasing dilution rate (D_3) causes a sharp drop in culture density ($X_{Pg,3}$) as D_3 approaches μ^{max}_{Nm}. This drop is sharper at lower $K_{Pg,Glu}$ values.
b) increasing D_3 causes a sharp rise in glucose concentration $R_{Glu,3}$ in a manner that mirrors plot (a).
c) propionic acid concentration $R_{Pa,3}$ switches from high to low as $P_{Pa,2,3}$ increases to be greater than D_3. The dotted purple line marks the value of D_3.
Parameters: $m = 5\,\text{mm}$, $\eta = 10$, $R^{in}_{Glu,3} = 15\,\text{mM}$, $D_3 = 6.58 \times 10^{-5}\,\text{s}^{-1}$, $pH_2 = 7.2$, $pH_3 = 6.0$. Other parameters are as listed in table 2.2.

.

However, this only applies when the dilution rate is low. As $D_3 \to \mu^{max}_{Pg}$ then the culture begins to "wash out": culture density decreases as the culture cannot grow fast enough to replace losses due to dilution, and glucose concentrations increase as the culture is not dense enough to utilise all of the glucose supply. This is shown in figure 2.16a&b and the steady state solution equations (equations 2.26): when $D_3 \to \mu^{max}_{Pg}$ then $R^*_{Glu,3}$ increases and so $X^*_{Pg,3}$ decreases. Figure 2.16a&b shows that the suddenness of the "washing out" is more pronounced at lower $K_{Pg,Glu}$ values: when $K_{Pg,Glu} =$

$1.94 \times 10^{-4}\,\mathrm{mM}$ (as in table 2.2) then "washing out" only begins when D_3 is practically equal to μ_{Pg}^{max}.

The solution for $R^*_{Pa,3}$ is not simple. However, given certain conditions, it can be simplified. When $R^*_{Glu,3} \approx 0$ then the simplified equation 2.27 can be used, and propionic acid in chamber 2 can be assumed to be immediately consumed ($R_{Pa,2} = 0$). Therefore

$$R^*_{Pa,3} = \frac{D_3}{D_3 + P_{Pa,2,3} \cdot J^*_{Pa,3}} \cdot Y_{Pg,Glu,Pa} \cdot R^{in}_{Glu,3}. \tag{2.28}$$

This is an important equation since it determines the concentration gradient of propionic acid between chamber 3 and chamber 2. Notably, $R^*_{Pa,3}$ is proportional to the input glucose concentration. Its relationship with D_3 and $P_{Pa,2,3} \cdot J^*_{Pa,3}$ is also important: when there is no diffusion (when $P_{Pa,2,3} = 0$) then D_3 has no effect, however when there is diffusion (when $P_{Pa,2,3} > 0$) then $R^*_{Pa,3}$ decreases. When $D_3 \gg P_{Pa,2,3} \cdot J^*_{Pa,3}$ then this decrease is small, however as $P_{Pa,2,3} \cdot J^*_{Pa,3}$ increases relative to D_3 then this decrease becomes larger (Fig2.16c). In other words, the significance of D_3 is that: when D_3 is higher then, although the concentration ($R^*_{Pa,3}$) is not any higher, the system can handle a higher "load" of propionic acid diffusion. At the same time, the high levels of propionic acid in chamber 3 may inhibit the growth of *P. gingivalis* (a factor that is not included in this model). Therefore it may be necessary to keep $R^*_{Pa,3}$ low. To achieve this without reducing the production rate of propionic acid, $P_{Pa,2,3} \cdot J^*_{Pa,3}$ must be greater than D_3.

It is therefore useful to measure the productivity ($R^P_{Pa,3}$) of the *P. gingivalis* culture (i.e. the rate of production of propionic acid). From equations 2.25, when at steady state, and when equation 2.27 applies, this is

$$R^P_{Pa,3} = D_3 \cdot Y_{Pg,Glu,Pa} \cdot R^{in}_{Glu,3}. \tag{2.29}$$

This equation shows the role of D_3 more clearly: it directly controls the production of propionic acid by the continuous culture of *P. gingivalis*.

2.7.4.3 Maintenance of anaerobic conditions by *N. meningitidis* adjacent to *P. gingivalis* continuous culture

The question of whether anaerobic conditions will be maintained at steady state by *N. meningitidis* growth can be answered using the analytical steady state solutions.

2.7.4.3.1 Conditions for anaerobic conditions Anaerobic conditions are maintained when the yield of *N. meningitidis* from utilisation of all available oxygen is less than the yield from utilisation of all available propionic acid (i.e. $y_{Nm,2,Ox} < y_{Nm,2,Pa}$, section 2.7.2.3). At steady state, the concentration of propionic acid in the *P. gingivalis* chamber is constant (with a concentration of $R^*_{Pa,3}$). Therefore, the partial yields are defined by equations 2.19 when $R_{Pa,3} = R^*_{Pa,3}$.

Analytical solutions to this condition ($y_{Nm,2,Ox} < y_{Nm,2,Pa}$) are shown in figure 2.17.

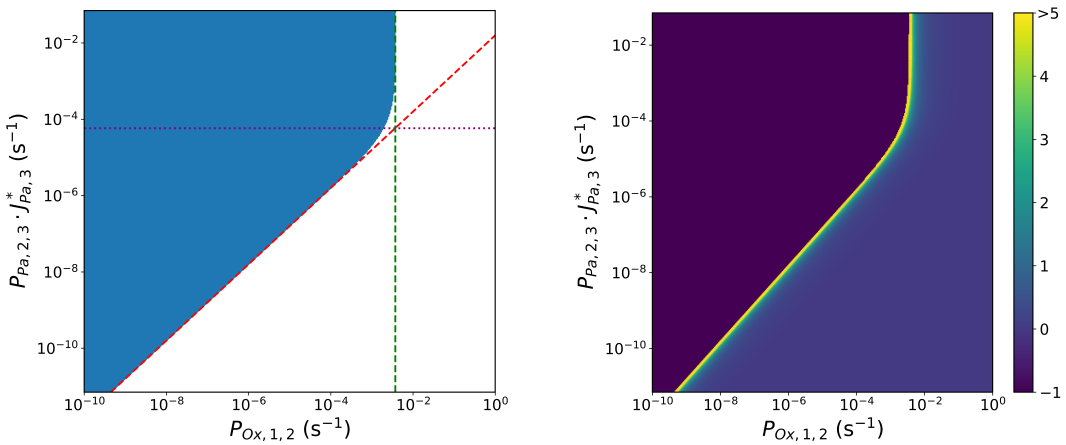

(a) **(b)**

Figure 2.17: Anaerobic conditions at steady state with continuous *P. gingivalis* culture at varying permeabilities.
a) Shaded blue areas indicate that *N. meningitidis* culture growth is being limited by propionic acid and therefore will maintain anaerobic conditions (as determined by analytical solutions). The dotted purple line indicates the dilution rate of chamber 3 (D_3). The dotted red line is the boundary between oxygen-limited and propionic acid-limited growth when permeability $P_{Pa,2,3}$ is much lower than D_3. The dotted green line is this boundary when $P_{Pa,2,3}$ is much higher than D_3.
b) Analytical solution for $y_{Nm,2,Pa}/(y_{Nm,2,Ox} - y_{Nm,2,Pa})$ (i.e. the duration of propionic acid depletion relative to duration of glucose depletion) over a range of oxygen ($P_{Ox,1,2}$) and propionic acid ($P_{Pa,2,3}$) permeabilities. A value of -1 indicates that $y_{Nm,2,Pa} > y_{Nm,2,Ox}$ and so propionic acid does not deplete. Parameters: $m = 5\,\text{mm}$, $\eta = 10$, $R_{Ox,1} = 100\%$ of saturation from air, $R^{in}_{Glu,3} = 15\,\text{mM}$, $D_3 = 6.58 \times 10^{-5}\,\text{s}^{-1}$, $pH_2 = 7.2$, $pH_3 = 6.0$. Other parameters are as listed in table 2.2.

As shown previously (section 2.7.4.2): when $P_{Pa,2,3}$ is less than D_3 then $R^*_{Pa,3} \approx Y_{Pg,Glu,Pa} \cdot R^{in}_{Glu,3}$, and so $y_{Nm,Pa,2}$ has a linear relationship with $P_{Pa,2,3}$. In this case, $y_{Nm,2,Ox} < y_{Nm,2,Pa}$ when $P_{Ox,1,2} < (Y_{Nm,Pa} \cdot Y_{Pg,Glu,Pa}/Y_{Nm,Ox}) \cdot (R^{in}_{Glu,3}/R_{Ox,1}) \cdot J^*_{Pa,3} \cdot P_{Pa,2,3}$ showing that the boundary is set by a linear relationship between $P_{Ox,1,2}$ and $P_{Pa,2,3}$. In other words, in order to maintain anaerobic conditions then the permeabilities must be at least proportional to each other. On this boundary, any increase in oxygen permeability must be met with a proportional increase in propionic acid permeability. This boundary is represented by the red dotted line in figure 2.17a.

When $P_{Pa,2,3} \cdot J^*_{Pa,3}$ is greater than D_3 then $R^*_{Pa,3} \approx 0$ (section 2.7.4.2) and so any further increases in $P_{Pa,2,3 \cdot J^*_{Pa,3}}$ will do nothing to increase the flux of propionic acid to chamber 2. Therefore, in this case, $y_{Pa,Nm}$ is not affected by $P_{Pa,2,3} \cdot J^*_{Pa,3}$. This is shown by the equations: when $P_{Pa,2,3} \cdot J^*_{Pa,3}$ is greater than D_3 then $R^*_{Pa,3} \approx (1/P_{Pa,2,3} \cdot J^*_{Pa,3}) \cdot Y_{Pg,Glu,Pa} \cdot R^{in}_{Glu,3}$ and so equation 2.19 becomes $y_{Nm,Pa,2} = Y_{Nm,Pa} \cdot Y_{Pg,Glu,Pa} \cdot R^{in}_{Glu,3}$ which is not a function of $P_{Pa,2,3}$. This imposes an upper limit on oxygen permeability of $\cdot P_{Ox,1,2} < \cdot (Y_{Nm,Pa} \cdot Y_{Pg,Glu,Pa}/Y_{Nm,Ox}) \cdot (R^{in}_{Glu,3}/R_{Ox,1})$. To exceed this limit, propionic acid production must be increased, either by increasing $R^{in}_{Glu,3}$ or D_3. This limit is represented by the green dotted line in figure 2.17a.

These two solutions form boundaries of the parameter sets for which anaerobic conditions are maintained at steady state (Fig2.17a). Which of the two boundaries apply is determined by whether $P_{Pa,2,3} \cdot J^*_{Pa,3}$ is greater or less than D_3 (represented by the purple dotted line in figure 2.17a).

Scenarios where $y_{Nm,2,Pa} < y_{Ox,2,Pa}$ (i.e. no anaerobic conditions at steady state), but that are also close to the $y_{Nm,2,Pa} = y_{Ox,2,Pa}$ boundary, are useful because they have an oxygen-limited phase of *N. meningitidis* growth followed by a propionic acid-limited phase (section 2.7.2). Measuring the duration of these phases can be used to quantify the metabolic interaction between the cultures. Figure 2.17b shows the degree to which this glucose depletion time is extended by the supply of propionic acid. The parameter sets for which it is extended to any practical degree lay very close to the boundary, therefore the oxygen and propionic acid permeabilities must be balanced. This is a simple, useful guideline for generating practical and useful parameter sets.

If the alternative experimental strategy of varying propionic acid supply is used (section 2.7.2), then the range of values used must still span this boundary, and so this same guideline is still useful.

2.7.4.3.2 Comparison with batch culture *P. gingivalis* in section 2.7.3.6 These results parallel the behaviour of two adjacent batch cultures (section 2.7.3.6). Both results (i.e. parameter sets for which anaerobic conditions are maintained) are bounded by a maximum $P_{Ox,1,2}$ value based on the rate of propionic acid production. Also, at lower $P_{Pa,2,3}$ values, there is an upper limit on the concentration of propionic acid meaning that $P_{Pa,2,3}$ values must fall within a boundary set by a linear relationship between $P_{Pa,2,3}$ and $P_{Ox,1,2}$. This means that there is no lower limit on the permeabilities.

However, the behaviours of batch and continuous culture systems are different in one key way. With a continuous culture of *P. gingivalis*, limit of the permeabilities may be shifted by varying the dilution rate and glucose input concentration (D_3 and $R^{in}_{Glu,3}$). In batch cultures, however, the limits are set by parameters intrinsic to the biology of the organisms (μ^{max}_{Pg}, $Y_{Pg,Glu}$ and $Y_{Pg,Glu,Pa}$) and so cannot be moved.

2.7.4.3.3 Practicality of experiment parameters with continuous *P. gingivalis* culture To determine which parameter values (i.e. *in vitro* apparatus design and experimental conditions) to use, the steady state analytical solutions are of vital importance for finding parameter values that are realistic, practical and that produce a useful result. If the following constraints are followed:

1. A convenient chamber size and mixing factor of $m = 5\,\mathrm{mm}$ and $\eta = 10$
2. Propionic acid concentrations should not exceed $10\,\mathrm{mM}$. Beyond these concentrations microbial growth is likely to be inhibited
3. PDMS membrane thicknesses not below $20\,\mu\mathrm{m}$
4. pH in each chamber that is compatible with microbial growth of their cultures
5. Reasonable culture density for *P. gingivalis*
6. Dilution rate less than the maximum *P. gingivalis* growth rate
7. Balanced partial yields from oxygen and propionic acid ($y_{Nm,2,Pa} \approx y_{Nm,2,Ox}$)
8. Generation of anaerobic conditions

then a practical approach is to start with the objective of maximising propionic acid diffusion (in order to maximise the measured growth response by *N. meningitidis*) by using the thinnest membrane thickness ($L_{2,3}$) of $20\,\mu\mathrm{m}$, a low pH in chamber 3 (pH 6.0) and the maximum propionic acid concentration in chamber 3 ($R_{Pa,3}$) of $10\,\mathrm{mM}$.

$R_{Pa,3}$ is dependent on $R^{in}_{Glu,3}$ and D_3. The values that are used for these *P. gingivalis* parameters are not relevant to the *N. meningitidis* culture as long as the propionic acid concentration gradient is maintained. A target culture density of *P. gingivalis* ($X_{Pg,3}$) can be used to pick parameter values. In this case, when $D_3 = P_{Pa,2,3} \cdot J^*_{Pa,3} = 1.75 \times 10^{-5}\,\mathrm{s}^{-1}$ then $R^{in}_{Glu,3} = 21.1\,\mathrm{mM}$ and $X_{Pg,3} = 2.54\ \mathrm{OD}_{600}$. Not only are these parameter values practical and consistent with the above constraints, but the fact that $D_3 = P_{Pa,2,3} \cdot J^*_{Pa,3}$ means that the system is sensitive to D_3 changes, a behaviour that be useful when making fine adjustments to an experiment.

These parameters give a partial yield from propionic acid of $y_{Nm,Pa,2} = 2.33 \times 10^{-3}\,\mathrm{g\,s}^{-1}$ (dw). When $y_{Nm,Ox,2} = y_{Nm,Pa,2}$ (and $R_{Ox,1}$ is at saturation concentration from oxygen in the atmosphere) then $L_{1,2} = 1.02\,\mathrm{mm}$. This value for $L_{1,2}$ represents the lower limit of the membrane thickness in this instance. If it was thinner than this, then excess oxygen would diffuse into the system and compromise the anaerobic conditions that *P. gingivalis* needs to thrive.

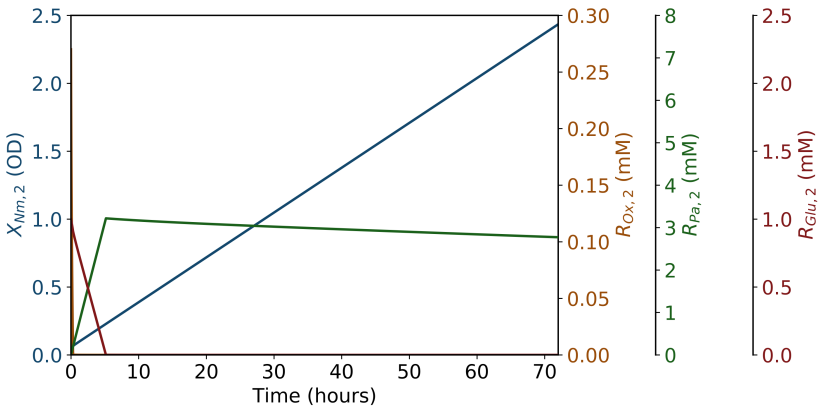

(a)

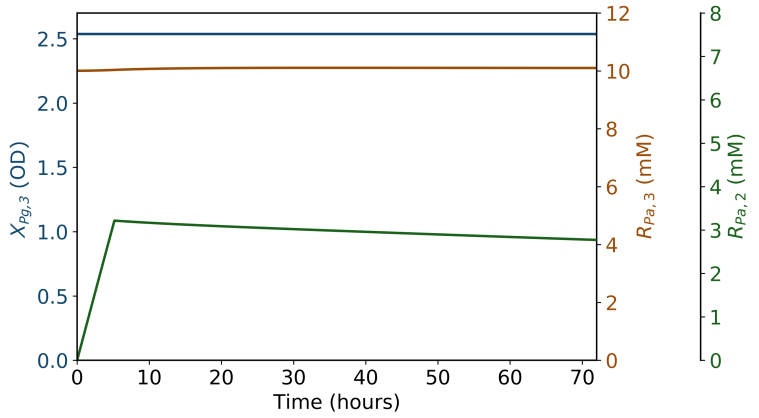

(b)

Figure 2.18: Continuous *P. gingivalis* culture dynamics showing viable co-culture with sensible parameter values.
a) Dynamics of culture density ($X_{Nm,2}$), and oxygen ($R_{Ox,2}$), propionic acid ($R_{Pa,2}$) and glucose ($R_{Glu,2}$) concentrations in the *N. meningitidis* culture chamber.
b) Dynamics of culture density ($X_{Pg,3}$) and propionic acid ($R_{Pa,3}$) in the *P. gingivalis* culture chamber, along with concentration of propionic acid in the adjacent *N. meningitidis* culture chamber ($R_{Pa,2}$).
Parameters: $m = 5\,\text{mm}$, $\eta = 10$, $R_{Ox,1} = 100\%$ of saturation from air, $R^{in}_{Glu,3} = 21.1\,\text{mM}$, $D_3 = 1.75 \times 10^{-5}\,\text{s}^{-1}$, $P_{Ox,1,2} = 7.80 \times 10^{-4}\,\text{s}^{-1}$, $P_{Pa,2,3} \cdot J^{*}_{Pa,3} = 1.75 \times 10^{-5}\,\text{s}^{-1}$, $L_{1,2} = 1.02\,\text{mm}$, $L_{2,3} = 20.0\,\mu\text{m}$, $pH_2 = 7.2$, $pH_3 = 6.0$, $X^{0}_{Nm,2} = 0.05$ OD_{600}, $R^{0}_{Glu,2} = 1\,\text{mM}$. Other parameters are as listed in table 2.2.

When these parameters are used, the dynamics of the numerical solution (Fig2.18) show that, as predicted by the analytical solutions, anaerobic conditions are maintained. The culture density of *N. meningitidis* in chamber 2 increases linearly with time. This growth is oxygen-limited, meaning the growth rate is equal to $y_{Nm,2,Ox}$, and so it is determined by oxygen diffusion into chamber 2. Once glucose is depleted, then the concentration of propionic acid in chamber 2 ($R_{Pa,2}$) starts to decrease. This is because

it approaches a steady state value in chamber 2. This steady state value is a function of the excess propionic acid remaining after consumption by *N. meningitidis* (i.e. the margin between $y_{Nm,2,Ox}$ and $y_{Nm,2,Pa}$), and the rate of loss of propionic acid as it diffuses from chamber 2 to chamber 1. If propionic acid was not lost from chamber 2 in this way then the equilibrium value would be determined by the propionic acid concentration in chamber 3 and the difference in pH (6.0 compared to 7.2). Therefore, the steady state concentration of propionic acid in chamber 2 would be more than 15 times greater than in chamber 3.

A $R_{Pa,2}$ that steadily increases to a very high steady state value could be useful for experiments since it could be used to assess how propionic acid inhibits bacterial growth in the system.

2.7.4.4 Time to steady state

A practical and useful set of parameters has been demonstrated, however the system has only been assessed with a steady state *P. gingivalis* culture. When the system is implemented *in vitro* then it will take some time to reach steady state. The time this takes must be factored in to any assessment of practicality and usefulness of a parameter set.

The factors that affect the time it takes for the system to reach steady state have been determined by analysing the dynamics of numerical solutions. Each variable ($X_{Pg,3}$ and $R_{Pa,3}$) is investigated in turn. In this analysis, the variable being investigated will start with an initial value of half the steady state value. The time taken for the variable to get within 5% of its steady state value will be used as a measure of how quickly the system approaches steady state.

Figure 2.19a shows that *P. gingivalis* culture density is not as quick to approach steady state as propionic acid concentration. This speed is dependent on dilution rate (D_3) with a higher D_3 resulting in a faster approach to steady state. However, the results show that, as D_3 approaches μ_{Pg}^{max}, then $X_{Pg,3}$ is slower to approach steady state.

Figure 2.19b shows that the speed at which $R_{Pa,3}$ approaches steady state is also dependent on the propionic acid permeability $P_{Pa,2,3}$ (in a similar way to D_3).

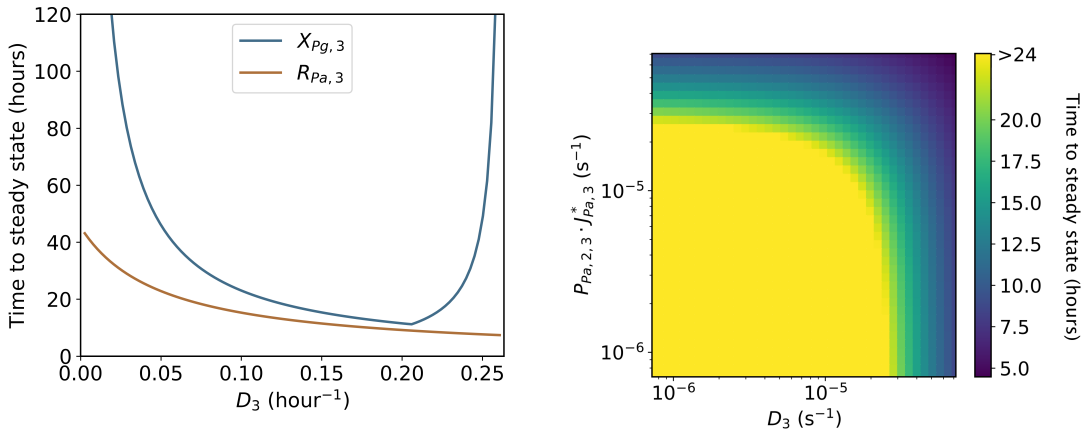

Figure 2.19: Time for *P. gingivalis* continuous culture to reach steady state is dependent on dilution rate and propionic acid permeability. Variables were perturbed to 50% of the steady state value. A return to steady state was defined as a return to within 5% of the steady state value. Each variable was perturbed independently.
a) Time for $X_{Pg,3}$ and $R_{Pa,3}$ to return to steady state at different dilution rates D_3.
b) Time for $R_{Pa,3}$ to return to steady state at different dilution rates D_3 and permeability values $P_{Pa,2,3}$. Parameters: $m = 5\,\mathrm{mm}$, $\eta = 10$, $R_{Ox,1} = 100\%$ of saturation from air, $R^{in}_{Glu,3} = 15\,\mathrm{mM}$, $P_{Ox,1,2} = 6 \times 10^{-4}\,\mathrm{s}^{-1}$, $P_{Pa,2,3} = 2 \times 10^{-4}\,\mathrm{s}^{-1}$, $L_{1,2} = 1.57\,\mathrm{mm}$, $L_{2,3} = 31.5\,\mu\mathrm{m}$, $pH_2 = 7.2$, $pH_3 = 6.0$. Other parameters are as listed in table 2.2.

The time scales in these time-to-steady-state analyses range between 10-100 h. This does not mean that, in an *in vitro* experiment, the system must be left for this long before the *N. meningitidis* culture is introduced to chamber 2. The *P. gingivalis* culture can instead be set up with initial values much closer to the steady state culture density than used in the time-to-steady-state analysis. Also, even when the *P. gingivalis* culture starts far from steady state (at 50% of the steady state value), *N. meningitidis* growth is unaffected when compared to a situation where the *P. gingivalis* culture starts at steady state (Fig2.20 and Fig2.18).

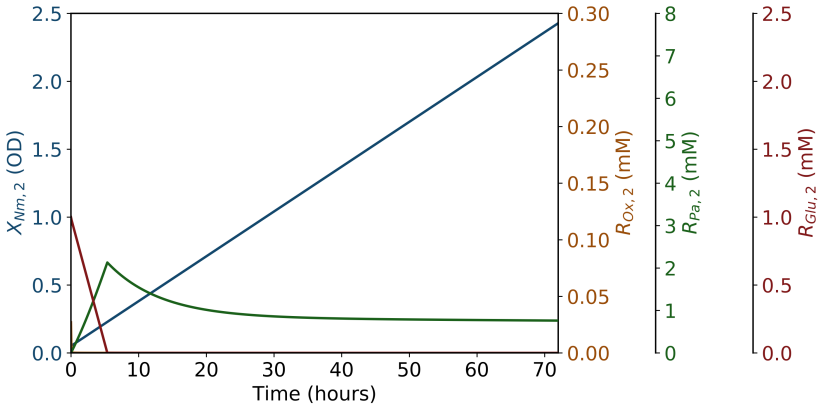

(a)

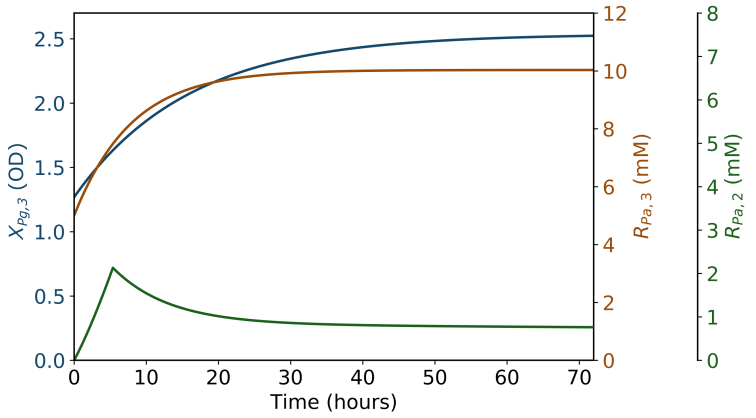

(b)

Figure 2.20: Non-steady-state *P. gingivalis* continuous cultures adjacent to a *N. meningitidis* batch culture. Initial culture density $X_{Pg,3}$ and propionic acid concentration $R_{Pa,3}$ are at 50% of steady-state.
a) Dynamics of culture density ($X_{Nm,2}$), and oxygen ($R_{Ox,2}$), propionic acid ($R_{Pa,2}$) and glucose ($R_{Glu,2}$) concentrations in the *N. meningitidis* culture chamber.
b) Dynamics of culture density ($X_{Pg,3}$) and propionic acid ($R_{Pa,3}$) in the *P. gingivalis* culture chamber, along with concentration of propionic acid in the adjacent *N. meningitidis* culture chamber ($R_{Pa,2}$).
Parameters: $m = 5\,\text{mm}$, $\eta = 10$, $R_{Ox,1} = 100\%$ of saturation from air, $R^{in}_{Glu,3} = 21.1\,\text{mM}$, $D_3 = 1.75 \times 10^{-5}\,\text{s}^{-1}$, $P_{Ox,1,2} = 7.80 \times 10^{-4}\,\text{s}^{-1}$, $P_{Pa,2,3} \cdot J^{*}_{Pa,3} = 1.75 \times 10^{-5}\,\text{s}^{-1}$, $L_{1,2} = 1.02\,\text{mm}$, $L_{2,3} = 20.0\,\mu\text{m}$, $pH_2 = 7.2$, $pH_3 = 6.0$, $X^{0}_{Nm,2} = 0.05$ OD_{600}, $R^{0}_{Glu,2} = 1\,\text{mM}$. Other parameters are as listed in table 2.2.

However, if anaerobic conditions are dependent on propionic acid accumulation while glucose in chamber 2 is utilised, then non-steady-state conditions of the *P. gingivalis* affect the duration of propionic acid depletion (Fig2.21). In the case shown in figure 2.21, when the initial propionic acid concentration and *P. gingivalis* culture density is less than the steady state values then propionic acid accumulation is slowed and depletion is faster. This is important since the duration of propionic acid depletion is a

key measurement that can be used to quantify the metabolic interaction between the two cultures. Therefore, the system must first be allowed to reach steady state when this experimental strategy is used.

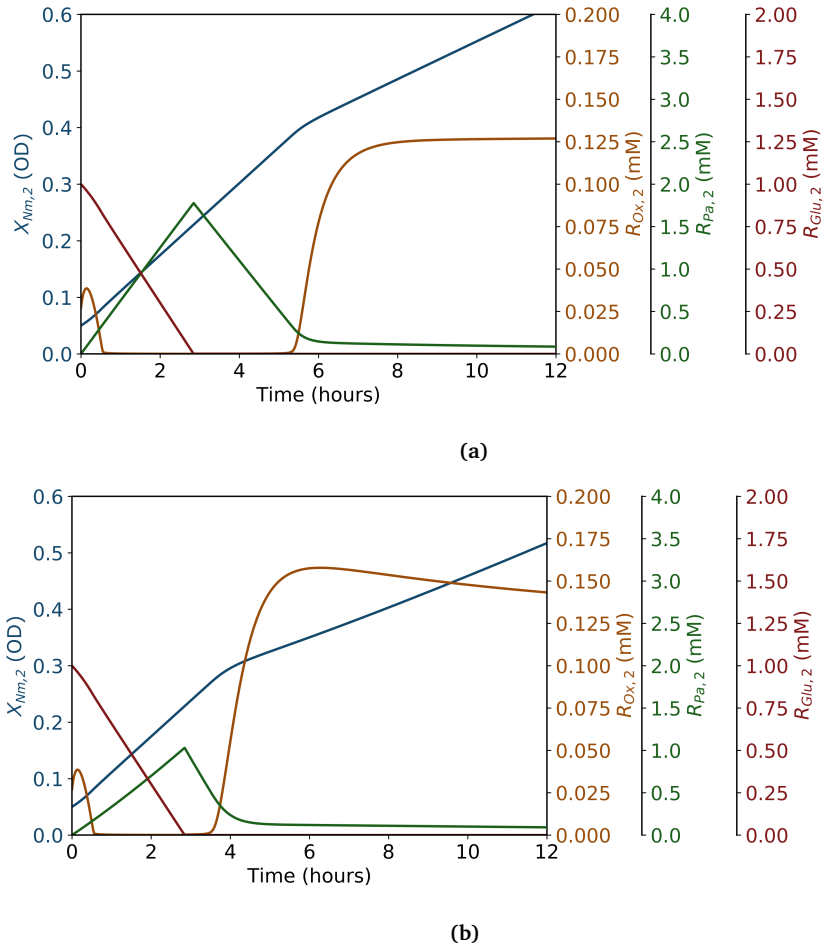

Figure 2.21: Propionic acid depletion with a steady-state and non-steady-state *P. gingivalis* continuous cultures adjacent to a *N. meningitidis* batch culture.
a) Variable values start at steady state.
b) Initial culture density $X_{Pg,3}$ and propionic acid concentration $R_{Pa,3}$ at 50% of steady-state.
Parameters: $m = 5\,\text{mm}$, $\eta = 10$, $R_{Ox,1} = 100\%$ of saturation from air, $R^{in}_{Glu,3} = 21.1\,\text{mM}$, $D_3 = 1.75 \times 10^{-5}\,\text{s}^{-1}$, $P_{Ox,1,2} = 1.50 \times 10^{-3}\,\text{s}^{-1}$, $P_{Pa,2,3} \cdot J^{*}_{Pa,3} = 1.75 \times 10^{-5}\,\text{s}^{-1}$, $L_{1,2} = 137\,\mu\text{m}$, $L_{2,3} = 20.0\,\mu\text{m}$, $pH_2 = 7.2$, $pH_3 = 6.0$, $X^{0}_{Nm,2} = 0.05$ OD_{600}, $R^{0}_{Glu,2} = 1\,\text{mM}$. Other parameters are as listed in table 2.2.

If the approach to steady state is too slow to be practical then it can be sped up by increasing D_3 and $P_{Pa,2,3}$, and the size of the chambers can be decreased. However, at the dimensions used in section 2.7.4.3.3, the approach to steady state is fast enough to be practical.

2.7.4.5 Comparison to batch culture *P. gingivalis*

A continuous culture of *P. gingivalis* was first proposed due to inadequacies of batch cultures (section 2.7.3.9). The use of continuous culture makes the system more convenient to use *in vitro* since the starting conditions of *P. gingivalis* culture do not need to be precise or consistent.

Continuous culture also gives a greater ability to fine tune the system using insight gained from the steady state analytical solutions. This gives more control over the propionic acid supply beyond setting the initial culture density of *P. gingivalis*, the pH or the permeability between chamber 2 and 3. In contrast, the propionic acid supply can also be controlled by varying dilution rate and input glucose concentration of chamber 3.

The stable concentration of propionic acid in chamber 3 is also beneficial since it can be kept at levels that are high enough to support *N. meningitidis* growth but low enough so that it does not inhibit growth. This contrasts with the batch culture system where propionic acid concentration may spike to levels that are high enough to inhibit growth and then drop to levels that limit *N. meningitidis* growth and compromise anaerobic conditions.

An increased possible concentration of propionic acid in chamber 3 is a potential benefit of continuous *P. gingivalis* culture. However, this may not be so useful since growth inhibition of propionic acid also places an upper limit on $R_{Pa,3}$. When choosing a practical set of parameters, a maximum propionic acid concentration of $10\,\mathrm{mM}$ was chosen for both of the chambers. Since the concentration is constant at steady state, the average concentration gradient of propionic acid is steeper (therefore increasing flux of propionic acid into chamber 2). However, similar to *P. gingivalis* batch culture, this flux is still limited by diffusion across the PDMS membrane.

The permeabilities that give rise to "successful" experiments (dynamics where anaerobic conditions are maintained by *N. meningitidis* oxygen consumption) are similar between batch and continuous *P. gingivalis* cultures, they are both limited by the same constraints. However, due to the greater consistency of propionic acid supply and greater fine-tuning possible with continuous cultures, the parameters are more practical (more convenient to create *in vitro*, and having a greater margin for error).

2.7.4.6 Further developments

There several extensions to the model and analysis that may be useful for studying the metabolic interaction between *N. meningitidis* and *P. gingivalis*.

Propionic acid has antimicrobial activity, inhibiting the growth of a wide variety of bacteria, including *P. gingivalis* (Huang *et al.*, 2011) and likely including *N. meningitidis* (section 1.3.3.5). This antimicrobial activity may be an important aspect of this metabolic relationship since *N. meningitidis* may remove this product inhibition to increase *P. gingivalis* growth. Therefore, the nature of this growth inhibition must be determined (whether it is simply concentration-dependent). Then the model must be parametrised based on *in vitro* experiments (e.g. growing batch cultures with varying concentrations of propionic acid in the growth medium).

In setting up an *in vitro* non-contact co-culture, it may be useful to start with a continuous culture of *N. meningitidis* in chamber 2. This culture could generate anaerobic conditions in preparation for establishing the *P. gingivalis* culture in chamber 3. Following this, the *N. meningitidis* could then be partially washed-out, and then the dilution rate could be cut to 0 to transition it to a batch culture. Alternatively, it may be possible to use the *N. meningitidis* culture as a continuous culture in experiments. These possibilities would first need to be explored in further variations of the current ODE model.

2.8 Quantification of metabolic interaction between *N. meningitidis* and *P. gingivalis*

The purpose of studying this non-contact co-culture between a *N. meningitidis* and a *P. gingivalis* culture is to detect and quantify the metabolic interactions between them.

When both cultures are grown as batch cultures, the duration of time that anaerobic conditions are maintained (as determined by when *N. meningitidis* growth slows down, or by the change in colour of an oxygen-sensitive dye) could be used as a feature to be detected. These are both possible to measure by monitoring the optical density of each culture chamber. Combined with knowledge of the permeabilities values (calculated with the assistance of other previous experiments such as described in section 2.7.2

with a known concentration of propionic acid prepared in chamber 3) and a control experiment with no *P. gingivalis* culture in chamber 3 then this feature could be used in model fitting. Data collected from an *in vitro* experiment could be fitted to the ODE system in order to calculate yields and verify assumptions (e.g. estimated values for the growth rate of *N. meningitidis* with propionic acid as carbon source, and half-rate constants). With knowledge about the oxygen and propionic acid permeabilities, it would be possible to calculate the relative yield of propionic acid production and propionic acid utilisation. If either of these yields are measured independently (e.g. by using gas chromatography to measure the concentration of propionic produced by a *P. gingivalis* culture) then the other value can be calculated. However, even without this, the relative yield (or in other words, yield of *N. meningitidis* from *P. gingivalis*) is an effective method of quantifying this microbial interaction.

When *P. gingivalis* is grown as a continuous culture, different methods can be used to measure the yield of *N. meningitidis* from propionic acid. With batch culture, the interaction can be quantified by measuring the point at which the co-culture is no longer viable. However, with a continuous culture, the production of propionic acid reaches steady state and so will continue to be produced indefinitely.

This is why, with a continuous *P. gingivalis* culture, it is necessary to either:

- balance the *N. meningitidis* partials yields from oxygen and propionic acid so that propionic acid slowly depletes once the initial glucose in the culture medium has been used up (section 2.7.2.4).
- vary the steady state propionic acid concentration, either by varying dilution rate or input glucose rate (section 2.7.4.6).

As propionic acid in the *N. meningitidis* chamber decreases, eventually anaerobic conditions become compromised and *N. meningitidis* growth rate begins to decrease. This can be measured with the same methods as with the batch culture. With knowledge about oxygen permeability and yield, then the yield of *N. meningitidis* from the propionic acid produced by the *P. gingivalis* culture can be calculated.

Another aspect of the metabolic interaction to be characterised and quantified is the release of *P. gingivalis* growth inhibition by the consumption of propionic acid by *N. meningitidis* (section 2.7.4.6). When the *P. gingivalis* culture productivity is high compared to the propionic acid permeability (i.e. $D_3 \gg P_{Pa,2,3} \cdot J^*_{Pa,3}$) then the consumption

of propionic acid has practically no effect on the concentration in the *P. gingivalis* chamber. Therefore, in this situation, there is no release of growth inhibition by propionic acid in that chamber. However, when $D_3 < P_{Pa,2,3} \cdot J^*_{Pa,3}$ then the diffusion gradient of propionic acid between the chambers has a strong effect on the concentration in the *P. gingivalis* chamber. In this scenario, the metabolic interaction is two-way, and it could be captured in an *in vitro* experiment. Growth inhibition by propionic acid would then be included in the mathematical model to interpret results and assess the importance of this factor *in vivo*.

It is possible that there are other aspects to the metabolic interaction between these two species. The primary strength of the non-contact co-culture method is that interactions via *all* volatile substances will be captured, even if it is not possible to determine the precise contribution of each individual substance. The purpose of this assay is to measure how one culture affects another via volatile substances. To this aim it may be useful to represent all of the volatile metabolites involved in the metabolic interaction as a single abstract resource.

The precision of the measurements taken using this non-contact co-culture system is not possible to ascertain at this point, although the use of a variety of different experimental conditions (e.g. different permeabilities and strategies) may be useful for increasing statistical confidence in these measurements. The suitability of the model, as outlined so far in this chapter, is also yet to be tested. The model assumptions have precedent (as laid out in each part of section 2.5), and further extensions to the model are possible if required. Implementation of this system, and collection of *in vitro* results, is needed to determine if this model is appropriate for the task of quantifying the metabolic interaction.

2.9 Time scale of experiments

The factors that determine the time scale of experiments are different for each experimental strategy.

When partial yields of *N. meningitidis* from oxygen and propionic acid are balanced, such that propionic acid is allowed to accumulate and then deplete (section 2.7.2.4), then the duration of viable co-culture (and therefore the experiment) is determined by:

1. the time it takes the initial glucose to be depleted, which is dependent on initial glucose concentration and oxygen flux into the *N. meningitidis* culture chamber.
2. the time it takes the accumulated propionic acid to be depleted, which is dependent on the balance of *N. meningitidis* partial yields from oxygen and propionic acid, and the amount of propionic acid that was able to accumulate while glucose was still present in the growth media.

When the source of propionic acid is from a batch culture of *P. gingivalis*, then the duration of viable co-culture (and therefore the experiment) is measured by how long *P. gingivalis* produces propionic acid for (which stops at stationary phase), and how long anaerobic conditions are maintained by *N. meningitidis* utilising this propionic acid. The time to reach stationary phase is determined solely by the initial culture density. When this is 0.2 OD_{600} then stationary phase is reached after around $24\,\mathrm{h}$ (section 2.7.3.7). Anaerobic conditions are maintained for around 6 times the amount of time taken for the initial $0.25\,\mathrm{mM}$ of glucose to be depleted by the *N. meningitidis* culture, which is anywhere from 0-$100\,\mathrm{h}$ depending on oxygen and propionic acid permeabilities (section 2.7.3.6).

The third experimental strategy of this chapter, where propionic acid diffusion rate starts high so that propionic acid is non-limiting and is then decreased to the point at which it limits *N. meningitidis* growth (section 2.8), has different factors affecting the experiment duration. The speed at which the system (in particular the growth rate of the *N. meningitidis* culture) responds to a change in propionic acid supply affects how fast it can be varied. When the source of propionic acid is a continuous culture of *P. gingivalis* then dilution rate and propionic acid permeability both affect the speed at which steady state is approached (section 2.7.4.4). Accumulated propionic acid in the *N. meningitidis* chamber may also affect how quickly the *N. meningitidis* growth rate responds to a drop in propionic acid supply. Enough time would have to be given for the *N. meningitidis* culture to reach a steady state (steady state of the growth resources, not the culture density).

The growth rate of the *N. meningitidis* culture itself can also influence the duration of co-culture needed for a useful experiment. Since the primary system variable to measure is the *N. meningitidis* culture density, this change must be of a magnitude that can be measured accurately by the apparatus (i.e. to a sufficient precision so that the calculated magnitude of metabolic interaction has a useful statistical power). These

limits would be determined by preliminary *in vitro* experiments and would depend on the apparatus used to measure, as well as the precision of the culture parameters (e.g. chamber dimensions, membrane thickness, mixing factor η, oxygen concentration) and the behaviour of the cultures (i.e. how valid the model is when compared to the observed *in vitro* behaviour of the system). Since the co-culture must be maintained long enough for *N. meningitidis* to grow by at least this minimum amount, the growth rate of the culture is a determining factor in the time scale of experiments.

In this system, when the co-culture is viable, then *N. meningitidis* growth is oxygen-limited. However, since oxygen diffusion is faster than propionic acid (section 2.10) then the primary factor placing a lower limit on experiment duration is propionic acid permeability. In section 2.10, the methods of increasing propionic acid permeability relative to oxygen permeability are discussed. However, an important method to vary both of these permeabilities is by modifying the scale (chamber unit length) of the system (section 2.11).

2.10 Propionic acid permeability limitation

The main limiting factor for parameter set viability is low propionic acid permeability relative to oxygen permeability (sections 2.7.1.4, 2.7.2.6, 2.7.3.7 and 2.7.4.3.3). This is due to the choice of PDMS as a membrane material. Because PDMS is hydrophobic, the predicted diffusion coefficient propionic acid is around 100 times lower than that of oxygen. On top of this, propionic acid can only diffuse through PDMS in its undissociated form. At pH 6.0, only 7.05% of propionic acid is undissociated, this effectively reduces the diffusion gradient meaning that diffusion only proceeds at 7.05% the rate compared to if all propionic acid was undissociated.

Oxygen and propionic acid permeability must be balanced in order to maintain the anaerobic conditions required for the *P. gingivalis* culture (sections 2.7.2.3, 2.7.3.5.1, 2.7.3.5.2 and 2.7.4.3.1). There are several methods that can be use to decrease the gap between oxygen and propionic acid diffusion rates:

- Propionic acid concentration in chamber 3 can be increased. This is possible with continuous *P. gingivalis* culture (section 2.7.4.3.1).
- Oxygen concentration in the oxygen supply chamber can be reduced, for instance

by mixing air with oxygen-free nitrogen. However, this would also make experiments less convenient to run, and the long-duration of experiments may present other technical challenges (such as dessication of the chamber contents).

- Membrane thicknesses can be adjusted. The lower limit is defined by the fragility of the membrane, the upper limit is defined by the fact that thicker membranes increase experiment time.
- pH in the *P. gingivalis* culture chamber can be lowered. This is limited by the growth requirements of the culture. In this analyses, the preferred limit is assumed to be pH 6.0 (or pH 5.5 if needed).
- Increase the surface area. This would require using a design other than cube chambers sharing faces with each other. For instance, thin-walled permeable tubing could be used: coils of tubing could be submerged in one culture chamber and then the contents of the other culture chamber could be circulated through this tubing. There are many such design options.
- Use of an alternative material for the membranes. This may not be possible. PDMS was chosen because it is impermeable to molecules in aqueous solution thereby allowing the two culture conditions to be distinct yet connected (section 3.2.2.4.1).

A combination of some of these methods were used when searching for a practical, useful parameter set with a good margin for error. In the parameter set for a *P. gingivalis* batch culture (section 2.7.3.7), a pH of 5.5 was used and an oxygen supply concentration 30% of that found in air. This is in contrast to the parameter set for a *P. gingivalis* continuous culture (section 2.7.4.3.3) where pH 6.0 and atmospheric oxygen concentration was used. However, vastly different membrane thicknesses were used ($1.02\,\mathrm{mm}$ and $20\,\mu\mathrm{m}$).

Therefore, although propionic acid permeability is a limitation inherent to this system (which requires diffusion of propionic acid across PDMS membranes), there are several methods for ensuring that it is balanced with oxygen permeability, and that the co-culture between the aerobic *N. meningitidis* and the anaerobic *P. gingivalis* is successful.

2.11 Choice of chamber dimensions

The scale (i.e. unit length m) of the culture chambers affects permeability of resources between the chambers. As described in section 2.5.4.1, permeability is the harmonic mean of permeability from diffusion across the membrane (P_{mem}) and permeability from diffusion through the chamber (P_{mix}). A smaller unit length will:

1. increase the surface area to volume ratio between the chambers thereby increasing P_{mem}
2. decrease the distance of diffusion within the chamber thereby reducing P_{mix}
3. allow for thinner membranes since they will be more structurally stable with a smaller area to cover. A thinner membrane increases P_{mem}.

Therefore, a smaller scale of chamber increases permeability.

N. meningitidis growth places limits on oxygen permeability, and this therefore limits the scale as well. In a viable co-culture, *N. meningitidis* growth is oxygen limited, and so oxygen partial yield cannot exceed the culture's growth when growing at the maximum growth rate. A useful, practical (for *in vitro* experiments) starting culture density is 0.02 OD_{600}. With the depletion of $0.25\,\mathrm{mM}$ glucose in the culture medium, this density rises to 0.0646 OD_{600}. At this culture density, the oxygen permeability is limited to $1.37 \times 10^{-3}\,\mathrm{s}^{-1}$. Beyond this, the culture is not able to consume all of the oxygen diffusing into the chamber and anaerobic conditions are not formed, at least not until the culture density has risen to a sufficient level.

There is an upper limit placed on chamber size by the need for a minimum *N. meningitidis* growth rate in a useful experiment 2.9. The exact requirements will only be known once the apparatus is implemented and preliminary experiments have been conducted, however a requirement for an increase in culture density of 0.4 OD_{600} over $24\,\mathrm{h}$ is a good place to start. This rate of culture growth requires an oxygen permeability of at least $3.94 \times 10^{-4}\,\mathrm{s}^{-1}$.

The relationship between culture chamber scale and oxygen permeability is shown in figure 2.22. For this analysis, the mixing factor (η) was set to 10 and the membrane thickness ($L_{1,2}$) was set to 10% of the unit length (m). This ratio of chamber size to membrane thickness was chosen to ensure that the membrane would not be too fragile at any of the scales. With these parameters, the upper and lower limits placed scale are

3.50 mm and 6.53 mm.

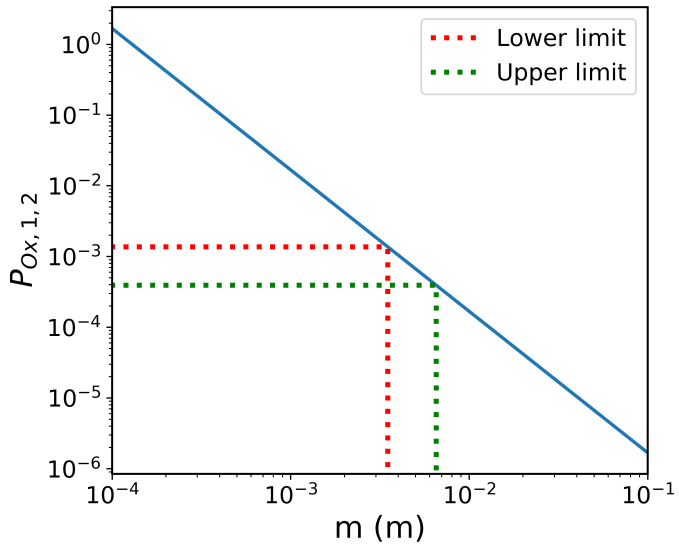

Figure 2.22: Limits placed on culture chamber scale by *N. meningitidis* growth parameters. Oxygen permeability ($P_{Ox,1,2}$) is plotted against chamber unit length (m) when membrane thickness ($L_{1,2}$) is 10% of m. The upper limit for this permeability is defined by μ_{Nm}^{max} when $X_{Nm,1} = 0.0646$ OD_{600}, the lower limit is defined by a minimum useful growth rate of 0.4 OD_{600} over $24\,h$ meaning that m must be between $3.50\,mm$ and $6.53\,mm$.
Parameters: $\eta = 10$, $R_{Ox,1} = 100\%$ of saturation from air. Other parameters are as listed in table 2.2.

These limits are not hard limits. Membrane thickness, degree of mixing and oxygen input concentration all affect oxygen permeability as well as the unit length. The effects of mixing, membrane thickness and chamber scale on diffusion are further explored in section 2.5.4.1.

Mixing is particularly important since it may be slowed in order to reduce the possible scale, or increased to allow for larger scale. However, a core assumption of the ODE model is that the chambers are well mixed. Although imperfect mixing is a feature of the equations describing permeability, imperfect mixing has other effects (e.g. due to unequal growth in different areas of the culture chambers) that are not modelled. Also, a chamber with heterogeneous culture density may reduce the accuracy of optical density measurements since the area being measured may not be representative of the whole culture. Therefore, although it may not be required for ensuring sufficient oxygen flux, it is best to ensure a high degree of mixing.

Of course, the chamber design is not limited to cubes, and the diffusion surfaces

between the chambers are not limited to flat membranes. The design has been limited to these simple constraints to bring out the essential factors that determine the effect of scale.

Chapter 3

Development of non-contact co-culture apparatus

3.1 Introduction

With the ultimate aim of studying metabolic interactions between *N. meningitidis* and *P. gingivalis*, and its role in invasive meningococcal disease (IMD), a non-contact co-culture assay between two liquid cultures was developed (as planned in section 1.8.3). This was based on mathematical modelling of the generation of anaerobic conditions by *N. meningitidis* and the metabolic interaction between the two cultures via propionic acid (chapter 2).

Implementation of this assay is essential to enable its use for testing the assumptions of the mathematical modelling, and then studying and quantifying the metabolic interaction between *N. meningitidis* and *P. gingivalis*. First, however, a suitable apparatus must be developed, and the technical challenges that limit the performance of the apparatus must be assessed.

3.2 Apparatus design

The mathematical modelling in chapter 2 assumes a simple two-chamber layout with an additional chamber for oxygen-supply. This is for the sake of simplicity to facilitate

the analysis, the intention being that study of this simple abstract system would be applied to a whole host of apparatus designs.

When choosing a design pattern, there are several types of non-contact co-culture to consider that have been described in the literature.

3.2.1 Possible apparatus designs

3.2.1.1 Semi-permeable bags

Non-contact co-culture has been achieved by encapsulating one culture in a tube (Kobayashi *et al.*, 2009) or dialysis bag (Fig3.1, Shi *et al.*, 2017) and immersing it in a flask containing a second culture. This technique is elegant and powerful in its simplicity, however there is limited access to the immersed culture which therefore limits the ability to take culture density measurements or control the growth conditions.

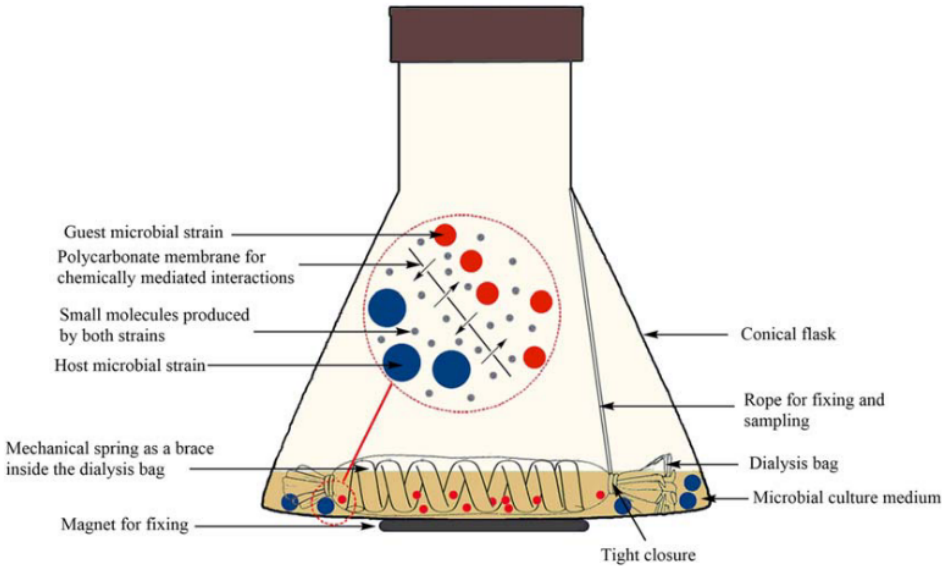

Figure 3.1: Method using a submerged semi-permeable bag for non-contact co-culture, used in Shi *et al.*, 2017

This method could be developed so that the aerobic *N. meningitidis* culture, for example in a $250\,\mathrm{mL}$ flask, maintains anaerobic conditions for *P. gingivalis* in the bag. Mixing could be by shaking or magnetic stirrer. Oxygen supply could simply be from the atmosphere. Optical density measurements of the *N. meningitidis* could be taken by a

shake flask reader system or by manually taking periodic samples and measuring with a benchtop spectrophotometer. Although this system would be simple due to its almost exclusive use of standard lab equipment, it is limited by its lack of flexibility and control over the culture conditions, in particular the culture in the semi-permeable bag. Cell counts of the culture in the bag are not possible without disrupting the co-culture or developing a complicated system of tubing. Mixing of the culture in the bag, and a consistent surface area of the bag cannot be ensured without further modifications that turn this simple method into a much more complicated one.

3.2.1.2 Adjacent culture chambers

An alternate option that allows equal control and monitoring of the two cultures is to have two directly adjacent culture chambers separated from each other by a semi-permeable material (e.g. a membrane). One study used two $100\,\mathrm{mL}$ flasks each containing a pure liquid culture connected with a $25\,\mathrm{mm}$ long $7.45\,\mathrm{mm}$ inner diameter tube filled with polyacrylamide to study the role of distance in a metabolic interaction between two cultures (Fig3.2a, Peaudecerf *et al.*, 2018). Compared to the scenarios described in chapter 2, these experiments were for a longer period of time (over the course of several weeks, compared to several days) and studied relatively slow-growing microbes (the bacteria *Mesorhizobium loti* and the unicellular alga *Lobomonas rostrata*). Therefore, the relatively large diffusion distance was not as important. Also, product inhibition was not an important factor therefore a very large concentration gradient was able to drive flux between the two flasks.

Another study used two glass vessels modified to each have a large flat open end (Fig3.2b, Paul *et al.*, 2013). A $0.22\,\mu\mathrm{m}$ polyvinylidene fluoride membrane was placed between these open ends and they were clamped together to form two culture chambers separated by the membrane. This apparatus was used to study metabolic interactions between algae and bacteria. Growth kinetics data collected was used to characterise metabolic interactions between the microbes.

A method using adjacent chambers separated by a polycarbonate membrane with $0.1\,\mu\mathrm{m}$ pores was developed to study interactions between batch cultures of human pathogens and other bacteria (Fig3.2c, Moutinho *et al.*, 2017). This method was particularly powerful since the device fits in a standard 96-well plate reader providing temperature control, shaking and frequent optical density readings.

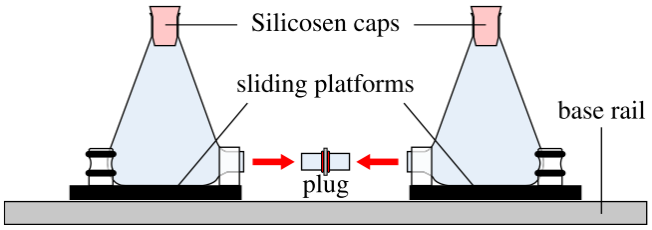

(a)

(b)

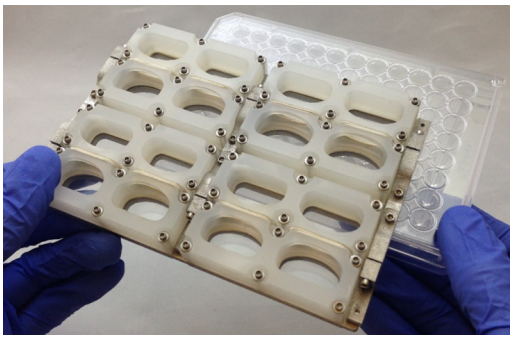

(c)

Figure 3.2: Adjacent chamber methods for non-contact co-culture in literature.
(a) Two cultures in separate flasks connected by a polyacrylamide plug used by Peaudecerf *et al.*, 2018.
(b) Modified glass vessels clamped together holding a polyvinylidene fluoride membrane between them, used by Paul *et al.*, 2013. The black bar corresponds to 100 mm.
(c) Array of culture chamber pairs with polycarbonate membranes between them, used by Moutinho *et al.*, 2017.

Using a slightly different approach, unicellular algae were cultured in 6-well plates with membrane inserts that separated an inner from an outer culture (Fig3.3, Yamasaki *et al.*, 2007). In this study, the culture density was monitored by taking regular cell-count measurements. This data was analysed by splitting the growth kinetics into distinct growth phases to study which phases of growth were affected by substances produced by other microbes (allelopathic interactions).

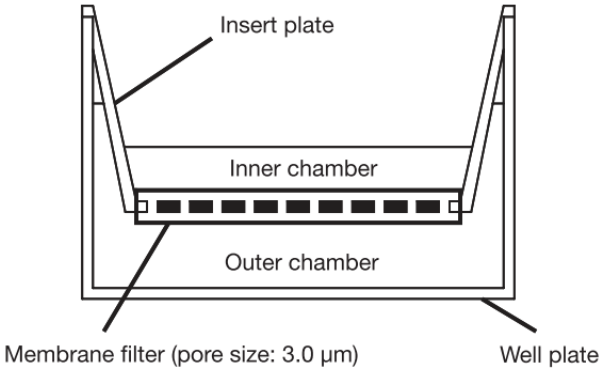

Figure 3.3: Method using standard well plate inserts for non-contact co-culture in literature, used by Yamasaki *et al.*, 2007

3.2.1.3 Microfluidic approaches

Small-scale devices and microfluidics have been used to construct non-contact co-culture vessels. One study (Fig3.4a, Kim *et al.*, 2008) set up three $200\,\mu\mathrm{m}$ diameter wells placed on top of a communication layer. The base of the wells was a polycarbonate membrane and substances could diffuse between the wells via the communication layer. The three wells were used as vessels for three different pure cultures which together formed a three-way syntrophic relationship. Also in the literature is a droplet-based approach (Fig3.4b, Park *et al.*, 2011), a capillary-based approach by which microfluidic chambers are be connected by capillaries that are too thin to allow the passage of cells (Fig3.4c, Groisman *et al.*, 2005), and gel-barrier-based approach where two chambers are separated by a polyethylene glycol (PEG) gel barrier (Fig3.4d, Patel *et al.*, 2015).

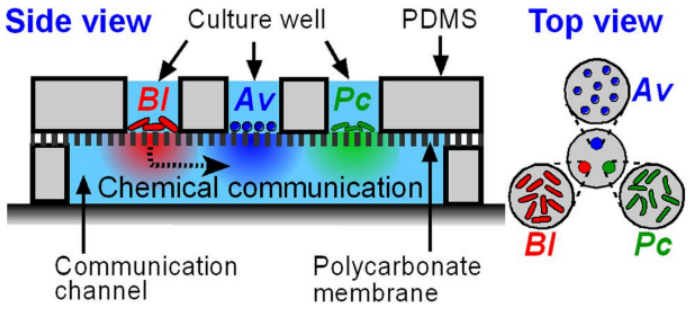

(a)

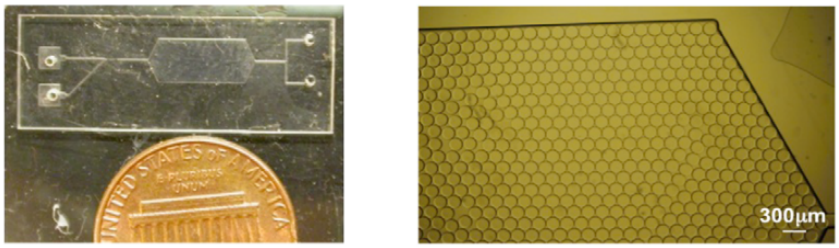

(b)

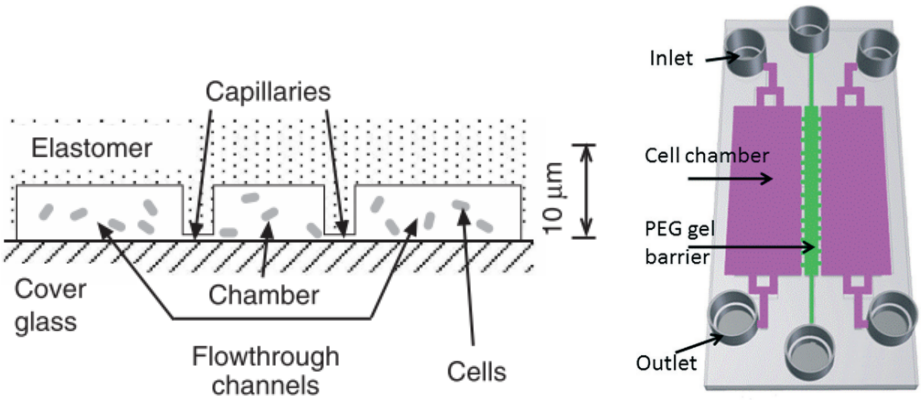

(c) (d)

Figure 3.4: Microfluidic methods for non-contact co-culture in literature.
(a) Three 200 μm diameter wells connected via a communication channel layer, used by Kim *et al.*, 2008.
(b) Droplet-based method used by Park *et al.*, 2011.
(c) Neighbouring culture chambers connected by thin capillaries used by Groisman *et al.*, 2005.
(d) Two neighbouring culture chambers separated by a polyethylene glycol (PEG) gel barrier, used by Patel *et al.*, 2015.

3.2.1.4 Oxygen control

Oxygen control is an important aspect of a co-culture between aerobic and anaerobic microorganisms. The mathematical modelling and analysis of non-contact co-culture in chapter 2 indicates that the co-culture will be viable when oxygen is fully consumed by the aerobic culture. Therefore, no other method of removing oxygen is needed (e.g. an oxygen "sink" as well as an oxygen source). And so, to maintain a viable co-culture *in vitro*, the apparatus must only prevent diffusion of oxygen directly into the anaerobic chamber while providing a controlled supply of oxygen to the aerobic chamber.

3.2.1.4.1 Selective supply and limitation of oxygen There are several examples in the literature of culture devices that control oxygen through diffusion with oxygen-rich and oxygen-poor liquids and gasses. One study used a microfluidic PDMS chip enclosed in a box flushed with an anaerobic N_2/CO_2 gas mix (Fig3.5a, Steinhaus *et al.*, 2007) to establish a range of oxygen concentrations by mixing varying degrees of oxygen-rich and oxygen-depleted aqueous solution. This principle, of excluding oxygen in the surrounding environment while delivering oxygen to where it is needed, is a powerful way to maintain growth conditions for strict anaerobes. Other examples include use of an Ussing chamber which is a two-chamber system separated by a section of animal tissue. Anaerobic conditions were maintained at the apical surface and aerobic conditions at the basal surface (Fig3.5b, Fang *et al.*, 2013) by circulating water which is constantly sparged by either micro-aerobic or oxygenated gas. This demonstrates the principle of removing oxygen by circulating an anaerobic fluid.

In another study (Shah *et al.*, 2016), a non-contact co-culture between epithelial cell cultures and mixed bacterial communities was established as a model to study interactions between gut epithelial cells and the human gut microbiome (the HuMiX system). An oxygen gradient between the two cultures (aerobic at the basal side of the epithelial cells, anaerobic bacterial culture) was maintained primarily by perfusion of aerobic and anoxic media.

Oxygen can be delivered to the aerobic culture across a polydimethylsiloxane (PDMS) membrane. This method was investigated for use in bioreactors as an alternative to standard aeration which produces bubbles and foam (Côté *et al.*, 1988). In another study (Lee *et al.*, 2006), supplying oxygen across a PDMS membrane enabled continuous monitoring of culture density by taking optical density (OD) measurements of

small bioreactor arrays (Fig3.5c) since no foams or bubbles were produced that could interfere with the OD measurements. Many PDMS microfluidic devices rely on oxygen diffusing across the PDMS to supply the culture's oxygen requirement. This process was been studied and quantified using devices constructed of PDMS and polycarbonate (PC) (Fig3.5d, Kirk *et al.*, 2016). These two materials were together used to control where oxygen could diffuse since PC is relatively impermeable to oxygen.

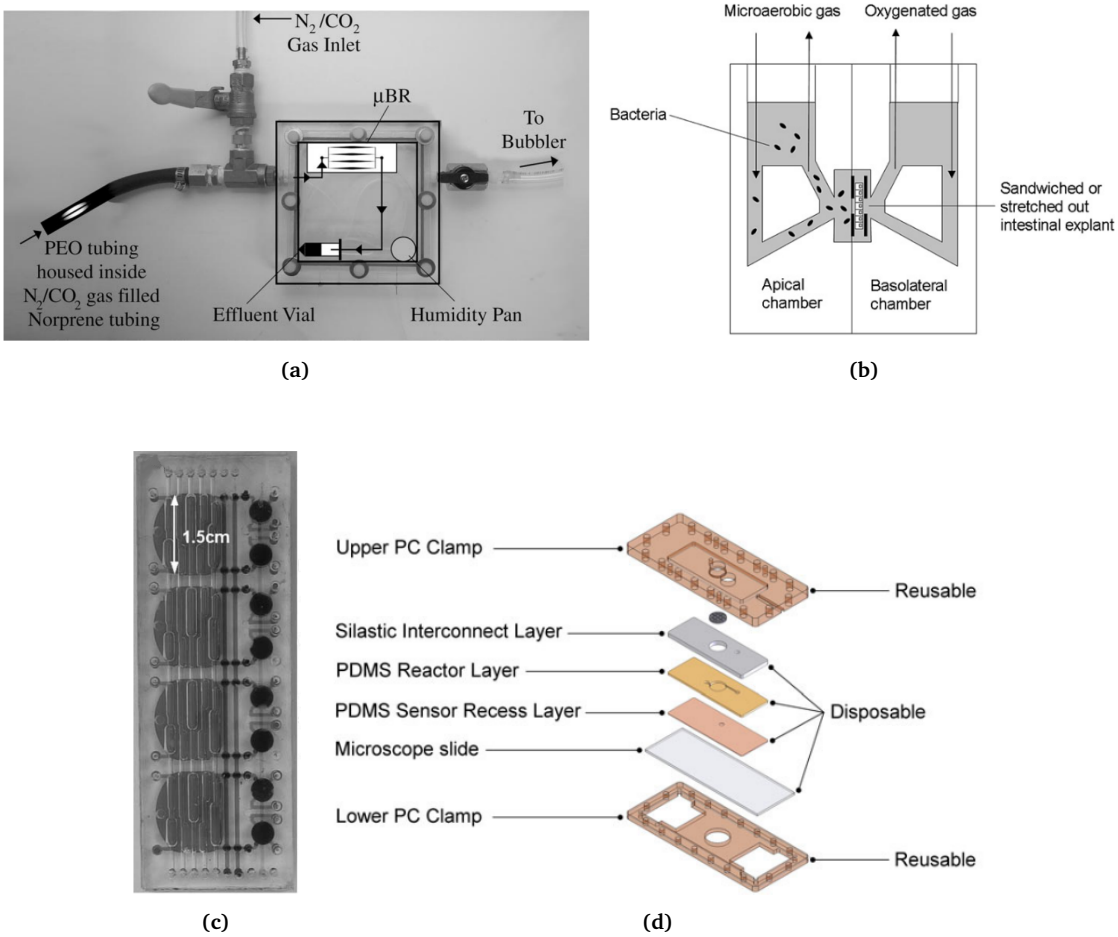

Figure 3.5: Methods for supplying and limiting oxygen for cultures in literature.
(a) Oxygen is excluded by anaerobic N_2/CO_2 gas and supplied selectively through delivery of oxygen-containing culture media, used by Steinhaus *et al.*, 2007.
(b) In Fang *et al.*, 2013 the culture medium is sparged by either microaerobic or oxygenated gas depending on the oxygen requirements of the culture.
(c) Array of four bioreactors used in Lee *et al.*, 2006.
(d) Apparatus used to study oxygen diffusion across PDMS in Kirk *et al.*, 2016.

3.2.1.4.2 Oxygen consumption The use of an aerobic culture to consume the oxygen and create the conditions for anaerobic culture has been demonstrated in the lit-

erature. One study showed that *P. gingivalis* and other anaerobes could be cultured in media sparged with 95% air (5% CO_2) (Bradshaw *et al.*, 1996). These anaerobes were part of a 10-member bacterial community including several facultative anaerobes and the aerobe *Neisseria subflava*. In this study *P. gingivalis* was most abundant in the biofilm (rather that the surrounding planktonic culture) accounting for around 26% of the cells, it also made up around 11% of the planktonic cells in the surrounding liquid media.

3.2.1.5 Diffusion device

Another design approach is to have two cultures in separate flasks where culture conditions can be controlled separately and culture density monitored separately (e.g. by OD measurements). Transfer of metabolites between the two cultures could be mediated by a device that facilitates diffusion, such as one study used to deliver oxygen to a culture (Côté *et al.*, 1988), or as used by another study to allow diffusion of metabolites between two flasks (Peaudecerf *et al.*, 2018), or by simply a length of tubing submerged in another culture (Fig3.6). Culture contents could be continually circulated through this diffusion device by peristaltic pumps to maintain the propionic acid concentration gradient. Diffusion could be controlled by modifying the diffusion area, for instance by adding more devices, changing the circulation speed, or changing the surface area within the device. The modular design and use of standard lab equipment and techniques mean that it would offer greater flexibility than the adjacent chamber method described previously. This would leave open possibilities such as more sophisticated control of the culture conditions by controlling pH, setting up continuous cultures or biofilms in the flasks, and the possibility of adding additional cultures and individually controlling the degree of diffusion between them. However, the additional tubing and pumps needed, and the need to develop a diffusion device means that this method is inherently more complicated than the other two options.

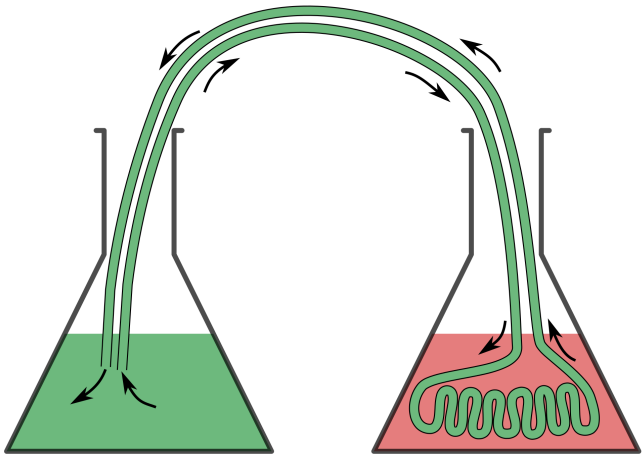

Figure 3.6: Diffusion device method for non-contact co-culture. The two cultures are held in separate flasks (or other containers), and one culture is circulated through semi-permeable tubing that is submerged in the other culture. This creates a diffusive connection between the cultures.

3.2.2 Chosen design

Due to simplicity of design, and fulfilment of requirements from the mathematical modelling and analysis (chapter 2), the chosen design for the non-contact co-culture device to study metabolic interactions between *N. meningitidis* and *P. gingivalis* was the adjacent chamber layout (section 3.2.1.2).

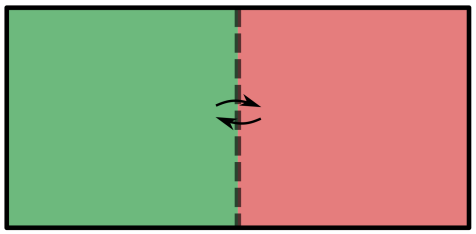

Figure 3.7: Adjacent chamber method for non-contact co-culture. The two cultures (green indicates *N. meningitidis*, red indicates *P. gingivalis*) are held in separate culture chambers that share a face, this shared face is made of a semi-permeable membrane (represented by a dotted line) that allows diffusion between the chambers but keeps the cultures separate (i.e. PDMS).

Specifically, the chosen design is to have two enclosed chambers containing only the liquid culture (i.e. no gas headspace) (Fig3.7). The enclosed nature of the chambers would prevent diffusion of oxygen into the anaerobic culture chamber. However, oxygen supply for the aerobic culture would have to be intentionally designed, for instance

as an adjacent oxygen supply chamber. Although this adds another aspect to be developed, it does mean that the oxygen supply could be modified by controlling this single source of oxygen. This would be a useful feature for generating the required culture conditions for an experiment.

The enclosed design means that liquid access to the chambers would have to be exclusively by tubing. The requirement for tubing means that development of the apparatus would take longer and use much less standard lab equipment. However, this chamber design allows for dilution of the chambers meaning that continuous cultures could be used. This is something highlighted in the mathematical model analysis as useful, if not essential, for quantification of the metabolic relationship between the two cultures (section 2.7.4.5). This design also allows for continuous monitoring of both cultures so that the necessary data for quantification of the metabolic interaction can be collected (section 2.8).

These advantages are true also for the diffusion-device-style design (section 3.2.1.5). However, the adjacent chamber design is simpler and so will minimise apparatus development time. The mathematical analysis indicates that this design can be used with practical chamber dimensions and membrane thickness (section 2.11).

When developing this apparatus, the construction must be flexible so that unforeseen technical challenges can be overcome. The choice of materials and fabrication methods must allow a rapid turn-around if modifications to the design are needed. Each aspect of the design has been chosen with these principles in mind.

3.2.2.1 Dimensions

Mathematical modelling of the non-contact co-culture system showed that a practical size for the chambers would be 3.50-$6.53\,\mathrm{mm}$ (section 2.11). Therefore, the chosen chamber dimensions were $5\,\mathrm{mm}\times5\,\mathrm{mm}\times5\,\mathrm{mm}$. The limits calculated using the mathematical modelling are not hard limits since the definition of what is "practical" is subjective and other scales fit this definition of practical when factors such as mixing and oxygen input concentration are varied. That being said, these limits are followed during development of the apparatus because they represent a good starting point.

The typical thickness of the membranes at this scale is shown in section 2.7.4.3.3 where results are predicted by the mathematical model using sensible parameter values. In

this analysis the membrane between the oxygen supply chamber and the *N. meningitidis* chamber is $1.02\,\mathrm{mm}$ thick, and the membrane between the *N. meningitidis* chamber and *P. gingivalis* chamber is $20.0\,\mu\mathrm{m}$ thick. These thicknesses are based on assumptions that may not be valid in the developed apparatus (e.g. degree of mixing may be different), so different membrane thicknesses may be needed. Also, in experiments for quantification of the metabolic interaction between the two cultures, several different diffusion rates should to be tested to ensure that the results have good statistical confidence (section 2.8).

The small footprint of the apparatus also allows for scaling up experiments by using many copies of the apparatus at once while still fitting in the lab space available. It also reduces the volume of media used which becomes more relevant in continuous culture experiments where volumes of around 10 to 50 times the chamber volume are pumped at precise and consistent rates over the course of several days. With a chamber volume of $125\,\mu\mathrm{L}$ (i.e. volume of a $5\,\mathrm{mm}$ cube) the entire reservoir of media for that chamber could be stored in a $10\,\mathrm{mL}$ syringe loaded in a syringe pump.

3.2.2.2 Measurement method

The proposed non-contact co-culture assay quantifies the metabolic interaction between *N. meningitidis* and *P. gingivalis* by observing population size dynamics and how they are affected by the co-culture (section 2.8). Therefore, it is essential that microbial population size measurements be recorded. Data with a high time-resolution, such as that collected from a plate reader, is advantageous in that it allows identification of features such as when growth phases transition, diauxic growth and allows measurement of properties such as lag phase and initial growth rate. Such data would be valuable when interpreting results and designing future experiments, and so it was determined that frequent measurements of cell counts was a desirable feature.

Optical density is the simplest and most established way to do this. For accurate results the culture being measured must be well-mixed and planktonic since in this case any region measured will be representative of the entire culture. Well-mixed cultures also have the advantage of maximising diffusion between the chambers by preventing the formation of boundary layers. It also means that spatial variation within chambers does not have to be accounted for in the mathematical model. Instead, diffusion rates of substances between the chambers can be modelled using Fick's Law, and the bacterial

cultures can be assumed to be homogenous and therefore modelled as a single culture density value. This means that the system can be modelled as ordinary differential equations (ODEs), a powerful and well-established method (section 1.8.3).

Optical density measurements can also be used in combination with an oxygen-sensitive dye (e.g. resazurin) to detect the presence or absence of oxygen in each culture chamber. This will be useful for testing the device and could also be used in experiments (section 2.7.3.8 & 2.8).

The culture densities of the growth chamber cultures are measured by optical density (OD). Light sources and light sensors are mounted in line with the chambers, OD is calculated by comparing measured light intensities to a blank measurement (where the culture density is 0).

3.2.2.2.1 Specification The main requirement for the optical density apparatus is that it must be sensitive enough to accurately measure culture density as it ranges from 0.0 to 2.0 OD_{600} (as measured by a standard lab spectrophotometer). Also, the measurements must be consistent over the course of $48\,\mathrm{h}$. All of the culture chambers (across all three triplicate chamber stacks) are to be monitored (be subject to frequent OD measurements), and the target frequency of the measurements is to take one every minute.

3.2.2.2.2 Design options To fulfil the requirement to monitor the OD of six chambers (two culture chambers in each of the three chamber stacks), either multiple sensors can be used or a single sensor moved from chamber to chamber. A moving light sensor would have greater consistency since the exact same equipment is used, slight variations between different electronics and optics do not need to be accounted for, and periodic blank measurements can be taken to re-calibrate the measurements.

However, to achieve this consistency, the sensor would have to be positioned in the same place for each repeated measurement. Slight variations could affect the result in an unpredictable manner. Stationary sensors fixed in place for each chamber would not have this problem. However, these sensors would have to be compact and be convenient to produce so that at least size of them can be prototyped. Also, these sensors would not be able to recalibrate during monitoring.

The method of using many stationary sensors was chosen for the sake of simplicity and speed of development. Developing a system that could precisely position a light sensor was deemed more technically challenging than developing a method for communicating with an array of stationary sensors.

3.2.2.2.3 Positioning of light sources, sensors and light masks It will be important that light following other paths (either originating from the apparatus light source, or light from the surrounding environment) do not affect the measured light intensity value (i.e. do not reach the light sensor).

A pinhole method of controlling the light beam is to be used, this involves passing the light through a series of masks (opaque sheets with two transparent circular holes). Lenses could be used instead, they would redirect the light rather than masking it and so would allow for a greater light intensity at the sensor. However, development of the light masks is quicker since they can be rapidly made by laser-cutting PMMA.

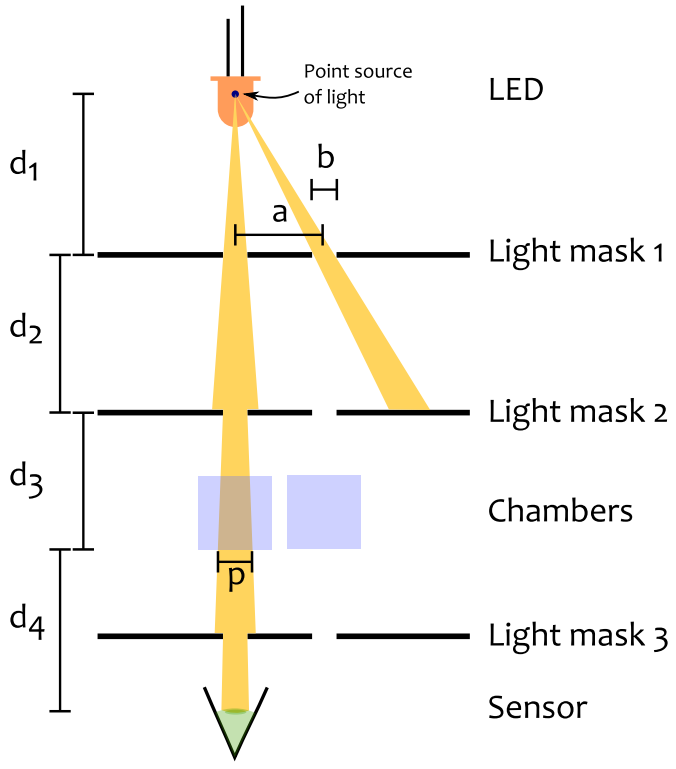

Figure 3.8: Model for understanding the principles of using light masks in OD measurement apparatus. The diagram shows how light masks can be used to direct the beam of light through the chamber being measured. Multiple light masks can be used to prevent alternate light paths between the light source and sensor, since this would introduce error into the measured OD value.

The light sources, light masks and light sensors are to be mounted as shown in figure 3.8). Since there are two sets of light holes, one for each chamber, alternate paths of light from light source to sensor are possible. In order to avoid these, a set of rules can be used to guide the placement of the light masks.

- Light mask 1 should be positioned such that light going through the adjacent hole is blocked before it can be scattered by the chamber stack or reflect off some other surface
- Light mask 2 should be positioned such that light going through the first light mask only goes through the aligned hole of the second light mask (not the adjacent hole)
- The chambers should be positioned such that light going through the chamber does not interact with the walls of the chamber, since this would result in internal reflection and scattering of the light beam

Although these conditions may not prevent all of the possible alternate light paths from affecting the measured result, they will keep these factors to a minimum. Keeping these rules will place limits on the positions of the light masks. These limits are described by the following mathematical relationships.

Using terminology from figure 3.8, d_1 is the distance between the light source and the first light mask, d_2 is the distance between the first and second light masks, d_3 is the distance between the second light mask and the bottom of the chamber, a is the distance between the two light holes: $5\,\mathrm{mm}$, and b is the diameter of the light holes: $2\,\mathrm{mm}$. L_{left}, L_{right}, R_{left} and R_{right} are the positions of the edges of the two holes in the 2D cross section of the apparatus displayed in figure 3.8, the hole L is on the left (the aligned hole), R is on the right (the adjacent hole). The positions of the points are as follows: $L_{left} = -\frac{1}{2} \cdot b$, $L_{right} = \frac{1}{2} \cdot b$, $R_{left} = a - \frac{1}{2} \cdot b$ and $R_{right} = a + \frac{1}{2} \cdot b$. In the following equations it is assumed that the LED is a point source of light.

Condition 1 is met when $\frac{d_1}{R_{left}} < \frac{d_1+d_2}{R_{right}}$ (i.e. when light passing by the inner edge of the adjacent hole of the first light mask lands past the outer edge of the adjacent hole of the second light mask). Condition 2 is met when $\frac{d_1}{L_{right}} > \frac{d_1+d_2}{R_{left}}$ (i.e. when light passing by the inner edge of the aligned hole of the first light mask does not make it to the inner edge of the adjacent hole of the second light mask). When both of these conditions are met, and when $a = 5\,\mathrm{mm}$ and $b = 2\,\mathrm{mm}$, then $\frac{1}{2} \cdot d_1 < d_2 < 3 \cdot d_3$.

For condition 3, a maximum diameter for the light beam in the chamber (q) must be defined. Condition 3 is met when $\frac{d_1+d_2}{L_{right}} > \frac{d_1+d_2+d_3}{\frac{1}{2}\cdot q}$ (i.e. when light passing by the inner edge of the aligned hole of the second light mask does not pass beyond the edge of the maximum light beam size when passing though the bottom of the chamber). And so, when $q = 3\,\mathrm{mm}$, $a = 5\,\mathrm{mm}$ and $b = 2\,\mathrm{mm}$ then $d_1 + d_2 > 2 \cdot d_3$.

An additional light mask, placed after the chamber, can be used to shield the sensor from light reflecting off other surfaces. This is not strictly necessary, however it may be useful for reducing light approaching via complicated routes.

These rules place limits on the relative distances of the various components. The absolute distance between light source and sensor is also important since it will affect the precision of optical density measurements. A greater distance would theoretically increase the change in light intensity per change in turbidity of a sample cell culture. This is because optical density of a culture is in part due to scattering, a larger distance offers more opportunity for scattered light to miss the sensor. However, a greater distance between the light source and the sensor would also mean a less intense signal and therefore a decreased precision of measurement.

3.2.2.3 Mixing

Since the cultures must be well-mixed (section 3.2.2.2) the apparatus must actively mix the culture chambers. However, the design choice of enclosed adjacent chambers with no headspace makes mixing the chamber contents more challenging. The lack of headspace means that shaking is less effective since the liquid cannot swirl around as in an open container. The requirement for tubing access and an uninterrupted path for optical density measurements means that there is no space for a magnetic stirrer bead to be used. There is an option to pulse a small volume of fluid back and forth through the chamber to generate currents and mix the contents. This would require additional pumping apparatus.

Shaking should be attempted and the pumping option used as an alternative if required. Another possible option is to leave the chambers un-mixed and adjust the results analysis to handle this scenario. This is less than ideal since the use of ODE models, assuming well-mixed chambers, has enabled insightful analysis of the system.

A mixing factor of between 5-10 is used in many evaluations and discussion in the

maths chapter. A mixing factor of 13 is known to correspond to a mixing time (time for a dye to mix in with clear water, as determined visually) of around 5 s (Lee *et al.*, 2006, section 2.6.3). Therefore a mixing factor of between 5-10 will have a marginally slower mixing time. This is a good target to aim for when developing the apparatus for mixing. The exact degree-of-mixing can be measured by measuring the diffusive flux between the chambers, for instance by measuring the time taken for oxygen to deplete in the chamber adjacent to the oxygen-limited aerobic culture.

3.2.2.4 Materials

3.2.2.4.1 Membranes The membranes must be permeable to gas while also keeping the cultures separate, and they must be biologically compatible with the cultures (i.e. not inhibit the viability of the cultures through some other interaction).

Polydimethylsiloxane (PDMS) is a silicone compound that has been used to construct culture chambers and supply oxygen to these cultures (Lee *et al.*, 2006). It has several properties that make its use appropriate for the apparatus. It is commonly used in microbiology and other fields (Li *et al.*, 2016), so it is known to be compatible with bacterial cultures and there is a lot of experience and literature to draw upon. It is permeable to gases and volatile substances including propionic acid and oxygen. Permeability to oxygen is demonstrated by its use for supplying oxygen to microbial cultures (Lee *et al.*, 2006). Permeability to fatty acids, including propionic acid, was shown by its use in removing volatile fatty acids from a product (Miyagi *et al.*, 2011). It is also impermeable to hydrophic molecules in aqueous solution due to its hydrophobic surface (Markov *et al.*, 2014). Therefore it would not permit the growth media contents (e.g. dissolved glucose, or amino acids) of the two cultures to mix.

PDMS is convenient to use in a biology lab. It can be made from a two-part mixture with a curing time of around 1 h at 70 °C, and it can be cast in a mould to make shapes, or spin-coated to make thin sheets and membranes (Sia & Whitesides, 2003). It is also available to purchase as pre-cured thin sheets, from a thickness of 2 mm to 0.02 mm (Silex Ltd., UK).

Heat and chemical resistance is an important factor for material choice since chambers must be sterilised in preparation for microbial cultures. PDMS can be autoclaved, exposed to ethanol and strongly acidic/alkaline solutions without any damage or de-

gradation (Lee *et al.*, 2003; Simmons *et al.*, 2006).

It is also visually transparent and therefore allows visual inspection of the contents of chambers, a feature that is especially useful when troubleshooting and developing a new method. This transparency is sufficient to allow for optical density measurements at $600\,\mathrm{nm}$ (Lee *et al.*, 2006).

3.2.2.4.2 Chamber walls The chamber walls must be made of a material that is optically transparent enough to enable $600\,\mathrm{nm}$ measurements. It must also be biologically compatible with the cultures, impermeable to gas diffusion, and it preferably should be convenient to rapidly fabricate and reuse.

PDMS could therefore be used for the chamber walls. However, its permeability to gas means that oxygen diffusion into the anaerobic chamber may compromise the strict anaerobic conditions required for *P. gingivalis* growth. The PDMS walls could be made very thick in order to reduce oxygen diffusion. They may, however, act as a reservoir for oxygen as well as other volatile substances. This may affect the flux of substances in and out of the chambers and so a more impermeable material would be preferable.

Poly(methyl methacrylate) (PMMA) is a synthetic resin that has been used in microfluidic devices (Zhang *et al.*, 2006), and so it is known to be compatible with microbial growth. It is also known as acrylic, or by the brand name Perspex®.

Diffusion of O_2 is around 1000 times slower in PMMA than PDMS: the diffusion coefficient for oxygen in PMMA at room temperature is $2.7 \times 10^{-12}\,\mathrm{m^2\,s^{-1}}$ (Klinger *et al.*, 2009) compared to $2.15 \times 10^{-9}\,\mathrm{m^2\,s^{-1}}$ for PDMS (Lee *et al.*, 2006). It is likely that there is a similar difference in diffusion coefficients for propionic acid.

PMMA is commonly used in the University of York Biology Department workshop and can be rapidly shaped by laser cutting. This material is also durable and so can easily be re-used. It cannot be used with ethanol and cannot be autoclaved without damaging the material (Münker *et al.*, 2018; Yavuz *et al.*, 2016), however it can be sterilised with strongly acidic or alkaline solutions ("Labware Chemical Resistance Table").

Polycarbonate and glass are other materials that could be used for the chamber walls. Glass in particular is completely impermeable to gas diffusion and is very re-usable and easily sterilised due to its excellent chemical and heat resistance. It also has suitable optical properties. However, for this project, rapid prototyping with glass is not as

convenient as with PMMA due to the facilities available. Polycarbonate was a suitable alternative and would not differ much from PMMA in this application, however PMMA was chosen since it was more readily available.

3.2.2.5 Schematic summarising the design choices

The chosen design is therefore as follows (Fig3.9). Three chambers of dimensions $5\,\mathrm{mm}$ cubed, adjacent to each other, spaced by membranes of thickness between approximately $20\,\mu\mathrm{m}$ and $1\,\mathrm{mm}$. The chamber walls are to be made of PMMA to prevent diffusion between the chambers and the outside environment, and to allow OD measurements of the chambers. Each chamber is to be accessed by tubing that passes through the PMMA chamber walls (Fig3.9b).

Optical density measurements of the culture chambers are to be calculated using light intensity measurements of a beam of light passing through the chamber from the top face to the bottom face (Fig3.9a).

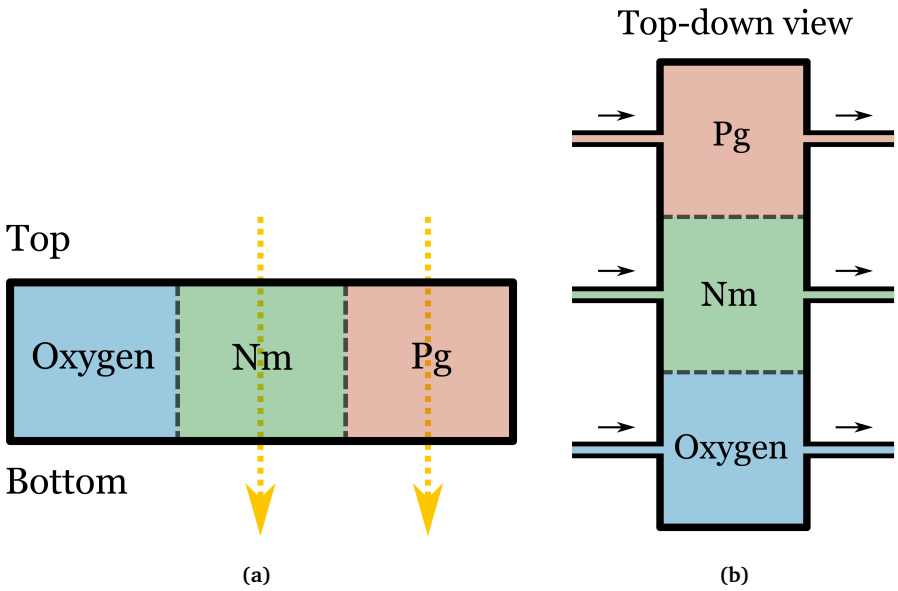

Figure 3.9: Chosen design for non-contact co-culture device. (a) Side view showing adjacent oxygen, *N. meningitidis* (Nm) and *P. gingivalis* (Pg) chambers separated by semi-permeable membranes and encapsulated by an impermeable barrier. The light beams for taking optical density measurements are indicated by the yellow dotted lines. (b) Top view showing the tubing that provides access to each of the chamber contents.

An air-tight enclosure, made up of an "anaerobic box" and hosing, will surround the chamber stacks and tubing to maintain anaerobic conditions around them (inspired by Steinhaus *et al.*, 2007). This box will also prevent the release of microbes into the lab in the event of a leak from some tubing or a chamber.

3.3 Methods

3.3.1 Chambers

3.3.1.1 Construction

The apparatus chambers were constructed as a stack of several "slices" in two forms: end pieces (Fig3.10a) and chamber slices (Fig3.10b and Fig3.10c). The slices were made by laser cutting $5\,\mathrm{mm}$ cast sheets of polymethylmethacrylate (PMMA) sourced from RS components. The actual width of the cast PMMA sheets varied widely from their nominal value (by $\pm 5\%$), therefore a single sheet of PMMA was used to make all of the slices. In the chamber slices, $1.2\,\mathrm{mm}$ tubing holes were created (by laser etching followed by hand-finishing with a drill bit) to allow access to the chamber (Fig3.10b and Fig3.10c). Gaskets (Fig3.10d) and membranes (Fig3.10e) were cut out of Polydimethylsiloxane (PDMS) sheets by hand with a scalpel and $2\,\mathrm{mm}$ hole punch. Gaskets were made of $0.1\,\mathrm{mm}$ PDMS. The PDMS for both the gaskets and the membranes were acquired as pre-cured sheets from Silex Ltd.

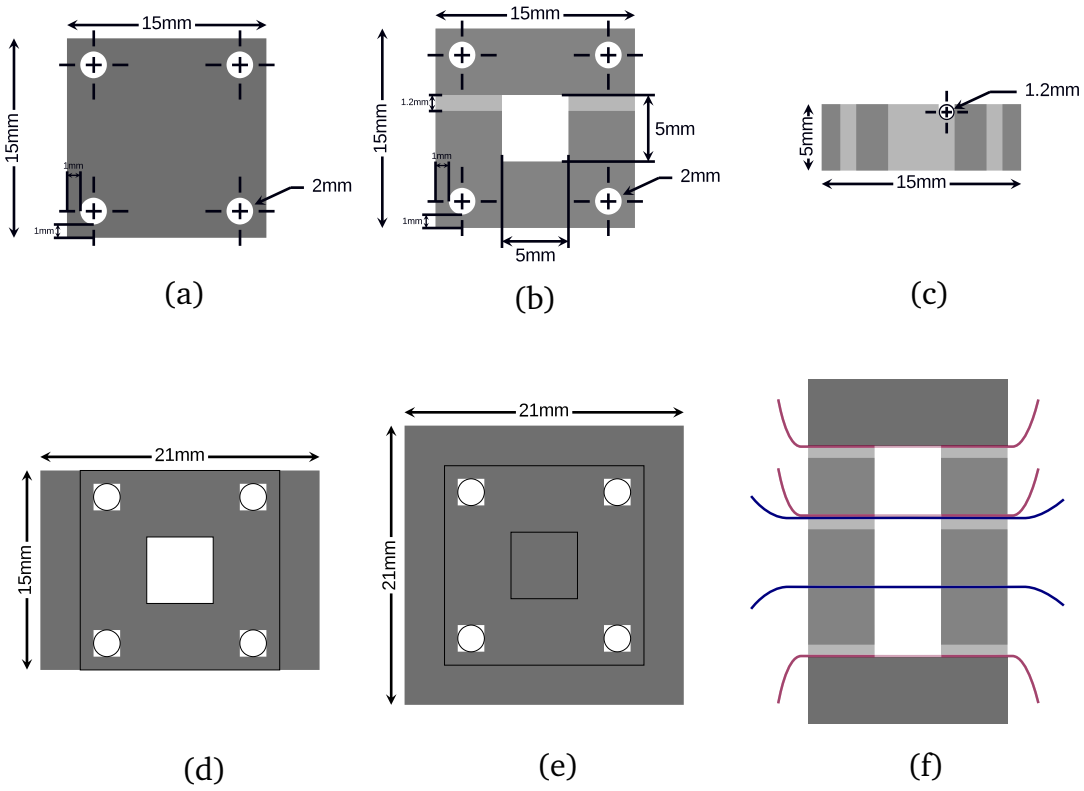

Figure 3.10: Schematics of chamber stack slices, gaskets and membranes. The end slices (a) and chamber slices (b&c) stack together to form chambers. Gaskets (d) were used to form a tight seal between each of these slices. Membranes (e) separate the adjacent chambers from each other. f) The complete stack of PMMA slices (grey), gaskets (red) and membranes (blue). The four $2\,\mathrm{mm}$ holes in each component were used to align and clamp the stack.

Figure 3.10f shows how the slices were stacked. Each chamber slice had either a membrane or an end piece on each side, this formed a chamber of dimensions $5\,\mathrm{mm} \times 5\,\mathrm{mm} \times 5\,\mathrm{mm}$. All slices, membranes and gaskets had four $2\,\mathrm{mm}$ holes in their corners that aligned when stacked. A $2\,\mathrm{mm}$ diameter bolt was inserted through each of the holes and the slices were clamped together by tightening a nut on each of the bolts. This held the slices in place and formed a tight seal between them (Fig3.13a, Fig3.13b).

Access to the chambers was via tubing which was inserted through the tubing holes. Side clamps (Fig3.11) were used to form a tight seal around these connections and hold the tubing in place. The side clamps were made of machined aluminium. They were $5.8\,\mathrm{mm}$ thick and had four $3\,\mathrm{mm}$ holes into which fitted $3\,\mathrm{mm}$ diameter bolts that

were used to clamp the side clamps together (Fig3.13c). The $1.2\,\mathrm{mm}$ holes in the side clamp lined up with the tubing holes in the chamber stack. Figures 3.12 and Fig3.13d show how the pieces fitted together: two side clamps were positioned on either side of the chambers stack, a $3\,\mathrm{mm}$ silicone gasket was placed in between the chamber stack and each of the side clamps, the tubing was inserted through the side clamps, silicone gaskets and tubing holes, and $3\,\mathrm{mm}$ diameter bolts joined the two side clamps together. When these were tightened then the silicone gaskets formed a tight seal with the chamber stack and the tubing. The silicone gaskets were made by manually drilling $1\,\mathrm{mm}$ holes through a sheet of $3\,\mathrm{mm}$ silicone rubber. This complete assembly was referred to as a "chamber stack".

All designs for laser cut parts were drawn up in OpenSCAD and laser cut in the University of York Biology Workshop. Other parts were machined or milled in the same workshop.

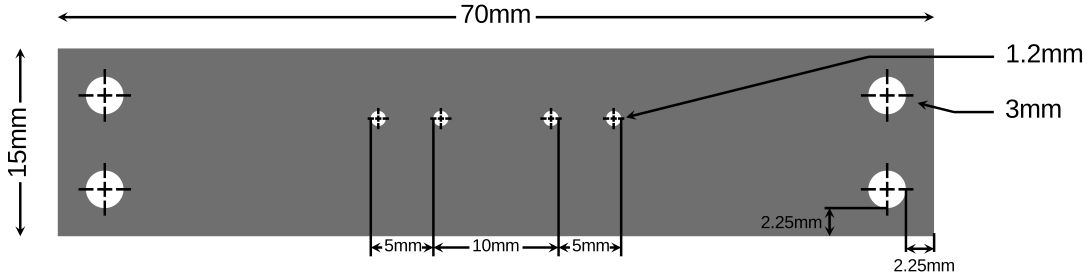

Figure 3.11: Side clamp schematic. The $3\,\mathrm{mm}$ holes were for clamping the two side clamps together (using nuts and bolts). The $1.2\,\mathrm{mm}$ holes allowed tubing through to connect to the chambers.

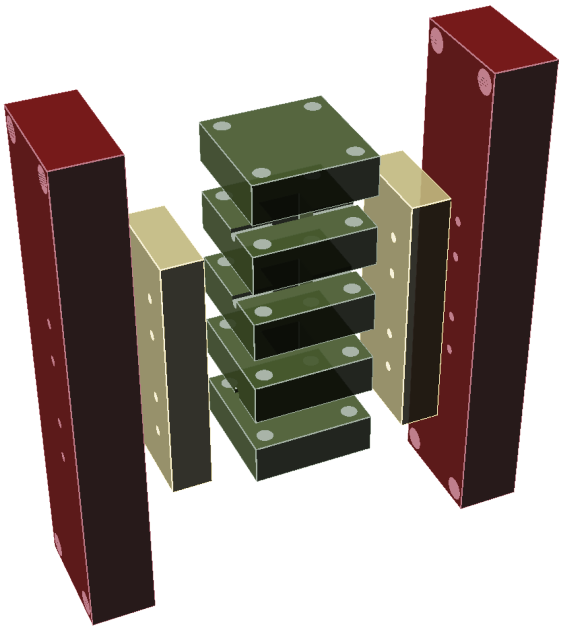

Figure 3.12: Components of chamber stack assembly. Chambers were formed from a stack of PMMA slices (green), tubing was attached to each of the chambers using the side clamps (red) with their gaskets (yellow).

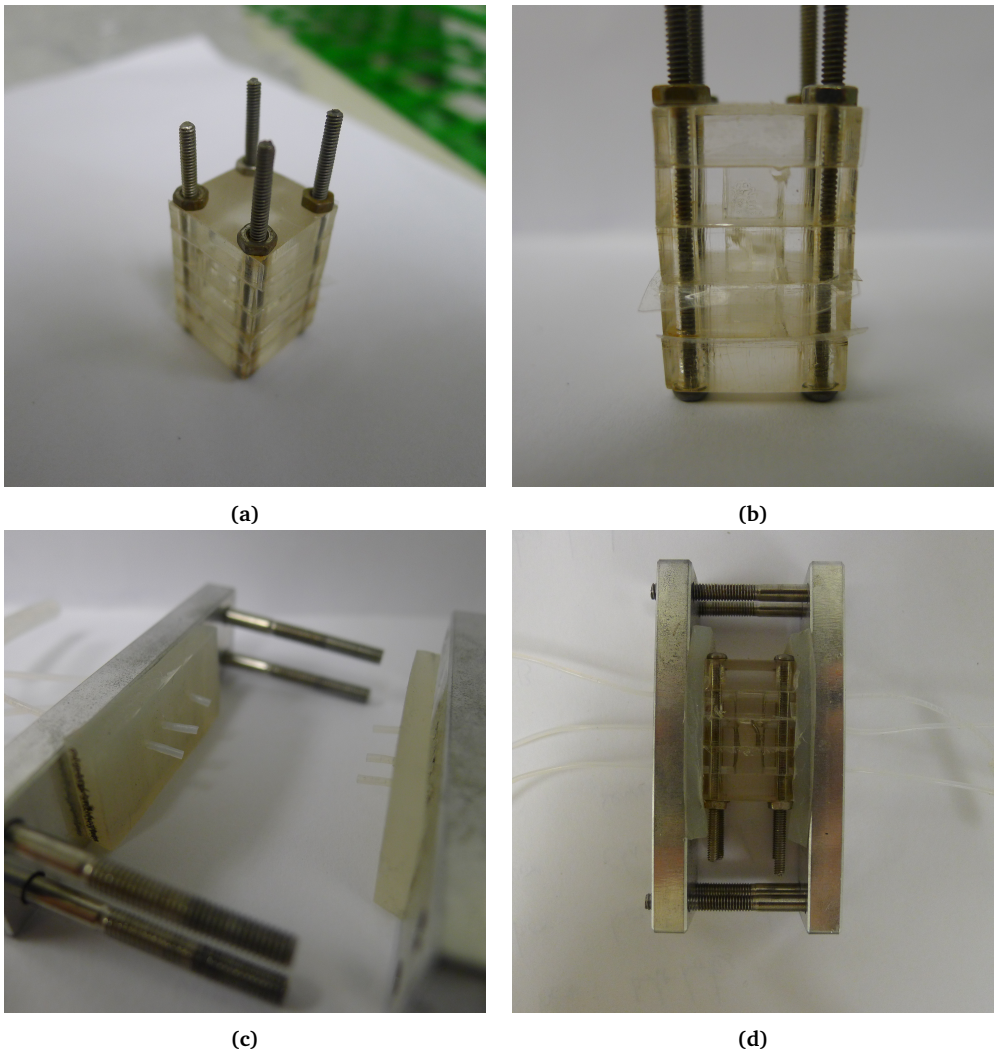

Figure 3.13: Photos of complete chamber stack assembly. a&b) Chambers were made of a stack of PMMA slices separated by gaskets and membranes, and clamped together with four nuts and bolts. c&d) Tubing was attached to the chambers using side clamps.

3.3.1.2 Earlier prototypes

This method for constructing the chambers was developed through a process of iteration. Several earlier prototypes were used for testing other aspects of the apparatus.

The first prototypes cast the chambers and membrane from PDMS in a single mould (Fig3.14a&b). A Dow Corning Sylgard 184 PDMS pre-polymer mixture of PDMS was prepared with a 10:1 (w:v) ratio of elastomer base to curing agent, mixed thoroughly in a plastic cup, de-gassed under vacuum for $15\,\mathrm{min}$, poured into the mould and cured

at $60\,^{\circ}\mathrm{C}$ for $1\,\mathrm{h}$. The mould was made by the University of York Biology Workshop by milling polytetrafluoroethylene (PTFE) (Fig3.14a&b).

The tubing that connected to the chambers were inserted through the PDMS walls. To enable this, holes were punched with a WellTech Rapid-Core $0.75\,\mathrm{mm}$ biopsy punch. The tubing was inserted and the area sealed by coating with PDMS pre-polymer mixture and curing with a heat-gun.

The PDMS cast was then attached to a $25\,\mathrm{mm}\times75\,\mathrm{mm}$ glass microscope slide by using PDMS pre-polymer mixture as an adhesive. A thin layer of PDMS pre-polymer was spread on the glass slide, the cast was placed on this and then the glass slide was placed on a hot plate at $80\,^{\circ}\mathrm{C}$ to rapidly cure the PDMS. The resulting chambers are shown in Fig3.14c&d.

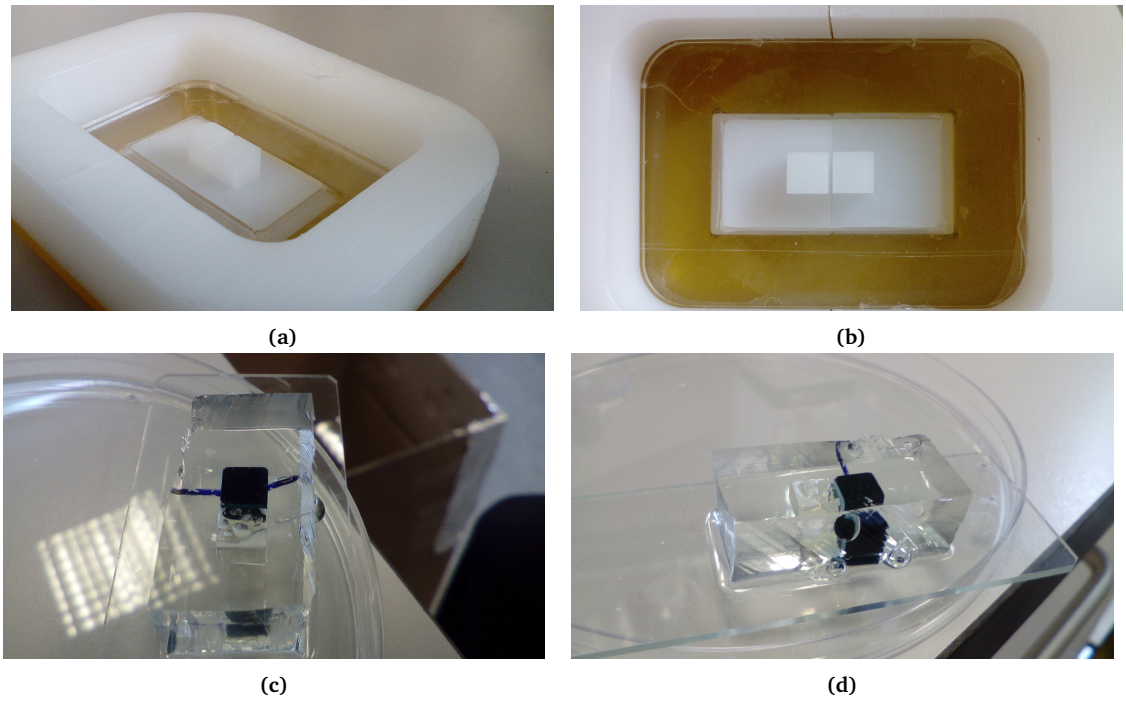

Figure 3.14: Photos of first test PDMS non-contact co-culture apparatus chambers. (a,b) the PTFE mould that was used to cast adjacent chambers in PDMS, (c&d) the PDMS cast attached to glass slide, one chamber was filled with methylene blue solution for visualisation, the tubing holes were punched with a needle.

The PDMS chambers were later refined to enable thinner, more consistent, membranes. PDMS chamber slices were cast (Fig3.15c&d) using a similar method to the previous PDMS casting. These slices were stacked with pre-cured PDMS membranes and bonded together using PDMS pre-polymer. The pre-polymer was applied and the stack clamped

tight and placed at $60\,^{\circ}\mathrm{C}$ for $1\,\mathrm{h}$. The whole PDMS chamber stack was again bonded to a glass slide for mounting with the other apparatus (e.g. light sensors). The resulting chamber construction is shown in figures 3.15a&b.

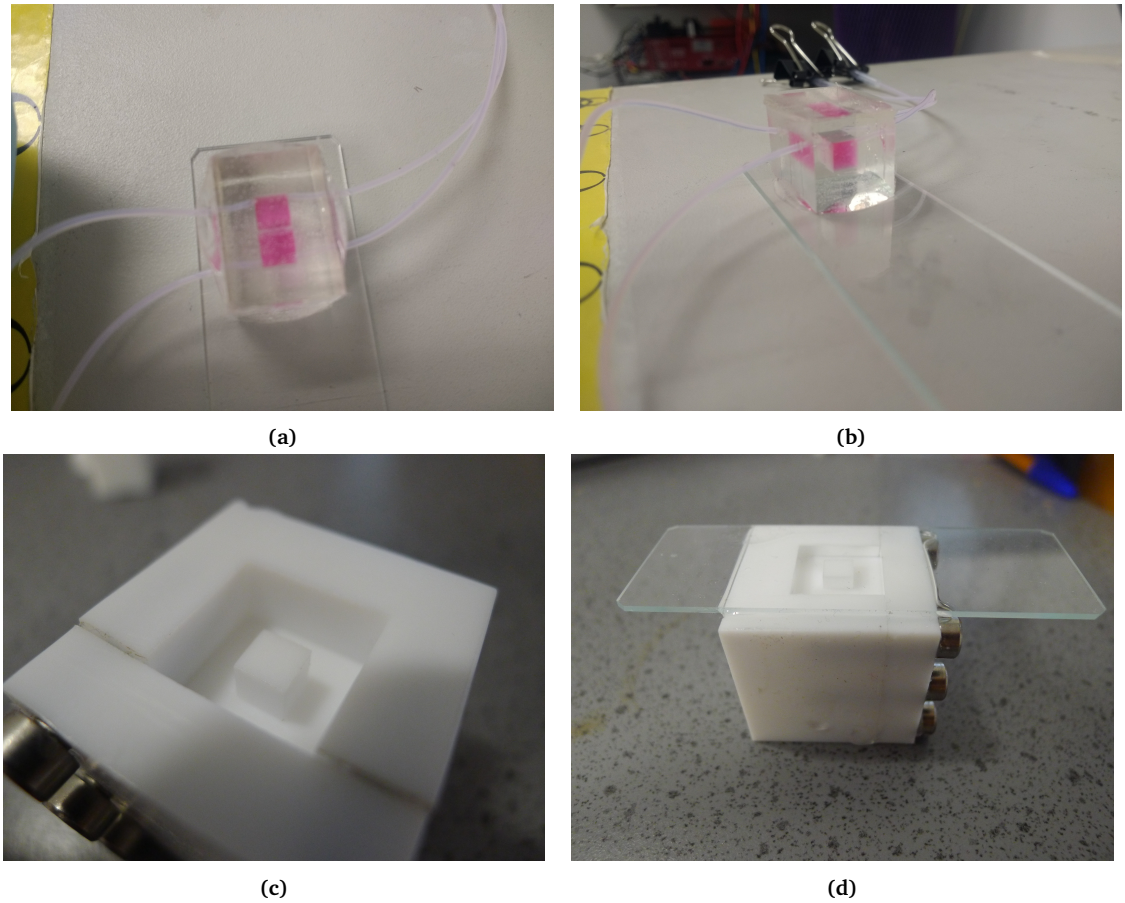

Figure 3.15: Photos of PDMS stack method of fabricating apparatus chambers. a&b) PDMS stack fully fabricated and attached to glass slide (so that it can be mounted), c) a mould used to cast a single PDMS slice of the stack, d) a cured PDMS slice cast in the mould.

These methods for constructing the chambers were not used due to the reasons outlined in section 3.2.2.4.2. Namely, that the PDMS walls may act as a route for oxygen to diffuse into the anaerobic chamber from the surrounding air, and the thick PDMS walls may act as a reservoir that affects the diffusion of substances in and out of each chamber. These earlier designs were however used for testing other aspects of the apparatus (e.g. light sensors, tubing, operating procedures).

3.3.2 Tubing

A system of tubing was used to connect the chambers to syringes and fluid reservoirs allowing the chambers to be prepared, inoculated, mixed and diluted (for continuous culture). This tubing was designed to ensure the sterility of the system and the exclusion/removal of bubbles that may interfere with the experiments, particularly interfering with optical density measurements.

3.3.2.1 Construction

The tubing used was Polytetrafluoroethylene (PTFE) tubing with inner diameter $0.5\,\mathrm{mm}$ and outer diameter $1\,\mathrm{mm}$ (manufactured by Bohlender). PTFE tubing was used due to its chemical and biological compatibility with all the substances to be used in the non-contact co-culture assay, and due to its physical flexibility allowing it to be easily bent into shape. The small inner diameter was useful for minimising the volume in the tubing relative to the volume in the chambers. The tubing effectively extended the chamber volume, however this could complicate modelling the system, so smaller diameter tubing was used to minimise this effect. PTFE was used to reduce the formation of biofilm in the tubing. Silicone tubing with inner diameter $0.5\,\mathrm{mm}$ and outer diameter $3.7\,\mathrm{mm}$ (manufactured by Watson Marlow) was used to connect the PTFE tubing at junctions and to connectors (e.g. to connect to syringes). Junctions were created with Cole Parmer™ Masterflex™ Polyvinylidene fluoride (PVDF) Y connectors (for $1.58\,\mathrm{mm}$ tubing). Syringes were connected with polypropylene (PP) female Luer lock connectors manufactured by Ibidi. Lengths of tubing were opened and closed by clamping the silicone tubing sections with standard medical tubing clamps.

The tubing was arranged for each culture chamber as shown in figures 3.17 and 3.16.

3.3.2.2 Operation

This tubing system was operated as follows: all substances were introduced to the system either via the injection or inoculation port (Fig3.18). Sterility of substances entering via the injection port was ensured by flooding the connector with 70% ethanol and then connecting a $0.22\,\mu\mathrm{m}$ syringe filter which filtered all the liquids entering via this port. The ethanol was removed from the system by ejecting the first $5\,\mathrm{mL}$ of in-

coming liquid through the ejection port. Sterility of the inoculation port was ensured by washing with 70% ethanol, this ethanol was then flushed with liquid from the reservoir syringe to prevent it mixing with the inoculum. Bubbles were removed from the system as needed via the ejection port. The volume of liquid held in the tubing from the syringe to the chamber was around $0.5\,\mathrm{mL}$.

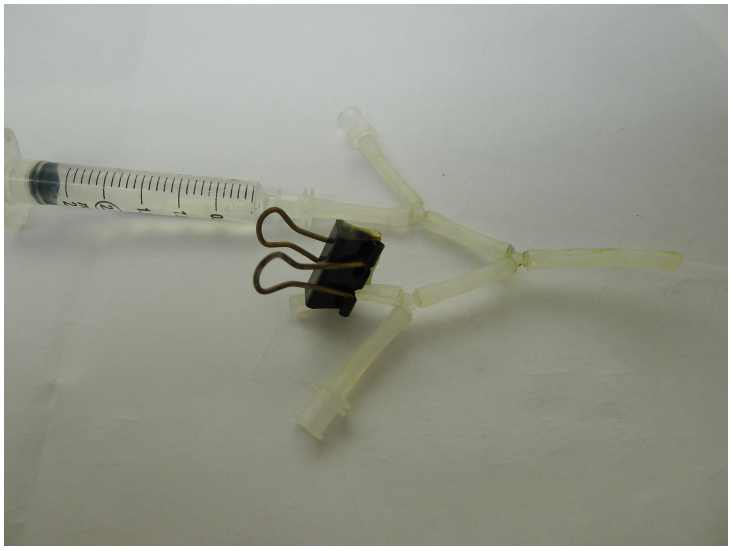

Figure 3.16: Photo of tubing system for one culture chamber. Silicone tubing was used to join connectors, junctions and thin PTFE tubing together. Silicone tubing was also used for controlling flow: sections of the tubing were pinched to prevent flow and released to allow flow.

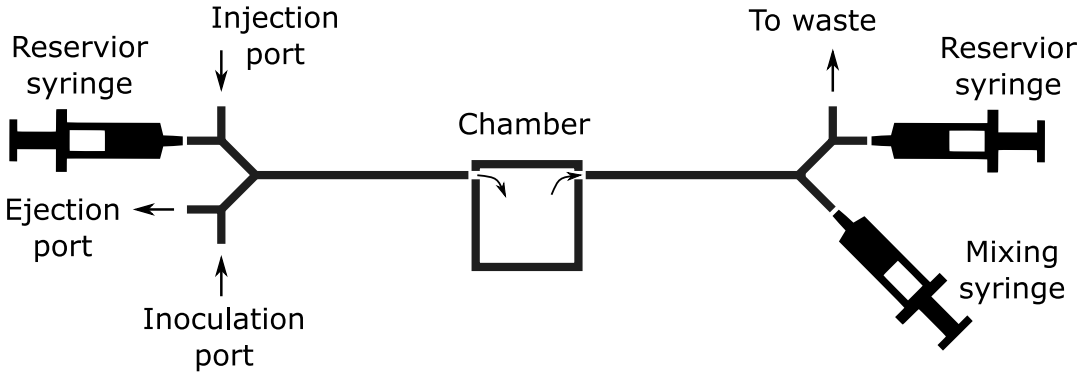

Figure 3.17: Tubing layout diagram for one culture chamber. The mixing syringe was used to pulse liquid in and out of the chamber to induce currents that mix the chamber contents. The reservoir syringes were used for washing, preparing and inoculating the chambers, and to dilute chambers when maintaining a continuous culture.

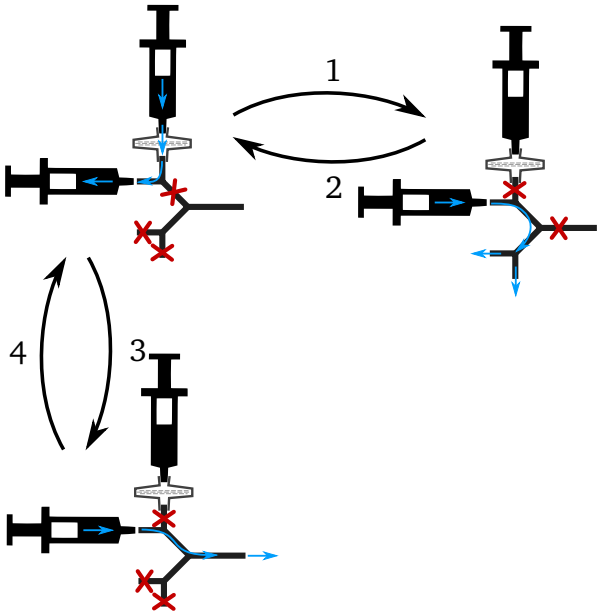

Figure 3.18: Sequence of syringe movements used to flush a chamber. All liquid entering the system was filter sterilised, the tubing was flushed first to remove previous contents and bubbles before being injected into the chamber.

3.3.3 Anaerobic box and hosing

The anaerobic box held up to four chamber stacks and aligned the chambers with the sensor apparatus used to measure absorbance. Three chamber stacks were used at once to carry out experiments in triplicate.

The anaerobic box was made up of a main body machined out of Nylon and a top and bottom plate each made of clear $6\,\mathrm{mm}$ PMMA. The gap between these sections was sealed with $2\,\mathrm{mm}$ closed-cell neoprene gaskets. Each of the plates was bolted to the body by a line of bolts around the edge of the top and bottom faces (Fig3.20a), these clamped the plates to the box to form an air-tight seal. To allow absorbance readings to be taken, the box body had openings that lined up with each of the four slots for the chamber stacks (Fig3.20a, Fig3.20b). Chamber stacks were held in place by the clamping of the top plate to the bottom plate.

The tubing was kept anaerobic by $10\,\mathrm{mm}$ outer diameter, $6\,\mathrm{mm}$ inner diameter PET-reinforced PVC hose that attached to the anaerobic box and surrounded the tubing. There were four connectors that attached this hosing to the box and allowed tubing to

enter the box (Fig3.20c, Fig3.20d). Where anaerobic conditions were required while preparing the contents of a chamber, the substances (e.g. media and wash solutions) were handled in a Sigma-Aldrich® AtmosBag glove bag (Fig3.20e) which is a polyethylene bag with glove-shaped impressions that allows tasks to be performed in a controlled gas mix on a lab bench.

As shown in figure 3.19, a nitrogen cylinder (oxygen-free) was connected to this anaerobic bag and to the anaerobic box which is in turn was connected to a Class II Biosafety Cabinet by hosing. The layout was such that gas from around chambers and tubing containing *N. meningitidis* (a hazard Group 2 organism) always flowed towards the cabinet, and movement through tubing of fluids from the chambers also always flowed towards the cabinet. Gas was allowed to exit the anaerobic bag through hosing with its opening submerged in water. This was to maintain a positive pressure in the anaerobic glove bag and to prevent gas from the atmosphere mixing with gas in the system. Nitrogen gas flow was regulated by a BOC Flowmeter, set at $1\,\mathrm{L\,min^{-1}}$. This value was determined empirically to be sufficient for maintaining anaerobic conditions, and to be convenient in terms to rate of gas use and ability of the lab apparatus to reliably maintain this flow rate.

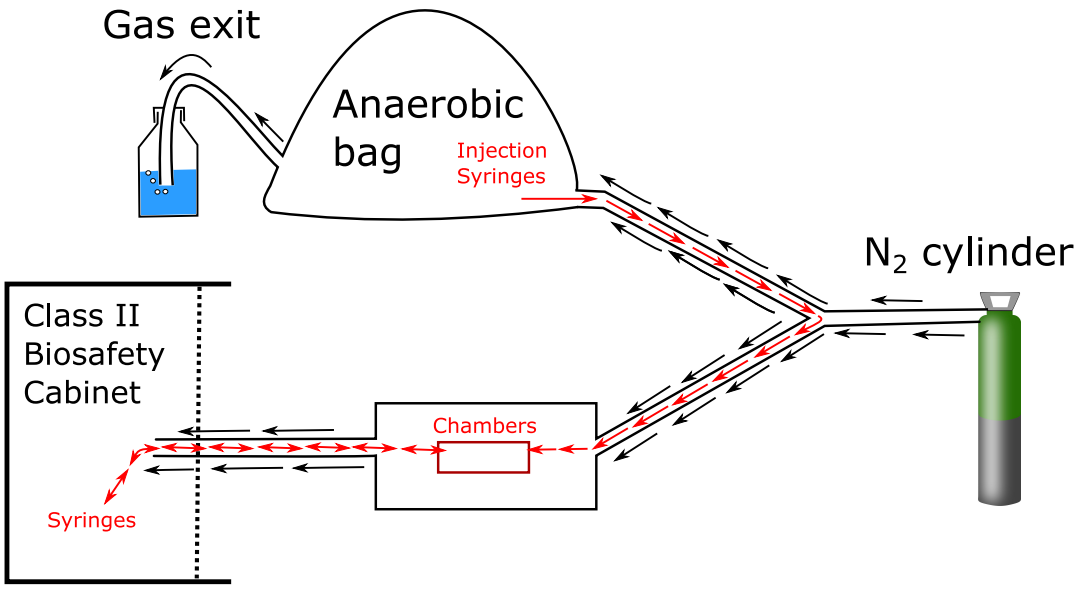

Figure 3.19: Hosing and tubing schematic of non-contact co-culture apparatus.
The outer hosing excluded oxygen from the area surrounding the tubing and chambers. The flow of gas in outer hosing (black) and fluids in tubing (red) through the system ensured that biological materials were confined either within the system or in the Class II Biosafety Cabinet. This is vital for safety when working with *N. meningitidis*.

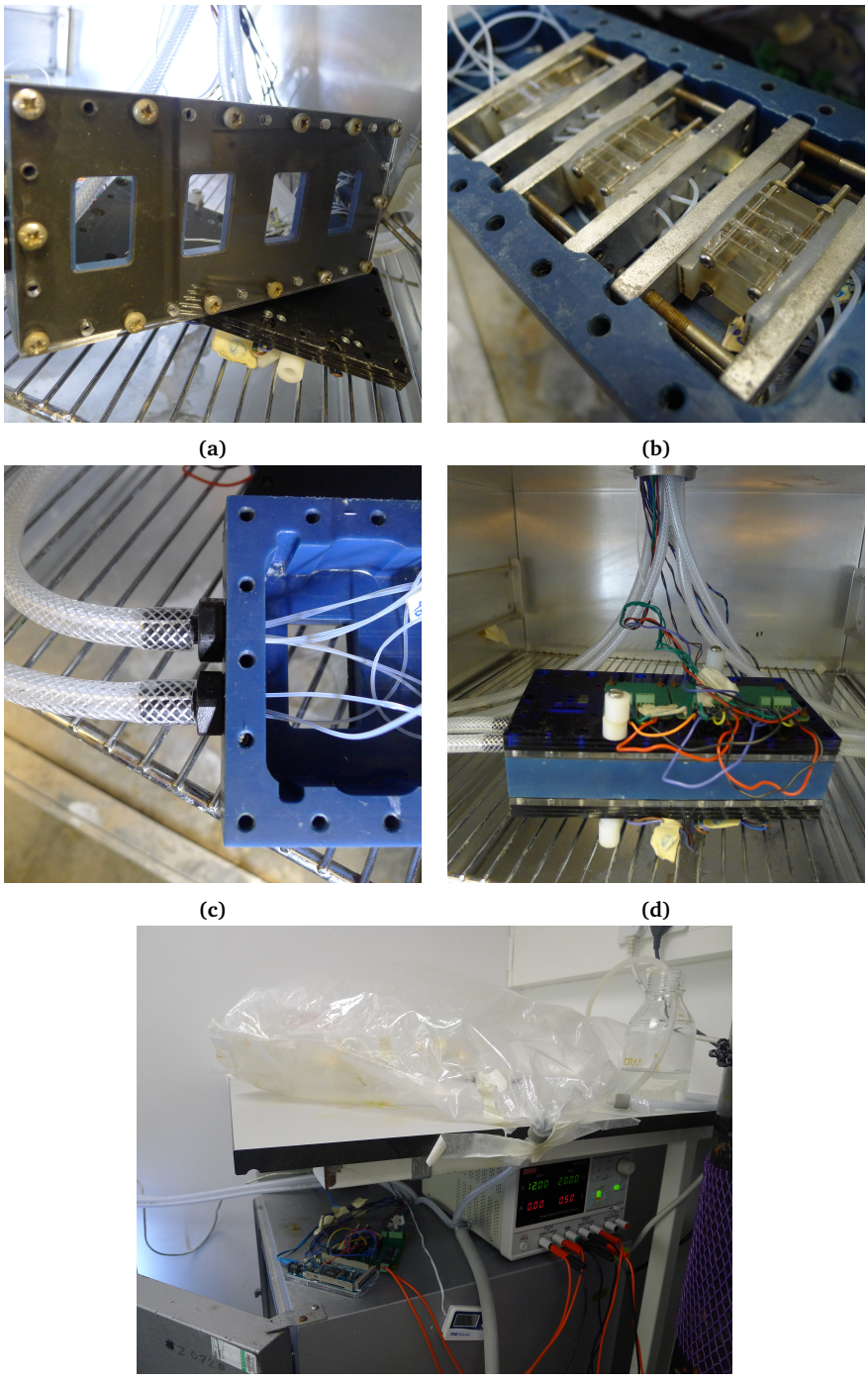

Figure 3.20: Photos of the anaerobic apparatus enclosing the chambers and tubing. The anaerobic box housed three chamber stacks (b) and had windows that enabled OD measurements of these chambers (a). Tubing was enclosed by hosing that attached to the anaerobic box (c), the whole box was placed in a lab oven for temperature control (d,e), the hosing connected to an anaerobic bag (e) in which materials could be handled while maintaining anaerobic conditions.

3.3.3.1 Electronics materials and printed circuit boards

Printed circuit boards (PCBs) were designed in KiCAD and manufactured by JLCPCB. The boards were originally designed to fit Arduino Micro microcontroller boards, however Arduino Dues were used instead because they provided greater flexibility when developing the firmware and troubleshooting the electronics. The Arduino Dues were connected with jumper wires to the Arduino Micro footprints on the boards.

Arduino Due microcontroller boards were used to control the optical density measurement apparatus, syringe pumps (for mixing) and temperature. The firmware was programmed in C. The microcontrollers were configured to receive serial commands from a laptop. This laptop controlled the scheduling of each of the operations (e.g. when to mix, and when to take a measurement) and stored the OD measurements to disk. A JuPyter Notebook running a Python kernel was used to implement this functionality and allow the human operator to configure the apparatus.

3.3.4 Chamber contents mixing

Mixing was achieved by pulsing liquid in and out of the chambers to generate currents within the chamber. Syringe pumps were used to do this because they could give precise control over the volume of displacement. This precision was needed to ensure that the chamber volumes did not change, something that was possible since the PDMS membranes were able to stretch. Additionally, the syringe pumps could be quickly configured for different mixing volumes, flow rates and frequencies, which was useful for developing the apparatus.

Shaking was tested as an alternative method for mixing, however the degree of mixing achieved was not high enough to even prevent the settling of microbial cultures.

3.3.4.1 Syringe pumps

The syringe pumps were based on a linear actuator kit from OozNest which used an ACME lead screw with an anti-backlash nut attached to a gantry on a V-Slot linear rail system, powered by a $1.68\,\mathrm{A}$ NEMA17 stepper motor. Custom-designed laser-cut plates were attached to the linear actuators to allow them to drive syringes (Fig3.21

and 3.22). Two plates were attached to the front of the linear actuator to clamp the syringe bodies in place, and two plates were attached to the moving gantry to clamp the syringe plungers. Moving the gantry back and forth therefore moved the syringe plungers in and out of the syringe bodies. The plates were designed to fit three $1\,\mathrm{mL}$ or $2\,\mathrm{mL}$ glass syringes (manufactured by Samco) each. The glass syringe plungers were coated with Dow Corning high vacuum silicone grease to seal the gap between the plunger and syringe body.

The linear actuator stepper motors were driven by SilentStepStick TMC2130 stepper motor driver boards. They were controlled by Arduino Due microcontrollers, which were in turn controlled by a PC via USB (connected as shown in figure 3.23).

The stepper motor driver boards were configured to split each full step into 16 microsteps, and each of these microsteps was further interpolated into 16 smaller steps. The stepper motors had 200 steps per full rotation, and the lead screw of the linear actuator moved the gantry by $8\,\mathrm{mm}$ for each full rotation, therefore the gantry moved at $\frac{200\times16}{8}$ microsteps per $1\,\mathrm{mm}$, or $2.5\,\mu\mathrm{m}$ per microstep.

With the $1\,\mathrm{mL}$ glass syringes, a plunger movement of $28.3\,\mathrm{mm}$ (3sf) displaced $1\,\mathrm{mL}$ giving a displacement of $35.3\,\mathrm{nL}\,\mu\mathrm{m}^{-1}$ (3sf), and with the $2\,\mathrm{mL}$ glass syringes, a plunger movement of $30.8\,\mathrm{mm}$ (3sf) displaced $2\,\mathrm{mL}$ giving a displacement of $64.9\,\mathrm{nL}\,\mu\mathrm{m}^{-1}$ (3sf). Therefore, when the $1\,\mathrm{mL}$ glass syringes were used, the syringe pumps operated at a displacement of $35.3 \times 2.5 = 88.3\,\mathrm{nL}$ per microstep (3sf), and at $64.9 \times 2.5 = 162\,\mathrm{nL}$ per microstep (3sf) when $2\,\mathrm{mL}$ glass syringes were used.

Syringe pumps were used for mixing by drawing in $25\,\mu\mathrm{L}$ of liquid from the chamber over the course of $3\,\mathrm{s}$ and then reversing this action to return the liquid to the chamber. The change in chamber volume caused the membranes to flex since the air chamber was able to compress and expand allowing this change in volume of the other chambers. It was essential that each mixing cycle resulted in no net change in chamber volume, otherwise the membrane may have remain flexed and interfered with optical density measurements of the culture chambers.

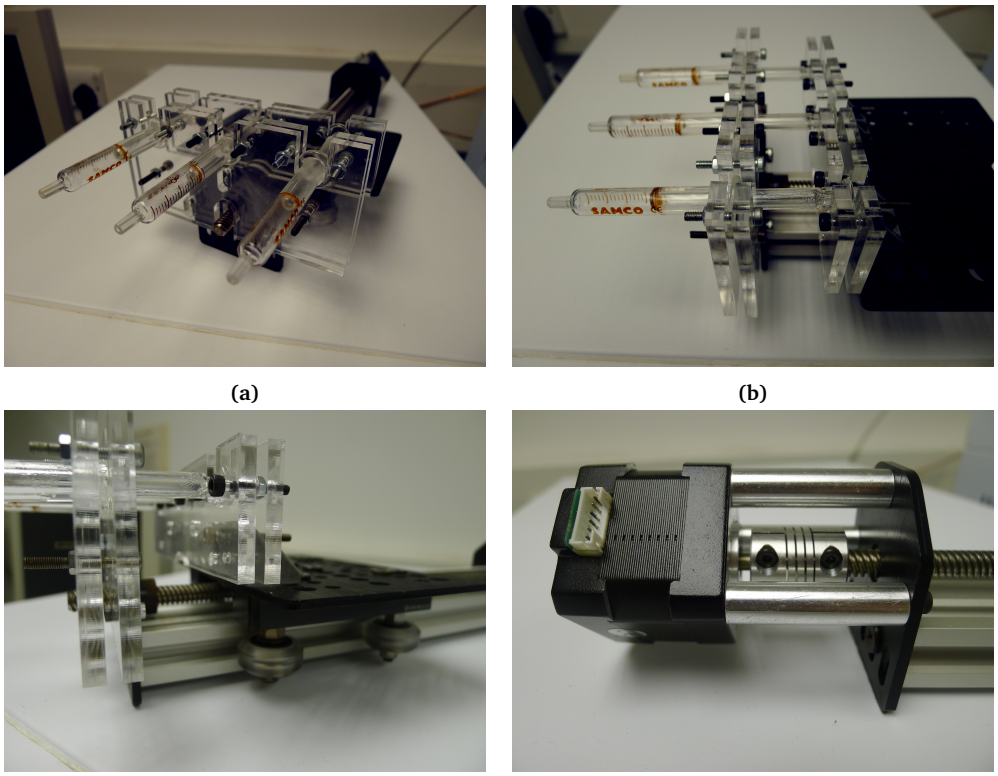

Figure 3.21: Photos of custom-made syringe pump. The complete syringe pump made from a modified linear actuator. a) the complete syringe pump, was made up of b) plates that clamp syringes, c) the linear rail system and d) the stepper motor attached to the lead screw.

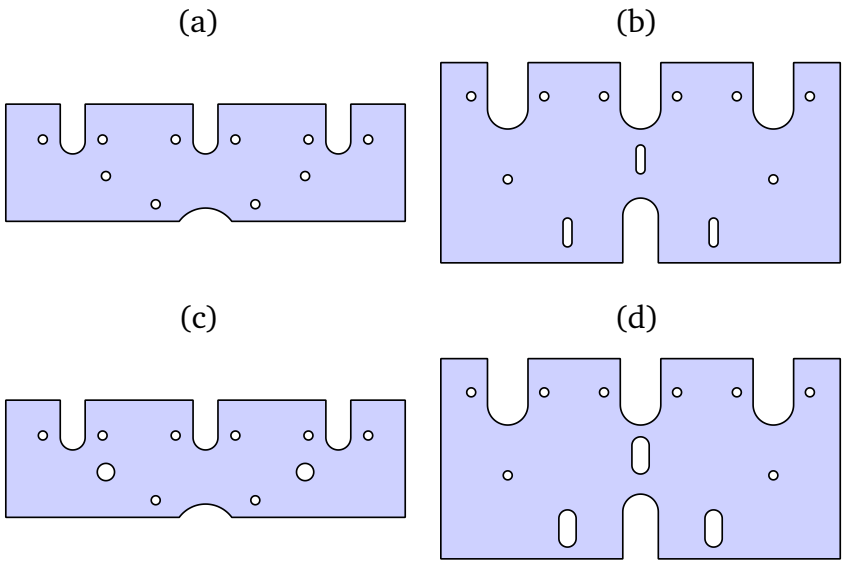

Figure 3.22: Syringe pump plate schematics. These plates attached to the linear actuator to attach syringes and so make it useful as a syringe pump. a&c) plates that clamped the syringe plungers, b&d) plates that clamped the syringe bodies.

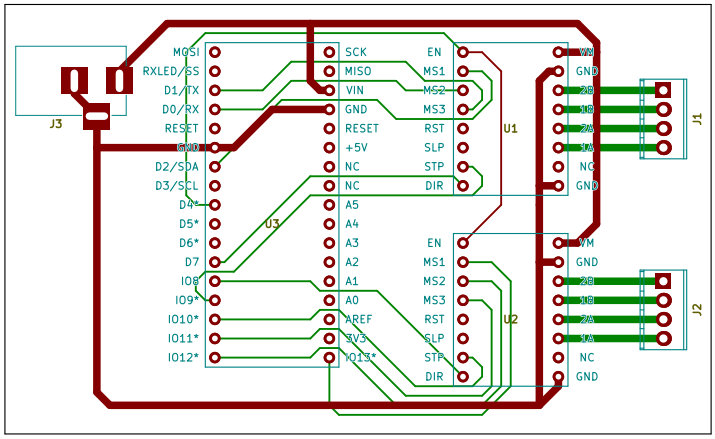

(a)

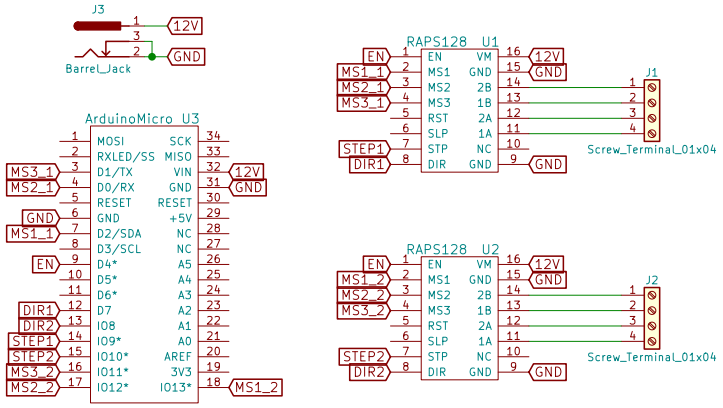

(b)

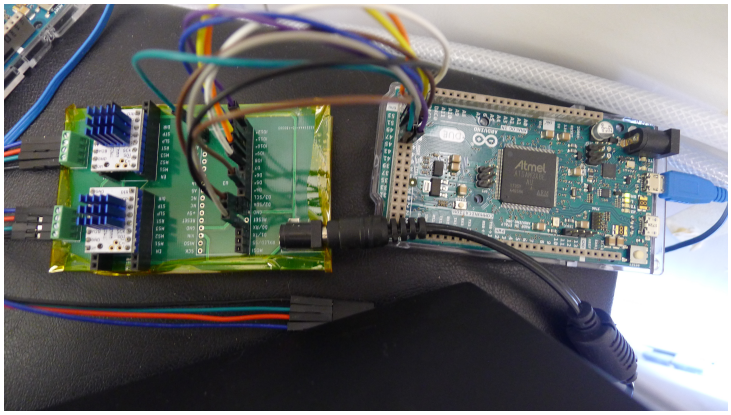

(c)

Figure 3.23: Stepper motor board a) PCB layout, b) schematic and c) photo. Used to control stepper motors in the syringe pumps. TMC2130 stepper motor drivers were connected to an Arduino Due microcontroller. The microcontroller was able to fully configure the drivers and operate the syringe pumps using these connections. The TMC2130 drivers were used in stand-alone operation (i.e. not in SPI mode).

3.3.4.2 Choice of mixing parameters

The mixing parameters were chosen with the aim of maximising the mixing rate. The mixing speed (the rate at which the syringe pumps pushed and pulled) was limited by the need to avoid pressure extremes (due to potential leak sites where the tubing meets the chamber stack, see section 3.4.2). The mixing volume was limited in order to avoid over-stretching the PDMS membranes, since this decreased their thickness, increased their surface area and would damage them to the point of leaking. The mixing rate was as frequent as is possible given the chosen mixing speed and volume, and given that mixing must be paused while optical density measurements are taken (to prevent the flexing membranes from interacting with the light passing through the chamber being measured). Determining these mixing speed and volume limitations was an empirical process of inspection of the apparatus following long periods (around $24\,\mathrm{h}$) of mixing.

3.3.4.3 Assessment of mixing rate

The mixing rate achieved by the apparatus was assessed visually. $0.1\,\mathrm{mM}$ methylene blue solution (a vivid blue dye) was injected gently into the chambers so that it settled at the bottom of the chamber remaining separate from the original chamber contents. The mixing was started and the time taken for the chamber contents to visually appear well-mixing (i.e. an even colour) was used to gauge the degree of mixing.

3.3.5 Optical density measurements

3.3.5.1 Light source

The light sources used were Kingsbright $3\,\mathrm{mm}$ round LEDs. They had a dominant wavelength of $601\,\mathrm{nm}$ and a luminous intensity of $800\,\mathrm{mcd}$. This dominant wavelength was used so that the measurements were as similar to standard OD_{600} (using light at $600\,\mathrm{nm}$) measurements as possible. The LEDs were mounted $5\,\mathrm{mm}$ apart on a PCB to line up with the growth chambers of the chamber stack (Fig3.25). They were powered by a standard LM317 current regulator circuit (Fig3.24) configured with a $68\,\Omega$ resistor to give an regulated output current of $18.4\,\mathrm{mA}$ (Fig3.29). This was used to ensure that the intensity of the light source was constant and not affected by temperature or an

inconsistent power source. Each LED was only powered when its corresponding light sensor was taking a measurement. This was to prevent interference with measurements of other chambers. The LEDs were switched on and off by TIP120 NPN Darlington transistors controlled by the Arduino Due (Fig3.29).

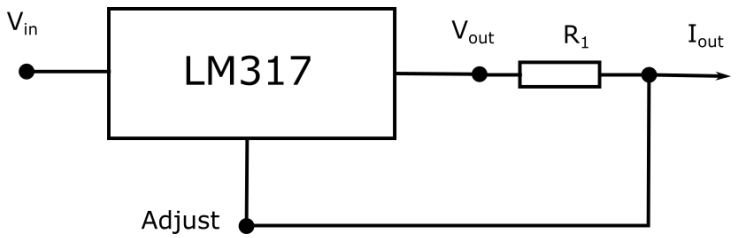

Figure 3.24: Standard LM317 current regulator circuit. Used to supply regulated power to the OD measurement apparatus light source.

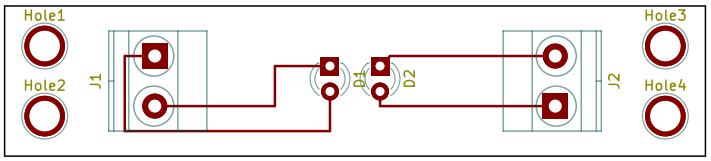

Figure 3.25: LED mount board schematic. The LEDs (D1 and D2) were positioned such that they could be mounted in the correct alignment with the rest of the OD measurement apparatus. Electrical connections (via screw-gate connectors J1 and J2) to the LEDs allowed them to be powered. These acted as light sources in the OD measurement apparatus. Holes at the corners (holes 1-4) allowed mounting to the apparatus and alignment with the chambers, light masks and light sensors.

3.3.5.2 Light sensor

The light sensors used were TSL2561 integrated circuits (IC). These were chosen because they output a digital signal that is not as subject to interference as an analogue output, and because use of these ICs with Arduino microcontrollers is well documented. These ICs were connected using a circuit based on the Adafruit TSL2561 Digital Luminosity/Lux/Light Sensor Breakout board but modified to contain two TSL2561 ICs. These two ICs were placed $5\,\mathrm{mm}$ apart so that they line up with the two culture chambers of the chamber stack (Fig3.26). The TSL2561 boards communicated with an Arduino Due microcontroller over I2C and provided a light reading as 16-bit digital output with a range of values from 0-65535.

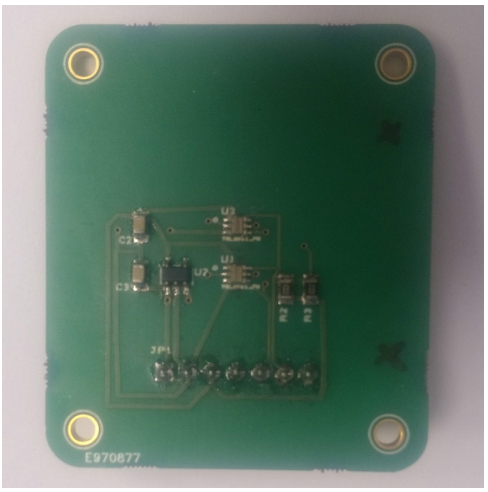

Figure 3.26: Photo of light sensor PCB. Two TSL2561 light sensor ICs (U1 and U2) were mounted on a custom-designed breakout board so that they were positioned correctly when mounted (aligned with the light sources and chambers), and so that they could be controlled by a microcontroller (via the pins at the bottom). These light sensors were used to measure OD as part of the non-contact co-culture apparatus.

3.3.5.3 OD sensor apparatus description

Light reaching the sensor was masked (Fig3.28c, Fig3.28f) as described in section 3.2.2.2.3. A stack of laser-cut light masks, made of opaque PMMA sheets, were attached to the anaerobic box using bolts (Fig3.28h, Fig3.27). These bolts aligned the light sources, sensors, chambers and light masks. The light mask holes were circular with diameter $1\,\mathrm{mm}$, the distance between light source and sensor was $110\,\mathrm{mm}$. The chamber stacks were positioned within the anaerobic box by slotting them into grooves in the box sides (Fig3.20b). They were held in place by the clamping of the top and bottom plates.

The distance of $110\,\mathrm{mm}$ was determined empirically based on the chosen light source, light sensor, light hole diameter and chamber size.

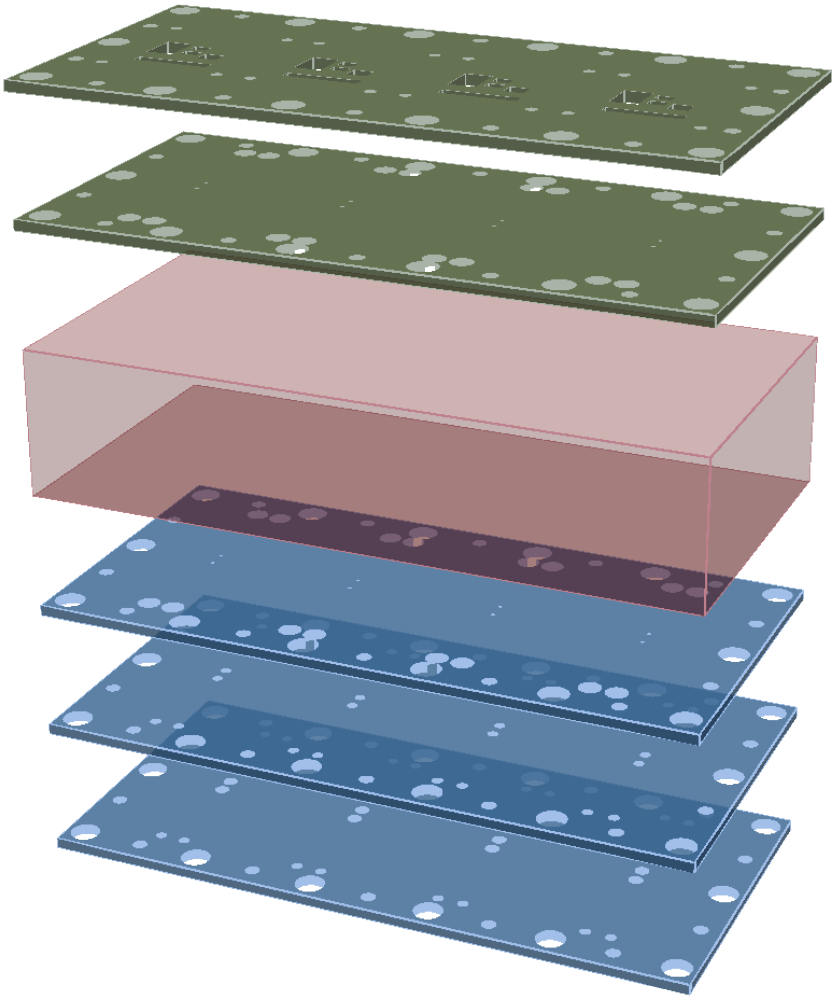

Figure 3.27: Diagram showing stack of light masks for optical density measurement apparatus. LED mounts (blue), light sensor mounts (green) were stacked with the anaerobic box (red) to align the light sources, sensors and chambers. This was essential for measuring OD of the chamber contents.

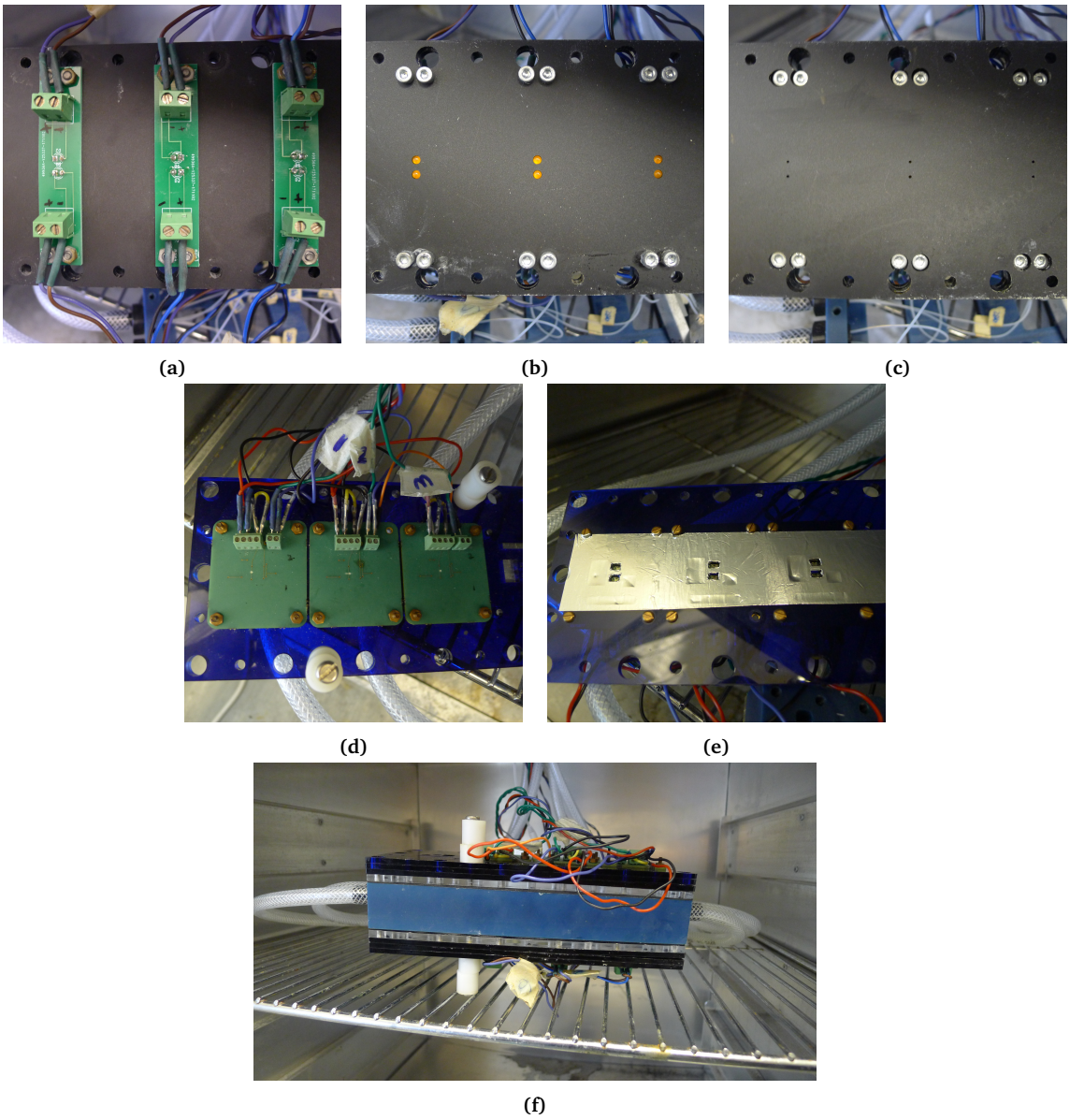

Figure 3.28: Photos of optical density measurement apparatus. Photos show the light sources (a,b), masks (c,f) and sensors (d), the measurement apparatus was mounted on the anaerobic box to measure the OD of the culture chambers contained inside.

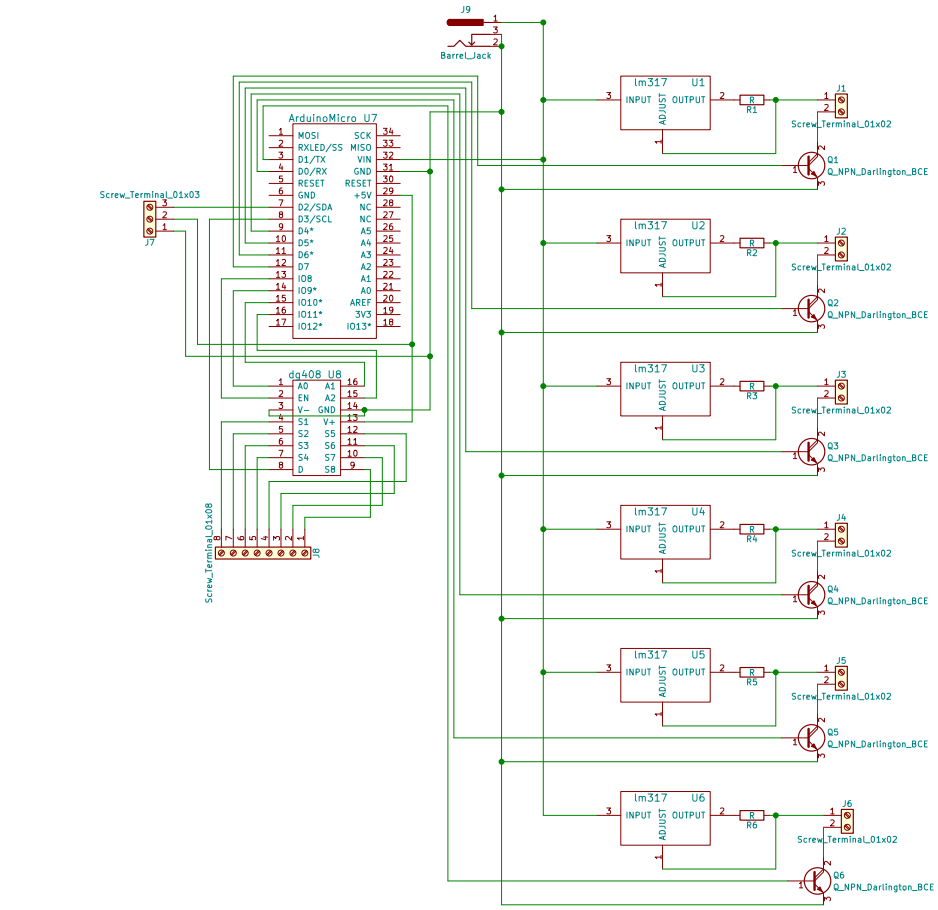

(a)

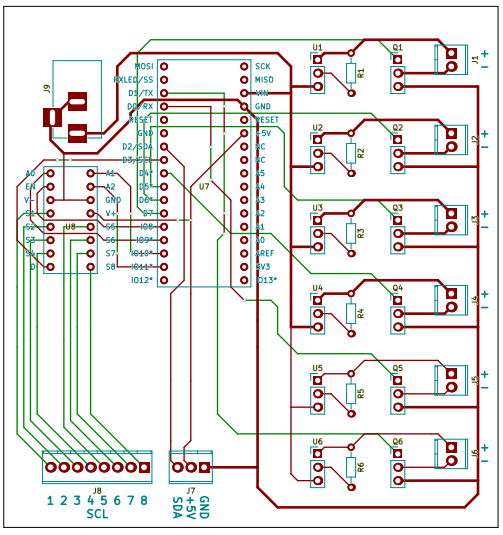

(b)

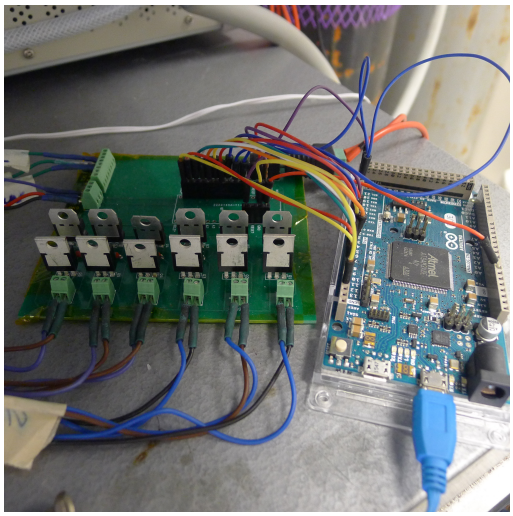

(c)

Figure 3.29: Light sensor controller a) schematic, b) PCB layout and c) photo. An Arduino Due microcontroller was connected to multiple TSL2561 light sensor boards via I2C (data line via J7 and clock line via J8). A DG408 IC (J8) switched the I2C clock line between different TSL2561 boards. The microcontroller controlled the LEDs using TIP120 transistors (Q1-6), the LM317 ICs (U1-6) provided a regulated power supply to the LEDs.

The TSL2561 light sensor ICs were configured as follows: $402\,\mathrm{ms}$ integration time (out of a choice of $13.7\,\mathrm{ms}$, $101\,\mathrm{ms}$ or $402\,\mathrm{ms}$), and $16\times$ gain (out of a choice of $1\times$ or $16\times$). A series of readings were taken over the course of $1\,\mathrm{min}$, and the mean of these readings was used an as a single light reading.

Optical density (OD) was calculated as

$$OD = log_{10}\left(\frac{\phi_0}{\phi_s}\right) \tag{3.1}$$

where ϕ_0 is the light intensity from a chamber with a blank sample, and ϕ_s with the sample being measured.

The six TSL2561 ICs were coordinated by one Arduino Due microcontroller. The TSL2561 ICs were able to share I2C communication connections and address each IC individually, however only three unique addresses were available. Therefore, a DG408 multiplexer was used to switch the I2C clock line (one of two lines that make up an I2C connection) from the Arduino Due to one of the three TSL2561 boards (Fig3.29). Once the TSL2561 board was selected, one of the two TSL2561 ICs on the board was selected by address. A $12\,\mathrm{V}$ $1\,\mathrm{A}$ switching power supply was used to power the microcontroller and the LEDs. A regulated $5\,\mathrm{V}$ supply from the Arduino Due microcontroller board powered the TSL2561 boards. The power supply to the LEDs was regulated by LM317 ICs.

3.3.6 Temperature control

A stable temperature was needed to maintain culture conditions. It was also needed to prevent temperature-dependent variations of the light sensors readings from affecting the results. To control the temperature, the entire anaerobic box with attached OD measurement apparatus was placed in a lab oven. The consistency of the temperature in this lab oven was improved by using a microcontroller (an Arduino Due with custom firmware). The microcontroller's firmware was an implementation of Proportional-Integration (PI) control, the input (temperature in the oven) was measured by an Adafruit HTU21DF board connected to the Arduino Due via I2C. The microcontroller firmware controlled the temperature by switching the oven on and off at the socket with a relay. This relay was a standard home remote control power socket which was operated

by sending radio control signals from the remote control. These signals were emulated by the microcontroller and sent using a radio transmitter board. The output from the PI control program controlled the proportion of time that the oven heater was on.

PI parameters were chosen manually with the aid of a first order plus dead time (FOPDT) model of the system. The model was fitted to the behaviour of the lab oven (e.g. rate of heat loss when heater is off, rate of heat gain when heater is on). Then PI control was added to this model and it was used to manually tune PI parameters to optimise accuracy and speed of the control.

3.3.7 Preparation of apparatus

To prepare the non-contact co-culture apparatus, all tubing and chamber stack slices were first washed with double-distilled water (ddH_2O) and constructed as described in sections 3.3.1.1 and 3.3.2.1. Air bubbles were removed from the system by manually pushing ddH_2O through with syringes. In order to prevent stretching and damaging of the PDMS membranes between the chambers, when one chamber was being flushed the other chamber's tubing was sealed at each end to prevent a change in volume in these other chambers.

The culture chambers and their associated tubing were sterilised by flushing with $100\,\mathrm{mM}$ NaOH. Each section of tubing was flushed in turn and then clamped shut, and then $5\,\mathrm{mL}$ of $100\,\mathrm{mM}$ NaOH was flushed through each chamber. The chambers and tubing were left to sit for $15\,\mathrm{min}$ filled with this sterilising solution. After the system was sterilised, all operations involving flushing of the chambers and tubing were carried out in a way that maintained the sterility of tubing and chambers (as described in section 3.3.2). The chambers and tubing were flushed with phosphate buffer (PB) ($3.10\,\mathrm{g\,L^{-1}}$ NaH_2PO_4, $10.9\,\mathrm{g\,L^{-1}}$ Na_2HPO_4 in ddH_2O) to remove the sterilising solution and neutralise any remaining alkalinity. The chambers and tubing were then flushed with the liquid needed for the operation of the apparatus (e.g. culture media for culture chambers).

The air supply chambers were simply washed with ddH_2O, the bubbles were removed, and then the system was sealed. This was done so that these chambers were not compressible while the other chambers are being flushed thereby preventing damage to the membranes.

When syringes (e.g. for the purpose of mixing or dilution) were connected to the tubing, the connector was first flooded with 70% ethanol. In order to remove the residual ethanol, the syringes were flushed with at least $5\,\mathrm{mL}$ of liquid (depending on the liquid held in their corresponding chamber). Mixing syringes were left filled with a volume of around $1\,\mathrm{mL}$ and media syringes were left full with around $2\,\mathrm{mL}$. $1\,\mathrm{mL}$ glass syringes were used for mixing, $2\,\mathrm{mL}$ glass syringes were used for dilution.

The chamber stacks were installed in the anaerobic box with care to position the tubing so that it did not interfere with light readings of the chambers. The anaerobic box was sealed and oxygen-free nitrogen (section 3.3.3) was set flowing through the hosing and box at a rate of $1\,\mathrm{mL\,min^{-1}}$.

3.3.8 Culturing of *E. coli* using the co-culture apparatus

3.3.8.1 Inoculation with *E. coli*

An *E. coli* DH5α inoculum was prepared by plating either *E. coli* DH5α glycerol stock or a previous *E. coli* DH5α liquid culture or plate onto an LB agar plate ($10\,\mathrm{g\,L^{-1}}$ Tryptone, $10\,\mathrm{g\,L^{-1}}$ NaCl, $5\,\mathrm{g\,L^{-1}}$ yeast extract, $15\,\mathrm{g\,L^{-1}}$ agar) and incubating at $37\,^{\circ}\mathrm{C}$ for around $8\,\mathrm{h}$. A single colony was picked off this plate and used to inoculate $10\,\mathrm{mL}$ LB medium ($10\,\mathrm{g\,L^{-1}}$ Tryptone, $10\,\mathrm{g\,L^{-1}}$ NaCl, $5\,\mathrm{g\,L^{-1}}$ yeast extract) which was incubated at $37\,^{\circ}\mathrm{C}$ for around $4\,\mathrm{h}$ shaking at $180\,\mathrm{RPM}$. This culture was then diluted in LB to an OD_{600} of 0.05 (as measured by a lab spectrophotometer).

This inoculum was injected into the relevant chamber by the sequence of syringe movements shown in figure 3.30. Before the procedure was started, the media syringe was filled with at least $2\,\mathrm{mL}$ of liquid media, and the ejection port adjacent to the inoculation port was connected to a sealed waste collection bottle via some PTFE tubing. The inoculation syringe connector was sterilised by flooding with 70% ethanol, and then the ethanol was flushed out of the system by the liquid media syringe. $5\,\mathrm{mL}$ of the inoculum was prepared in a sterile $5\,\mathrm{mL}$ syringe. The inoculation connector was flushed with media, and then the inoculation syringe was immediately attached. $1\,\mathrm{mL}$ of inoculum was flushed through the connector into the waste collection bottle to further flush the tubing and remove air bubbles. Then the inoculation syringe was used to fill the chamber with inoculum.

Once the inoculation syringe was emptied, the tubing connecting the inoculation connector to the chamber was clamped shut and the inoculation port was sterilised again by flushing with 70% ethanol. This was for safety to prevent release of the inoculum to the surrounding environment.

Immediately following inoculation, the adjacent air supply chamber was flushed of all liquid by pushing air through it with a syringe. This was to begin use of this chamber for supplying oxygen to the newly inoculated culture chamber. To achieve a sufficiently unhindered flow of air though the air-supply chamber, the tubing had to be thoroughly flushed with around $200\,\mathrm{mL}$ of air to remove any droplets of water that remained.

Finally, the volumes of the chambers were adjusted so that the membranes between the chambers showed no visible signs of flexing. This was to ensure that the chamber volumes, membrane thicknesses and surface areas were as intended, and so that the light beams used to measure OD were not interrupted by flexed membranes.

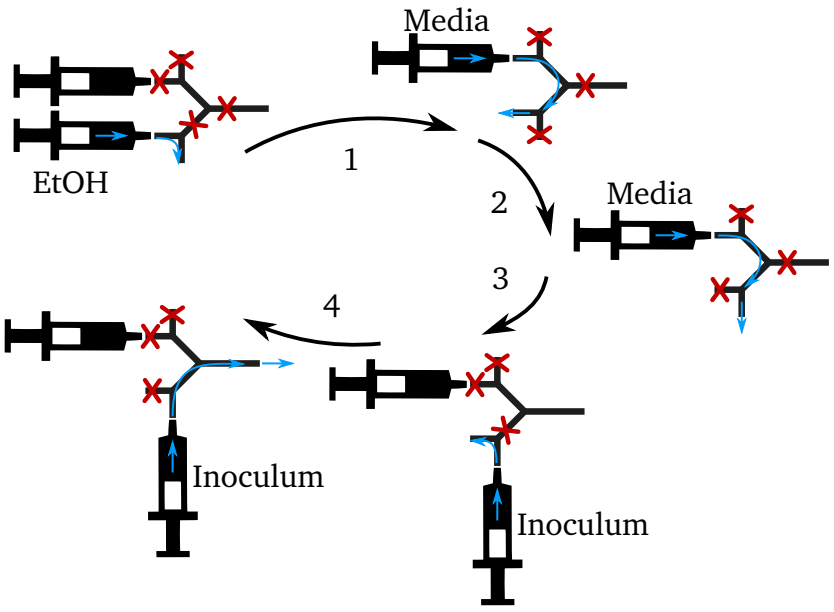

Figure 3.30: Sequence of syringe movements used to inoculate a culture chamber. Ethanol was used to sterilise the inoculation connector which was then flushed by sterile media already in the system before connecting the inoculum. The inoculum was first pushed to waste in order to prevent injection of any bubbles to the culture chamber. Then it was injected into the culture chamber.

3.3.8.2 Operation

Once the chambers were prepared and the culture chambers inoculated, they were monitored by periodic OD measurements. The chambers were also mixed. This was achieved for the two adjacent culture chambers, A and B, by drawing in liquid from A, then pushing back liquid to A while simultaneously drawing in liquid from B, then finally pushing liquid back in to B. This staggered mixing minimised flexing of the membranes. The volume of liquid displaced in each syringe movement was $25\,\mu$L over the course of $3\,\mathrm{s}$.

Chamber mixing was coordinated with OD measurements to avoid artefacts caused by the flexing membrane interfering with the passage of light through the chambers. Three cycles of mixing were carried out and then an optical density measurement was taken for one of the culture chambers. For each chamber, five readings were taken over a period of $4\,\mathrm{s}$ and averaged to be used as a single measurement. The complete mixing/measurement cycle of all six culture chambers was carried out every $1.5\,\mathrm{min}$.

Air was flowed though the air supply chambers by the push-pull cycle of a syringe pump loaded with $2\,\mathrm{mL}$ plastic syringes. Each syringe pump movement had a displacement of $0.882\,\mathrm{mL}$ over the course of $30\,\mathrm{s}$. The syringes pumped air to and from a humid air source (a bottle containing warm water). This limited evaporation of water from the adjacent culture chamber.

The temperature was set to $37\,^{\circ}\mathrm{C}$. The temperature was recorded every $1\,\mathrm{min}$ to verify that the correct temperature had been maintained throughout the experiment.

3.3.9 Testing of sterility of the apparatus methods

The ability of the apparatus to maintain sterile conditions was tested by combining the tubing operation procedures with a chamber-sterilisation procedure. To sterilise the chambers and tubing, the whole system was filled with $100\,\mathrm{mM}$ NaOH aqueous solutions for $30\,\mathrm{min}$, washed with phosphate buffer ($3.10\,\mathrm{g\,L^{-1}}$ NaH_2PO_4, $10.9\,\mathrm{g\,L^{-1}}$ Na_2HPO_4 in ddH_2O) and then filled with Mueller-Hinton broth. These injections were made using the operating procedure described in section 3.3.2. The chamber contents are considered to be "changed" once $10\,\mathrm{mL}$ of the new solution is flowed through the chamber thus diluting the previous chamber's contents and replacing them with the new solu-

tion. The chambers were incubated at $37\,^{\circ}\mathrm{C}$ for $24\,\mathrm{h}$, and were then visually inspected for cloudiness that would indicate microbial growth by a contaminating organism.

3.3.10 Detection of anaerobic conditions

A resazurin solution ($10\,\mu\mathrm{M}$ resazurin, $4.13\,\mathrm{mM}$ cysteine) was used as an indicator of the level of oxygen in the chamber. Under anaerobic conditions, resazurin is irreversibly reduced to resorufin resulting in a colour change from purple to pink. Resorufin can be further reduced, and this is associated with a colour change from pink to colourless. This change can be reversed by oxidation and so makes a useful indicator to detect if anaerobic conditions have been compromised. These colour changes are useful as both a visual change that can be observed and a change in OD that can be measured. In this solution, cysteine acts as a reducing agent. It is added to ensure that the resorufin is able to fully reduce under anaerobic conditions so that any influx of oxygen then produces a clear colour change.

3.3.10.1 Testing of oxygen diffusion into apparatus

The ability of the chamber stack with attached tubing to prevent oxygen entering the system was tested by filling the chambers with an oxygen-sensitive solution (section 3.3.10). Anaerobic conditions were established by leaving the apparatus in an anaerobic hood overnight. Then the apparatus was exposed to air and observed for any colour change that would indicate the presence of oxygen.

3.3.10.2 Generation of anaerobic conditions

Three PDMS chamber stacks (section 3.3.1.2) were used. Two different conditions were tested. In two chamber stacks, *E. coli* was grown in one chamber and an oxygen-sensitive solution (section 3.3.10) was injected into the adjacent chamber. In a third co-culture device, both chambers were filled with just the oxygen-sensitive solution.

3.3.11 Analysis of OD time series data

The starting OD of the inoculum was measured in a lab spectrophotometer before injection into the co-culture device. However, since this value could not be translated to a value measured by the device sensor apparatus, the starting OD was defined as 0 in the data presented. If a calibration curve was collected before each use of the apparatus then this could have been used to adjust the starting OD accordingly. However, this was impractical since it would have greatly increased the time taken to prepare the apparatus, and also increased the opportunities for introduction of bubbles in the system or damage to the membranes.

The starting $30\,\mathrm{min}$ of the OD time series was a period of time in which the temperature was still adjusting (Fig3.33). This affected the light sensors and so the data from this period was discarded. The culture was likely in lag phase (and the temperature was lower) so it is unlikely that the culture density changed much in this time period.

3.3.12 Testing of optical density measurements

The ability of the apparatus to measure OD of cell cultures was tested by filling the chamber with dilutions of either an *E. coli* DH5α culture or a resazurin solution. Resazurin was chosen simply because it is a soluble dye that is absorbent to light at around $600\,\mathrm{nm}$. To test that the measured OD is proportional to the actual OD of the chamber contents, the results were compared to OD_{600} measurements by a Thermo Fisher Scientific Spectronic™ 20D+ spectrophotometer. To test consistency of measurements between chambers (and their corresponding OD measurement equipment), this process was performed with one chamber in each of three chamber stacks (so three chambers were compared). Four different liquids with OD_{600} ranging between 0.1-1.2 were used.

3.4 Results

3.4.1 Apparatus re-use, sterility and temperature control confirmed

3.4.1.1 Re-use of PMMA chamber stack

Re-use of the chambers between experiments was quick since the PMMA slices only had to be cleaned before re-use. The gaskets and membranes were not suitable for re-use because the membranes stretched as liquids were pumped through the chambers, and the gaskets often got damaged as the chamber stack clamping bolts were tightened. Therefore, new gaskets and membranes were cut by hand each time a new chamber stack was constructed.

3.4.1.2 Maintenance of apparatus sterility

The sterilisation procedure (section 3.3.7) and did not result in any degradation confirming that it was compatible with all of the materials used. When the sterility was tested (section 3.3.9), no contamination was observed.

3.4.1.3 Temperature control testing

The temperature of the lab oven that contained the co-culture apparatus reached $37\,^{\circ}\mathrm{C}$ in around $20\,\mathrm{min}$ and was stable from $40\,\mathrm{min}$ onwards (Fig3.31).

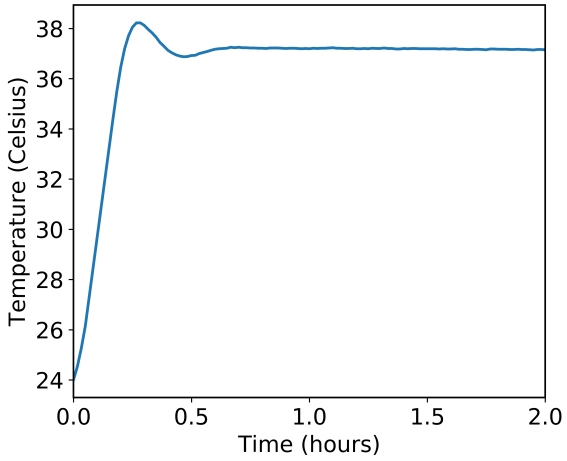

Figure 3.31: Temperature of lab oven under PI control

3.4.2 Leaking from chambers

The chambers, constructed by stacking PMMA slices (section 3.3.1.1), were able to hold liquid contents. Leaks of liquid from the chambers were rare. When this did happen, it was the result of a damaged gasket or a loose clamp and so they could be easily fixed. However, when under negative pressure (e.g. during mixing by pulsing liquid through the chambers), gas was able to leak in to the system. This was a problem because the bubbles interrupted the light beams and made the optical density measurements unreliable. Also, the gas displaced liquid cultures from their growth chambers meaning the co-culture was not as planned and modelled. The leaks may have been due to gaps in the gaskets, particularly those surrounding the tubing holes. Attempts were made to plug these entry routes with adhesives or by curing PDMS in place. However, a bond was not able to form on both the PDMS and the PMMA to seal them together. This problem was therefore managed by avoiding highly negative pressures in the chambers.

3.4.3 Mixing rate testing

At short tubing lengths (around $30\,\mathrm{cm}$) and over short time periods (around $10\,\mathrm{min}$), rapid mixing times of around $3\,\mathrm{s}$ were achieved. However, with the long tubing used in the complete apparatus, mixing speeds had to be lower to avoid large negative pressures. Also, over longer periods of time (i.e. over the course of several days), the effects

from leaks and membrane stretching were greater. Therefore, a modest mixing stroke of $25\,\mu$L over the course of $3\,\mathrm{s}$ was used. This yielded a mixing time of around $30\,\mathrm{s}$.

3.4.4 Exclusion of oxygen by anaerobic enclosure

When the apparatus was tested (section 3.3.10.1) without a surround anaerobic box and hosing, colour change was observed within a few minutes. The colour change started in the tubing and then moved to the chambers. This indicated that oxygen was able to rapidly enter the system, either by diffusing across the $0.25\,\mathrm{mm}$ PTFE tubing walls or through leaks at the tubing junctions (particularly the junction between tubing and chambers).

Testing for the generation of anaerobic conditions by *E. coli* cultures (section 3.3.10.2) in the apparatus without an anaerobic box or hosing resulted in no observable colour change. This indicated that anaerobic conditions were not generated.

However, when the apparatus filled with aerobic oxygen-sensitive dye solution was placed in the anaerobic closure, the solution turned colourless indicating that anaerobic conditions were generated. This showed that the oxygen was removed as it diffused out of the tubing and so oxygen was completely excluded from the system.

3.4.5 Optical density measurement testing

3.4.5.1 Proportionality with standard OD measurements

The ability of the apparatus to measure the OD of cell cultures was tested (section 3.3.12) by using a range of *E. coli* DH5α culture dilutions.

The results (Fig3.32) showed a linear relationship between measurements from the lab spectrophotometer and from the custom sensor apparatus. Linear regression analysis showed an R^2 value of 0.998 (3sf), y-intercept of -0.00896 (3sf) and gradient of 0.305 (3sf) indicating that there was a direct linear relationship. This means that measurements would only need to be scaled by a single factor to convert them to standard OD_{600} measurements. In this case, that factor (the gradient) was 0.305 (3sf).

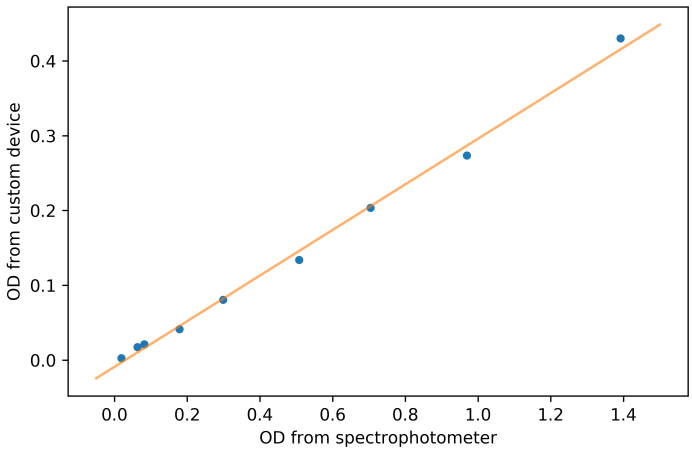

Figure 3.32: Optical density measurement calibration to test light mask method. Different densities of *E. coli* DH5α cultures were used as samples. A single reading was recorded for each sample. There was a linear relationship between OD measurements by the test sensor apparatus and OD_{600} by the lab spectrophotometer. Linear regression analysis showed a gradient of 0.305 (3sf) and y-intercept of -0.00896 (3sf) (n$=9$, $R^2 = 0.998$ (3sf), standard error $= 0.00726$ (3sf)).
The test apparatus used light masks to direct a beam of light through the chamber being measured.

These results were collected at an early stage in development and used a different light source (World Precision Instruments LED light source, model F-O-LITEH), sensor (Ocean Optics S2000, average intensity of light between $595\,\mathrm{nm}$ and $605\,\mathrm{nm}$ was used as a single reading), and different light mask arrangement ($d_1 = 60\,\mathrm{mm}$, $d_2 = 80\,\mathrm{mm}$, $d_3 = 7\,\mathrm{mm}$ and $d_4 = 70\,\mathrm{mm}$, light holes all had diameter of $2\,\mathrm{mm}$).

3.4.5.2 Consistency of measurements between chambers

Varying dilutions of a resazurin solution were used to test consistency between OD measurements of each chamber (section 3.3.12).

The results (Fig3.33) showed that the measurements from each chamber were proportional to the lab spectrophotometer measurements. However, each of the proportional relationships were different, showing that the OD measurements of each chamber were not consistent with each other.

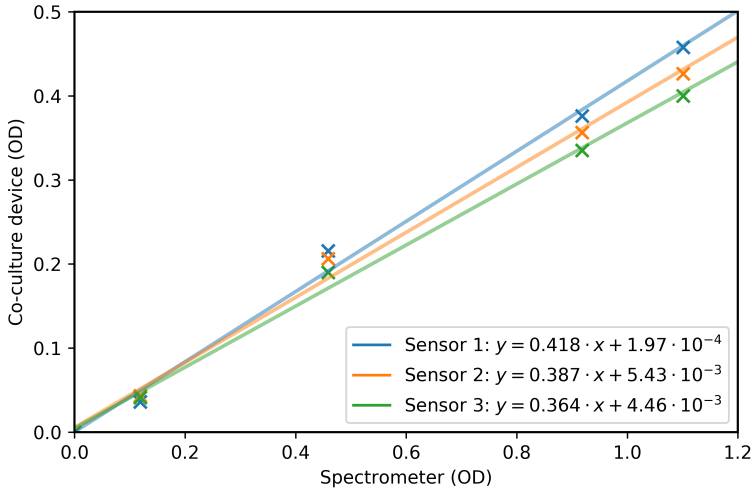

Figure 3.33: Optical density measurement consistency between sensors. Linear relationships are shown between OD measurements by the sensors developed for the non-contact co-culture apparatus and a lab spectrometer. Gradients and y-intercepts of the linear relationships were calculated by linear regression analysis (n$= 4$, R^2 values were 0.997, 0.998 and 0.998, standard errors were 0.0172, 0.0156 and 0.0125 (3sf) for sensors 1, 2 and 3 respectively).

3.4.6 Apparatus testing with *E. coli* cultures

3.4.6.1 Aerobic growth in triplicate

Three chamber stacks were prepared and operated in triplicate as described in section 3.3.8 but with several differences: 1) a PDMS stack design was used for the chambers (section 3.3.1.2, Fig3.14c&d), 2) an anaerobic enclosure was not used (the OD measurement apparatus was still aligned with the chambers using a similar method), and 3) mixing was by shaking rather than syringe pumps.

The results (Fig3.34b) showed exponential, linear and stationary phases of growth. There appear to have been two distinct exponential phases (transition around the $2.5\,\mathrm{h}$ mark) which may indicate diauxic growth. They also showed good consistency for the first $15\,\mathrm{h}$ in both the timings of the growth and also the absolute OD values.

After $15\,\mathrm{h}$, the OD measurements of the three triplicates deviated from each other (Fig3.34a). Visual inspection of the chambers revealed that the likely cause of this was bubbles that had formed in some of the chambers, probably due to evaporation through leaky connections between the chambers and their tubing.

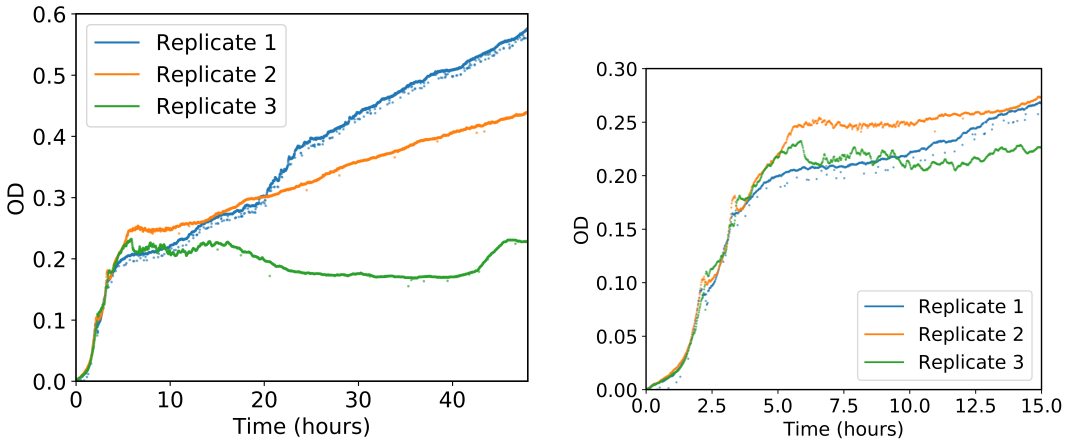

Figure 3.34: Scatter plot showing growth of *E. coli* cultures in non-contact co-culture apparatus. a) OD readings from the three replicate chamber stacks over a time period of 50 h. b) The first 15 h of this data showing the exponential growth phase in more detail.
OD measurement values are relative to the initial OD (at 0 h).

3.4.6.2 Generation of anaerobic conditions

When testing for generation of anaerobic conditions (section 3.3.10.2), no colour change was observed when the anaerobic box was not used. This indicated that the oxygen consumption of the *E. coli* cultures was not sufficient to generate anaerobic conditions in the adjacent chamber.

The results when the anaerobic box was used (Fig3.35) showed that anaerobic conditions were formed after 1 h. This is indicated by the drop in OD of the resazurin solution containing chamber as *E. coli* grew in the adjacent chamber (Fig3.35a). This contrasts with the control conditions (Fig3.35b) where OD dropped slightly, but not to the same extent as when adjacent to an *E. coli* culture. This indicates that oxygen may have been diffusing out of the chamber and therefore generating slightly more anaerobic conditions. The OD values for the resazurin solution containing chambers were calculated using a blank reading collected after the time-series data had been collected (the chambers were flushed with water and a blank reading was taken). The resazurin solution was visually confirmed to be colourless when adjacent to *E. coli* cultures and purple/pink in the control.

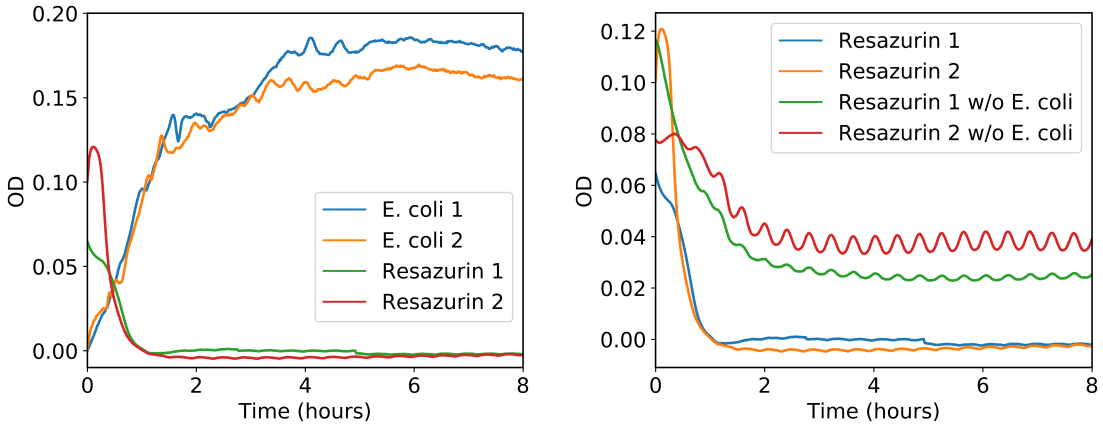

Figure 3.35: Anaerobic conditions were generated by *E. coli* culture in non-contact co-culture apparatus. a) *E. coli* cultures were grown adjacent to chamber filled with oxygen-sensitive resazurin solution, in both chamber stacks the resazurin OD dropped as *E. coli* grew. b) A control, with both adjacent chambers filled in resazurin solution (labelled "Resazurin 1/2 w/o E. coli"), did not show the same drop in OD compared to a) (labelled "Resazurin 1/2").

In these results the OD measurements undulate. This is particularly noticeable in figure 3.35b in the control data series. This undulation was found to be associated with the undulation of temperature in the lab oven before it was upgraded with PI control (section 3.3.6).

3.5 Discussion

3.5.1 Design and implementation process

An apparatus to carry out non-contact co-culture experiments has been developed. The design was inspired by devices that have been reported in scientific journals. There are many designs for non-contact co-culture apparatus reported, however none were suitable for studying metabolic interactions between *N. meningitidis* and *P. gingivalis*. The unique aspects of this application are 1) the maintenance of adjacent anaerobic and aerobic cultures, and 2) for these to be well-mixed liquid cultures (to aid interpretation of system behaviour by mathematical modelling). Aspects from several different apparatus designs have been combined in order to develop apparatus that is able to meet these requirements.

Implementation of this design was iterative and several key technical challenges had to be overcome, namely: mixing of the chambers, leaking from the connections, exclusion of oxygen, sterilising the apparatus, and taking reliable OD measurements. A simpler design could potentially have been used to avoid these technical challenges. A semi-permeable bag (section 3.2.1.1) could have been used to prove the concept. Cultures in separate flasks could have been grown in separate environments and "connected" using a diffusion device (section 3.2.1.5). The use of standard glassware would have allowed the use of standard mixing and optical density monitoring apparatus. However, these solutions would likely have had their own unique set of associated technical challenges.

By implementing the chosen design for the non-contact co-culture apparatus, each technical challenge has been identified and addressed.

3.5.2 Mixing rate and culture duration is limited by leakiness of the tubing and chambers

It is important that the apparatus does not leak, not just in order to maintain sterility and a constant culture volume, but also for safety since it is to be used for culturing a Biosafety level 2 organism (*N. meningitidis*). No leaks of liquid coming out of the apparatus were detected during testing. However, when the chamber contents were under negative pressure (when liquid was being drawn from the chamber) then gas leaked in to the system.

To prevent this, pumping could instead be performed solely by positive pressures (relative to the surrounding air) rather than a combination of positive and negative pressures. This would require the oxygen-supply chamber to be filled with water and its volume actively controlled (by another set of syringe pumps), otherwise it would be compressed. Having all of the chambers constantly under either neutral or positive pressure would prevent air from entering the system. To achieve this, a pressure monitoring and feedback system would have to be developed to prevent damage due to overpressure and keep the volumes of the chambers constant.

Bonding of the leaking junctions with an adhesive would most likely require surface modification of the PDMS (e.g. with an oxygen plasma treatment) to increase its wettability (i.e. make the surface more hydrophilic). This was not convenient to attempt in this project, and so the problem was instead managed by avoiding highly negative

pressures in the chambers.

Shorter tubing lengths could be used so that less extreme pressures are needed to achieve the same flow rate (e.g. for mixing). However, long lengths of tubing were needed to connect the separate anaerobic, temperature controlled and Biosafety Level II cabinet environments, and this exacerbated leaking at the tubing connections.

The relatively low degree of mixing achieved by the developed apparatus was a consequence of the requirement to use less extreme pressures. The demonstrated mixing rate of $30\,\mathrm{s}$ was significantly slower than the $5\,\mathrm{s}$ to $10\,\mathrm{s}$ target set earlier in section 3.2.2.3. A lower degree of mixing causes decreased diffusion rates between the chambers. This could be compensated for when results are interpreted with the mathematical model. However, a lower degree of mixing also means that the well-mixing assumption of the ODE models is less valid. This may reduce the relevance and utility of the models for designing experiments and interpreting results.

Leaking of gas into the apparatus will also decreases the duration of experiments since the gradual build-up of gas bubbles eventually interferes with OD measurements and changes the volume of the cultures.

3.5.3 Effectiveness of OD measurement apparatus

It was not expected that the OD measurements from the developed apparatus and the lab spectrophotometer would be the same. The path length through the sample ($10\,\mathrm{mm}$ for the lab spectrophotometer, $5\,\mathrm{mm}$ in the developed apparatus), and the distance from sample to sensor were both different, meaning that the opportunity for light to miss the sensor due to scattering was different. What is important is that any measurement is proportional to a standard OD measurement (by a lab spectrophotometer). The measurement apparatus (the electronics equipment and use of light masks) produced measurements proportional to optical density across a range of 0.014 OD_{600} demonstrating that it is suitable for use in co-culture experiments.

Although the measurements from each chamber were each proportional with a standard measurement, they did not have the same proportional relationships. This means that the OD measurements cannot be quantitatively compared between the different chamber stacks. However, qualitative features, such as the shape and timings of events

in a time series of OD measurements, can still be compared. The inconsistency of measurements between the chambers was due to slight misalignments of the chambers in the anaerobic box meaning that the light did not follow a simple straight-line path through the chamber. Evidence for why the anaerobic box is the cause of the misalignment is shown by the fact that OD measurements appeared much more consistent when the anaerobic box was not used.

The positioning of the chamber stacks within the anaerobic box should be made more precise in order to increase the quality of the OD measurements. The quality of the readings may be also improved by changing the manufacturing method for the chamber walls. Currently they are made by laser cutting PMMA, however this process leaves an uneven finish on the surface that scatters light as it passes through. The surface finish may be improved by machining the edge and polishing to ensure it is without distortion. This process, however, is more suitable for producing a final product rather than a development prototype, and so it should only be used once the complete design specification is finalised.

3.5.4 Generation of anaerobic conditions by aerobic of *E. coli*

The apparatus is able to support aerobic growth of *E. coli* and is able to supply sufficient oxygen to that culture to support a prominent exponential growth phase. The consistency of the results for each of the triplicates shows that the growth conditions between the three chamber stacks are consistent. There was inconsistency between the triplicates after $15\,\mathrm{h}$, however this was determined to be due to bubbles developing in the chambers rather than differences in the behaviour of the cultures.

Anaerobic conditions were formed and maintained in the apparatus, but only when the anaerobic box and hosing was used. When no anaerobic enclosure was used, oxygen entered into the apparatus via the tubing rapidly. Therefore, to generate and maintain anaerobic conditions, the co-culture apparatus must be surrounded by anaerobic gas.

Alternatively, different materials which prevent oxygen diffusion could have be used for the tubing (e.g. metals or glass). However, thin tubing made of these materials is rigid and fragile making it unsuitable for a method that requires significant manual manipulation of the tubing to prepare the apparatus, and that requires tubing to span between a Class II Biosafety Cabinet and a lab oven (Fig3.19). Even with these materials, oxygen

may still have been able to enter via junctions between the tubing and chambers, or via other routes that would only be detected once diffusion into the tubing was stopped. Rather than overcoming these challenges, an anaerobic enclosure was chosen since this method has already been demonstrated (section 3.2.1.4.1, Steinhaus *et al.*, 2007).

With the anaerobic enclosure, when oxygen was supplied to an *E. coli* culture, the generation of anaerobic conditions was not compromised. This shows that the oxygen was depleted by aerobic metabolism of the culture. This demonstrates that the apparatus is able to generate the conditions required for simultaneous aerobic and anaerobic cultures in adjacent chambers separated only by a semi-permeable PDMS membrane.

3.5.5 Anaerobic enclosure will not prevent diffusion of other substances

The rapid diffusion of oxygen into the apparatus (section 3.4.4) shows that undesirable exchange of volatile substances is able to occur across the tubing walls. Volatile metabolites may be lost via this route thereby reducing transfer of these metabolites between the culture chambers and weakening the measured effect of this microbial interaction. In particular, it is possible that propionic acid may diffuse via this route and ultimately be lost to diffusion through the tubing wall.

Use of metal or glass tubing would provide more of a barrier to diffusion. However, as mentioned previously, this would be impractical. One possible solution is the use of continuous culture rather than batch cultures. This may reduce diffusion from the tubing since the dilution flow would push substances from the tubing back into the chamber.

Loss of substances via this route must be taken into account when interpreting results from the developed assay. The amount of propionic acid lost due to diffusion across the tubing walls should be low compared to that diffusing into the adjacent chamber. This is because the tubing walls ($250\,\mu\mathrm{m}$) are much thicker than the PDMS membrane ($20\,\mu\mathrm{m}$ was the thinnest practical PDMS membrane that could be used in this project), and the permeability of PTFE to other substances is generally lower than PDMS (Pasternak *et al.*, 1970; Merkel *et al.*, 2000).

3.5.6 Ability to dilute chambers for continuous culture

Dilution of the chambers was not tested. However, the developed apparatus is, in principle, capable of this by using two reservoir syringes. With one syringe pump pushing and the other pulling, the liquid would be drawn through the chamber while the pressure and volume remains unchanged. For slow dilutions of the chambers, a smoother (less "stepped") flow would be desirable. To achieve this, 100:1 or 51:1 planetary gearboxes could be placed between the stepper motors and the lead screws of the syringe pumps to reduce the volume displaced per microstep.

3.5.7 Suitability of apparatus for non-contact co-culture between *N. meningitidis* and *P. gingivalis*

The apparatus has been shown to be capable of maintaining an aerobic microbial culture while generating strict anaerobic conditions for an adjacent anaerobic culture. The preparation and operation procedures are suitable for preventing contamination of the cultures. The developed apparatus is also convenient to re-use since only the membranes need replacing between experiments. The re-use is is not vital, but it will be useful for increasing the number of experiments that can be performed. The various electronics components have been shown to able to keep the chambers at a constant temperature while monitoring OD and keeping the chambers mixed.

The chamber mixing is limited by leaks in the chambers, this also limits the duration of experiments since gas leaks into the chambers and gradually accumulates. The OD measurements are limited to being used only to detect qualitative changes in culture density.

Despite these limitations, the tests have demonstrated that a non-contact co-culture between *N. meningitidis* and *P. gingivalis* in this apparatus should be possible. Therefore, this apparatus is ready to be tested further with these organisms. Experiments should be carried out to test the key assumptions of the mathematical modelling, particularly the diffusion of propionic acid across a PDMS membrane. The diffusion rates of oxygen and propionic acid across the membranes should be measured since these values are fundamental to determining the conditions for a viable non-contact co-culture.

Chapter 4

Preparation for non-contact co-culture experiments with *N. meningitidis* and *P. gingivalis*

4.1 Introduction

The non-contact co-culture apparatus, tested with aerobic *E. coli* cultures, is to be used to culture aerobic *N. meningitidis* cultures.

Compared to *E. coli*, *N. meningitidis* has more specific growth requirements. It is a strict aerobe, whereas *E. coli* is a facultative anaerobe. Also, *N. meningitidis* requires CO_2 to initiate growth. The mechanism for this is likely due to it being used by phosphoenolpyruvate carboxylase to produce oxaloacetate for the citric acid cycle (Baart *et al.*, 2007). Additionally, it is a biosafety level 2 organism and so must always be handled within a biosafety class 2 cabinet. Therefore, the apparatus must be tested with *N. meningitidis* cultures to see if this organism is capable of growing in this environment, and to assess its ability to generate anaerobic conditions by aerobic growth. Additionally, *N. meningitidis* growth should be characterised so that experiments using the non-contact co-culture assay can be planned. This mainly should involve the measurement of parameters such as growth rate and yields from glucose and propionic acid. Cultures should be studied so that other aspects of growth, that may be important in a metabolic interaction with *P. gingivalis*, can be identified and characterised.

Experimental conditions from Catenazzi *et al.*, 2014 have been used as a starting point to test these aspects of *N. meningitidis* growth. This study is used because it demonstrated propionic acid utilisation by *N. meningitidis* liquid cultures.

P. gingivalis growth should also be characterised in preparation for culturing using the apparatus. Characteristics such as growth rate, lag phase and carrying capacity should be measured along with any other important aspects. Following this, *P. gingivalis* cultures will then be able to be grown in the non-contact co-culture apparatus in preparation for running experiments using this assay.

4.2 Methods

4.2.1 *Neisseria meningitidis* growth media

4.2.1.0.1 Columbia Blood Agar $39\,\mathrm{g\,L^{-1}}$ Oxoid Columbia Blood Agar base (CM0331) in ddH_2O was heated and sterilised by autoclaving ($120\,^{\circ}\mathrm{C}$ for $40\,\mathrm{min}$) then placed in a water bath at $60\,^{\circ}\mathrm{C}$ for $30\,\mathrm{min}$. 5% v/v defibrinated horse blood was added and poured into Petri dishes. Plates were stored at $4\,^{\circ}\mathrm{C}$ for up to one month.

4.2.1.0.2 Mueller-Hinton Broth $21\,\mathrm{g\,L^{-1}}$ Oxoid Mueller-Hinton Broth (CM0405) in ddH_2O was sterilised by autoclaving ($120\,^{\circ}\mathrm{C}$ for $40\,\mathrm{min}$). 1% v/v of $1\,\mathrm{M}$ $NaHCO_3$ in ddH_2O was added immediately before *N. meningitidis* inoculation.

4.2.1.0.3 Chemically defined media Chemically defined media (CDM) (Catlin, 1973) was prepared by mixing ddH_2O with 2.5% (v/v) solution 1, 5% solution 2, 5% solution 3, 1% solution 5, and varying quantities of solution 4a, 4b or 6 (table 4.1). The CDM was filter sterilised with a $0.22\,\mu\mathrm{m}$ syringe filter before use. The final pH of CDM ranged from 7.1 to 7.3.

All stock solutions were stored at $4\,^{\circ}\mathrm{C}$. Solutions 1,2 and 4a were replaced monthly, solutions 3, 4b, 5 and 6 were replaced weekly.

Solution 1 (x40)	$MgCl_2$	1.95 mM	78 mM	Stir at 50 °C
	$CaCl_2$	0.2 mM	8.15 mM	overnight, filter
	Ferric citrate	0.15 mM	6.5 mM	sterilise
Solution 2 (x20)	NaCl	100 mM	2 M	Stir 10 min, pH 6.3,
	K_2SO_4	5.75 mM	114.8 mM	autoclave
	K_2HPO_4	235 mM	460 mM	
	NH_4Cl	185 mM	360 mM	
Solution 3 (x20)	Glycine	3.8 mM	75.6 mM	Stir 1 h at 40 °C, filter
	L-cysteine HCl	0.4 mM	8.3 mM	sterilise
	L-arginine	0.7 mM	14 mM	
	L-glutamine	4 mM	80 mM	
	L-serine	4.75 mM	95 mM	
Solution 4a (x224)	Glucose	2.5 mM	560 mM	Autoclave
Solution 4b (x40)	Sodium pyruvate	5 mM	200 mM	Stir 30 min, filter sterilise
Solution 5 (x100)	$NaHCO_3$	10 mM	1 M	Stir 20 min at 50 °C, filter sterilise
Solution 6 (x200)	Propionic acid	5 mM	1 M	pH 7.0, filter sterilise
	NaOH	5 mM	1 M	

Table 4.1: Component solutions of *N. meningitidis* chemically defined media (CDM). From Catlin, 1973

4.2.2 Preparation of *N. meningitidis* inocula

N. meningitidis MC58 (serogroup B) was the only strain of *N. meningitidis* used. Inocula for liquid culture experiments (in the plate reader or the non-contact co-culture assay) were prepared by first streaking 50 μL of *N. meningitidis* glycerol stock onto a Columbia Blood Agar plate. The plate was then incubated at 35 °C in a 5% CO_2 atmosphere for 12-

$24\,\mathrm{h}$. Large sparse colonies were scraped off a plate with a sterile loop and resuspended in $1\,\mathrm{mL}$ of liquid media by mixing and repeatedly pipetting up and down ($100\,\mu\mathrm{L}$ with P200 pipette). This thick cell suspension was then diluted to the desired cell density to be used as an inoculum.

4.2.3 Creation of *N. meningitidis* glycerol stocks

A Columbia Blood Agar plate was streaked with $50\,\mu\mathrm{L}$ of *N. meningitidis* glycerol stock and incubated at $35\,^{\circ}\mathrm{C}$ in a 5% CO_2 atmosphere for 12-24 h. $10\,\mathrm{mL}$ Mueller-Hinton Broth in a $50\,\mathrm{mL}$ Falcon tube was inoculated from a single colony on the plate. The culture tube was sealed in a second container for safety and incubated at $37\,^{\circ}\mathrm{C}$ for $4\,\mathrm{h}$ shaking at $200\,\mathrm{rpm}$. This culture was mixed 1:1 with sterile 50% v/v glycerol in ddH_2O, aliquoted ($1\,\mathrm{mL}$) and placed in a $-80\,^{\circ}\mathrm{C}$ freezer for freezing and storage.

4.2.4 Growth of *N. meningitidis* in CDM using plate reader

A Tecan Sunrise™ 96-well plate reader was used to maintain a temperature of $37\,^{\circ}\mathrm{C}$, measure absorbance at $620\,\mathrm{nm}$ every $1\,\mathrm{min}$ and mix the cultures by shaking for $30\,\mathrm{s}$ between each absorbance reading. The sample wells of the 96-well plates were prepared with a final well volume of $160\,\mu\mathrm{L}$ ($150\,\mu\mathrm{L}$ media and $10\,\mu\mathrm{L}$ inoculum). The outer wells were filled with $200\,\mu\mathrm{L}$ H_2O to reduce evaporation from sample wells. Water blanks and growth media blanks were included as controls. OD was calculated from the measured absorbance readings by subtracting the media blank absorbance.

A range of experimental conditions were tested. Two different serial dilutions of propionic acid in CDM media were used: one serial dilution was in CDM supplemented with $2.5\,\mathrm{mM}$ glucose, the other was CDM supplemented with $5\,\mathrm{mM}$ pyruvate. Each serial dilution started with $10\,\mathrm{mM}$ propionic acid and was diluted by 1:1 (v/v) mixing with the next well. There were 8 dilutions in the serial dilution plus one condition with $0\,\mathrm{mM}$ propionic acid. So, in total, there were 18 different experimental conditions. The concentrations of glucose and pyruvate were taken from Catenazzi *et al.*, 2014, and this study was also used as the basis for the range of propionic acid concentrations.

The *N. meningitidis* inoculum was prepared in CDM and diluted to a final starting OD_{600} of 0.25 (as measured by a lab spectrophotometer). This starting OD_{600} was chosen after

cultures with lower starting OD_{600} failed to grow reliably.

4.2.5 Measurement of *N. meningitidis* growth parameters

Data from *N. meningitidis* culture growth in the plate reader was used to measure maximum growth rate and yield from propionic acid.

The maximum growth rate of *N. meningitidis* for each of the conditions was measured by fitting an exponential function to the OD readings spanning the time period 0.5-$2\,\mathrm{h}$. This period of time spanned the exponential phase of growth.

To measure a yield of *N. meningitidis* from propionic acid, first the yield from glucose and pyruvate were calculated. The maximum density (measured by OD) of the culture growing in media supplemented by just one of these carbon sources was measured. The known quantity of the carbon source and the measured change in OD generated were used to calculate a yield.

The change in *N. meningitidis* culture OD due to propionic acid was calculated by measuring the height of the peak in OD due to propionic acid. The growth due to glucose or pyruvate was removed by subtracting a control data series. For the control, a low concentration of propionic acid ($0.0781\,\mathrm{mM}$) was used rather than 0 propionic acid. This was because at concentrations $<0.3125\,\mathrm{mM}$, decreasing propionic acid further had no effect on growth dynamics, however the dynamics were slightly different to the 0 propionic acid control (Fig4.2b). This may have been because the cultures with low propionic acid concentrations were prepared as part of the dilution series whereas the 0 propionic acid control was not. Therefore, the $0.0781\,\mathrm{mM}$ propionic acid condition acted as a better control for propionic acid addition. This control data series was subtracted from a subject data series, and the peak height was measured as the maximum value. A yield was then calculated in the same way as with glucose and pyruvate.

To calculate a yield in terms of biomass of *N. meningitidis* (rather than OD), the yield from propionic acid was expressed as a proportion of the yield from glucose or pyruvate. This relative yield was multiplied by a known yield value for glucose or pyruvate (reported in literature) to estimate a yield from propionic acid.

4.2.6 Testing of *N. meningitidis* cultures in non-contact co-culture apparatus

The non-contact co-culture apparatus was prepared and operated as described in section 3.3.7.

An inoculum with OD_{600} of 0.05 was used. CDM supplemented with $2.5\,\mathrm{mM}$ glucose was used as the culture medium. The oxygen-free gas inside the anaerobic enclosure was 90% N_2, 10% CO_2. This was to fulfil the CO_2 requirement of *N. meningitidis*. 10% CO_2 was used instead of the more conventional 5% CO_2 since 10% was the minimum partial pressure that could be accurately delivered by the equipment available.

Three chamber stacks were operated in triplicate. Each chamber stack had three chambers: one air supply chamber, one chamber containing the *N. meningitidis* culture in supplemented CDM, and one chamber containing an oxygen indicating solution (section 3.4.6.2). The *N. meningitidis* chamber was the middle of the three chambers, adjacent to both the oxygen-supply chamber and the resazurin chamber. A $0.02\,\mathrm{mm}$ PDMS membrane separated the air supply chamber from the *N. meningitidis* chamber, and a $0.1\,\mathrm{mm}$ PDMS membrane separated the *N. meningitidis* chamber from the resazurin chamber.

The model of oxygen diffusion between the resazurin and *N. meningitidis* chambers was tested by using the timing of this change in OD, together with parameter values taken from literature or estimated, to calculate the mixing rate factor η. This factor was chosen because it was the only value that could not be taken from literature, since it is affected by device dimensions and it had not yet been measured by some other means (although a plausible value between 5-10 was estimated, section 2.6.3).

4.2.7 Anaerobic methods for culturing *P. gingivalis*

Anaerobic conditions were used in the preparation of *P. gingivalis* liquid media, agar plates, anaerobic wash solutions, *P. gingivalis* inocula, and for the streaking, inoculating and passaging *P. gingivalis* cultures. Materials used in this anaerobic work, such as syringes, needles and filters, were stored either in an anaerobic hood or in anaerobic jars. Anaerobic conditions were generated either in an anaerobic hood or an anaerobic glove bag (part of the non-contact co-culture apparatus). The anaerobic glove bag

was only used instead of the anaerobic hood if the anaerobic materials needed to be injected directly into the non-contact co-culture device, or if the anaerobic hood was unavailable.

Anaerobic hood oxygen concentrations were kept below 10 PPM, they typically were stable at around 0-2 PPM. O_2 was removed by a reaction with H_2 over a catalyst. Entry and exit of materials to and from the anaerobic hood was through an airlock. Gas mix in the hood was a 1:1 N_2:CO_2 mix plus an H_2 concentration of 2-$4\,\%$. Sterilisation of gloves and surfaces was by bleach spray, and sterilisation of injection surfaces was by 70% ethanol. Liquid media were made anaerobic by leaving in the hood loosely covered overnight, or by heat sparging with N_2 over a flame.

4.2.8 *P. gingivalis* growth media

4.2.8.0.1 Supplemented tryptic soy broth ATCC Medium 2722 Supplemented Tryptic Soy Broth was prepared in sealed glass tubes to maintain anaerobic culture conditions.

Glass tubes with neck inner diameter of $12.7\,\mathrm{mm}$, outer diameter of $18\,\mathrm{mm}$ and length $150\,\mathrm{mm}$ (Fig4.1) were prepared as follows: $200\,\mu$L ddH_2O was pipetted into each tube, and each tube was sealed with a $20\,\mathrm{mm}$ butyl rubber stopper (sourced from Chemglass Life Sciences) and $20\,\mathrm{mm}$ aluminium crimp (manufactured by Chromacol). A gas mixture (80% N_2, 10% CO_2 and 10% H_2) was flowed through each tube using $0.5\,\mathrm{mm} \times 16\,\mathrm{mm}$ needles for $30\,\mathrm{min}$ and the tubes were sterilised in an autoclave ($120\,^{\circ}\mathrm{C}$ for $20\,\mathrm{min}$).

Tryptic Soy Broth (TSB) was prepared according to the supplier's instructions (ATCC): aqueous $30\,\mathrm{g\,L^{-1}}$ TSB (Merck product number 22092), $5\,\mathrm{g\,L^{-1}}$ yeast extract, $0.5\,\mathrm{g\,L^{-1}}$ L-cysteine HCl, $1\,\mathrm{mL\,L^{-1}}$ resazurin $100\,\mathrm{mM}$ pH-balanced to 7.6. The TSB was heat-sparged in a round bottom flask over a flame with N_2 bubbling moderately through the media until pigmentation from the resazurin became colourless. A pH of 7.6 before heat-sparging gave a final pH of 7.0-7.4 .

The TSB was immediately moved into the anaerobic hood with the prepared glass tubes. 20-$50\,\mathrm{mL}$ anaerobic ddH_2O was added to the TSB to compensate for evaporation during the heat-sparge. $1\,\mathrm{mL\,L^{-1}}$ Hemin stock ($5\,\mathrm{mg\,mL^{-1}}$, $10\,\mathrm{mM}$ K_2HPO_4 in ddH_2O boiled and

stored at $4\,^{\circ}\mathrm{C}$) and $200\,\mu\mathrm{L\,L^{-1}}$ Vitamin K_1 stock ($5\,\mathrm{mg\,mL^{-1}}$ in EtOH stored at $4\,^{\circ}\mathrm{C}$) was added to the TSB. The surface of each glass tube's rubber stopper was sterilised with EtOH and $10\,\mathrm{mL}$ TSB was filter-injected into each tube using $0.5\,\mathrm{mm} \times 16\,\mathrm{mm}$ needles and a $0.22\,\mu\mathrm{m}$ syringe filter (a second needle was used to release pressure from the sealed tube). Each tube was immediately wrapped in aluminium foil to protect light-sensitive compounds in the media.

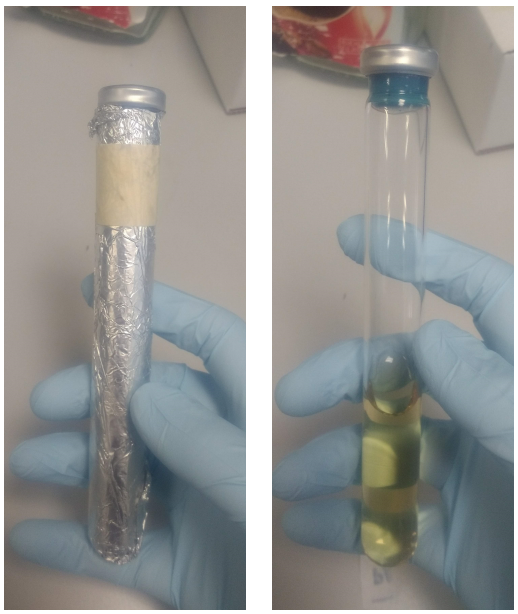

(a) **(b)**

Figure 4.1: Glass tubes containing anaerobic TSB media. Photographed a) with, and b) without the aluminium foil used to reduce degradation of light-sensitive compounds.

4.2.8.0.2 Supplemented TSB blood agar plates Blood agar plates, made with ATCC Medium 2722 Supplemented Tryptic Soy Agar, were prepared as follows.

$30\,\mathrm{g\,L^{-1}}$ TSB (Merck product number 22092), $5\,\mathrm{g\,L^{-1}}$ yeast extract, $0.5\,\mathrm{g\,L^{-1}}$ L-cysteine HCl, $1\,\mathrm{mL\,L^{-1}}$ resazurin $100\,\mathrm{mM}$ in ddH_2O pH balanced to 7.6. The TSB was heat-sparged in a round bottom flask over a flame with N_2 bubbling moderately through the media until pigmentation from the resazurin became colourless.

The TSB was immediately moved into the anaerobic hood. 20-$50\,\mathrm{mL}$ anaerobic ddH_2O was added to the TSB to compensate for evaporation during the heat-sparging. Once the TSB had cooled to around $60\,^{\circ}\mathrm{C}$ (to the touch), $1\,\mathrm{mL\,L^{-1}}$ Hemin stock ($5\,\mathrm{mg\,mL^{-1}}$ in ddH_2O), $200\,\mu\mathrm{L\,L^{-1}}$ Vitamin K_1 stock ($1\,\mathrm{mg\,mL^{-1}}$ in EtOH) and 5% v/v defibrinated horse blood was added to the TSB. The TSB was poured into $100\,\mathrm{mm}$ Petri dishes. For

storage, the plates were placed in an anaerobic jar that was wrapped in aluminium foil. The sealed anaerobic jar was removed from the chamber and gas mixture (80% N_2, 10% CO_2 and 10% H_2) was immediately flowed through it for $30\,\mathrm{min}$. The plates were stored at room temperature for at least $24\,\mathrm{h}$ before use, and used within one month of being made.

4.2.9 Inoculation of anaerobic liquid media with *P. gingivalis*

Initially, inocula were prepared from *P. gingivalis* ATCC® 33277™ Thermo Scientific™ Culti-Loops™. Subsequently, inocula were prepared either from glycerol stocks. Both Culti-Loops™ and glycerol stocks were used to streak an anaerobic TSB plate. The Culti-Loops™ used as per their instructions: in the anaerobic hood, a Culti-Loop™ was buried in an anaerobic TSB plate for $30\,\mathrm{s}$ and then streaked on the plate. Glycerol stocks were used by pipetting $40\,\mu\mathrm{L}$ onto a TSB plate and streaking. The plate was immediately sealed in an anaerobic jar which had been wrapped in aluminium foil. The anaerobic jar was removed from the anaerobic hood and an anaerobic gas mixture (80% N_2, 10% CO_2 and 10% H_2) was immediately flowed through it for $30\,\mathrm{min}$. The plate was incubated in the anaerobic jar at $37\,^{\circ}\mathrm{C}$ for 48-$96\,\mathrm{h}$.

Once visible colonies formed on the plate, in the anaerobic hood a $1.2\,\mathrm{mm} \times 40\,\mathrm{mm}$ blunt-ended needle and $1\,\mathrm{mL}$ syringe was used to extract a single colony on a "plug" of agar from the plate into the syringe. The needle was then swapped to a $0.5\,\mathrm{mm} \times 16\,\mathrm{mm}$ needle, the surface of the glass tube's rubber stopper was sterilised by EtOH, and the agar plug was injected into the glass tube. Liquid media was repeated drawn into the syringe and pushed back out until the agar plug was sufficiently broken up and injected.

4.2.10 Creation of *P. gingivalis* glycerol stocks

An anaerobic and sterile glycerol solution (50% v/v) was prepared by heat-sparging with N_2 and autoclaving. A liquid culture of *P. gingivalis* was inoculated and grown at $37\,^{\circ}\mathrm{C}$ to an OD_{600} of 0.6-0.8. In the anaerobic hood, the glycerol solution and *P. gingivalis* culture were mixed 1:1 (v/v) and aliquoted ($50\,\mu\mathrm{L}$) into snap-cap $1.5\,\mathrm{mL}$ micro-centrifuge tubes. They were then immediately placed in a sealed plastic bag, removed from the anaerobic hood and transported to a $-80\,^{\circ}\mathrm{C}$ freezer for freezing and storage.

4.2.11 Monitoring of *P. gingivalis* growth in liquid culture

Supplemented anaerobic TSB was prepared in triplicate tubes. Each tube was inoculated from the same *P. gingivalis* liquid culture and then incubated at $37\,^{\circ}\mathrm{C}$. These cultures were monitored by periodic OD_{600} measurement. A Thermo Fisher Scientific Spectronic™ 20D+ spectrophotometer was used to measure the OD_{600} of liquid cultures in glass tubes. A glass tube containing sterile supplemented anaerobic TSB was used as a blank.

A logistic growth function (Verhulst, 1838, described in section 2.5.2) was fitted to the data in order to measure the maximum growth rate and carrying capacity of the cultures.

4.2.12 Confirmation of *P. gingivalis* culture purity by 16S rDNA PCR and sequencing

16S sequencing was used to verify the identity of the culture after inoculation from a Thermo Scientific™ Culti-Loop™.

The PCR reaction mixture was made up as follows: $25\,\mu$L Master Mix (Invitrogen 2xPlatinum SuperFi PCR Master Mix), $2.5\,\mu$L forward primer (27F, 5'-AGAGTTTGATCCTGGCTCAG-3', OD_{260} of 7.6), $2.5\,\mu$L reverse primer (1492R, 5'-GGTTACCTTGTTACGACTT-3', OD_{260} of 8.2), $0.5\,\mu$L DNA (template), made up to $50\,\mu$L with nuclease-free water.

The thermocycle parameters were as follows: $98\,^{\circ}\mathrm{C}$ for $5\,\mathrm{min}$ to lyse cells. 30 cycles of $98\,^{\circ}\mathrm{C}$ for 5-10 s, $56\,^{\circ}\mathrm{C}$ for $10\,\mathrm{s}$ and $72\,^{\circ}\mathrm{C}$ for 15-30 s. The sequence was finished at $72\,^{\circ}\mathrm{C}$ for $5\,\mathrm{min}$ to allow any reactions to finish and then Left at $4\,^{\circ}\mathrm{C}$ (until the PCR products were collected).

The PCR product was prepared for sequencing with a Qiagen PCR purification kit. The PCR product was confirmed by gel electrophoresis (1.2% agarose, $50\,\mathrm{V}$ for $45\,\mathrm{min}$, $5\,\mu$L loading). The DNA concentration was quantified with a NanoDrop™ spectrophotometer, and then samples were diluted to $10\,\mathrm{ng}\,\mu\mathrm{L}^{-1}$ and submitted to Source Bioscience for Sanger sequencing.

4.2.13 Confirmation of *P. gingivalis* culture purity by Gram stain

Gram staining and confocal microscopy were used to verify the identity and purity of cultures before use in inoculation and after culture-based experiments (e.g. after monitoring the growth of a batch culture). This was important due to the high risk of contamination from handling the cultures in the anaerobic hood.

On a microscope slide, 3-4 drops of liquid culture were left to dry ($10\,\mathrm{min}$ at $37\,^{\circ}\mathrm{C}$). The slide was treated with crystal violet for $60\,\mathrm{s}$, washed with ddH_2O, treated with iodine solution for $30\,\mathrm{s}$, washed with ddH_2O, treated with a 1:1 v/v EtOH:acetone mixture for $5\,\mathrm{s}$, washed with ddH_2O, treated with safranin for $20\,\mathrm{s}$ and then washed with ddH_2O. The slide was air-dried and then examined under a confocal microscope (100$\times$ oil-immersion objective, 10$\times$ viewfinder).

Crystal violet, iodine and safranin solutions were sourced from Pro-Lab Diagnostics.

4.3 Results

4.3.1 Plate reader experiments to study *N. meningitidis* growth dynamics

4.3.1.1 Growth inhibition by propionic acid in media supplemented with glucose

Results of *N. meningitidis*, growing with glucose as a the primary source with varying concentrations of propionic acid, showed that *N. meningitidis* utilised both glucose and propionic acid for growth (Fig4.2). The change in OD_{600} in CDM supplemented only with $2.5\,\mathrm{mM}$ glucose (and no propionic acid) was 0.180 (Fig4.2b). Therefore yield of *N. meningitidis* from glucose was 0.0720 OD_{600} mM^{-1}.

An exponential decay of OD started immediately after the end of the linear growth phase. When glucose was the only carbon source, the rate of decline was such that there was a $50\,\%$ decline in culture density over the course of $\sim 3\,\mathrm{h}$.

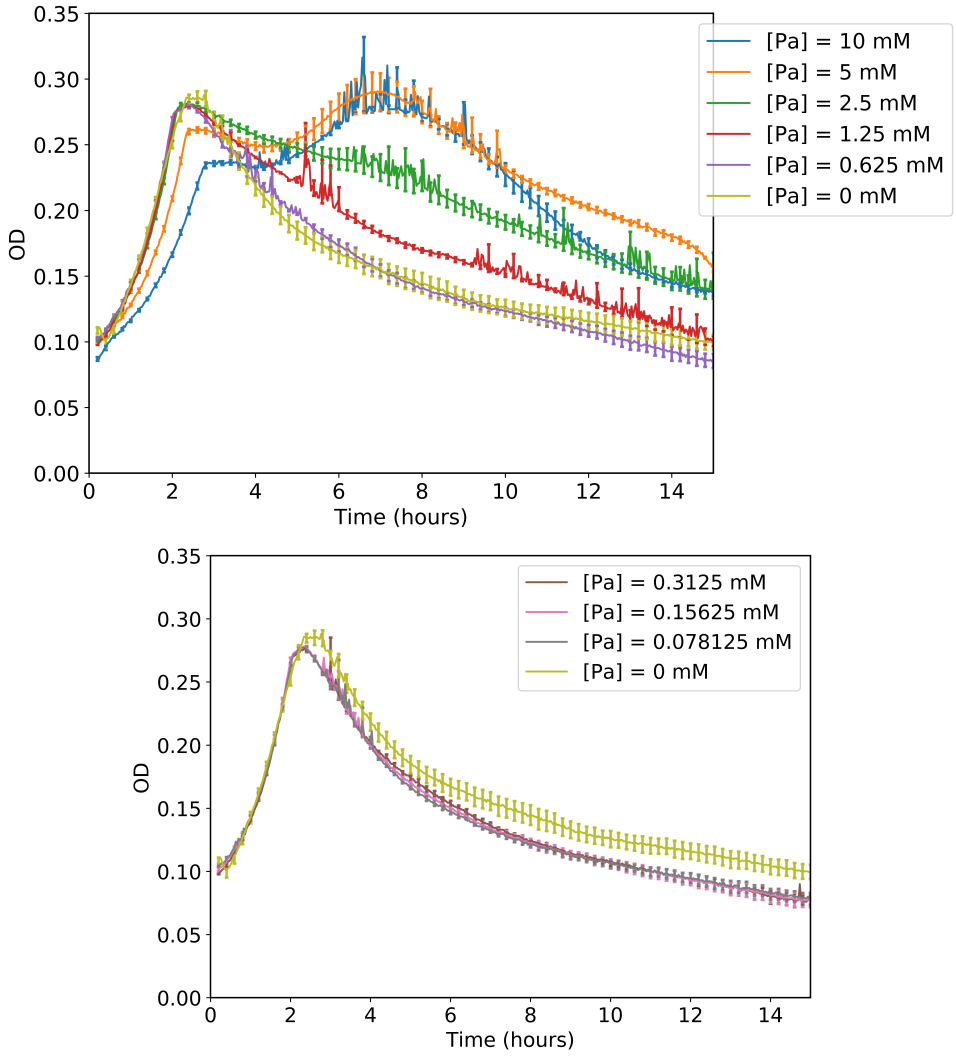

Figure 4.2: Growth of *N. meningitidis* in CDM supplemented with $2.5\,\mathrm{mM}$ glucose and varying concentrations of propionic acid.
a) Higher concentrations of propionic acid (0.625-$10\,\mathrm{mM}$)
b) Lower concentrations of propionic acid (0.0781-$0.313\,\mathrm{mM}$)
Error bars show standard error of measurement of three replicates.

When propionic acid was present the growth media, the cultures grew in a second peak, after which the OD decreased back to the same level as the controls (Fig4.3a). The second peak reached a higher OD at higher propionic concentrations, but beyond a propionic acid concentration of $5\,\mathrm{mM}$ the second peak height did not increase any further (Fig4.3b).

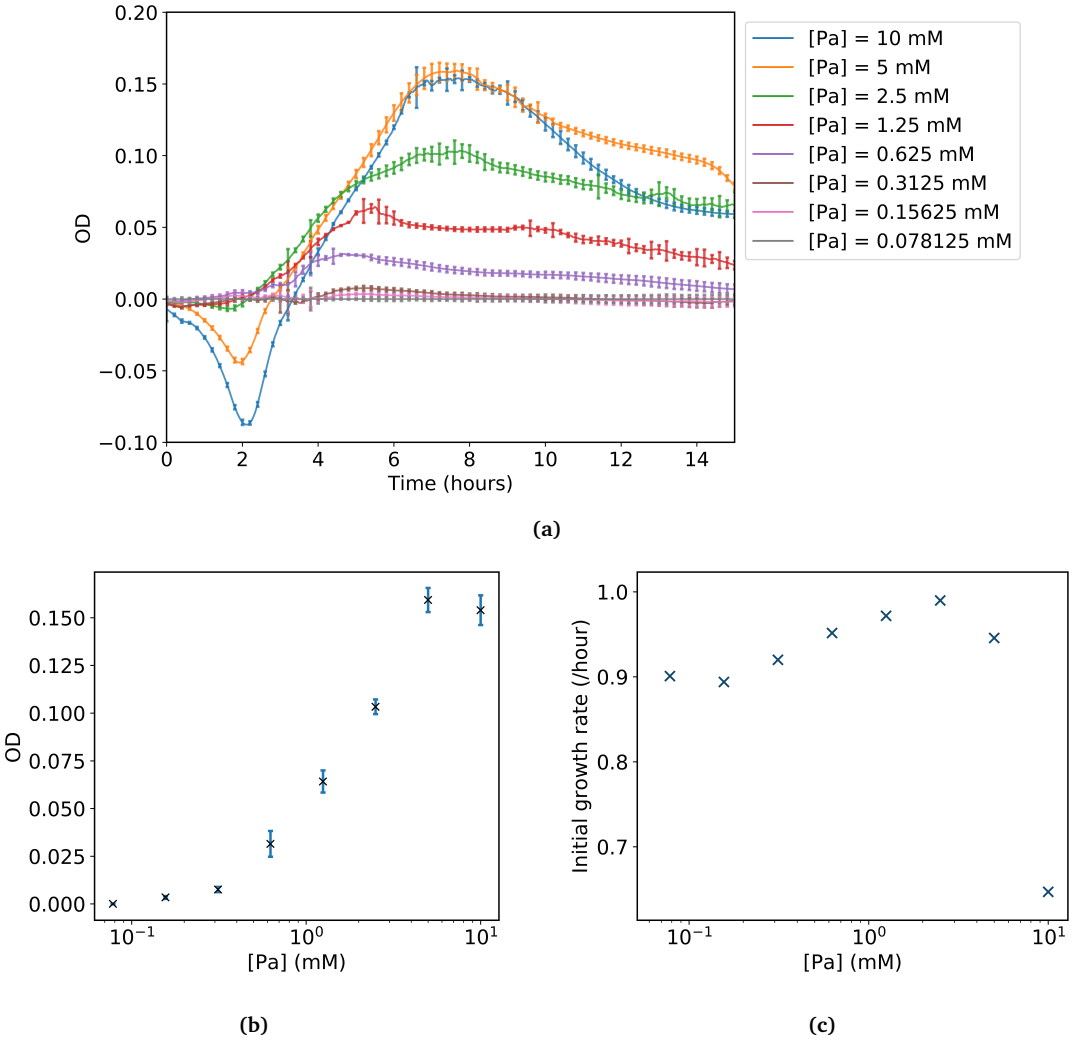

Figure 4.3: Effect of propionic acid concentration on yield and maximum growth rate of *N. meningitidis* in CDM supplemented with $2.5\,\mathrm{mM}$ glucose.
a) *N. meningitidis* growth curves with control data ($0.0781\,\mathrm{mM}$ propionic acid) subtracted to measure just the growth from propionic acid.
b) Relationship between measured peak height from (a) and propionic acid concentration.
c) Relationship between propionic acid concentration and maximum growth rate, measured by fitting an exponential function to the time series data between 0.5-$2\,\mathrm{h}$.
Error bars show standard error of measurement or three replicates.

The maximum growth rate of *N. meningitidis* growing in CDM supplemented with $2.5\,\mathrm{mM}$ glucose ranged between around 0.6-$1.0\,\mathrm{h}^{-1}$ depending on the propionic acid concentration (Fig4.3c). The growth rate was inhibited at high propionic acid concentrations, particularly at $10\,\mathrm{mM}$, and to a lesser extent at $5\,\mathrm{mM}$. However, at propionic acid concentrations between 0.0781-$2.5\,\mathrm{mmol\,dm^{-3}}$, higher concentrations of propionic acid were associated with higher growth rates.

The maximum growth rate of *N. meningitidis* unaffected by propionic acid was $0.9\,\mathrm{h}^{-1}$.

4.3.1.2 Yield from propionic acid in media supplemented with pyruvate

The results for growth conditions with $5\,\mathrm{mM}$ pyruvate also showed a second period of growth associated with propionic acid. However, the shape of this second peak was more prolonged (Fig4.4).

There was also a decline in OD that started immediately after the end of the linear growth phase. When pyruvate was the only carbon source this decrease in OD was at a constant rate of $\sim 0.018\,\mathrm{h}^{-1}$.

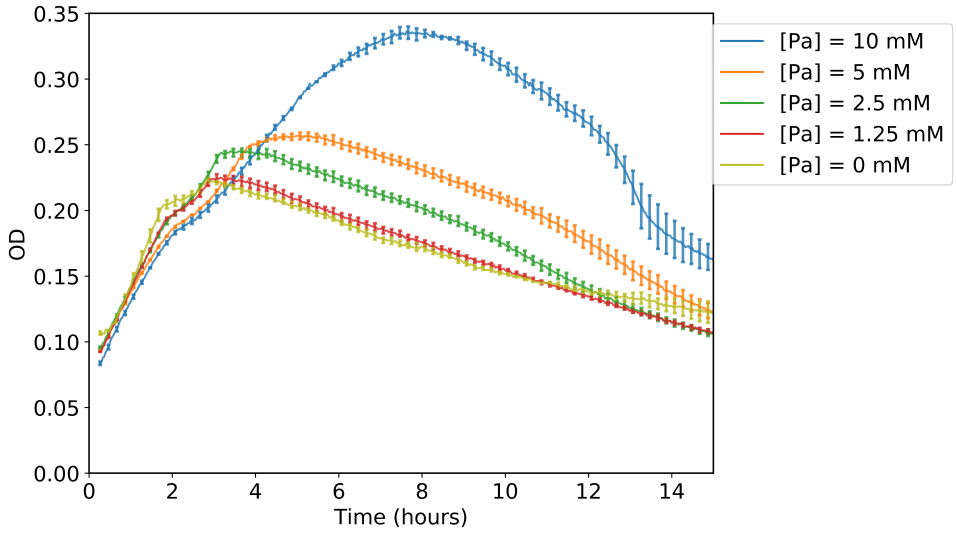

(a)

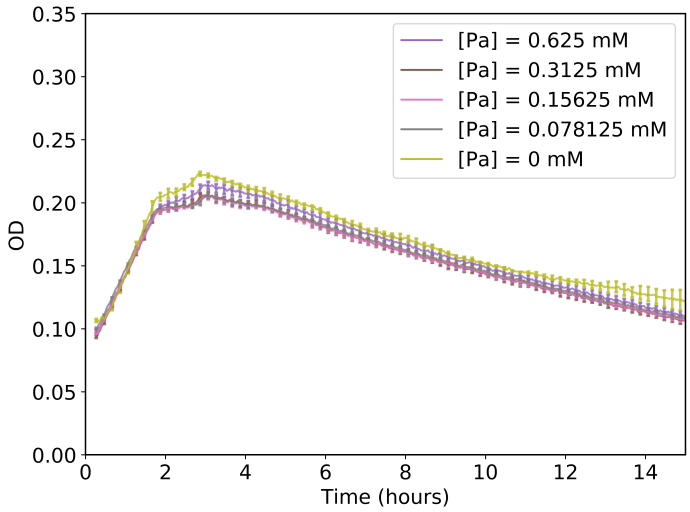

(b)

Figure 4.4: Growth of *N. meningitidis* in CDM supplemented with $5\,\mathrm{mM}$ pyruvate and varying concentrations of propionic acid.
a) Higher concentrations of propionic acid (1.25-$10\,\mathrm{mM}$)
b) Lower concentrations of propionic acid (0.0781-$0.625\,\mathrm{mM}$)
Error bars show standard error of measurement of three replicates.

The change in OD_{600} in CDM supplemented with $5\,\mathrm{mM}$ pyruvate (with 0 propionic acid) was 0.110, therefore the yield of *N. meningitidis* from pyruvate was 0.0220 OD_{600} mM^{-1}. There is a linear relationship between peak height (due to propionic acid utilisation) and propionic acid concentration, it has gradient of 0.0172 (Fig4.5b). Therefore, the yield of *N. meningitidis* from propionic acid was 0.0172 OD_{600} mM^{-1}.

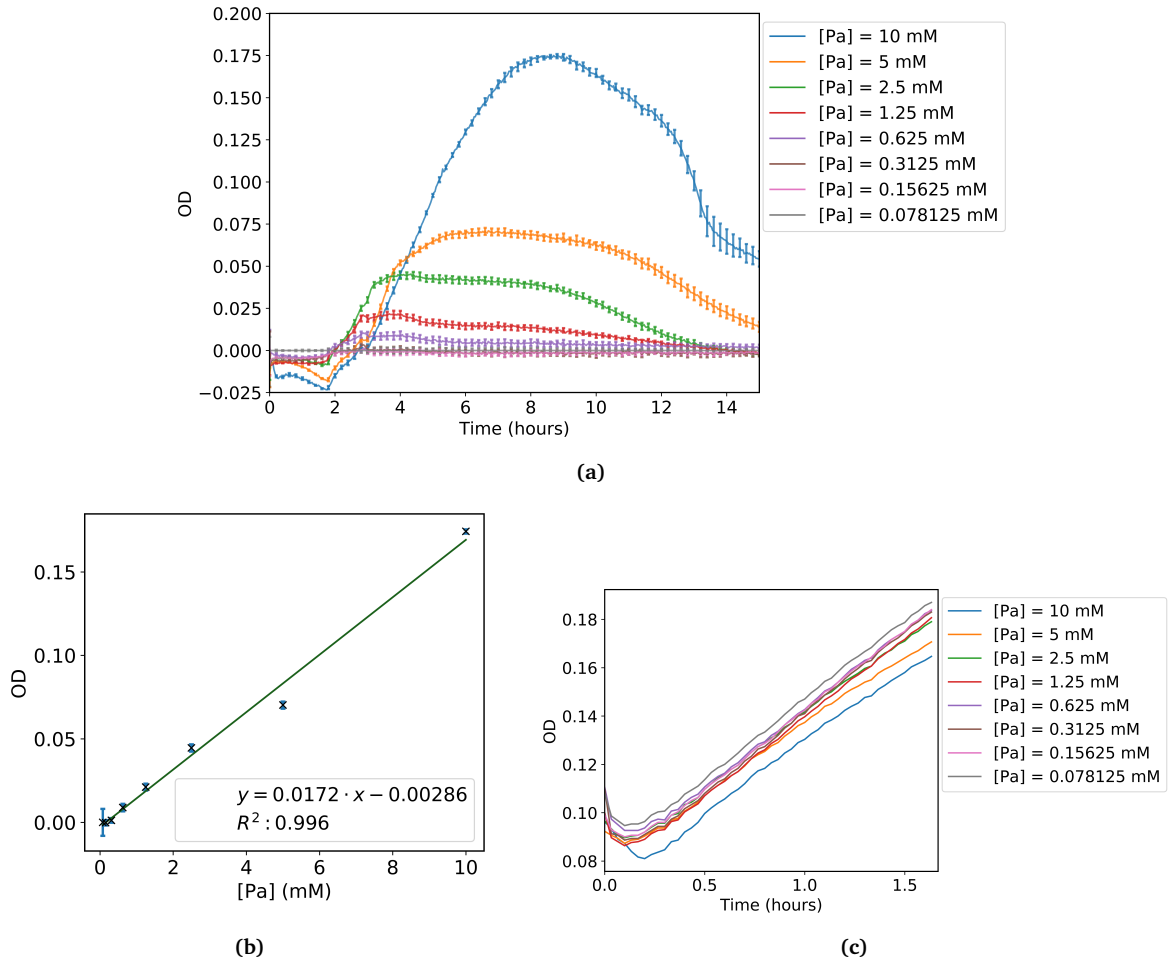

Figure 4.5: Effect of propionic acid concentration on yield and maximum growth rate of *N. meningitidis* in CDM supplemented with $5\,\mathrm{mM}$ pyruvate.
a) *N. meningitidis* growth curves with control data ($0.0781\,\mathrm{mM}$ propionic acid) subtracted to measure just the growth from propionic acid.
b) Linear relationship between measured peak height from (a) and propionic acid concentration, fitted to linear function by linear regression analysis.
c) Initial phase of *N. meningitidis* visually slight variation in initial growth rate due to propionic acid.
Error bars show standard error of measurement of three replicates.

To convert this yield from propionic acid into a dry weight yield of *N. meningitidis*, the yield as a proportion of the yield from glucose was calculated ($0.0720\ \mathrm{OD_{600}\ mM^{-1}}$ for glucose, $0.0172\ \mathrm{OD_{600}\ mM^{-1}}$ for propionic acid). This relative yield was multiplied by the dry weight yield of *N. meningitidis* from glucose ($64.2\,\mathrm{g\,mol^{-1}}$, Baart *et al.*, 2007) to give a yield from propionic acid of $15.3\,\mathrm{g\,mol^{-1}}$.

The pyruvate-supplemented CDM data could not be used to measure initial growth rates because there was no apparent exponential growth phase. Visually, there did

appear to be some growth inhibition by propionic acid (Fig4.5c), however this was not as pronounced as in glucose-supplemented media.

4.3.2 Testing of *N. meningitidis* growth in non-contact co-culture apparatus

4.3.2.1 Aerobic growth

To test growth aerobic growth of *N. meningitidis* cultures in the non-contact co-culture apparatus, the experiment was prepared with air surrounding the chamber stacks instead of 90% N_2, 10% CO_2. The results (Fig4.6) show clear exponential, linear and stationary phases.

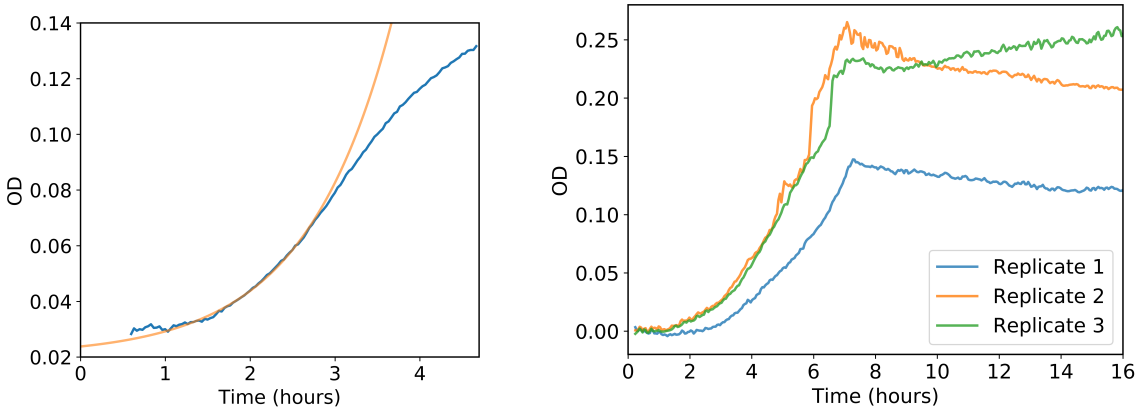

(a) **(b)**

Figure 4.6: Exponential growth of *N. meningitidis* in non-contact co-culture apparatus.
a) Maximum growth rate measured by fitting an exponential function to initial section of figure 4.7b.
b) Growth with air surrounding the chambers and tubing.

When the anaerobic enclosure was filled with oxygen-free 90% N_2, 10% CO_2, the growth was more linear (Fig4.7b) indicating greater oxygen limitation. Oxygen was still supplied by flowing air through the oxygen-supply chamber.

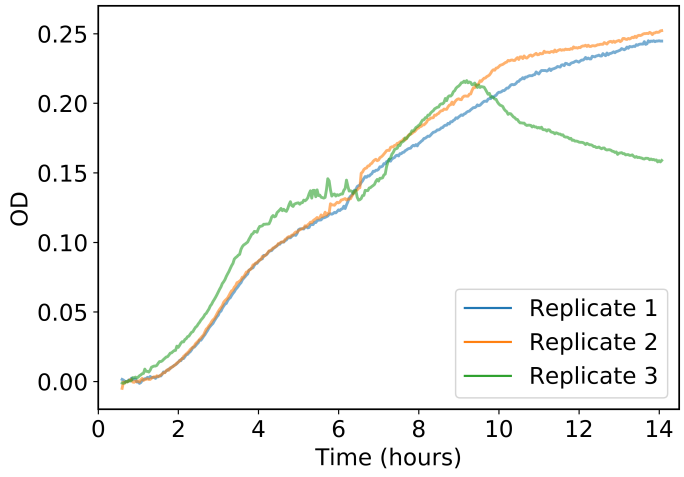

(a)

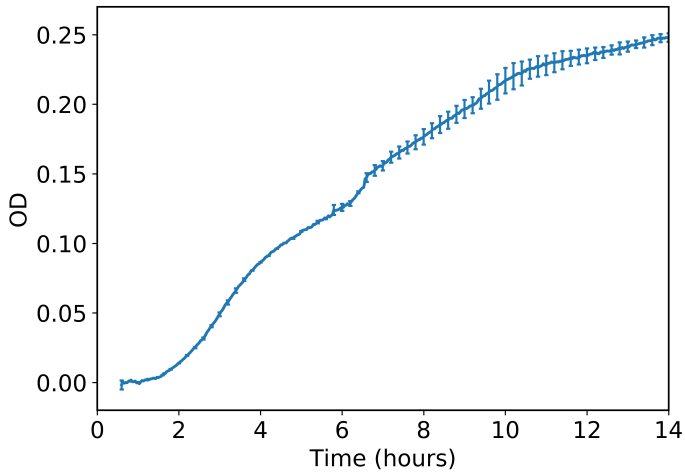

(b)

Figure 4.7: *N. meningitidis* growth in co-culture non-contact apparatus.
a) OD of *N. meningitidis* chamber from each of the triplicate chamber stacks.
b) Average of two replicates, error bars indicate standard error of measurement. Triplicate 3 is excluded due to fault in syringe pump causing errors.

One of the triplicates (Fig4.7a) showed a qualitatively different result to the other triplicates. Upon inspection of the apparatus, it was determined that this was due to a jamming of one of the syringes which both prevented mixing of the chamber and resulted in an inconsistent chamber volume. Therefore, data from this chamber stack was not used to generate the averaged results (Fig4.7b).

4.3.2.2 Generation of anaerobic conditions

The OD measurements of the resazurin chamber shift from an initial high OD to a low OD indicating that anaerobic conditions were established the chamber.

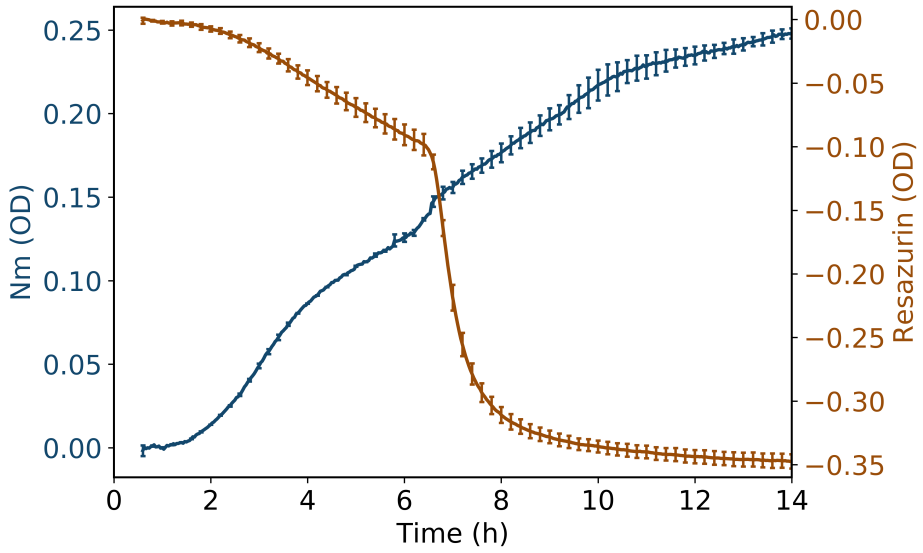

Figure 4.8: Oxygen depletion associated with *N. meningitidis* growth. The *N. meningitidis* culture and oxygen-sensitive resazurin solutions were in adjacent culture chambers of the non-contact co-culture device. The drop in resazurin OD corresponds to the generation of anaerobic conditions.
Error bars indicate standard error of measurement of two replicates.

These results were used to calculate mixing rate of the chambers. First, the concentration of oxygen in the resazurin chamber when the OD of this oxygen indicator transitioned was calculated.

Resazurin reduction has a standard reduction potential of $-0.45\,\mathrm{V}$ (Besant *et al.*, 2015) which means that at that redox potential half of the resazurin in the solution will be in a colourless reduced state. The relationship between redox potential and [DO] (dissolved oxygen concentration) is not clear when solutions have many components (e.g. a microbial culture), especially at [DO] $<3.13\,\mu\mathrm{M}$ (Myers *et al.*, 2006). However, data from activated sludge reactors indicated a relationship of

$$E_H = a \cdot log\big([DO] \cdot 32\big) + b \tag{4.1}$$

where E_H is the redox potential and a and b have a range of values, the upper and lower

parameter sets were $a = 0.091, b = 0.264$ and $a = 0.180, b = 0.148$ (Heduit & Thevenot, 1989). And so, when $E_H = -0.45\,\mathrm{V}$ (i.e. the potential at which half of resazurin is in a reduced state) then [DO] ranged from between 0.012-$1.13\,\mu\mathrm{M}$.

This point, at which half the resazurin is in a reduced colourless state, is shown by the results to be at the $6.83\,\mathrm{h}$ time-point. Therefore, this value of 0.012-$1.13\,\mu\mathrm{M}$ at the known time-point of $6.83\,\mathrm{h}$ can be used, with a starting [DO] value at time $0\,\mathrm{h}$, to calculate the permeability of oxygen between the resazurin chamber and the *N. meningitidis* chamber. When oxygen diffuses from one chamber with [DO] of R to another with a [DO] of 0 then the rate of oxygen diffusion is $P \cdot R$ (where P is the permeability). And so, [DO] at time t (R_t) is given by

$$R_t = R_0 \cdot e^{-P \cdot t} \tag{4.2}$$

where R_0 is [DO] at time 0.

When this equation is evaluated for $t = 6.83\,\mathrm{h}$, $R_t = 0.012$-$1.13\,\mu\mathrm{M}$ and $R_0 = 0.27\,\mathrm{mM}$ then $P = 1.81$-$2.48\,\mathrm{h}^{-1}$.

As described in section 2.5.4.1, permeability (P) is a function of the membrane thickness (L), the characteristic length of the chamber (m, i.e. the volume divided by the diffusion surface area), a mixing factor (η), the diffusion coefficient of oxygen in water ($C_{Ox,aq}$) and PDMS ($C_{Ox,pdms}$), and the saturation concentrations of oxygen in water ($S_{Ox,aq}$) and PDMS ($S_{Ox,pdms}$).

The experimental conditions for *N. meningitidis* growing in the co-culture device were $L = 0.1\,\mathrm{mm}$ and $m = 5\,\mathrm{mm}$. When $C_{Ox,aq}$, $C_{Ox,pdms}$, $S_{Ox,aq}$ and $S_{Ox,pdms}$ take their respective values from table 2.2, and when P is between 1.81-$2.48\,\mathrm{h}^{-1}$, then η is between 5.95-8.26.

4.3.3 *P. gingivalis* anaerobic growth

Following demonstration of the generation of anaerobic conditions in the non-contact co-culture apparatus, preparations were made for culturing *P. gingivalis* and *N. meningitidis* in adjacent chambers.

First, liquid cultures were inoculated from Culti-Loops™ (section 4.2.9). The identity

of the culture was tested by 16S rDNA sequencing (section 4.2.12) and confirmed to be *P. gingivalis*. The culture was tested for contamination by Gram stain and confirmed to be a pure culture of *P. gingivalis* (Fig4.9). This liquid culture was used to create glycerol stocks which were then used for subsequent experiments.

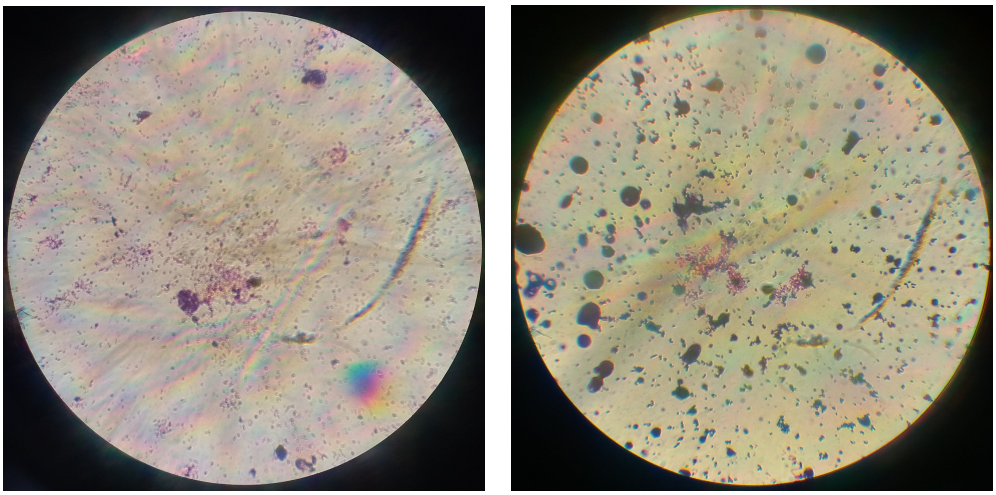

(a) (b)

Figure 4.9: Gram stain of *P. gingivalis* liquid culture to verify purity.
a) A pure culture, consistent with *P. gingivalis*.
b) For comparison, an example of a *P. gingivalis* culture with a Gram positive contamination.

P. gingivalis pure cultures were grown, and the OD monitored, in order to determine the conditions required, and to measure parameters (i.e. growth rate and carrying capacity) while identifying other important aspects of the culture growth. The purity of these cultures was verified by Gram stain. The results (Fig4.10) were consistent between the the triplicates, therefore the mean of the triplicates was used for further analysis.

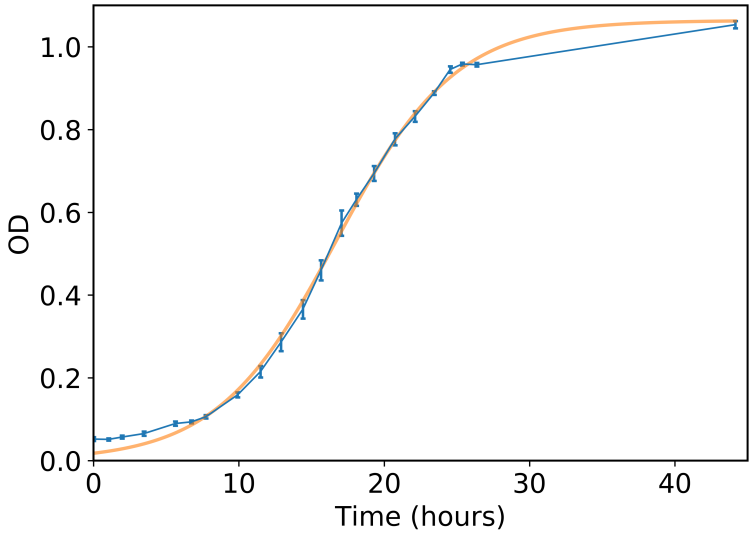

Figure 4.10: *P. gingivalis* liquid batch culture results with fitted logistic growth function. These results show a maximum growth rate of $0.259\,\mathrm{h}^{-1}$ and a maximum OD of 1.06.
Data is the mean of triplicates. Error bars indicate standard error of measurement.

The *P. gingivalis* cultures grew with a characteristic exponential phase, linear phase and stationary phase. The fitted maximum growth rate was $0.259\,\mathrm{h}^{-1}$, the carrying capacity (maximum OD) was 1.06.

4.4 Discussion

4.4.1 Plate reader experiments enabled reliable measurement of *N. meningitidis* yield from propionic acid

The presence of second peak in culture density due to growth utilising propionic acid is consistent with previously reported results (Catenazzi *et al.*, 2014). Also, the difference in the shape of this second peak between media supplemented with glucose and pyruvate was also observed in this previous study.

The range of propionic acid concentrations tested enabled a yield of *N. meningitidis* from propionic acid to be calculated. There were large differences in the second peak height between the pyruvate and glucose results. In particular, the peak height at

$5\,\mathrm{mM}$ propionic acid was lower than the equivalent height in media supplemented with $2.5\,\mathrm{mM}$ glucose. This was probably due to an overestimation of peak height with glucose-supplemented media caused by a faster degradation rate of *N. meningitidis* in the death phase of the control data. The data for pyruvate-supplemented media showed a slower, more steady OD decrease in death phase. Also, there was a linear relationship between peak height and propionic acid concentration in CDM supplemented with pyruvate, but not with glucose.

A linear relationship is to be expected if propionic acid is being utilised as a carbon source. It is not clear why this was not observed in glucose-supplemented media. It is not due to an artefact in the way that yield of *N. meningitidis* is calculated from the data since other measurement methods (such as integrating to measure the area of the peak) also do not show an increase in yield between $5\,\mathrm{mM}$ and $10\,\mathrm{mM}$ propionic acid in media supplemented with $2.5\,\mathrm{mM}$ glucose (Fig4.2). It may be that the decrease of OD in the stationary/death phase may cause artefacts when control data (with a prominent death phase) is subtracted from data with less of a death phase due to propionic acid. The mechanism for the difference between the two data series's may not be as simple as resource utilisation. Instead, propionic acid may modulate the rate of culture population size decrease by some other mechanism. Whether the difference is due to measurement artefacts to unknown biological mechanisms, the data from pyruvate-supplemented media does not appear to be affected by these factors. Therefore, this data provides a reliable measure of yield from propionic acid.

4.4.2 Calculated growth parameter values will be useful for the non-contact co-culture assay

The measured values for yields and maximum growth rates are useful for preparing to culture *N. meningitidis* in the non-contact co-culture assay.

A value of for yield from an acetate/glutamate mixture of $18.9\,\mathrm{g\,mol^{-1}}$ was used as a rough estimate for the yield of *N. meningitidis* from propionic acid in the mathematical analysis of the non-contact co-culture assay (section 2.6.1). The similarity of this to the measured value of $15.3\,\mathrm{g\,mol^{-1}}$ shows that this yield measured by the plate reader experiments is consistent with what was expected.

The measured maximum growth rate value is consistent with a reported mean growth

rate (averaged from various *N. meningitidis* strains) of $0.9\,\mathrm{h}^{-1}$ (Schoen *et al.*, 2014). This indicates that *N. meningitidis* is able to grow in the non-contact co-culture apparatus in a similar manner to other standard *in vitro* culture methods.

The measured maximum growth rate and the yield from propionic acid are important parameters values in the mathematical model of the system. Verification of these values indicates that the outcomes of the analysis of this model are valid. An accurate yield value is also important for interpreting results from the non-contact co-culture assay, since it could be used to calculate the diffusion rate of propionic acid between the culture chambers (e.g. from measurements of the growth of *N. meningitidis* when cultured adjacent to a propionic-acid-supply chamber). These values could then be used to calculate the production rate of propionic acid by a *P. gingivalis* culture in that adjacent chamber. This is significant because these quantities would represent an initial quantification of the metabolic relationship between *N. meningitidis* and *P. gingivalis*, and they would be useful for designing further experiments.

4.4.3 Growth inhibition by propionic acid places limits on non-contact co-culture assay parameters

The decrease in maximum growth rate due at higher propionic acid concentrations indicates that propionic acid inhibits *N. meningitidis* growth. This was expected since propionic acid is known to inhibit the growth of many bacterial species, including *N. gonorrhoeae* (section 1.3.3.5).

The measured increase in growth rate due to increased propionic acid when propionic acid concentrations were between 0.0781-$2.5\,\mathrm{mmol\,dm}^{-3}$ appear to contradict this. However, this may be an artefact due to propionic acid lengthening the lag phase and causing the growth rate in the 0.5-$2\,\mathrm{h}$ time window to appear more rapid.

Inhibition of *N. meningitidis* growth by propionic acid is a factor that may be important in interpreting non-contact co-culture assay results (section 2.7.4.6). The mathematical analysis of this assay recognised the need for oxygen to be fully consumed by the *N. meningitidis* culture to maintain anaerobic conditions, but it also recognised that propionic acid should be consumed as much as possible (while still having oxygen-limited *N. meningitidis* growth) in order to prevent inhibition of microbial growth (sections 2.7.4.3.3). These results indicate that if propionic acid concentrations exceed $5\,\mathrm{mM}$

then the maximum growth rate of *N. meningitidis* will be significantly inhibited.

Mathematical modelling of the system showed that *P. gingivalis* batch cultures will produce $15.8\,\mathrm{mM}$ of propionic acid (section 2.7.3.3), and that this may accumulate at higher concentrations in the *N. meningitidis* chamber due to a difference in pH (section 2.5.4.2). Therefore, in any non-contact co-culture experiments designed to study the utilisation of propionic acid by *N. meningitidis*, this should be avoided (or at least taken into account during interpretation of the results).

4.4.4 *N. meningitidis* culture death rate may be important to model

There is a significant amount of cell death observed in the plate reader experiment results. This was at a much higher rate when glucose was the primary carbon source (section 4.3.1.1) compared to pyruvate (section 4.3.1.2). Also, culture density decayed exponentially with glucose, as opposed to pyruvate where the decline was more linear. It is unknown if there is a constant death rate for the culture, or if this death rate increases as glucose or propionic acid is depleted, or if it operates by some other mechanism (e.g. depletion of another resource, or accumulation of a product).

This death rate, however, is not observed in results from the non-contact co-culture assay (section 4.3.2.1). Therefore, it is unclear whether culture death rate is an important factor that should be taken into account. Knowledge about the cause of the death phase in the plate reader experiments would be useful to determine whether culture in the non-contact co-culture apparatus could experience a similar death phase. If it found to be an important factor then it should be included in any mathematical model used to interpret non-contact co-culture assay results.

4.4.5 *N. meningitidis* growth in non-contact co-culture apparatus

The plate reader *N. meningitidis* experiments provided an important demonstration of conditions in which growth was sensitive to propionic acid concentration. This information aided testing of the non-contact co-culture assay by inspiring the experimental conditions for the tests, and by providing a point of comparison for identifying factors particular to the non-contact co-culture assay that must be taken into account when interpreting results.

4.4.5.1 Maximum growth rate is similar to plate reader results

Although the *N. meningitidis* culture growths in the non-contact co-culture apparatus were oxygen-limited, there was a brief exponential phase that was be used to calculate a maximum growth rate of the culture. The measured growth rate of $0.983\,\mathrm{h}^{-1}$ is consistent with the growth of *N. meningitidis* in the plate reader (section 4.3.1) which (when uninhibited by propionic acid) ranged between 0.9-$1.0\,\mathrm{h}$.

4.4.5.2 Growth dynamics are more prolonged compared to plate reader results

Growth of cultures is more prolonged in the non-contact co-culture apparatus compared to the plate reader. When the anaerobic enclosure was filled with oxygen-free gas, *N. meningitidis* growth did not have the distinct exponential, linear and stationary phases that were observed in the plate reader cultures. This will in part be due to oxygen-limitation since, as previously stated, a longer exponential phase was observed when oxygen was allowed to leak into the culture chambers. An oxygen-limited culture should grow at a rate determined by the constant rate at which oxygen diffuses into the culture chamber. This linear growth was previously displayed in the oxygen-limited *E. coli* growth in (Fig3.35). However, the growth of the *N. meningitidis* cultures are not linear, they instead appear to gradually approach a value. This may be due to the mixing method causing a slight dilution of the chambers.

Mixing was achieved by pumping liquid in and out of the chambers, 20% of the volume of the chambers ($25\,\mu$L of $125\,\mu$L) was drawn out and then pushed back in. This has the potential to cause dilution as liquid from the chambers is exchanged with the tubing contents. Dilution due to the mixing method was confirmed by filling the chambers with a dye and observing the passage of that dye out thought the tubing. Therefore, the culture can be considered as a continuous culture of sorts since the culture is diluted as it spreads up the tubing and growth substrates are replenished as they spread from the tubing into the chamber. This provides an explanation for why the *N. meningitidis* culture densities appear to approaching an asymptote, since a continuous culture will approach an equilibrium state in a similar manner (section 2.7.4).

4.4.6 Generation of anaerobic conditions are slower than with *E. coli* cultures

Anaerobic conditions are generated by the aerobic growth of a *N. meningitidis* in a similar manner to what was first demonstrated with *E. coli* (section 3.5.4). However, the rate at which *N. meningitidis* cultures generate the anaerobic conditions are much slower than *E. coli* cultures (Fig3.35). This may be explained by the *N. meningitidis* culture's apparent longer lag phase which would delay the consumption of oxygen.

Additionally, the chambers used with the *E. coli* culture tests were made of bonded PDMS slices rather than separate PMMA slices. The PMMA slices showed leakiness, particularly at the connections between the tubing and the chambers (section 3.4.2), which could increase or reduce oxygen concentrations in the chambers depending on the oxygen concentration in the anaerobic enclosure. Although the anaerobic chamber was flushed with oxygen-free gas, early on in the experiment some oxygen may have remained. If this was the case then this would have been able to diffuse in to the *N. meningitidis* culture chambers (and adjacent chambers). Both of these factors would lengthen the time it would take for anaerobic conditions to be generated.

4.4.7 Initial test indicates that the mathematical model is appropriate

The mathematical model, with estimated and measured parameter values, was used to interpret results from the generation of anaerobic conditions and calculate the mixing rate of the chambers. The result (between 5.95-8.26) is a reasonable value given that a mixing factor of 13 corresponds to a mixing time of around $5\,\mathrm{s}$ (Lee *et al.*, 2006, section 2.6.3) and the mixing time of the apparatus chambers is around $30\,\mathrm{s}$.

The calculated mixing factor value may be slightly higher than expected. A more precise comparison is not possible since the method of measuring mixing times is subjective. However, a higher value may be explained by diffusion out of the chambers via leaky connections artificially inflating the apparent permeability of oxygen between the chambers resulting in a higher calculated value for the mixing rate.

Given that the calculated mixing factor is reasonable, this shows that there are no major differences between the results and the model predictions of how oxygen diffuses

between the chambers.

4.4.8 *P. gingivalis* growth rate is faster than expected

The measured growth rate is faster than the values reported in the literature (Milner *et al.*, 1996). This may be due the use of different culture media: a maximum growth rate of $0.12\,\mathrm{h}^{-1}$ was reported in the chemically defined media "KGB", and $0.15\,\mathrm{h}^{-1}$ in Brain-Heart Infusion media. The value used in the mathematical analysis (section 2.6.2) is around half the measured value.

A faster growth rate will not fundamentally affect the behaviour or limitations of the system, although a faster growth rate could be beneficial in speeding up experiments. However, accurate parameters for *P. gingivalis* growth are important for designing experiments. This is particularly true in an experiment where both *P. gingivalis* and *N. meningitidis* are grown in batch cultures since coordination of the two cultures will be vital (section 2.7.3.5). Accurate growth parameter values are also required for a continuous *P. gingivalis* culture so that an appropriate dilution rate can be chosen.

4.4.9 Practical steps needed to study *N. meningitidis*/*P. gingivalis* non-contact co-culture

The growth of *N. meningitidis* and generation of anaerobic conditions has been demonstrated. Before *P. gingivalis* is cultured in the anaerobic chamber adjacent to *N. meningitidis*, the diffusion of propionic acid between the chambers should be tested. Experimental conditions, presented in the mathematical analysis of the co-culture as practical and useful (section 2.7.4.3.3), should be used (i.e. membrane thickness of $20\,\mu\mathrm{m}$, propionic acid concentration of $10\,\mathrm{mM}$, pH 6.0 in the propionic acid chamber).

Once this has been demonstrated and the propionic acid diffusion rate measured, then the propionic acid production of a *P. gingivalis* culture in the non-contact co-culture assay can be tested. This can be done by injecting the contents of a liquid *P. gingivalis* culture, in exponential phase, into the adjacent chamber once it has been made anaerobic. Comparison of *N. meningitidis* culture growth between the different adjacent chamber conditions (empty, propionic acid solution and *P. gingivalis* culture) can then

be used to measure the rate of propionic acid production by *P. gingivalis* in the non-contact co-culture environment.

The leakiness of the apparatus, allowing diffusion of oxygen with the surrounding gas (in the anaerobic enclosure), and the dilution due to the mixing method used, has introduced uncertainty in the analysis of the non-contact co-culture results. This is a barrier to quantifying the metabolic interaction, and so a solution should be found. To do this, an exploration of different materials and fabrication method could be conducted to find ways to seal the leaks. In addition to this, the diffusion through the leaks and the dilution due to the mixing method could both be quantified and included in the mathematical model. Modelling of dilution has already been described and analysed (section 2.7.4), and modelling of diffusion would be modelled in a similar way to diffusion between chambers (section 2.5.4.1). This updated model could then be used to interpret experiment results. If the impact of these changes is significant then the recommendations and guidelines from the mathematical analysis would also have to be updated to include these additional factors.

Even without these modifications, the apparatus can be used for confirmation of the core capabilities of the assay, and for measurement the growth dynamics of *N. meningitidis* and *P. gingivalis* in non-contact co-culture.

Chapter 5

Discussion

5.1 Quantification of metabolic relationship between *N. meningitidis* and *P. gingivalis*

Mathematical analysis has shown that the non-contact co-culture assay can be used to quantify the metabolic relationship, due to volatile substances, between *N. meningitidis* and *P. gingivalis* (section 2.8). Specific conditions must be met so that *N. meningitidis* growth is initially oxygen-limited, but that at some point it shifts to being limited by propionic acid (or other substances produced by *P. gingivalis*). This is so that anaerobic conditions can be generated while also having propionic acid production and utilisation cause a change in *N. meningitidis* growth that can be measured.

5.1.1 Aspects of the metabolic relationship that are important to capture

There are many facets of the metabolic relationship that could potentially be quantified. In the mathematical model used in chapter 2, the magnitude of the metabolic interaction can be fully quantified by two yield parameters: 1) the yield of propionic acid from *P. gingivalis* growth, and 2) the yield of *N. meningitidis* from propionic acid. This model, however, does not include some factors (e.g. growth inhibition by propionic acid, or difference in *N. meningitidis* maximum growth rate between glucose

and propionic acid) that are likely to be important.

Culturing of *N. meningitidis* in pure culture using a plate reader (section 4.3.1) showed that propionic acid inhibits growth rate in a concentration-dependent manner at concentrations relevant to conditions in the non-contact co-culture assay. These experiments also showed a prominent death phase and clear differences in growth dynamics between when glucose or pyruvate is the primary carbon source, the mechanisms of which are unknown. This clearly shows that the growth dynamics of the *N. meningitidis* culture are not as simple as the monodic growth model used in mathematical analysis of the system. These additional aspects of growth may need to be captured since a close agreement between assay results and model predictions would aid in the process of fitting model parameters to quantify all relevant aspects of the metabolic relationship.

5.1.2 Process for capturing additional aspects of growth

The importance of capturing each of these factors in the model could be assessed by using a mixture of pure culture and co-culture experiments. The co-cultures would be used, with model predictions, to detect and identify important factors that are not yet included in the model. The pure cultures (e.g. using similar methodology to the plate reader culture experiments in section 4.3.1) would be used to make clear measurements of single factors in isolation (e.g. effect that addition of a single substance has). These experiments could be used together to iteratively refine the model until it captures all relevant factors of the metabolic interaction. This is important so that the verified and fitted model is a suitable representation of the metabolic interaction, and so that a subset of the model parameters (related to the metabolic interaction) can be used to assign a "quantity" to the metabolic relationship.

5.2 Translation from metabolic interaction quantification to combatting IMD

The metabolic interactions between *N. meningitidis* and propionic acid-producing bacteria of the URT are hypothesised to be important in IMD (section 1.8).

And so, quantification of the metabolic relationship between *N. meningitidis* and *P. gingivalis* has applications in combatting IMD. A quantification would allow :

1. the *in vivo* significance of propionic acid-producing bacteria on *N. meningitidis* growth to be determined
2. the conditions which modify this interaction (e.g. growth substrates available, pH, genetics of the microbial strains) to be characterised and their *in vivo* importance assessed (e.g. as an event that triggers IMD, or a factor that suppresses IMD).

Modification of this metabolic interaction *in vivo* (e.g. using probiotics, or prebiotics) could be a novel approach to combatting IMD (Moir, 2015), something that could be used alongside the vaccines and antibiotics currently employed (section 1.6). Results from the non-contact co-culture would be an important step in determining if a metabolic interaction with propionic acid-producing bacteria would make a good therapeutic target (i.e. a target that can modify the ecological niche and so reduce the risk of IMD).

The non-contact co-culture assay has fundamental differences to the *in vivo* environment it models. For instance, the specific experimental conditions required for quantification using the non-contact co-culture assay would not be required for a metabolic interaction *in vivo*. Instead, *N. meningitidis* and *P. gingivalis* are hypothesised to interact in biofilms (or by diffusion/transport of propionic acid between distant sites). These biofilms have an oxygen gradient between the inner and outer regions (section 1.8.4, Fig1.7). Propionic acid would be produced by *P. gingivalis* in the anaerobic inner part of the biofilm and diffuse to the outer regions of the biofilm where oxygen is non-limiting and where it can be fully utilised by *N. meningitidis*. Therefore, results from the non-contact co-culture assay must be carefully translated before they can be used to make *in vivo* predications.

Quantification of the metabolic interaction using the non-contact co-culture assay has not been carried out. Only preparations to carrying out these experiments have been made (chapter 4). In lieu of a verified and fitted model of the metabolic interaction, the steps likely to be required for translating such results to *in vivo* insights and applications in combatting IMD are discussed.

5.2.1 Aspects of the co-culture expected to be important *in vivo*

The aspects of the co-culture important to an *in vivo* metabolic interaction must be captured in the model and quantified. Some of these aspects, such as yields (section 4.4.2), propionic acid growth inhibition (section 4.4.3) and culture death rate (section 4.4.4), have already been identified from culture-based experiments.

Of these, the yields (i.e. yield of propionic acid from *P. gingivalis*, and yield of *N. meningitidis* from propionic acid) will be important *in vivo* since they represent the most basic measure of how much *N. meningitidis* will grow in response to *P. gingivalis* growth.

Growth inhibition by propionic acid is also likely to be important since propionic acid concentrations in gingival crevices are known to reach $9.5\,\mathrm{mM}$ during peridontitis (Niederman *et al.*, 1997). This concentration of propionic acid is enough to significantly inhibit *N. meningitidis* growth rate (section 4.4.3). The *in vivo* significance of this would be in determining how close *P. gingivalis* and *N. meningitidis* can grow in biofilms, since high concentrations of propionic acid in the deeper anaerobic regions (where *P. gingivalis* would produce propionic acid as a fermentative end product) may exclude *N. meningitidis*. It would also be useful to determine how this inhibition balances with the increase in *N. meningitidis* growth due utilisation of propionic acid.

There are other factors, not captured in the growth dynamics of the experiments in chapter 4, that are likely to be important in an *in vivo* metabolic interaction.

The effect of pH on inhibition of *N. meningitidis* growth by propionic acid may be important. The antimicrobial properties of organic acids are typically dependent on a combination of pH and concentration (Levison, 1973; Ghorbani *et al.*, 2015). pH does not appear to vary significantly from neutral in the gingival crevice or periodontal pocket (i.e. the gingival crevice in disease) (Eggert *et al.*, 1991). However, within the microstructure of dental biofilms, pH ranges between 5.5-7.4 (Schlafer *et al.*, 2011) with pH less than 5.5 in the centre of microcolonies (Xiao *et al.*, 2017). These sites are significant to the metabolic interaction with *N. meningitidis*, mediated by propionic acid, since they are located in the URT and are known habitats of *P. gingivalis* (Tan *et al.*, 2014).

Potential *P. gingivalis* growth inhibition by propionic acid may be important *in vivo* since this would limit the production rate of propionic acid. Additionally, if utilisation

of propionic acid by *N. meningitidis* is able to release this inhibition then it could cause a positive feedback loop in which the population sizes of *N. meningitidis* and *P. gingivalis* increase dramatically.

The sufficiency of propionic acid as a carbon source for *N. meningitidis* would be important to assess. It appears as though propionic acid is not sufficient to act as a sole carbon source for *N. meningitidis* since in the plate reader experiments (section 4.3.1) another carbon source (either glucose or pyruvate) was required for growth to start. This would be important *in vivo* if the abundance of other growth substrates affects the ability of *N. meningitidis* to utilise propionic acid (which is the primary basis of the metabolic interaction between *N. meningitidis* and *P. gingivalis*).

The role of different growth substrates on the rate of propionic acid production by *P. gingivalis* may be important since these different conditions may strengthen or weaken any metabolic interaction based on propionic acid. This would have an effect *in vivo* and may represent a method of interrupting the metabolic interaction and reducing *N. meningitidis* carriage to prevent IMD.

5.2.2 Further studies for translating *in vitro* results to *in vivo* insights

Further modelling and experiments would be used to predict the *in vivo* significance of the metabolic interaction between *N. meningitidis* and *P. gingivalis*.

Parameter values from a quantified mathematical model of the metabolic interaction could be used in further mathematical models that capture spatial aspects of microbial growth in a biofilm (e.g. with an agent-based model) and include other relevant factors (such as the growth substrates available *in vivo* in the URT).

These predictions could be compared to results from *in vitro* biofilm culture experiments to identify other important factors not captured by the non-contact co-culture assay. Since this assay separates the cultures with a PDMS membrane, interactions via non-volatile diffusible factors (which may include toxins) or contact-dependent interactions, will not be captured. However, a biofilm-based assay would capture these factors. These additional factors may be important for an *in vivo* metabolic interaction and so they should be identified.

Information about the *in vivo* environment would be useful for appropriate translation of the results. The locations of *P. gingivalis* and *N. meningitidis* in the human body, especially whether they share a site in the body, is important for determining if the metabolic relationship is close or distant. If they occur in the same locations then information about whether they co-occur in the same biofilm structures, and the microstructure of these biofilms would be useful. Other propionic acid producers have been detected at sites where *N. meningitidis* is known to reside. *Porphyromonas* spp and *Fusobacterium* spp (which are likely to be producers of propionic acid) are associated with disease in many sites in the URT, including the tonsils (Brook, 2002, section 1.4.4). *N. meningitidis* biofilm has been found to be commonly associated with tonsils that have been surgically removed (Sim *et al.*, 2000). The relevance of this to healthy tonsils is unclear, however this does show that *N. meningitidis* is found in tonsils that are likely infected with many other bacterial species including *Porphyromonas* spp and *Fusobacterium* spp. It is likely that this is not the only site of co-occurrence between propionic acid-producing bacteria and *N. meningitidis* in the URT. More information about the distance of the metabolic interaction is important because if propionic acid diffuses within a biofilm then the concentration of propionic acid that *N. meningitidis* would be exposed to is much higher than if it must diffuse from biofilms containing *P. gingivalis* and be transported to a site containing *N. meningitidis* (e.g. via flow of mucus, as described in section 1.3.3.2).

Also, information about the size of *N. meningitidis* populations *in vivo* associated with IMD, compared to population sizes during non-invasive carriage, would be essential since this would allow model predictions to be translated to a risk of IMD.

5.2.3 Use of this information for studying importance of the metabolic interaction

The ODE-based mathematical model of the non-contact co-culture assay could be modified, based on information about the *in vivo* environment, to make *in vivo* predictions. The chambers in the model would represent different spatially separated compartments, such as different regions of biofilms or sites within the URT. The strength of starting with this model is that the analytical methods developed for interpreting non-contact co-culture assay results and quantifying the metabolic relationship can be used to quantify its importance in the *in vivo* context. This analysis would be used to

identify conditions that control the importance of this metabolic relationship (e.g. pH, presence of different carbon sources, or presence of bacterial species). The ODE model is particularly useful as a starting point because it can be solved analytically to reveal clear mathematical relationships. Further analysis, using methods that are able to represent other important aspects of the *in vivo* environment, could then be layered on top of these findings. Partial differential equations (which model spatial dimensions as well as temporal, such as used by Phalak *et al.*, 2016) and agent-based methods (which model groups of individual bacterial cells, such as used by Sweeney *et al.*, 2019) may be particularly useful for modelling the spatial structure of biofilms and contact-based interactions.

This strategy effectively uses the parametrised model from the non-contact co-culture assay as a quantitative representation of the metabolic relationship. This allows different conditions to be tested *in vitro* and then translated *in vivo*. Conditions such as pH, presence of other carbon sources, different strains (for both *N. meningitidis* and *P. gingivalis*) and alternative propionic acid producers (to replace *P. gingivalis*) should be tested *in vitro*. Conditions such as population sizes and relative locations of the different bacterial populations should be tested *in silico* by modifying the parametrised non-contact co-culture model.

However, not all aspects of the *in vivo* interaction will be captured by the non-contact co-culture assay (e.g. contact-based interactions, and interactions mediated by non-volatile substances). Therefore, *in vivo* data should be used to test *in silico* predictions. Useful experiments that discern between different hypotheses could be designed by modelling each of these hypotheses to search out conditions that will produce measurably different outcomes. The manner in which this is done would depend on the prediction made, and some *in vivo* validation could be performed with existing data. Predictions about the effect on different strains on the significance of the metabolic interaction could be compared to the known virulence of these meningococcal strains (with consideration for all the other factors involved in strain virulence, discussed in section 1.5.2). Predictions about the role of different propionic acid-producers could be tested by examining 16S sequencing datasets from different age groups, similar to the methodology used in Catenazzi *et al.*, 2014.

5.2.4 Application in pro-active prevention of sporadic IMD and containment of outbreaks

Knowledge about what factors could disrupt a potential metabolic interaction between *N. meningitidis* and *P. gingivalis* (or other propionic acid producers) could be used to combat IMD. It may be that there is a single propionic acid producing niche, and the species or strain that fills this niche affects the population size of *N. meningitidis* in the URT. And so, inoculation with an alternative propionic acid producing culture may cause a reduction in *N. meningitidis* carriage. Or it may be that introduction of another propionic acid consuming population may disrupt the metabolic interaction with *N. meningitidis* and cause a reduction in carriage. If pH, size and location of biofilms, or carbon sources are found to be significant, then specific interventions (e.g. pre-biotics) could be investigated. This knowledge may also lead to general diet and hygiene advice for reducing *N. meningitidis* carriage.

A microbiome-based approach to combatting IMD has already been studied. Inoculation of college students with *N. lactamica* caused a rapid, short-term (several months) reduction of *N. meningitidis* carriage levels (Deasy *et al.*, 2015). This reduction in carriage should correspond to a reduction in IMD risk (section 1.7), and so this approach may represent an alternative to antibiotics and vaccines to combat IMD. It could be used pro-actively (before any cases of IMD have been detected) in high-risk groups (e.g. university students, pilgrims or military recruits) to lower the risk of sporadic cases or an outbreak. This would be a valuable contribution since antibiotic use is limited by AMR and only applied as a prophylactic in direct contacts of an individual with IMD (section 1.6.1). Vaccines are deployed to the general population as a preventative measure, and are targetted to high-risk sub-populations. However, they are generally deployed strategically to respond to long-term global trends in IMD. In contrast, a microbiome approach may be useful for more short-term, localised events. Also, it may be effective against a wide range of *N. meningitidis* serogroups and strains meaning it could be applied as a general preventative measure. This broad protection may also enable it to be used to combat newly emerging meningococcal strains that do not yet have effective corresponding vaccines. This would be a valuable contribution since there is a risk of global antigenic changes that could nullify currently effective vaccines (Harrison *et al.*, 2009).

5.3 Non-contact co-culture assay suitability

The non-contact co-culture assay was designed to isolate metabolic interactions between *N. meningitidis* and *P. gingivalis* via propionic acid. The co-culture aspect of the method means that interactions via unknown mechanisms can be detected and measured. The non-contact aspect of the method limits the ways in which the cultures can interact to give greater clarity in the interpretation of results. Interpretation of results is also aided by limiting metabolic interactions to those mediated by volatile substances (e.g. propionic acid).

Since the assay was, from the start, tightly linked to an ODE model of the system, this model can be refined by comparison to results and ultimately used as quantitative representation of the metabolic relationship.

This non-contact co-culture between *N. meningitidis* and *P. gingivalis* was not demonstrated *in vitro* using the developed apparatus. However, the feasibility and usefulness of the apparatus has been demonstrated *in silico* using mathematical models of the non-contact co-culture system. Also, limitations of the theoretical approach, and of the apparatus, have been identified.

This assay could be extended in response to some of the limitations that have been discovered. For example, the conditions for a useful experiment are limited by the need to have the *N. meningitidis* culture go through an oxygen-limited growth phase (to generate anaerobic conditions) and then a propionic acid-limited phase (so that its effect on growth can be measured) (section 2.7.2.1). This requirement could instead be fulfilled by splitting the *N. meningitidis* culture chamber in two so that there is an oxygen-limited chamber (adjacent to the *P. gingivalis* chamber) and a propionic acid-limited chamber (adjacent to the oxygen supply chamber). This, in effect, would model an oxygen gradient from the anaerobic core of a biofilm to the more oxygen-rich outer regions.

To decrease the diffusion distance between the two cultures, or allow interactions via a greater variety of factors, the non-contact concept could be relaxed. Instead, a biofilm-based assay could be used, where a mixed biofilm is submerged in a planktonic *N. meningitidis* culture (similar to methods used in Bradshaw *et al.*, 1996). This approach could be taken further and the cultures could be mixed completely in a well-mixed planktonic co-culture. These co-cultures should be viable on the condition that the

growth of the aerobic population is oxygen-limited. However, this would limit the ability to measure the density of each population and would not isolate the interactions mediated by volatile substances. Therefore, these methods (that allow contact between cultures) could be used alongside the non-contact co-culture assay to verify predictions and determine the role of interactions mediated by non-volatile compounds (e.g. toxins, non-volatile metabolites) and contact-dependent interactions.

5.4 Further applications of the non-contact co-culture assay

The non-contact co-culture assay should be well-suited to investigating how different microbial strains and species affect the metabolic interactions (and so study the genetic component of the metabolic interactions). This is because it should be able to culture any strain that can grow in a pure planktonic liquid culture, and since the environments for the two cultures are kept separate, incompatibilities between the two liquid cultures should not present a problem.

Interactions between *N. meningitidis* and other propionic acid-producing bacteria of the URT could be studied, such as *Propionibacterium* spp, *Bacteroides loescheii*, *F. nucleatum*, and others identified in section 1.4.4. Also, interactions involving other pathogens and propionic acid-producers could be studied, such as interactions between *S. aureus* and *Propionibacterium* spp in the URT (Brugger *et al.*, 2016), or between *Salmonella* Typhimurium and *Bacteroides* spp in the gut (Jacobson *et al.*, 2018).

Although this assay is well-suited to studying interactions via propionic acid, it could also be used to study other types of metabolic interaction. For example, *N. meningitidis* is able to utilise lactate, produced in the URT by lactic acid bacteria, in a metabolic interaction that is known to have a significant effect on *N. meningitidis* population size (Schoen *et al.*, 2014). In order to study this interaction with the non-contact co-culture assay, a porous membrane could be used to separate the two cultures chambers (similar to the membranes used for non-contact co-culture experiments in Paul *et al.*, 2013 and Moutinho *et al.*, 2017). This would allow diffusion of lactate between the chambers, but would also allow diffusion of other culture media contents (e.g. sugars, salts, amino acids). Therefore, the culture conditions between the chambers would

not be as distinct compared to when a PDMS membrane is used. Because of this, metabolic interactions due to competition for resources would have to be factored in when planning experiments and interpreting results.

The non-contact co-culture assay could also be applied to studying the role of metabolic interactions in the gut microbiome. Cross-feeding (a form of metabolic interaction) between microbial populations, utilising resources from the host's diet, determines the structure (i.e. presence and abundance of microbial populations) and metabolic activity of the gut microbiome (Hoek & Merks, 2017). Variations in the structure and metabolic activity of the gut microbiome are associated with disease (e.g. obesity, and irritable bowel syndrome). The metabolites involved in these cross-feeding relationships include products of anaerobic metabolism, including propionic acid (Vernocchi *et al.*, 2016). Therefore, the non-contact co-culture assay would be well-suited to studying the role of microbial metabolic interactions in this site as well as many other sites in the human body (e.g. lower respiratory tract, vagina, skin).

Applied to studying these microbial interactions, the non-contact co-culture assay would be of use in investigating metabolic relationships predicted from analysis of 16S sequencing datasets. For example, co-occurrence evidence backed up with knowledge of the metabolic activity of the members of proposed interaction (such as in Catenazzi *et al.*, 2014) could be verified and characterise by the non-contact co-culture assay. This *in vitro*, well-defined system could be used to quantify the important aspects of the metabolic interaction, and so would help assess the potential role that the interaction could play *in vivo*.

Study of these microbial metabolic interactions is vital for the development of therapeutics that push the human microbiome towards a state that encourages health rather than disease.

References

Abreu NA, Nagalingam NA, Song Y, Roediger FC, Pletcher SD, Goldberg AN & Lynch SV (2012). "Sinus Microbiome Diversity Depletion and *Corynebacterium tuberculostearicum* Enrichment Mediates Rhinosinusitis". *Sci Transl Med* **4**(151). DOI: 10.1126/scitranslmed.3003783.

Abu Kwaik Y & Bumann D (2013). "Microbial quest for food *in vivo*: 'Nutritional virulence' as an emerging paradigm". *Cellular Microbiology* **15**(6):882–890. DOI: 10.1111/cmi.12138.

Acevedo R *et al.* (2019). "The Global Meningococcal Initiative meeting on prevention of meningococcal disease worldwide: epidemiology, surveillance, hypervirulent strains, antibiotic resistance and high-risk populations". *Expert Review of Vaccines* **18**(1):15–30. DOI: 10.1080/14760584.2019.1557520.

Agarwal S, Vasudhev S, DeOliveira RB & Ram S (2014). "Inhibition of the Classical Pathway of Complement by Meningococcal Capsular Polysaccharides". *The Journal of Immunology* **193**(4):1855–1863. DOI: 10.4049/jimmunol.1303177.

Allen EK, Koeppel AF, Hendley JO, Turner SD, Winther B & Sale MM (2014). "Characterization of the nasopharyngeal microbiota in health and during rhinovirus challenge". *Microbiome* **2**(1):1–11. DOI: 10.1186/2049-2618-2-22.

Anderson GG & O'Toole GA (2008). "Innate and induced resistance mechanisms of bacterial biofilms". *Curr Top Microbiol Immunol* **322**:85–105. DOI: 10.1007/978-3-540-75418-3_5.

Baart GJE, Zomer B, Haan A de, Van der Pol LA, Beuvery C, Tramper J & Martens DE (2007). "Modeling *Neisseria meningitidis* metabolism: From genome to metabolic fluxes". *Genome Biology* **8**(7). DOI: 10.1186/gb-2007-8-7-r136.

Balmer P, Burman C, Serra L & York LJ (2018). "Impact of meningococcal vaccination on carriage and disease transmission: A review of the literature". *Human Vac-*

cines and Immunotherapeutics **14**(5):1118–1130. DOI: 10.1080/21645515.2018.1454570.

Batty EM *et al.* (2020). "The spread of chloramphenicol-resistant *Neisseria meningitidis* in Southeast Asia". *International Journal of Infectious Diseases*. DOI: 10.1016/j.ijid.2020.03.081.

Besant JD, Sargent EH & Kelley SO (2015). "Rapid electrochemical phenotypic profiling of antibiotic-resistant bacteria". *Lab on a Chip* **15**(13):2799–2807. DOI: 10.1039/c5lc00375j.

Beutler B, Du X & Poltorak A (2001). "Identification of toll-like receptor 4 (Tlr4) as the sole conduit for LPS signal transduction: genetic and evolutionary studies". *Journal of Endotoxin Research* **7**(4):277–280. DOI: 10.1179/096805101101532846.

Black S, Pizza M, Nissum M & Rappuoli R (2012). "Toward a Meningitis-Free World". *Science Translational Medicine* **4**(123). DOI: 10.1126/scitranslmed.3003859.

Bogaert D, Keijser B, Huse S, Rossen J, Veenhoven R, Gils E van, Bruin J, Montijn R, Bonten M & Sanders E (2011). "Variability and Diversity of Nasopharyngeal Microbiota in Children: A Metagenomic Analysis". *PLoS ONE* **6**(2):e17035. DOI: 10.1371/journal.pone.0017035.

Borrow R *et al.* (2017). "Meningococcal disease in the Middle East and Africa: Findings and updates from the Global Meningococcal Initiative". *Journal of Infection* **75**(1):1–11. DOI: 10.1016/j.jinf.2017.04.007.

Bozza G *et al.* (2014). "Role of ARF6, Rab11 and external Hsp90 in the trafficking and recycling of recombinant-soluble *Neisseria meningitidis* adhesin A (rNadA) in human epithelial cells". *PLoS ONE* **9**(10). DOI: 10.1371/journal.pone.0110047.

Bradshaw DJ, Marsh PD, Allison C & Schilling KM (1996). "Effect of oxygen, inoculum composition and flow rate on development of mixed-culture oral biofilms". *Microbiology* **142**(3):623–629. DOI: 10.1099/13500872-142-3-623.

Brook I (2002). "Anaerobic Bacteria in Upper Respiratory Tract and other Head and Neck Infections". *Annals of Otology, Rhinology & Laryngology* **111**(5):430–440. DOI: 10.1177/000348940211100508.

— (2006). "The role of anaerobic bacteria in sinusitis". *Anaerobe* **12**(1):5–12. DOI: 10.1016/j.anaerobe.2005.08.002.

Brugger SD, Bomar L & Lemon KP (2016). "Commensal-Pathogen Interactions along the Human Nasal Passages". *PLoS Pathogens* **155315**:1–9. DOI: 10.1371/journal.ppat.1005633.

Catenazzi MCE, Jones H, Wallace I, Clifton J, Chong JPJ, Jackson MA, Macdonald S, Edwards J & Moir JWB (2014). "A large genomic island allows *Neisseria meningitidis* to utilize propionic acid, with implications for colonization of the human nasopharynx". *Molecular Microbiology* **93**(2):346–355. DOI: 10.1111/mmi.12664.

Catlin BW (1973). "Nutritional profiles of *Neisseria gonorrhoeae*, *Neisseria meningitidis*, and *Neisseria lactamica* in chemically defined media and the use of growth requirements for gonococcal typing". *Journal of Infectious Diseases* **128**(2):178–194. DOI: 10.1093/infdis/128.2.178.

Charlson ES, Chen J, Custers-Allen R, Bittinger K, Li H, Sinha R, Hwang J, Bushman FD & Collman RG (2010). "Disordered Microbial Communities in the Upper Respiratory Tract of Cigarette Smokers". *PLoS ONE* **5**(12):e15216. DOI: 10.1371/journal.pone.0015216.

Chen M *et al.* (2015). "Shifts in the Antibiotic Susceptibility, Serogroups, and Clonal Complexes of *Neisseria meningitidis* in Shanghai, China: A Time Trend Analysis of the Pre-Quinolone and Quinolone Eras". *PLoS Medicine* **12**(6):1–22. DOI: 10.1371/journal.pmed.1001838.

Christensen H, May M, Bowen L, Hickman M & Trotter CL (2010). "Meningococcal carriage by age: a systematic review and meta-analysis". *The Lancet Infectious Diseases* **10**(12):853–861. DOI: 10.1016/S1473-3099(10)70251-6.

Côté P, Bersillon Jl, Huyard A, Faup G, Pierre C & Huyard A (1988). "Bubble-Free Aeration Using Membranes: Process Analysis"**.** **60**(11):1986–1992.

Coureuil M, Jamet A, Bille E, Lécuyer H, Bourdoulous S & Nassif X (2019). "Molecular interactions between *Neisseria meningitidis* and its human host". *Cellular Microbiology* **21**(11):1–11. DOI: 10.1111/cmi.13063.

Davila S *et al.* (2010). "Genome-wide association study identifies variants in the CFH region associated with host susceptibility to meningococcal disease". *Nature Genetics* **42**(9):772–779. DOI: 10.1038/ng.640.

Deasy AM, Guccione E, Dale AP, Andrews N, Evans CM, Bennett JS, Bratcher HB, Maiden MCJ, Gorringe AR & Read RC (2015). "Nasal inoculation of the commensal *Neisseria lactamica* inhibits carriage of *Neisseria meningitidis* by young adults: A controlled human infection study". *Clinical Infectious Diseases* **60**(10):1512–1520. DOI: 10.1093/cid/civ098.

Deghmane AE, Hong E & Taha MK (2017). "Emergence of meningococci with reduced susceptibility to third-generation cephalosporins". *Journal of Antimicrobial Chemotherapy* **72**(1):95–98. DOI: 10.1093/jac/dkw400.

Dellicour S & Greenwood B (2007). "Impact of meningococcal vaccination on pharyngeal carriage of meningococci". *Tropical Medicine and International Health* **12**(12):1409–1421. DOI: 10.1111/j.1365-3156.2007.01929.x.

Diaz PI, Zilm PS & Rogers AH (2002). "*Fusobacterium nucleatum* supports the growth of *Porphyromonas gingivalis* in oxygenated and carbon-dioxide-depleted environments". *Microbiology* **148**(2):467–472. DOI: 10.1099/00221287-148-2-467.

Difilippo EL & Eganhouse RP (2010). "Assessment of PDMS-water partition coefficients: Implications for passive environmental sampling of hydrophobic organic compounds". *Environmental Science and Technology* **44**(18):6917–6925. DOI: 10.1021/es101103x.

Donati C *et al.* (2016). "Uncovering oral *Neisseria* tropism and persistence using metagenomic sequencing". *Nature Microbiology* **1**(7). DOI: 10.1038/nmicrobiol.2016.70.

Dretler AW, Rouphael NG & Stephens DS (2018). "Progress toward the global control of *Neisseria meningitidis*: 21st century vaccines, current guidelines, and challenges for future vaccine development". *Human Vaccines and Immunotherapeutics* **14**(5):1146–1160. DOI: 10.1080/21645515.2018.1451810.

Duineveld PC, Lilja M, Johansson T & Inganäs O (2002). "Diffusion of solvent in PDMS elastomer for micromolding in capillaries". *Langmuir* **18**(24):9554–9559. DOI: 10.1021/la025831s.

Dunn LA & Stokes RH (1965). "The diffusion of monocarboxylic acids in aqueous solution at 25°C". *Australian Journal of Chemistry* **18**:285–296. DOI: 10.1071/CH9650285.

Earl JP *et al.* (2018). "Species-level bacterial community profiling of the healthy sinonasal microbiome using Pacific Biosciences sequencing of full-length 16S rRNA genes". *Microbiome* **6**(190):1–26. DOI: 10.1186/s40168-018-0569-2.

Echenique-Rivera H, Muzzi A, Del Tordello E, Seib KL, Francois P, Rappuoli R, Pizza M & Serruto D (2011). "Transcriptome analysis of *Neisseria meningitidis* in human whole blood and mutagenesis studies identify virulence factors involved in blood survival". *PLoS Pathogens* **7**(5). DOI: 10.1371/journal.ppat.1002027.

Eggert FM, Drewell L, Bigelow JA, Speck JE & Goldner M (1991). "The pH of gingival crevices and periodontal pockets in children, teenagers and adults". *Archives of Oral Biology* **36**(3):233–238. DOI: 10.1016/0003-9969(91)90091-8.

Fang SB, Schüller S & Phillips AD (2013). "Human intestinal *in vitro* organ culture as a model for investigation of bacteria-host interactions". *Journal of Experimental and Clinical Medicine(Taiwan)* **5**(2):43–50. DOI: 10.1016/j.jecm.2013.02.006.

Fastenberg JH, Hsueh WD, Mustafa A, Akbar NA & Abuzeid WM (2016). "Biofilms in chronic rhinosinusitis: Pathophysiology and therapeutic strategies". *World Journal of Otorhinolaryngology - Head and Neck Surgery* **2**(4):219–229. DOI: 10.1016/j.wjorl.2016.03.002.

Firpo G, Angeli E, Repetto L & Valbusa U (2015). "Permeability thickness dependence of polydimethylsiloxane (PDMS) membranes". *Journal of Membrane Science* **481**:1–8. DOI: 10.1016/j.memsci.2014.12.043.

Flynn JM, Niccum D, Dunitz JM & Hunter RC (2016). "Evidence and Role for Bacterial Mucin Degradation in Cystic Fibrosis Airway Disease". *PLoS Pathogens* **12**(8):1–21. DOI: 10.1371/journal.ppat.1005846.

Freilich S, Zarecki R, Eilam O, Segal ES, Henry CS, Kupiec M, Gophna U, Sharan R & Ruppin E (2011). "Competitive and cooperative metabolic interactions in bacterial communities". *Nature Communications* **2**:589. DOI: 10.1038/ncomms1597.

Füchslin HP, Schneider C & Egli T (2012). "In glucose-limited continuous culture the minimum substrate concentration for growth, Smin, is crucial in the competition between the enterobacterium *Escherichia coli* and *Chelatobacter heintzii*, an environmentally abundant bacterium". *The ISME journal* **6**(4):777–89. DOI: 10.1038/ismej.2011.143.

Gabutti G, Stefanati A & Kuhdari P (2015). "Epidemiology of *Neisseria meningitidis* infections: Case distribution by age and relevance of carriage". *Journal of Preventive Medicine and Hygiene* **56**(3):E116–E120. DOI: 10.15167/2421-4248/jpmh2015.56.3.478.

Galimand M, Gerbaud G, Guibourdenche M, Riou JY & Courvalin P (1998). "High-level Chloramphenicol Resistance in *Neisseria meningitidis*". *New England Journal of Medicine* **339**(13):868–874.

Ghorbani P, Santhakumar P, Hu Q, Djiadeu P, Wolever TMS, Palaniyar N & Grasemann H (2015). "Short-chain fatty acids affect cystic fibrosis airway inflammation and bacterial growth". *European Respiratory Journal* **46**(4):1033–1045. DOI: 10.1183/09031936.00143614.

Grifantini R *et al.* (2002). "Previously unrecognized vaccine candidates against group B meningococcus identified by DNA microarrays". *Nature Biotechnology* **20**(9):914–921. DOI: 10.1038/nbt728.

Groisman A, Lobo C, Cho H, Campbell JK, Dufour YS, Stevens AM & Levchenko A (2005). "A microfluidic chemostat for experiments with bacterial and yeast cells". **2**(9):685–689. DOI: 10.1038/NMETH784.

Hanly TJ & Henson MA (2013). "Dynamic metabolic modeling of a microaerobic yeast co-culture: predicting and optimizing ethanol production from glucose/xylose mixtures". *Biotechnology for biofuels* **6**(1):1–16. URL: http://www.biomedcentral.com/content/pdf/1754-6834-6-44.pdf.

Harrison LH, Trotter CL & Ramsay ME (2009). "Global epidemiology of meningococcal disease". *Vaccine* **27 Suppl 2**:B51–63. DOI: 10.1016/j.vaccine.2009.04.063.

Hasanoglu A, Salt Y, Keleser S & Dincer S (2009). "The esterification of acetic acid with ethanol in a pervaporation membrane reactor". *Desalination* **245**(1-3):662–669. DOI: 10.1016/j.desal.2009.02.034.

Hedman AK, Li MS, Langford PR & Kroll JS (2012). "Transcriptional profiling of serogroup B *Neisseria meningitidis* growing in human blood: An approach to vaccine antigen discovery". *PLoS ONE* **7**(6). DOI: 10.1371/journal.pone.0039718.

Heduit A & Thevenot D (1989). "Relation between redox potential and oxygen levels in activated-sludge reactors". *Water Science and Technology* **21**:947–956.

Hey A, Li MS, Hudson MJ, Langford PR & Simon Krolla J (2013). "Transcriptional profiling of *Neisseria meningitidis* interacting with human epithelial cells in a long-term *in vitro* colonization model". *Infection and Immunity* **81**(11):4149–4159. DOI: 10.1128/IAI.00397-13.

Hoek MJA & Merks RMH (2017). "Emergence of microbial diversity due to cross-feeding interactions in a spatial model of gut microbial metabolism". *BMC Systems Biology* **11**(1):1–18. DOI: 10.1186/s12918-017-0430-4.

Hron P, Jost D, Bastian P, Gallert C, Winter J & Ippisch O (2014). "Numerical simulation of growth of *Escherichia coli* in unsaturated porous media". *arXiv*:1–14. arXiv: 1407.3743.

Huang CB, Alimova Y, Myers TM & Ebersole JL (2011). "Short- and medium-chain fatty acids exhibit antimicrobial activity for oral microorganisms". *Archives of Oral Biology* **56**(7):650–654. DOI: 10.1016/j.archoralbio.2011.01.011.

Jacobson A *et al.* (2018). "A Gut Commensal-Produced Metabolite Mediates Colonization Resistance to *Salmonella* Infection". *Cell Host & Microbe* **24**(2):296–307.e7. DOI: 10.1016/j.chom.2018.07.002.

Janowski AB & Newland JG (2017). “From the microbiome to the central nervous system, an update on the epidemiology and pathogenesis of bacterial meningitis in childhood”. *F1000Research* **6**:86. DOI: 10.12688/f1000research.8533.1.

Kapoor G, Saigal S & Elongavan A (2017). “Action and resistance mechanisms of antibiotics: A guide for clinicians”. *Journal of Anaesthesiology Clinical Pharmacology* **33**(3):300–305. DOI: 10.4103/joacp.JOACP.

Kettle H, Louis P, Holtrop G, Duncan SH & Flint HJ (2015). “Modelling the emergent dynamics and major metabolites of the human colonic microbiota”. *Environmental Microbiology* **17**(5):1615–1630. DOI: 10.1111/1462-2920.12599.

Kim HJ, Boedicker JQ, Choi JW & Ismagilov RF (2008). “Defined spatial structure stabilizes a synthetic multispecies bacterial community”. *Proceedings of the National Academy of Sciences of the United States of America* **105**(47):18188–18193. DOI: 10.1073/pnas.0807935105. arXiv: arXiv:1408.1149.

Kim KS (2003). “Pathogenesis of Bacterial Meningitis: From Bacteraemia to Neuronal Injury”. *Nature Reviews Neuroscience* **4**(May):376–385. DOI: 10.1038/nrn1103.

Kirk TV, Marques MP, Radhakrishnan ANP & Szita N (2016). “Quantification of the oxygen uptake rate in a dissolved oxygen controlled oscillating jet-driven microbioreactor”. *Journal of Chemical Technology and Biotechnology* (October 2015). DOI: 10.1002/jctb.4833.

Klinger M, Tolbod LP, Gothelf KV & Ogilby PR (2009). “Effect of polymer cross-links on oxygen diffusion in glassy PMMA films”. *ACS Applied Materials and Interfaces* **1**(3):661–667. DOI: 10.1021/am800197j.

Klouwenberg PK & Bont L (2008). “Neonatal and infantile immune responses to encapsulated bacteria and conjugate vaccines”. *Clinical and Developmental Immunology* **2008**. DOI: 10.1155/2008/628963.

Kobayashi K, Takata Y & Kodama M (2009). “Direct contact between Pseudo-nitzschia multiseries and bacteria is necessary for the diatom to produce a high level of domoic acid”. *Fisheries Science* **75**(3):771–776. DOI: 10.1007/s12562-009-0081-5.

Könönen E (2005). “Anaerobes in the upper respiratory tract in infancy”. *Anaerobe* **11**(3):131–136. DOI: 10.1016/j.anaerobe.2004.11.001.

Koyfman A & Takayesu JK (2011). “Meningococcal disease”. *African Journal of Emergency Medicine* **1**(4):174–178. DOI: 10.1016/j.afjem.2011.07.007.

Kumar PS (2013). “Sex and the subgingival microbiome: Do female sex steroids affect periodontal bacteria ?” *Periodontology 2000* **61**:103–124.

Kurita-Ochiai T, Fukushima K & Ochiai K (1995). "Volatile Fatty Acids, Metabolic By-products of Periodontopathic Bacteria, Inhibit Lymphocyte Proliferation and Cytokine Production". *J DENT RES* **74**:1367–1373.

Law DKS, Lorange M, Ringuette L, Dion R, Giguère M, Henderson AM, Stoltz J, Zollinger WD, De Wals P & Tsang RSW (2006). "Invasive meningococcal disease in Québec, Canada, due to an emerging clone of ST-269 serogroup B meningococci with serotype antigen 17 and serosubtype antigen P1.19 (B:17:P1.19)". *Journal of Clinical Microbiology* **44**(8):2743–2749. DOI: 10.1128/JCM.00601-06.

Lee HLT, Boccazzi P, Ram RJ & Sinskey AJ (2006). "Microbioreactor arrays with integrated mixers and fluid injectors for high-throughput experimentation with pH and dissolved oxygen control". *Lab on a chip* **6**(9):1229–1235. DOI: 10.1039/b608014f.

Lee IH, Fredrickson AG & Tsuchiya HM (1974). "Diauxic Growth of *Propionibacterium shermanii*". *Applied Microbiology* **28**(5):831–835.

Lee JN, Park C & Whitesides GM (2003). "Solvent Compatibility of Poly(dimethylsiloxane)-Based Microfluidic Devices". *Analytical Chemistry* **75**(23):6544–6554. DOI: 10.1021/ac0346712.

Levison ME (1973). "Effect of colon flora and short chain fatty acids on growth *in vitro* of *Pseudomonas aeruginosa* and *Enterobacteriaceae*". *Infection and Immunity* **8**(1):30–35. DOI: 10.1128/iai.8.1.30-35.1973.

Lewis LA & Ram S (2014). "Meningococcal disease and the complement system". *Virulence* **5**(1):98–126. DOI: 10.4161/viru.26515.

Lewis VP & Yang ST (1992). "Propionic acid fermentation by *Propionibacterium acidipropionici*: effect of growth substrate". *Applied Microbiology and Biotechnology* **37**(4):437–442. DOI: 10.1007/BF00180964.

Li R, Lv X, Zhang X, Saeed O & Deng Y (2016). "Microfluidics for cell-cell interactions: A review". *Frontiers of Chemical Science and Engineering* **10**(1):90–98. DOI: 10.1007/s11705-015-1550-2.

MacLennan J *et al.* (2006). "Social behavior and meningococcal carriage in British teenagers". *Emerging Infectious Diseases* **12**(6):950–957. DOI: 10.3201/eid1206.051297.

Markov DA, Lillie EM, Garbett SP & McCawley LJ (2014). "Variation in diffusion of gases through PDMS due to plasma surface treatment and storage conditions". *Biomedical Microdevices* **16**(1):91–96. DOI: doi:10.1007/s10544-013-9808-2.

Martels JZH von, Sadaghian Sadabad M, Bourgonje AR, Blokzijl T, Dijkstra G, Faber KN & Harmsen HJM (2017). "The role of gut microbiota in health and disease: *In*

vitro modeling of host-microbe interactions at the aerobe-anaerobe interphase of the human gut". *Anaerobe* **44**:3–12. DOI: 10.1016/j.anaerobe.2017.01.001.

Martinon-Torres F *et al.* (2016). "Natural resistance to Meningococcal Disease related to CFH loci: Meta-analysis of genome-wide association studies". *Scientific Reports* **6**(October):1–9. DOI: 10.1038/srep35842.

Maruyama K & Kitamura H (1985). "Mechanisms of growth inhibition by propionate and restoration of the growth by sodium bicarbonate or acetate in *Rhodopseudomonas sphaeroides* S". *Journal of Biochemistry* **98**(3):819–824. DOI: 10.1093/oxfordjournals.jbchem.a135340.

McCarthy PC, Sharyan A & Moghaddam LS (2018). "Meningococcal vaccines: Current status and emerging strategies". *Vaccines* **6**(1). DOI: 10.3390/vaccines6010012.

McCoy RD, Vimr ER & Troy FA (1985). "CMP-NeuNAc:poly-α-2,8-sialosyl sialyltransferase and the biosynthesis of polysialosyl units in neural cell adhesion molecules". *Journal of Biological Chemistry* **260**(23):12695–12699.

Medlock GL, Carey MA, McDuffie DG, Mundy MB, Giallourou N, Swann JR, Kolling G & Papin JA (2018). "Metabolic mechanisms of interaction within a defined gut microbiota". *bioRxiv* **7**(3):250860. DOI: 10.1101/250860.

Merkel TC, Bondar VI, Nagai K, Freeman BD & Pinnau I (2000). "Gas Sorption, Diffusion, and Permeation in Poly(dimethylsiloxane)". *Journal of Polymer Science, Part B: Polymer Physics* **38**:415–434. DOI: 10.1021/acs.macromol.5b02578.

Miller RD, Brown KE & Morse SA (1977). "Inhibitory action of fatty acids on the growth of *Neisseria gonorrhoeae*". *Infection and Immunity* **17**(2):303–312. DOI: 10.1128/iai.17.2.303-312.1977.

Milner P, Batten JE & Curtis Ma (1996). "Development of a simple chemically defined medium for *Porphyromonas gingivalis*: requirement for $alpha$-ketoglutarate". *FEMS microbiology letters* **140**(2-3):125–130. DOI: 0378-1097(96)00159-0[pii].

Miyagi A, Nabetani H & Subramanian R (2011). "Purification of crude fatty acids using a PDMS-based composite membrane". *Separation and Purification Technology* **77**(1):80–86. DOI: 10.1016/j.seppur.2010.11.023.

Moir JWB (2015). "Meningitis in adolescents: the role of commensal microbiota". *Trends in Microbiology* **23**(4):181–182. DOI: 10.1016/j.tim.2015.02.004.

Momeni B, Xie L & Shou W (2017). "Lotka-Volterra pairwise modeling fails to capture diverse pairwise microbial interactions". *eLife* **6**:1–34. DOI: 10.7554/eLife.25051.001.

Monod J (1949). “The Growth of Bacterial Cultures”. *Annual Review of Microbiology* **3**(1):371–394. DOI: 10.1146/annurev.mi.03.100149.002103.

Mourelatos K, Eady EA, Cunliffe WJ, Clark SM & Cove JH (2007). “Temporal changes in sebum excretion and propionibacterial colonization in preadolescent children with and without acne”. *British Journal of Dermatology* **156**(1):22–31. DOI: 10.1111/j.1365-2133.2006.07517.x.

Moutinho TJ, Panagides JC, Biggs MB, Medlock GL, Kolling GL & Papin JA (2017). “Novel co-culture plate enables growth dynamic-based assessment of contact-independent microbial interactions”. *PLoS ONE* **12**(8):1–12. DOI: 10.1371/journal.pone.0182163.

Moxon ER & Jansen VAA (2005). “Phage variation: understanding the behaviour of an accidental pathogen”. *Trends in Microbiology* **13**(12):563–565. DOI: 10.1016/j.tim.2005.10.003.

Münker TJAG, Vijfeijken SECM van de, Mulder CS, Vespasiano V, Becking AG & Kleverlaan CJ (2018). “Effects of sterilization on the mechanical properties of poly(methyl methacrylate) based personalized medical devices”. *Journal of the Mechanical Behavior of Biomedical Materials* **81**(January):168–172. DOI: 10.1016/j.jmbbm.2018.01.033.

Myers M, Myers L & Okey R (2006). “The use of oxidation-reduction potential as a means of controlling effluent ammonia concentration in an extended aeration activated sludge system”. *WEFTEC*:5901–5926.

Nadel S & Ninis N (2018). “Invasive meningococcal disease in the vaccine era”. *Frontiers in Pediatrics* **6**(November):1–11. DOI: 10.3389/fped.2018.00321.

Neil RB & Apicella MA (2009). “Clinical and laboratory evidence for *Neisseria meningitidis* biofilms”. *Future Microbiology* **4**(5):555–563. DOI: 10.2217/fmb.09.27.

Netke SA, Sawant SB, Joshi JB & Pangarkar VG (1995). “Sorption and permeation of acetic acid through zeolite filled membrane”. *Journal of Membrane Science* **107**(1-2):23–33. DOI: 10.1016/0376-7388(95)00099-X.

Niederman R, Buyle-Bodin Y, Lu BY, Robinson P & Naleway C (1997). “Short-chain Carboxylic Acid Concentration in Human Gingival Crevicular Fluid”. *Journal of Dental Research* **76**(1). DOI: https://doi.org/10.1177/00220345970760010801.

Park J, Kerner A, Burns MA & Lin XN (2011). “Microdroplet-Enabled Highly Parallel Co-Cultivation of Microbial Communities”. *PLoS ONE* **6**(2). Ed. by A Herrera-Estrella:e17019. DOI: 10.1371/journal.pone.0017019.

Pasternak RA, Christensen MV & Heller J (1970). “Diffusion and Permeation of Oxygen, Nitrogen, Carbon Dioxide, and Nitrogen Dioxide through Polytetrafluoroethylene”. *Macromolecules* **3**(3):366–371. DOI: 10.1021/ma60015a020.

Patel D, Gao Y, Son KJ, Siltanen C, Neve RM, Ferrara KW & Revzin A (2015). “Microfluidic Co-Cultures with Hydrogel-Based Ligand Trap to Study Paracrine Signals Giving Rise to Cancer Drug Resistance”. *Lab Chip*. DOI: 10.1039/C5LC00948K.

Pathan N, Faust SN & Levin M (2003). “Pathophysiology of meningococcal meningitis and septicaemia”. *Archives of Disease in Childhood* **88**(7):601–607. DOI: 10.1136/adc.88.7.601.

Paul C, Mausz MA & Pohnert G (2013). “A co-culturing/metabolomics approach to investigate chemically mediated interactions of planktonic organisms reveals influence of bacteria on diatom metabolism”. *Metabolomics* **9**(2):349–359. DOI: 10.1007/s11306-012-0453-1.

Peaudecerf FJ, Bunbury F, Bhardwaj V, Bees MA, Smith AG, Goldstein RE & Croze OA (2018). “Microbial mutualism at a distance: The role of geometry in diffusive exchanges”. *Physical Review E* **97**(2):1–14. DOI: 10.1103/PhysRevE.97.022411. arXiv: 1708.01716.

Phalak P, Chen J, Carlson RP & Henson MA (2016). “Metabolic modeling of a chronic wound biofilm consortium predicts spatial partitioning of bacterial species”. *BMC Systems Biology* **10**(1):1–20. DOI: 10.1186/s12918-016-0334-8.

Poolman J & Borrow R (2011). “Hyporesponsiveness and its clinical implications after vaccination with polysaccharide or glycoconjugate vaccines”. *Expert Review of Vaccines* **10**(3):307–322. DOI: 10.1586/erv.11.8.

Press WH, Flannery BP, Teukolsky SA & Vetterling WT (1992). “Runge-Kutta Method”. *Numerical Recipes in FORTRAN: The Art of Scientific Computing*. 2nd ed. Cambridge, England: Cambridge University Press. Chap. 16:704–716.

Pridmore AC, Jarvis G, John CM, Jack DL, Dower SK & Read RC (2003). “Activation of Toll-Like Receptor 2 (TLR2) and TLR4/MD2 by *Neisseria* is Independent of Capsule and Lipooligosaccharide (LOS) Sialylation but Varies Widely among LOS from Different Strains”. *Microbiology* **71**(7):3901–3908. DOI: 10.1128/IAI.71.7.3901.

PubChem Compound Database. “1-Propanol | C3H8O - PubChem”. *[online]* (). URL: https://pubchem.ncbi.nlm.nih.gov/compound/1031.

— “Propionate | C3H5O2 - PubChem”. *[online]* (). URL: https://pubchem.ncbi.nlm.nih.gov/compound/104745.

Ram S, Lewis LA & Agarwal S (2011). "Meningococcal group W-135 and Y capsular polysaccharides paradoxically enhance activation of the alternative pathway of complement". *Journal of Biological Chemistry* **286**(10):8297–8307. DOI: 10.1074/jbc.M110.184838.

Ramakrishnan VR, Feaze LM, Gitomer SA, Ir D, Robertson CE & Frank DN (2013). "The microbiome of the middle meatus in healthy adults". *PLoS ONE* **8**(12):1–10. DOI: 10.1371/journal.pone.0085507.

Ramakrishnan VR, Gitomer S, Kofonow JM, Robertson CE & Frank DN (2017). "Investigation of sinonasal microbiome spatial organization in chronic rhinosinusitis". *International Forum of Allergy and Rhinology* **7**(1):16–23. DOI: 10.1002/alr.21854.

Read RC *et al.* (2014). "Effect of a quadrivalent meningococcal ACWY glycoconjugate or a serogroup B meningococcal vaccine on meningococcal carriage: An observer-blind, phase 3 randomised clinical trial". *The Lancet* **384**(9960):2123–2131. DOI: 10.1016/S0140-6736(14)60842-4.

Ren Q, Henes B, Fairhead M & Thöny-Meyer L (2013). "High level production of tyrosinase in recombinant *Escherichia coli*". *BMC Biotechnology* **13**(1):18. DOI: 10.1186/1472-6750-13-18.

Riley G & Brown S (1991). "Penicillin resistance in *Neisseria meningitidis*". *New England Journal of Medicine* **324**(14):997. DOI: 10.1056/NEJM199104043241416.

Rouphael NG & Stephens DS (2012a). *Neisseria meningitidis: Advanced Methods and Protocols*. Ed. by M Christodoulides. Vol. 799. 1. New York Dordrecht Heidelberg London: Humana Press. DOI: 10.1007/978-1-62703-239-1_1. arXiv: arXiv:1011.1669v3.

— (2012b). "*Neisseria meningitidis*: Biology, Microbiology, and Epidemiology". *Methods Mol Biol* **799**:1–20. DOI: 10.1007/978-1-61779-346-2.

Schlafer S, Raarup MK, Meyer RL, Sutherland DS, Dige I, Nyengaard JR & Nyvad B (2011). "pH landscapes in a novel five-species model of early dental biofilm". *PLoS ONE* **6**(9):1–11. DOI: 10.1371/journal.pone.0025299.

Schmitter T, Pils S, Weibel S, Agerer F, Peterson L, Buntru A, Kopp K & Hauck CR (2007). "Opa proteins of pathogenic neisseriae initiate src kinase-dependent or lipid raft-mediated uptake via distinct human carcinoembryonic antigen-related cell adhesion molecule isoforms". *Infection and Immunity* **75**(8):4116–4126. DOI: 10.1128/IAI.01835-06.

Schoen C, Kischkies L, Elias J & Ampattu BJ (2014). "Metabolism and virulence in *Neisseria meningitidis*". *Frontiers in Cellular and Infection Microbiology* **4**(August):1–16. DOI: 10.3389/fcimb.2014.00114.

Shah P *et al.* (2016). "A microfluidics-based *in vitro* model of the gastrointestinal human-microbe interface". *Nature Communications* **7**(May). DOI: 10.1038/ncomms11535. arXiv: arXiv:1507.02142v2.

Shi Y, Pan C, Wang K, Chen X, Wu X, Chen CTA & Wu B (2017). "Synthetic multispecies microbial communities reveals shifts in secondary metabolism and facilitates cryptic natural product discovery". *Environmental Microbiology* **19**(9):3606–3618. DOI: 10.1111/1462-2920.13858.

Shu M, Wang Y, Yu J, Kuo S, Coda A, Jiang Y, Gallo RL & Huang CM (2013). "Fermentation of *Propionibacterium acnes*, a Commensal Bacterium in the Human Skin Microbiome, as Skin Probiotics against Methicillin-Resistant *Staphylococcus aureus*". *PLoS ONE* **8**(2). DOI: 10.1371/journal.pone.0055380.

Shultz TR, Tapsall JW, White PA, Ryan CS, Lyras D, Rood JI, Binotto E & Richardson CJL (2003). "Chloramphenicol-resistant *Neisseria meningitidis* containing catP isolated in Australia". *Journal of Antimicrobial Chemotherapy* **52**(5):856–859. DOI: 10.1093/jac/dkg452.

Sia SK & Whitesides GM (2003). "Microfluidic devices fabricated in poly(dimethylsiloxane) for biological studies". *Electrophoresis* **24**(21):3563–3576. DOI: 10.1002/elps.200305584.

Siegel SJ & Weiser JN (2015). "Mechanisms of Bacterial Colonization of the Respiratory Tract". *Annual Review of Microbiology* **69**(1):425–444. DOI: 10.1146/annurev-micro-091014-104209.

Sim RJ, Harrison MM, Moxon ER & Tang CM (2000). "Underestimation of meningococci in tonsillar tissue by nasopharyngeal swabbing". *The Lancet* **356**:1653–1654.

Simmons A, Hyvarinen J & Poole-Warren L (2006). "The effect of sterilisation on a poly(dimethylsiloxane)/poly(hexamethylene oxide) mixed macrodiol-based polyurethane elastomer". *Biomaterials* **27**(25):4484–4497. DOI: 10.1016/j.biomaterials.2006.04.017.

Stein RR, Bucci V, Toussaint NC, Buffie CG, Rätsch G, Pamer EG, Sander C & Xavier JB (2013). "Ecological Modeling from Time-Series Inference: Insight into Dynamics and Stability of Intestinal Microbiota". *PLoS Comput Biol* **9**(12):e1003388. DOI: 10.1371/journal.pcbi.1003388.

Steinhaus B, Garcia ML, Shen AQ & Angenent LT (2007). "A Portable Anaerobic Microbioreactor Reveals Optimum Growth Conditions for the Methanogen *Methanosaeta concilii*". **73**(5):1653–1658. DOI: 10.1128/AEM.01827-06.

Stephens DS, Hoffman LH & McGee ZA (1983). "Interaction of *Neisseria meningitidis* with Human Nasopharyngeal Mucosa: Attachment and Entry into Columnar Epithel". *The Journal of Infectious Diseases* **148**(3):369–376.

Stephens DS, Greenwood B & Brandtzaeg P (2007). "Epidemic meningitis, meningococcaemia, and *Neisseria meningitidis*". *Lancet* **369**(9580):2196–2210. DOI: 10.1016/S0140-6736(07)61016-2.

Stolper Da, Revsbech NP & Canfield DE (2010). "Aerobic growth at nanomolar oxygen concentrations." *Proceedings of the National Academy of Sciences of the United States of America* **107**(44):18755–18760. DOI: 10.1073/pnas.1013435107.

Stork M, Grijpstra J, Bos MP, Mañas Torres C, Devos N, Poolman JT, Chazin WJ & Tommassen J (2013). "Zinc Piracy as a Mechanism of *Neisseria meningitidis* for Evasion of Nutritional Immunity". *PLoS Pathogens* **9**(10). DOI: 10.1371/journal.ppat.1003733.

Sutherland TC, Quattroni P, Exley RM & Tang CM (2010). "Transcellular passage of *Neisseria meningitidis* across a polarized respiratory epithelium". *Infection and Immunity* **78**(9):3832–3847. DOI: 10.1128/IAI.01377-09.

Sweeney EG, Nishida A, Weston A, Banuelos MS, Potter K, Conery J & Guillemin K (2019). "Agent-Based Modeling Demonstrates How Local Chemotactic Behavior Can Shape Biofilm Architecture". *mSphere* **4**(3):1–13. DOI: 10.1128/msphere.00285-19.

Taha MK *et al.* (2007). "Target gene sequencing to characterize the penicillin G susceptibility of *Neisseria meningitidis*". *Antimicrobial Agents and Chemotherapy* **51**(8):2784–2792. DOI: 10.1128/AAC.00412-07.

Takahashi H, Kim KS & Watanabe H (2011). "Meningococcal internalization into human endothelial and epithelial cells is triggered by the influx of extracellular L-glutamate via GltT L-glutamate ABC transporter in *Neisseria meningitidis*". *Infection and Immunity* **79**(1):380–382. DOI: 10.1128/IAI.00497-10.

Takeda I, Stretch C, Barnaby P, Bhatnager K, Rankin K, Fub H, Weljie A, Jha N & Slupsky C (2009). "Understanding the human salivary metabolome". *NMR in Biomedicine* **22**(6):577–584. DOI: 10.1002/nbm.1369.

Tala A, Cogli L, Stefano M, Cammarota M, Spinosa MR, Bucci C & Alifano P (2014). "Serogroup-specific interaction of *Neisseria meningitidis* capsular polysaccharide

with host cell microtubules and effects on tubulin polymerization". *Infection and Immunity* **82**(1):265–274. DOI: 10.1128/IAI.00501-13.

Tan KH *et al.* (2014). "*Porphyromonas gingivalis* and *Treponema denticola* Exhibit Metabolic Symbioses". *PLoS Pathogens* **10**(3). DOI: 10.1371/journal.ppat.1003955.

ThermoFisher Scientific. "Labware Chemical Resistance Table" (). URL: http://tools.thermofisher.com/content/sfs/brochures/D20480{~}.pdf.

Toussi DN, Wetzler LM, Liu X & Massari P (2016). "*Neisseriae* internalization by epithelial cells is enhanced by TLR2 stimulation". *Microbes and Infection* **18**(10):627–638. DOI: 10.1016/j.micinf.2016.06.001..

Trivedi K, Tang CM & Exley RM (2011). "Mechanisms of meningococcal colonisation". *Trends in Microbiology* **19**(9):456–463. DOI: 10.1016/j.tim.2011.06.006.

Trotter CL & Maiden MCJ (2014). "Meningococcal vaccines and herd immunity: lessons learned from serogroup C conjugate vaccination programmes". *Expert Rev Vaccines* **8**(7):851–861. DOI: 10.1586/erv.09.48.Meningococcal.

Tzeng YL, Thomas J & Stephens DS (2016). "Regulation of capsule in *Neisseria meningitidis*". *Critical Reviews in Microbiology* **42**(5):759–772. DOI: 10.3109/1040841X.2015.1022507.

Tzeng YL & Stephens DS (2000). "Epidemiology and pathogenesis of *Neisseria meningitidis*". *Microbes and Infection* **2**(6):687–700. DOI: 10.1016/S1286-4579(00)00356-7.

Vaveilin VA & Lokshina LY (1996). "Modeling of volatile fatty acids degradation kinetics and evaluation of microorganism activity". *Bioresource Technology* **57**:69–80.

Verhulst PF (1838). "Notice sur la loi que la population poursuit dans son accroissement". *Corresp. Math. Phys* **10**:113–121.

Vernocchi P, Del Chierico F & Putignani L (2016). "Gut Microbiota Profiling: Metabolomics Based Approach to Unravel Compounds Affecting Human Health". *Frontiers in Microbiology* **7**(July). DOI: 10.3389/fmicb.2016.01144.

Vieusseux M (1805). "Mιmoire sur la maladie qui a regnι a Genκve au printemps de 1805". *J Med Chir Pharmacol* **11**:163.

Vos MGJ de, Zagorski M, McNally A & Bollenbach T (2017). "Interaction networks, ecological stability, and collective antibiotic tolerance in polymicrobial infections". *Proceedings of the National Academy of Sciences* **114**(40):201713372. DOI: 10.1073/pnas.1713372114.

WHO (2016). "Weekly epidemiological record". *The Weekly Epidemiological Record* **16**(91):209–216. DOI: 10.1016/j.actatropica.2012.04.013.. arXiv: 436830.

Wade MJ *et al.* (2016). “Perspectives in mathematical modelling for microbial ecology”. *Ecological Modelling* **321**:64–74. DOI: 10.1016/j.ecolmodel.2015.11.002.

Wade WG (2013). “The oral microbiome in health and disease”. *Pharmacological Research*. SI:Human microbiome and health **69**(1):137–143. DOI: 10.1016/j.phrs.2012.11.006.

Weichselbaum A (1887). “Ueber die Aetiologie der akuten *Meningitis cerebrospinalis*”. *Fortschr Med* **5**:573–583.

Weintraub A (2003). “Immunology of bacterial polysaccharide antigens”. *Carbohydrate Research* **338**(23):2539–2547. DOI: 10.1016/j.carres.2003.07.008.

Welch JLM, Rossetti BJ, Rieken CW, Dewhirst FE & Borisy GG (2016). “Biogeography of a human oral microbiome at the micron scale”. *Proceedings of the National Academy of Sciences* **113**(6):E791–E800. DOI: 10.1073/pnas.1522149113. arXiv: arXiv:1408.1149.

Weyand NJ (2017). “*Neisseria* models of infection and persistence in the upper respiratory tract”. *Pathogens and Disease* **75**(3):1–13. DOI: 10.1093/femspd/ftx031.

Xiao J, Hara AT, Kim D, Zero DT, Koo H & Hwang G (2017). “Biofilm three-dimensional architecture influences in situ pH distribution pattern on the human enamel surface”. *International Journal of Oral Science* **9**(2):74–79. DOI: 10.1038/ijos.2017.8.

Yaesoubi R, Trotter C, Colijn C, Yaesoubi M, Colombini A, Resch S, Kristiansen PA, LaForce FM & Cohen T (2018). “The cost-effectiveness of alternative vaccination strategies for polyvalent meningococcal vaccines in Burkina Faso: A transmission dynamic modeling study”. *PLoS Medicine* **15**(1):1–18. DOI: 10.1371/journal.pmed.1002495.

Yamasaki Y, Nagasoe S, Matsubara T, Shikata T, Shimasaki Y, Oshima Y & Honjo T (2007). “Allelopathic interactions between the bacillariophyte *Skeletonema costatum* and the raphidophyte *Heterosigma akashiwo*”. *Marine Ecology Progress Series* **339**(Honjo 1993):83–92. DOI: 10.3354/meps339083.

Yavuz C, Oliaei SNB, Cetin B & Yesil-Celiktas O (2016). “Sterilization of PMMA microfluidic chips by various techniques and investigation of material characteristics”. *Journal of Supercritical Fluids* **107**:114–121. DOI: 10.1016/j.supflu.2015.08.019.

Yogev R & Tan T (2011). “Meningococcal disease: The advances and challenges of meningococcal disease prevention”. *Human Vaccines* **7**(8). DOI: 10.4161/hv.7.8.16270.

Zaccaria M, Dedrick S & Momeni B (2017). “Modeling Microbial Communities: A Call for Collaboration between Experimentalists and Theorists”. *Processes* **5**(4):53. DOI: 10.3390/pr5040053.

Zahlanie YC, Hammadi MM, Ghanem ST & Dbaibo GS (2014). “Review of meningococcal vaccines with updates on immunization in adults”. *Human Vaccines and Immunotherapeutics* **10**(4):995–1007. DOI: 10.4161/hv.27739.

Zhang Z, Boccazzi P, Choi HG, Perozziello G, Sinskey AJ & Jensen KF (2006). “Microchemostat-microbial continuous culture in a polymer-based, instrumented microbioreactor”. *Lab on a chip* **6**(7):906–913. DOI: 10.1039/b518396k.

de Steenhuijsen Piters WAA, Sanders EAM & Bogaert D (2015). “The role of the local microbial ecosystem in respiratory health and disease”. *Philosophical Transactions of the Royal Society B: Biological Sciences* **370**(1675). DOI: 10.1098/rstb.2014.0294.